Novel therapeutic options in models of nephropathy

by

Muh Geot Wong

A thesis submitted in the fulfilment of the requirements for the degree of

Doctor of Philosophy

Faculty of Medicine

University of Sydney

December 2010

Declaration

This thesis is the result of my full-time study during the years of 2007- 2010. The work is my own and has not been submitted for the award of any other degree at any other University. Where other workers have made valuable contributions, they have been acknowledged.

.....

Muh Geot Wong

Acknowledgements

First and foremost, I would like to thank my supervisor Professor Carol Pollock for her encouragement, kindness and support throughout my PhD. She has been an inspirational role model for me as a clinician scientist, and it was an enormous privilege to have worked in her laboratory.

My co-supervisors, Dr. Xin-Ming Chen and Dr. Weier Qi have also provided invaluable support and technical expertise. They hold the credits in teaching me most of the techniques used in this thesis. I would like to thank our collaborator, Professor Darren Kelly and his laboratory members from St Vincent's Hospital, Melbourne and Assoc Professor Vlado Perkovic and his team from the George's institute who have been most generous in providing samples and technical expertise used in this thesis. Special thank to the Urology department of Royal North Shore hospital and Concord Repatriation hospital in procuring kidney tissues used for primary cell culture and immunohistochemistry for this thesis. Also to the pathology departments, RNSH and Dr. Diego G Silva from Pharmaxis Ltd and their staff members who have been most generous and helpful.

Thank you Usha Panchapakesan, Sonia Saad, John Holian, Sylvie Shen, Ellein Mreich, Siska Sumual who were always available and understand what I am going through, and understand the trials and tribulations of a programme of PhD study. To Owen, Dania, Rachel Yong, Hashimi, Kate for their friendship and technical assistance. Special thanks to Sanaz Maleki, Michael Hann, Vivve Howell, and every member on Level 9 of the Kolling Building.

I appreciate all others in the Royal North Shore Hospital department of renal medicine, David Waugh, Michael Field, Stella McGinn, Bruce Cooper, Yvonne Shen, Amanda Mather, Sarah Roxbourg, Paul Collette, Marnie and all the renal nurses who taught me the art of renal medicine. Special thanks to Margaret, Helen, Noriah and Jacqueline for their cakes and countless cups of tea.

I thank the University of Sydney for awarding me Endeavour International Post-graduate Research Scholarship and International Post-graduate Awards, the University Post-graduate Awards, the Northern Clinical School for additional fundings, the Australian and New Zealand Society of Nephrology and the Royal North Shore Hospital staff specialist awards. Without these funds, completion of a PhD would be impossible.

Finally but not the least, special thanks to my lovely wife, Pei Chee for her patience and love during this difficult period, and my adorable daughter, Samantha who grows with my PhD and keeps me going. To my mum, dad, Muh Rong, Chi Ching, Muh Jiun, Crystal, Maria, Jimmy, Channa, Richard and Tammie, who constantly remind me of the value and joy of a family, and never once make me feel that distance is keeping us apart.

Publications

1. Muh Geot Wong, Yusuke Suzuki, Chiaki Tanifuji, Hisaya Akiba, Ko Okumura, Takeshi Sugaya, Tokunori Yamamoto, Satoshi Horikoshi, Si Yen Tan, Carol Pollock, and Yasuhiko Tomino. Peritubular ischemia has more impact on tubular damage than proteinuria in immune-mediated glomerulonephritis. *J Am Soc Nephrol* 2008 Feb; 19:290-297.

2. Muh Geot Wong , Usha Panchapakesan, Weier Qi, Deigo G Silva, Xin-Ming Chen and Carol Pollock. Cation independent mannose 6-phosphate receptor inhibitor (PXS25) inhibits fibrosis in human proximal tubular cells by inhibiting conversion of latent to active transforming growth factor-β1. *Am J Renal Physiol*, June 2010 (In press).

3. Muh Geot Wong Weier Qi, Xin-Ming Chen, Carol Pollock. TGFβ1 and Krüppel-like factor-6 synergistically suppress bone morphogenetic protein receptors-IA (BMRPIA) in renal proximal tubule cells. Under review by *Am J Pathol (Submitted).*

Manuscript in preparation

1. Muh Geot Wong, Sonia Saad, Weier Qi, Xin-Ming Chen and Carol A. Pollock. Activation of farnesoid X receptors inhibits extracellular matrix deposition in human kidney proximal tubular epithelial cells.

2. Muh Geot Wong, Vlado Perkovic, Qiang Li and Carol Pollock. Circulating bone morphogenetic protein-7 and transforming growth factor-β1 as predictive biomarkers of renal outcome in patients with type 2 diabetes mellitus.

3. Usha Panchapakesan, Sonia Saad, Siska Sumual, Muh Geot Wong, Dania Yagobian. Compensatory adaptive responses of human proximal tubule cell to high glucose.

4. Sonia Saad, Rachel Yong, Muh Geot Wong, Darren Kelly and Carol Pollock. The role of EGF receptor in mediating peroxisome proliferator activated receptors gamma induced sodium and water transport in human proximal tubule cells.

Abstracts/ oral presentations arising from this work

1. Muh Geot Wong, Sonia Saad, Weier Qi, Xin Ming Chen and Carol Pollock. Activation of Farnesoid X receptors (FXR) inhibits extracellular matrix (ECM) deposition in human kidney proximal tubular epithelial cells (PTCs). 2nd Kidney molecular biology, Queenstown, New Zealand 2010.

2. Muh Geot Wong, Sonia Saad, Weier Qi, Xin Ming Chen and Carol Pollock. Activation of farnesoid X receptors (FXR) inhibits extracellular matrix (ECM) deposition in human kidney proximal tubular epithelial cells (PTCs). 46th Annual scientific meeting of Australian and New Zealand Society of Nephrology (ANZSN), September 2010, Perth Western Australia. Abstract no. 153.

3. Usha Panchapakesan, Muh Geot Wong, Siska Sumual, Dania Yaghobian, Huiling Wu, Stephen Chadban, Carol Pollock, and Sonia Saad. Compensatory adaptive responses of human proximal tubule cells to high glucose. 46th Annual scientific meeting of Australian and New Zealand Society of Nephrology (ANZSN), September 2010. Abstract no. 146

4. Muh Geot Wong. "Antifibrotic therapy in kidney disease: Are we any closer in finding a solution?" PReSS seminar Kolling Institute of Medical Research, RNSH, 31st July 2009 (oral presentation)

5. Sonia Saad, Rachel Yong, Muh Geot Wong, Darren Kelly and Carol Pollock. The role of EGF receptor in mediating peroxisome proliferator activated receptors gamma induced sodium and water transport in human proximal tubule cells. 45th Annual scientific meeting of Australian and New Zealand Society of Nephrology (ANZSN), September 2009, Hobart, Tasmania. Abstract No. 131.

6. Muh Geot Wong, Siska Sumual, Usha Panchapakesan, Weier Qi, Xin Ming Chen, Carol Pollock. Effects of mannose 6-phosphate receptor inhibitor (PSX25) in transforming growth factor β1 production in HK2 cells in high glucose and hypoxic conditions. American Society of Nephrology (ASN), 27th October -1st November 2009, San Diego, USA. Abstract No. SA-PO2935.

7. Muh Geot Wong, Siska Sumual, Usha Panchapakesan, Weier Qi, Xin Ming Chen, Carol Pollock. Role of mannose 6-phosphate receptor inhibitor on active transforming growth factorβ1 production in HK-2 cells. 45th Annual scientific meeting of Australian and New Zealand Society of Nephrology (ANZSN), September 2009, Hobart, Tasmania. Abstract No. 125

8. Muh Geot Wong Weier Qi, Xin Ming Chen, Carol Pollock. Mesenchymal epithelial transdifferentiation Action of BMP-7 is inhibited by TGF-β1 and KLF-6 via suppression of BMP receptors of expression in human kidney. World Congress of Nephrology (WCN) 2009, 22nd -26th May 2009, Milan, Italy. Abstract No: Sa248.

9. Muh Geot Wong. "Role of cationic independent mannose 6-phosphate inhibitor (PXS-25) in renal fibrosis?" Invited speaker by Pharmaxis Ltd, 20 Rodborough Road, Frenchs Forest, 7th July 2009. (oral presentation)

10. 8th-19th November 2008: 25th Annual Scientific Research Meeting, 2008. RNSH/UTS/USYD/Kolling Institute combined (Young investigator free communication category). Mesenchymal epithelial transition (MET) action of bone morphogenetic protein-7 is inhibited by transforming growth factor-β1 and Krüppel-like factor-6 via suppression of bone morphogenetic protein receptors expression in human proximal tubular cells. (O12)

11. Muh Geot Wong, Weier Qi, Xin Ming Chen, Carol Pollock. The Effects of transforming growth factor-β1 and Krüppel-like factor-6 on bone morphogenetic proteins receptors expression in human proximal tubular cells. Renal Week, ASN 4th-9th November 2008, Philadelphia, USA. Abstract No. TH-PO395

12. Stella McGinn, Phillip Wong, Liza Nery, Muh Geot Wong, Phillip Clifton Bligh, Rory Clifton Bligh. A high incidence of prevalent fractures in dialysis patients and a role for peripheral quantitative computerised tomography. Renal Week, ASN 4th-9th November 2008, Philadelphia, USA, Abstract No. TH-FC019

13. Muh Geot Wong, Weier Qi, Xin Ming Chen and Carol Pollock. The effects of transforming growth factor-β1 and Krüppel-like factor-6 on bone morphogenetic proteins

receptors expression in human proximal tubular cells. 44th Australia and New Zealand Society of Nephrology (ANZSN), September 2008, Newcastle, NSW, Abstract no. 150.

14. Phillip Wong, Roderick Clifton-Bligh, Muh Geot Wong, Bruce Cooper, Susie Baird, Lisa Nery, Valda Wilson, Philip Clifton-Bligh, Stella McGinn. The use of peripheral quantitative computerised tomography (pQCT) to predict fracture risk in dialysis patients. 44th Australia and New Zealand Society of Nephrology (ANZSN), September 2008, Newcastle, NSW, Abstract no. 187.

15. Muh Geot Wong, Ellein Mreich, John Holian, Weier Qi, Xin-Ming Chen and Carol Pollock. Interaction of BMP receptors with high glucose and TGF beta in a human proximal tubular cell line. Annual Scientific meeting of Australia and New Zealand Society of Nephrology (ANZSN), Gold Coast, 10th to 12th September 2007, Gold Coast. Abstract No: 1189.

16. Free oral communication session. 8th-11th November 2007: 24th Annual Scientific Research Meeting, 2007. RNSH/UTS/USYD/Kolling Institute combined. Bone morphogenetic protein receptors and its interaction with TGF-β1 and high glucose in human proximal tubule cells.

Awards

2007

Endeavour International Post-graduate Research Scholarship (EIPRS), University of Sydney.

International Post-graduate Awards (IPA), University of Sydney.

Top-up Scholarship, Northern clinical school, Royal North Shore Hospital.

Australia and New Zealand Society of Nephrology (ANZSN) World Congress of Nephrology travel awards, Rio de Janerio, Brazil.

2008

Winner, young investigator category, 23rd Annual Scientific Research Meeting, RNSH/UTS/USYD/Kolling Institute combined, November 2008

ANZSN International travel grant, ASN renal week, November 2008, Philadelphia, USA

2009

University Post-graduate Awards (UPA), University of Sydney 2009-2010

Winner, best presentation by PhD student more than 18 months into their candidature, PReSS student seminar series

ISN World Congress of Nephrology (WCN) Travel Awards 2009

ANZSN ASM Travel Awards 2009

Beryl & Jack Jacobs Postgraduate research award 2009.

PReSS International Travel Awards 2009.

Co-investigator of Neorecormon Research Grant Award

2010

Don and Lorraine Jacquot Research Fellowship by Royal Australasian College of Physician (RACP), 2010.

Table of contents

List of figures and tables

Figures

Tables

List of abbreviations

ACE	angiotensin converting enzyme
AGEs	advanced glycation end-products
ALK	activin like kinases
ARB	angiotensin receptor blockers
BMI	body mass index
BMP-7	bone morphogenetic protein-7
BMPR	bone morphogenetic protein receptors
BSEP	bile salt export pump
CA	cholic acid
CARM-1	coactivator-associated arginine (R) methyltransferase-1
CDCA	chenodeoxycholic acid
CI-M6PR	cationic mannose 6-phosphate receptor
CKD	chronic kidney disease
CTGF	connective tissue growth factor
CVD	cardiovascular disease
CYP7A1	cholesterol 7α-hydroxylase
DM	diabetes mellitus
dNTPs	deoxyribonucleotide triphosphates
ECL	Enhanced chemiluminescence
ECM	extracellular matrix
EGF	epidermal growth factor
eGFR	estimated glomerular filtration rate
EMT	epithelial mesenchymal transition
EndoMT	endothelial mesenchymal transition
ERR	estrogen-related receptors
ESKD	End stage kidney disease
ET-1	endothelin-1
FSP-1	fibroblast specific protein-1
FXR	Farnesoid X receptors
Fzd	Frizzled receptors
GDF	growth and differentiation factors
HGF	hepatocyte growth factor
HIF	hypoxia inducible factors
HNF4α	hepatocyte nuclear factor 4α
IBABP	intestinal bile acid binding protein
IGF-II	insulin-like growth factor-II
IL-1	interleukin-1
ILK	integrin-linked kinases

KCP	kielin/ chordin-like protein
KLF	Krüppel-like factor
KSFM	keratinocyte-serum free medium
LAP	latency-associated peptide
LEF-1	lymphoid enhancer-binding factor-1
LTBP	latency binding protein
LXR	liver X receptor
M6PR	mannose 6-phosphate receptor
MAPK	mitogen-activated protein kinase
MCP-1	monocyte chemotactic protein-1
MET	mesenchymal-epithelial transition
MMP	matrix metalloproteinases
NO	nitric oxide
OP	osteogenic proteins
PAI-1	plasminogen activator inhibitor-1
PAS	periodic acid shift
PDGF	platelet derived growth factor
PEPCK	phosphoenolpyruvate carboxykinases
PGC-1α	peroxisome-proliferator-receptors coactivator-1α
PLTP	phospholipid transfer proteins
PMSF	phenylmethylsulphonyl fluoride
PPARs	peroxisome proliferator-activated receptors
PRA	plasma renin activity
PRMT-1	protein arginine (R) methyl transferase-1
PTC	proximal tubular epithelial cell
RAS	renin-angiotensin system
ROS	reactive oxygen species
RXR	retinoic acid receptor
SHP	short heterodimer partner
SRC-1	steroid receptors coactivator-1
SREBP	sterol regulatory element-binding protein
STZ	streptozotocin
TBP	TATA binding protein
TGF-β1	transforming growth factor-β1
TIMP	tissue inhibitors of matrix metalloproteinases
TNF	tumour necrosis factor
tPA	tissue plasminogen activator
TSP-1	thrombospondin-1
Txnip	thioredoxin-interacting protein
UDCA	ursodeoxycholic acid
uPA	urokinase plasminogen activator

uPAR	urokinase plasminogen activator receptors
USAG-1	uterine sensitization-associated gene-1
UUO	unilateral ureteric obstruction
VDR	vitamin D receptor
VEGF	vascular endothelial growth factor
VLDL	very low density lipoprotein
VLDL	very low density lipoprotein
αSMA	alpha smooth muscle actin

Abstract

Despite a better understanding of the pathogenesis and progression of chronic kidney disease (CKD), the functional decline of kidney function in patients with any form of nephropathy remains the greatest challenge to clinicians. Renal fibrosis is considered the 'point of no return' for any form of chronic kidney disease, including diabetic nephropathy, and renal dysfunction induced by inflammation, hypoxia, reactive oxygen species, and lipotoxicity. However, there are limited therapeutic options to mitigate against kidney fibrosis, and therefore novel agents are required to add to the armamentarium of therapies for slowing the progression of CKD.

In this thesis HK-2 cells were used as an *in vitro* model to study the cellular response to known mediators of renal injury. HK-2 cells are derived from proximal tubular cells (PTCs) from normal adult human renal cortex. They retain phenotypic and functional characteristics indicative of well-differentiated PTCs. These cells were cultured in conditions inherent in diabetes mellitus (DM) mimicking the microenvironment of CKD.

The functional relationship between transforming growth factor-β1 (TGF-β1), bone morphogenetic protein-7 (BMP-7) and Krüppel-like factor-6 (KLF-6) in epithelial mesenchymal transition (EMT) was studied using recombinant human TGF-β1 and BMP-7. The BMP receptors and markers of EMT were assessed in HK-2 cells after exposure to 0.5 ng/ml of TGF-β1 for 48 hours. Overexpression of BMP-7 was induced and BMP receptor expression was assessed in KLF-6 overexpressing and silenced cells. TGF-β1 significantly down-regulated bone morphogenetic protein receptor-IA (BMPR-IA) expression. Cells overexpressing KLF-6 showed decreased expression of BMPR-IA and

other type I BMP receptors, and silencing of KLF-6 increased BMPR-IA expression. Cells overexpressing BMP-7 had significantly higher E-cadherin and phosphorylated Smad1/5/8, which was not observed with concurrent TGF-β1 exposure. *In vivo* studies confirmed a reduction in BMP-7 and BMPR-IA but an increase in KLF-6 expression in established diabetic nephropathy. TGF-β1 and KLF-6 synergistically induced suppression of BMPR-IA and downstream reduction of BMP-7 signalling. These findings suggest that the presence of TGF-β1 in multiple forms of nephropathy mitigates against the use of rhBMP-7 as an antifibrotic therapeutic agent.

Hyperglycemia and hypoxia have independent and convergent roles in the development and progression of renal disease. TGF-β1 is a key cytokine promoting the production of extracellular matrix proteins. The cationic-independent mannose 6-phosphate receptor (CI-M6PR) is a cell membrane protein that binds M6P containing proteins. A key role is to activate latent TGF-β1. PXS-25, a novel CI-MPR inhibitor, has been shown to have antifibrotic properties in skin fibroblasts. In the experiments described in this chapter, HK-2 cells were exposed to high glucose (30mM) ± 100μM PXS-25 in both normoxic (20% O2) and hypoxic (1% O2) conditions for 72 hours. Cellular fibronectin, collagen IV and matrix metalloproteinase-2 (MMP-2) and MMP-9 were assessed. Total and active TGF-β1 proteins were measured by ELISA. High glucose and hypoxia independently induced active and total TGF-β1 production. Active TGF-β1, but not total TGF-β1 was reduced with concurrent PXS-25 in the presence of high glucose, but not when hyperglycemia and hypoxia were both present. Hyperglycemia induced fibronectin ($p < 0.01$) and collagen IV ($p < 0.05$) production, as did hypoxia, but only hyperglycemia induced increases in matrix proteins were suppressed by concurrent PXS-25exposure. This

was not evident when hypoxia and hyperglycemia coexist. High glucose induced MMP-2 and -9 in normoxic and hypoxic conditions, which was not modified in the presence of PXS-25. This chapter demonstrates that high glucose and hypoxia can independently induce endogenously active TGF-β1 production in human PTCs. PXS-25 inhibits conversion of high glucose induced latent to active TGF-β1, which translates to a reduction of extracellular matrix proteins only in the absence of hypoxia.

Farnesoid X receptor (FXR) plays a key role in regulating lipid and carbohydrate metabolism, fibrosis and inflammation in *in vivo* and *in vitro* models of diabetes mellitus. The mechanisms underpinning this regulation, and the relationship with the broader nuclear hormone receptor superfamily, particularly PPARγ, remain unclear. In this chapter, we aimed to study these questions. HK-2 cells were exposed to 10μM of pioglitazone or rosiglitazone, 1μM of GW4064 (FXR agonist) in 5mM or 30mM D-glucose. RNA was obtained at 24 hours for real-time PCR of FXR target genes, sterol regulatory element binding protein-1 (SREBP-1), short heterodimer protein (SHP) and TGF-β1. Fibronectin, collagen IV and monocyte chemoattractant protein-1 (MCP-1) protein were measured at 48 hours. FXR siRNA was used to silence FXR prior to study in the above experimental conditions. We showed that high glucose suppressed FXR mRNA and protein expression, suppressed SHP and induced SREBP-1 mRNA. High glucose-induced fibronectin accumulation were suppressed equally by FXR and PPARγ agonists ($p<0.01$). FXR, but not PPARγ agonists, suppressed collagen IV ($p<0.01$). Both suppressed high glucose induced TGF-β1 mRNA. However, only PPARγ agonists reduced MCP-1 production. FXR silenced cells had increased SREBP-1 expression parallel to increased ECM production, which was further increased by high glucose.

Diabetes mellitus (DM) is an independent risk factor for CKD. At present, proteinuria and eGFR are the best known predictors for the future functional decline of the kidneys in patients with diabetic nephropathy. However, the presence of macroalbuminuria and impaired renal function usually reflects irreversible advanced nephropathy. Therefore, there is a need for biomarkers that can predict poor renal outcome in the early stage of renal dysfunction so as to better deploy community and hospital resources. The Action in Diabetes and Vascular Disease: Preterax and Diamicron Modified Release Controlled Evaluation (ADVANCE) Collaborative Group study is a factorial randomised, double blinded controlled trial involving 11,140 patients with type 2 diabetes. Baseline serum from 64 patients who developed renal end points (defined as doubling of serum creatinine to at least 200umol/l, need for renal replacement therapy, or death due to renal disease), were used in this study. To obtain the matched controls, propensity scores methods are used. The characteristics matched for include age, sex, race, baseline estimated glomerular filtration rate (eGFR) (<60 vs. >60), urinary albumin: creatinine ratio (UACR), baseline blood pressure, baseline HbA1c, known macrovascular disease, history of retinopathy and treatment allocation (BP lowering intensive glucose lowering, both or neither). Enzyme linked immunosorbent assays were used to analyse total and active circulating TGF-β1 and BMP-7. In this study, we showed that those who developed renal endpoints have higher baseline total circulating TGF-β1 ($p=0.0003$), and lower BMP-7 ($p<0.0001$) as compared to controls, even after adjusting for various variables. We also demonstrated that circulating BMP-7 is strong and independent predictor of poor renal outcomes in individuals with type 2 DM, which may have prognostic potential in predicting poor renal outcomes.

CHAPTER 1: Literature review

1.1 Chronic kidney failure

1.1.1 Chronic kidney disease and diabetic nephropathy

Chronic kidney disease (CKD) is a condition in which renal excretory function progressively and irreversibly decreases as a consequence of renal injury and nephron loss. Decreased excretory function leads to an accumulation of metabolic and waste products in the blood and organs, which causes azotemia and multiorgan damage. Eventually patients may die either due to renal failure or associated co-morbidity, the most important being cardiovascular disease, or needing renal replacement therapy in the form of transplantation or dialysis[1]. It is estimated that 10-20% of the adult population have some degree of CKD, and that dialysis consumes about at least 2% of total health expenditure in many developed conuntries[2]. Because of its high incidence and prevalence, and the disproportionate cost of dialysis, CKD represents a heavy human, clinical and socioeconomic burden. CKD is a growing epidemic worldwide, driven largely by the rise in obesity, hypertension and diabetes mellitus in the Western world.

Diabetic nephropathy is the leading cause of end stage kidney disease (ESKD). The worldwide prevalence of diabetes mellitus has been predicted to reach 366 million by 2030, up from 171 million in 2000[3]. The growing number of patients with diabetes mellitus in developed countries is partly due to the ageing population, increased urbanization, and increased prevalence of obesity. Almost one million Australians aged 25 years and over

have overt diabetes mellitus, though the Australian Diabetes, Obesity and Lifestyle Study (AusDiab) would suggest many more remain undiagnosed[4]. In the non-indigenous population the prevalence is approximately 7% rising to 30 % in some Aboriginal and Torres Strait islander communities[5]. The 2005 AusDiab study estimated the incidence of diabetes mellitus for Australian adults at approximately 275 cases every day (almost 90% of whom have type 2 diabetes)[4]. More than one third of these will go on to develop diabetic nephropathy characterised by albuminuria, declining glomerular filtration rate (GFR), arterial hypertension and increased cardiovascular risk[6].

While diabetic nephropathy continues to be the leading cause of ESKD in Australia (34% of all new ESRD patients)[7], CKD is 30-60 times more prevalent than ESKD among patients with diabetes mellitus, and its incidence is increasing exponentially. CKD is one of the most potent known risk factors for cardiovascular disease (CVD) such that individuals with CKD have a 10-20 fold greater risk of cardiac death than age and sex matched controls without CKD[8, 9]. Moreover, patients with CKD are at least 20 times more likely to die from a CVD than survive to reach dialysis[10]. There is an independent relationship between reduced eGFR (particularly in individual with eGFR <45ml/min/1.75m^2), and microalbuminuria, with CVD risk in many cross sectional analysis[11, 12]. It has been shown these patients have higher prevalence of surrogate markers of CVD such as left ventricular hypertrophy, carotid arterial intimal thickening, and brain white matter hyperintensity volume. Microalbuminuria is also an independent marker associated with poor cardiovascular outcome and all-cause mortality in those with[13] and without diabetes[14]. Intervention with ACE inhibitor in patients with microalbuminuria has been proven to reduce CVD outcome and delay renal progression[11]. It is believed that microalbuminuria

represents more than just kidney disease itself but may be a manifestation of systemic endothelial dysfunction.

In addition to the traditional risk factors for CVD, CKD patients have other risk factors such as anaemia, chronic volume overload, electrolyte imbalance, uremic toxin, and other neurohormonal factors[15]. The latter includes the activation of sympathetic nervous system and renin-angiotensin-aldosterone system, endothelins, vasopressin, prostaglandins, adenosine, oxidative stress, and systemic inflammation.

1.1.2 CKD and metabolic syndrome

Metabolic syndrome also called syndrome X or insulin-resistance syndrome, was first described by Reaven in 1988 as a set of metabolic and cardiovascular risk factors that occur together more often than would be expected by change alone[16, 17]. Although there are serial definitions of metabolic syndrome, the unifying definition includes insulin resistance, impaired glucose tolerance or type 2 diabetes, hypertension, atherogenic dyslipidemia (low level of high-density lipoprotein or high levels of triglycerides), central obesity, hyperuricemia, microalbuminuria, and hypercoagulability[18]. Metabolic syndrome is associated with a two fold increase in the risk of atherosclerotic cardiovascular disease and a fivefold increase in the risk of type 2 diabetes mellitus[19]. The concept of the metabolic syndrome was originally devised to identify cohort of patients at high risk of CVD and diabetes, but not CKD. However, prospective data are emerging to indicate that the metabolic syndrome is associated with a modest but independent and additive risk of new-onset CKD[20, 21], even after adjusting for newly diagnosed diabetes and hypertension[22]. The

association between the metabolic syndrome and CKD was noted by Chen *el al.* in a cross-sectional analysis of the NHANES III cohort (n=6,217), that demonstrated the significant association between the metabolic syndrome and presence of CKD (estimated glomerular filtration rate (eGFR) <60ml/min/1.73m2; odd ratio (OR=2.60) and microalbuminuria (OR=1.89), after adjusting for age, gender and lifestyle factors. These results persisted even after excluding patients with diabetes[23]. These findings are not surprising as patients with chronic renal insufficiency frequently exhibit many of the major components of the metabolic syndrome and are at high risk for cardiovascular mortality.

The exact pathophysiology and cellular mechanism caused by the metabolic syndrome is still not fully understood. However, insulin resistance is considered the hallmark of the metabolic syndrome and is believed to be the underlying reason for the associated systemic metabolic derangements of hypertension, dyslipidemia and hyperglycemia[24]. Insulin resistance causes compensatory hyperinsulinemia and hyperglycaemia, which are considered the fundamental pathogenetic factors for cardiac and cerebrovascular disease. The other potential mechanisms underpinning renal damage in the metabolic syndrome are thought to be a combination of renal lipotoxic effects of VLDL and triglycerides[25], dysfunctional secretion of adiponectin[26] and leptin[27], local inflammatory cell recruitment leading to inflammatory cytokine production, (such as interleukin 6 and tumour necrosis factor); activation of the renin-angiotensin-aldosterone system, endothelial dysfunction, oxidative stress, mesangial cell proliferation and extracellular matrix deposition[28, 29]. The glomeruli and tubules are exposed to numerous injurious factors in the metabolic syndrome including systemic hypertension, hyperinsulinemia, hyperglycemia, hyperlipidemia and systemic inflammation, all of which

results in direct or hyperfiltration-induced renal injury[30]. In addition, glomerulopathy, proteinuria and focal segmental glomerulosclerosis are all associated with obesity[31].

CKD may not be just a consequence of metabolic syndrome, it may be actively involved in the development and progression of metabolic syndrome, since the kidney is an important organ in glucose and lipid homeostasis. However, few studies have examined whether interventions targeting the metabolic syndrome can improve renal outcomes, mainly due to poorly designed studies and renal parameters are generally assessed as secondary outcomes. Recently, the so called "adopted nuclear receptors" which have been found to have regulatory roles in the disposal of physiologically dietary lipid and metabolites such as bile salts, fatty acids and eicosanoids. The most well known subfamilies of these nuclear receptors are peroxisome proliferator-activated receptors (PPARs) and the farnesoid X receptors (FXR), both of which have a regulatory role in the renal response to factors inherent in the metabolic syndrome and diabetes mellitus[32, 33]. Nuclear hormones receptors are well established targets for small molecule modulators. Therefore both biomedical and pharmaceutical researchers have strived to develop synthetic ligands that selectively modify nuclear hormone receptor function. This approach is currently under investigation as a strategy for the treatment of endocrine and metabolic disease including diabetic nephropathy[34].

1.1.3 Therapies for CKD

As cardiovascular disease is the principal cause of morbidity and mortality in the CKD population, the primary aims of treatment in patients with CKD are both to slow or

prevent the progression of CKD and to prevent cardiovascular disease. Although regression of CKD is described frequently in laboratory animals, regression is rare in humans and difficult to quantify. In fact, all therapies currently available for human CKD are only partially effective against the accepted renal end points of ESKD or decline in glomerular filtration rate (GFR). Most studies have demonstrated a reduction in risk of renal end points of only 15-30% and delay to ESKD of only a few months. For examples, in the Reduction of Endpoints in Non-insulin dependent diabetes mellitus with the Angiotensin II receptor Antagonist Losartan (RENAAL) study, losartan reduced the level of proteinuria by only 35%, the incidence of doubling of serum creatinine level by 25% and the incidence of ESKD by 28%, after a mean follow up of 3.4 years[35]. Hence significant treatment gap exists.

Even though conventional non-pharmacological therapies such as weight reduction, dietary and lifestyle changes have been shown to be effective, they are unlikely to adequately reduce the risk of CKD. The best evidence based pharmacological therapy currently available for CKD focuses primarily on blood pressure control and maximizing renin-angiotensin aldosterone blockade. Several large, randomised controlled trials have shown the effectiveness of angiotensin receptor blockers (ARBs) and angiotensin-converting enzyme (ACE) inhibitors[36, 37], alone or (less convincingly) in combination[38]. Although some studies have shown dual blockade to be most beneficial, this enthusiasm was recently dampened by the results of the ONTARGET trial in 2008, which showed that the secondary outcome of renal end points (a composite of dialysis, doubling of serum creatinine and death), occurred more frequently in patients assigned to combination therapy than in patients assigned to either monotherapy. So, although combination therapy is more

effective at limiting the progression of proteinuria, a surrogate marker of renal disease, it did not reduce progression of CKD. Thus, the most effective therapies currently available for slowing progression of CKD are only partially effective and newer agents are needed.

To date, several emerging therapies aimed at slowing the progression of renal disease have shown great promise in animal studies, but they have been less effective in humans. This could either due to species difference, differences in side effect tolerance, or the agents being too narrowly targeted against a single pathophysiology event when human CKD is likely to be due to a myriad of factors and multiple therapies are likely to be required. These agents include Tranilast[39, 40], Sulodexide[41, 42], target against advanced glycation end-products (AGEs)[43], protein kinase C inhibitors[44], pentoxifylline[45], endothelin antagonists[46, 47], statins[48, 49], erythropoiesis-stimulating agents[50, 51], Vitamin D analogues[52, 53] and many more. However, many of these agents have lacked proven efficacy in slowing the progression of CKD[54, 55], caused significant unwanted side effects[56, 57], have not reported long term outcomes[58-60] or renal outcomes were adjudicated as secondary outcomes[61, 62], and hence lacked sufficient power to draw valid conclusions. Therefore more novel agents are required to add to the armamentarium of therapies for slowing the progression of CKD in humans.

For emerging therapeutic strategies to find clinical application they need to be more effective than, treatment targeting the inhibition of the renin-angiotensin-aldosterone system. In addition, successful drugs will need to demonstrably impact on the hard end points such as decline in GFR, need for dialysis and mortality, and not just show beneficial effects on surrogate markers of disease progression such as proteinuria. It also raises the

question as to whether alternative biomarkers may better predicting the likelihood of progression of CKD.

1.2 Pathophysiology of renal fibrosis

1.2.1 Renal tubulointerstitium and tubulointerstitial fibrosis

The tubulointerstitium encompasses the tubular epithelium, vascular structures, and interstitium together accounting for more than 90% of the kidney volume[63]. The renal interstitium acts as a tissue skeleton giving structural support to the kidney, modulating the exchange among tubular and vascular elements of the renal parenchyma, regulating glomerular filtration through its effect on tubuloglomerular feedback, and involvement in the synthesis of systemic hormones such as erythropoietin and vitamin D. It is divided into the cortical and medullary tubulointerstitial space. The interstitial space is composed of resident fibroblasts, immune regulatory cells, peritubular vasculature and its perivascular cells, and extracellular components.

Renal fibrosis is regarded as a central event in the progression of CKD regardless of the aetiology. The kidney's response to injury resembles the generalized wound healing response that occurs elsewhere. Renal fibrosis is probably initiated as a beneficial response to injury, which if uncontrolled leads to a self perpetuated pathological process. Histologically ESKD manifests itself as glomerulosclerosis, vascular sclerosis, and tubulointerstitial fibrosis, with tubulointerstitial fibrosis consistently shown to be the best histological predictor of progression of CKD. Indeed, even in glomerulopathies,

tubulointerstitial fibrosis correlates better than glomerular injury with evolution and prognosis[64, 65].

1.2.2 Interstitial fibroblast and myofibroblasts

The normal adult renal interstitium contains fibroblasts and dendritic cells[66]. Fibroblasts are stellate shaped cells with a stellate nucleus and abundant rough endoplasmic reticulum, collagen secreting granules, actin filaments under the plasma membrane and multiple cell processes, which connect them to tubular and capillary basement membranes. Mechanical stress, cytokines and various other factors induce fibroblasts to acquire a myofibroblast phenotype[67]. Myofibroblasts differ from fibroblasts in that they contain stress fibres, sparse myofilaments, fibronexin (transmembrane connections between extracellular fibronectin and actin microfilaments), more frequent attachments to basement membranes and a rather rounded nucleus[68]. A key feature of myofibroblasts is their contractile function. α-smooth muscle actin (αSMA) and fibroblast S100A4 (FSP-1) are the most well known myofibroblast markers. Other markers include vimentin and the fibronectin splice variant, ectodomain A. However, none of these markers, including α-SMA, are unique to the myofibroblasts. Moreover, myofibroblasts are often stated to represent activated or differentiated fibroblasts.

The origin of the myofibroblast is rather controversial but it is thought to be derived from a number of sources. These include a) proliferation of resident mesenchymal cells (including fibroblasts[69], pericytes and perivascular cells[70], b) tubular epithelial cells or endothelial cells through a process called epithelial mesenchymal transition (EMT)[71] or

endothelial mesenchymal transition (EndoMT)[72], and c) recruitment of blood-borne precursors[73]. Myofibroblasts are thought to be the major source of extracellular matrix (ECM) production followed by tubular epithelial cells, macrophages and fibrocytes[74]. Myofibroblast differentiation, proliferation and collagen synthesis are stimulated by a variety of paracrine and circulating factors derived from tubular cells, leukocytes/ macrophages and fibroblasts themselves. A hierarchy exists among the profibrotic growth factors, with compelling evidence for the importance of transforming growth factor-β1 (TGF-β1), angiotensin II and platelet derived growth factor[75]. It is also recognised that fibroblasts are stimulated by disease-specific factors such the high glucose concentrations in diabetes, mechanical strain and the by factors inherent in the surrounding ECM[76].

1.2.3 Extracellular matrix (ECM)

Tubulointerstitial fibrosis occurs due to a net deposition of ECM (mainly collagen), resulting from a disproportionate increase in production, and an altered degradation of ECM components. It is well known that the normal ECM provides survival signalling to adjoining cells. In addition, when epithelial cells are in contact with an abnormal ECM, they undergo a specific form of cell death called anoikis[77]. It is also known that the ECM is a reservoir of a variety of growth factors including TGF-β[78]. Thus, alterations in the composition or structure of the ECM must influence tissue trophic status and homeostasis. Although matrix synthesis is part of the normal repair process, excessive synthesis of ECM is in itself deleterious, further exacerbating injury in a vicious cycle[79]. The dysregulation of the normal turnover of the ECM for basement membrane and tissue repair into a

pathological process is thought to be the consequence of a) persistent stimulation by the injurious agent, and b) imbalance of other homeostatic signalling factors such as other anti-fibrotic cytokines, for examples bone morphogenetic protein-7 (BMP-7)[80] and hepatocyte growth factor (HGF)[81] that counteract the profibrotic cytokines, in particular TGF-β1 (Figure 1.2.3.1).

The increase in ECM production is also accompanied by a loss of renal parenchyma as a result of the fibrocontractive nature of fibrotic scarring. This is reflected in end-stage kidneys being smaller than their normal counterparts[79]; and the indirect observation that a decrease in renal size parallels loss of renal function[82]. Fibrosis also leads to progressive renal tissue destruction through the disruption of the peritubular capillary network and the consequent reduction of renal blood flow and local tissue hypoxia[83, 84]. This, in turn, induces the expression of hypoxia-inducible factors which also promotes fibrosis in chronic disease[85, 86].

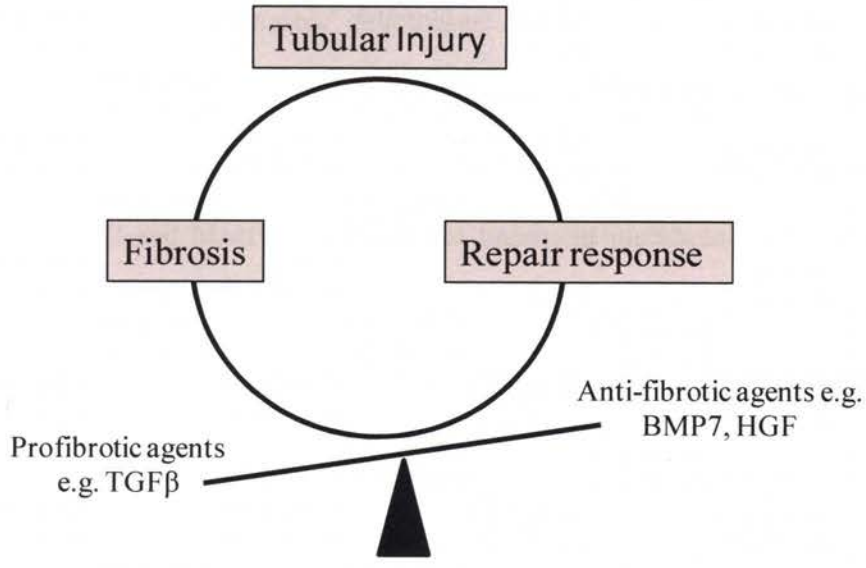

Figure 1.2.3.1 Balance between tubular injury, repair and fibrosis.

Initially common mechanisms are activated in response to the stimulus of tubular injury. At some point, the imbalance between the opposing effects of pro-fibrotic cytokines e.g. TGF-β1 and the counterregulators, such as hepatocyte growth factor (HGF) and bone morphogenetic protein-7 (BMP-7), impedes critical components of tissue repair, disrupts tissue homeostasis, and leads to the process of self perpetuated, progressive fibrosis.

1.2.4 Extracellular matrix protease system

Normal matrix turnover is maintained through a combination of synthesis and degradation, due to the usually coordinated actions of two protease systems: The matrix metalloproteinases (MMP)/ tissue inhibitors of matrix metalloproteinases (TIMP) system, and the plasminogen activator (PA)/ plasmin/ plasminogen activator inhibitor (PAI) system. Most collagen degradation in the kidney is under the regulation of matrix metalloproteinases (MMPs), a family of zinc-dependent endopeptidases, subdivided into

four groups, namely collagenases, gelatinases, stromelysins and elastases, which are typically secreted as latent zymogens. Four members of the collagenase group, MMP-1, MMP-2, MMP-8 and MMP-13, have the ability to degrade fibrillar collagens. The two gelatinases, MMP-2 and MMP-9 both degrade basement membrane collagen and gelatin. MMP-2 is substrate specific to fibronectin and laminin, whereas MMP-9 is more specific to type IV and V collagen[87]. Collectively, they are capable of degrading all ECM proteins.

Four major tissue inhibitors of MMPs have been identified: TIMP-1-2,-3 and -4 but only TIMP-1 and TIMP-2 have been implicated in renal disease[88]. These inhibitors are capable of inhibiting activation of latent prometalloproteinases and found to be significantly induced in progressive renal disease[89, 90].

In addition to the MMP family, the second proteolytic cascade to play a role in renal interstitial fibrosis is the plasmin-dependent pathway[91]. Plasmin not only activates latent procollagenases but also may directly degrade other matrix proteins such as fibronectin and laminin. Latent plasminogen is activated by proteolytic cleavage by tissue plasminogen activator (tPA) and urokinase plasminogen activator (uPA), which is produced in significant quantities by proximal and distal tubular cells, as well as by macrophages and myofibroblasts[92]. As with the MMPs, these enzymes are regulated by parallel inhibitory systems, in this case plasminogen activator inhibitor (PAI). TGF-β1 is known to be a potent inducer of PAI-1 expression, as are high glucose and endothelin-1 (ET-1), which collectively act to inhibits matrix degradation[93].

If the ability to remodel collagen is an important counterbalance to upregulated ECM synthesis, theoretically renal fibrosis could be explained by a reduction in protease

system activity. However, almost all MMP knock-out mice do not have a fibrotic phenotype[94], and overexpression of MMP-2 induces fibrosis[95], suggesting that such an assumption is an oversimplification of the remodelling process. It is increasingly recognized that MMPs have both antifibrotic and profibrotic roles. Studies of MMP expression and activity *in vivo* remain controversial. Sustained MMP expression has consistently been seen in experimental models[96] and in human renal disease[97]. However, it is unclear if this reflects compensatory mechanisms trying to limit matrix accumulation or a reflection of profibrotic activity.

1.2.5 Epithelial mesenchymal transition (EMT)

Strutz *et al.* first described tubular epithelial cells as being capable of transitioning to a fibroblastic phenotype via a process known as epithelial mesenchymal transition (EMT)[98]. EMT is a process in which differentiated epithelial cells undergo a phenotypic conversion that gives rise to the matrix-producing fibroblasts and myofibroblasts, which is accompanied by the sequential loss of epithelial markers and *de novo* acquisition of mesenchymal markers[99]. EMT and its reverse process, mesenchymal-to-epithelial transition, are well recognized in normal ontogenesis. Multiple comprehensive reviews have been written about EMT[99, 100] and it is believed EMT is an integral part of tissue fibrogenesis after injury which plays an important role in the progression of renal fibrosis[101-104]. EMT is thought be an adaptive response of epithelial cells to a hostile or changing microenvironment.

A large number of *in vivo* and *in vitro* studies have demonstrated that renal tubular cells undergone EMT in response to leukocyte infiltration, stress signals and various mediators, in particular TGF-β1[105]. However, EMT is not an easy process to study, especially *in vivo*. EMT is generally assessed *in vivo* by the appearance of fibroblastoid markers such as αSMA, FSP-1 or vimentin in tubule cells co-expressing general or specific epithelial markers, in association with actin re-organization and basement membrane disruption[106]. Even though Iwano *et al*[107]. have provided convincing evidence that EMT contributes to interstitial fibroblasts using genetically tagged PTCs. Although they concluded that EMT accounts for up to 36% of all FSP-1 positive interstitial fibroblasts, the actual frequency of documented EMT in fibrotic kidneys is low in most studies[71]. Despite this, evidence for EMT and its role in renal fibrosis *in vivo* is emerging in both animal models of CKD and human renal disease including obstructive nephropathy[108], 5/6 remnant kidney nephropathy[109, 110], lupus nephritis[111], IgA nephropathy[112], diabetic nephropathy[113, 114], and chronic allograft nephropathy[115-117].

Depending on the specific pathophysiologic circumstances, EMT can be induced by a wide variety of stimuli (Table 1.2.5.1). Of which, TGF-β1 is possibly the most potent inducer and will be the focus of this thesis. TGF-β1 initiates and completes the EMT process *in vitro* and *in vivo* [118]. This is consistent with the observation that TGF-β1 expression is universally upregulated in experimental models of CKD and in clinical diseases[119].

In rodents, TGF-β1-mediated EMT is inhibited by endogenous modulators such as BMP-7[80], HGF[120] and cell-to-cell contact[121]. *In vivo*, tubular EMT only occurs after a sustained injury. Similarly, TGF-β1 cannot induce EMT in an intact confluent cell

monolayer. This suggests that EMT can only be induced by TGF-β1 in the presence of epithelial injury, which is inherent in the repair process and distorted within the pathological scenario. In this setting, EMT would result in damage, rather than in repair, which in turn would further stimulate a vicious cycle of exacerbated damage. Hence, pathological EMT observed in CKD can be viewed as a consequence of skewed repair processes. Therefore, inhibition of TGF-β1 action would potentially result in a beneficial effect in the setting of renal injury. The role of BMP-7 and HGF in modulating renal fibrosis in patients with CKD needs to be further explored.

Table 1.2.5.1

Inducers and suppressors of EMT in the interstitial space

Factors that promote or induce EMT	**Factors that suppress or inhibit EMT**
a) Growth factors TGF-β1[101, 118] FGF-2[122] Connective tissue growth factor (CTGF)[123]	**a) Growth factor** BMP-7[80] HGF[120]
b) Cytokines IL-1[125] Oncostatin-M[126, 127]	**b) Nuclear receptor activator** Vitamin D[124]
c) Renin angiotensin system Angiotensin II[129]	**c) Renin-angiotensin system inhibitors** Angiotensin converting enzymes (ACE) inhibitor & Angiotensin II receptor blockers[128]
d) Proteases MMP-2[133] tPA[108] Plasmin[134]	**d) Others** Statins[130] Rapamycin[131, 132]
e) **Environmental stresses** hypoxia/ reactive oxygen species[135, 136] advanced glycation end products[123, 137]	

1.2.6 Endothelial-to-mesenchymal transition (EndoMT)

Endothelial cells, like tubular cells, have been proposed as a source of renal fibroblasts via a process known as endothelial-to mesenchymal transition (EndoMT). Zeisberg *et al.* have recently used lineage tracing techniques to demonstrate EndoMT in a variety of murine models of renal disease. They demonstrated that 30-50% of myofibroblasts co-expressed myofibroblast markers and the endothelial antigen CD31, after sustained renal injury[72]. Using a similar approach in a diabetic mice model, up to 23% of interstitial myofibroblasts were shown to be of endothelial origin[138]. Conversely, there are studies which have found no evidence that EndoMT exists[74, 139]. Since endothelial cells are a specialized type of epithelial cells, EndoMT may represent another form of EMT that occurs in the injured kidney. Although the role of EndoMT in fibrosis is unresolved, these studies all indicate that the vasculature may be an important contributor to renal fibrosis. It also illustrates that the origin of interstitial fibroblast in the diseased kidney is much more complex than had been previously thought.

1.2.7 Role of inflammation in renal tubulointerstitial fibrosis

EMT is often preceded by and closely associated with chronic interstitial inflammation. Only in the embryo can loss or damage of tissue be repaired without an inflammatory response[140]. After birth, injury and repair are always associated with an inflammatory process, irrespective of the eventual outcome. Local injury to the renal cells triggers the release of soluble factors, an increase in local vascular permeability, activation of endothelial cells and the emigration of leukocytes[141]. Such soluble factors include

chemokines, cytokines, growth factors (e.g. TGFβ, BMP7, platelet derived growth factor (PDGF), vascular endothelial growth factor (VEGF), insulin like growth factor) and lipid mediators (e.g. leukotrienes, lipoxins etc). Stimuli for the generation of mediators by tubular cells include proteinuria, high glucose, altered lipid, hypoxia, infectious agents, uric acid, paraproteins and many others[141].

The fibrotic process involves a similar set of players including leucocytes, cytokine and chemokines release. In fibrosis, macrophages and lymphocytes play major roles via the production of proinflammatory and profibrotic cytokines which activate fibroblasts and tubular cells in the tubulointerstitial compartment[142]. As capillary blood supply is lost because of tissue injury, the chronically hypoxic state that exists in local tissues renders it susceptible to progressive inflammation unless adequate neo-vascularisation occurs. More recently, Toll like receptors (TLRs), which are expressed by cells of the immune system, have been found to be expressed in non-immune cells in the kidney such as renal tubular epithelial cells, podocytes, mesangial cells and endothelial cells. Even though their functions are not clear they are believed to play a role in fibrosis[143, 144].

Both tubular cells and interstitial fibroblasts produce chemokines when exposed to hypoxia and hyperglycemia[145, 146] following stimulation with proinflammatory cytokines and after TLR activation[147]. Furthermore, activated renal fibroblasts secrete chemokines such as macrophage chemotactic protein-1 (MCP-1), which in turn potentiates macrophage accumulation. Renal fibroblasts produce interstitial matrix components including collagen upon stimulation by activated macrophages, indicating that chemokines, acting either directly or indirectly through macrophage recruitment, contribute to interstitial collagen deposition and fibrosis. Chemokines may also contribute to the recruitment of bone

marrow-derived cells to the renal interstitium in progressive renal disease[148]. The functional role of chemokines in interstitial disease has been confirmed by several animal studies using chemokine antagonists or chemokine-deficient mice. The models used have studies the interstitial involvement of immune complex mediated glomerulonephritis, Alport's disease, nephrotic syndrome, diabetic nephropathy, and obstructive nephropathy[147]. At present, there are insufficient data to assign a specific chemokine and receptor ligand to tubulointerstitial injury. However, it highlights the role for chemokines and their receptors in leukocyte mediated progressive tubulointerstitial damage and fibrosis[149].

1.2.8 The role of hypoxia in tubulointerstitial fibrosis

The oxygen tension within the kidney is disproportionately low due to the anatomical arrangement of the renal arterioles and veins, allowing shunt diffusion of descending and ascending vasa recta. The medullary interstitial renal oxygen tension is 5-15 mmHg as compared to 95 mmHg in the renal artery. As a consequence, the S3 segment of the proximal tubule is particularly vulnerable to ischemic injury. The importance of chronic hypoxia in the pathogenesis of tubulointerstitial injury in the pathogenesis of CKD is increasingly recognized[150, 151]. This has been validated in a variety of human and experimental kidney diseases, including diabetic nephropathy[136,146]. Wong *et al.* reported that hypoxia may be a more potent inducer for tubulointerstitial injury than proteinuria in immune mediated glomerulonephritis[84].

Chronic hypoxia in CKD occurs as result of a reduced number and density of peritubular capillaries. Glomerular and vascular damage to the efferent arterioles causes reduction in oxygen diffusion to tubulointerstitial cells, eventually leading to tubular dysfunction and fibrosis[152]. Vasoactive substances such as angiotensin II and nitric oxide (NO) further decrease postglomerular peritubular blood flow. NO, which is an endogenous regulator of renal hemodynamics, regulates oxygen availability with its levels being reduced in individuals with diabetes and other form of CKD. Furthermore, metabolic demands are increased in the outer medulla tubules as remaining nephrons compensate for tubular nephron loss by an increase in single nephron tubular transport, resulting in more energy consumption. The anaemia associated with CKD additionally hinders oxygen supply to the tissues[153]. Hypoxia per se then has an impact on various biological reactions such as oxidative stress, mitochondrial dysfunction, endoplasmic reticulum stress, and particularly in diabetic nephropathy, advanced glycation and carbonyl stress[154].

Hypoxia inducible factors (HIF) are central to the adaptive response occurring in hypoxic conditions. HIF-α is constitutively transcribed and translated, and its levels are regulated by its rate of degradation. Oxygen affects the stability of HIF-α through enzymatic hydroxylation involving the von Hippel Lindau protein[155]. Defence against hypoxia hinges upon HIF activation, which induces the expression of a broad range of genes that participate in erythrocytosis, angiogenesis, glucose metabolism and more recently recognised in EMT[83, 85]. Genes that have been implicated in EMT and upregulated by HIF include NotchIC, Snail, Lysyl oxidase-like 2 (Loxl2), and Hairy and Enhancer Split-1 (Hes1)[83]. Various potential therapeutic strategies have been explored targeting the abnormal oxygen metabolism associated with CKD. As yet, none have proved successful.

1.3 Transforming growth factor-β (TGF-β)

TGF-β is the archetypal member of the TGF-β superfamily that encompasses a large group of soluble extracellular peptides including TGF-β, activins, BMPs, inhibins and growth and differentiation factors (GDF). This family is recognised as playing big roles in mammalian development, homeostasis, differentiation, apoptosis, immune response, and extracellular matrix remodelling, depending on the physiological context. There are three isoforms of TGF-β found in mammals that are designated as TGF-β1, TGF-β2 and TGF-β3[156]. The TGF-β isoforms are located on chromosomes 19q13, 1q41 and 14q24 respectively, with their receptors, are ubiquitously expressed in normal tissues and most cell line[157].

1.3.1 The role of TGF-β1 in tubulointerstitial fibrosis

In the context of renal fibrosis, TGF-β is described as a central mediator of fibrosis, this occurs due to its role in inducing ECM production and proliferation of the myofibroblast, and also through its immune-regulatory function. It is recognised as the prototypical fibrogenic and hypertrophic cytokine and was first described as an inducer of EMT in normal mammary epithelial cells by signalling through receptor serine/ threonine kinase complexes[158]. It has been shown to stimulate ECM synthesis, decrease matrix degradation by inhibiting protease systems and promote cell-matrix interaction by upregulating integrins, all of which have been identified as crucial intermediary steps in the development of tubulointerstitial fibrosis in CKD. In diabetic mellitus, the chronic

hyperglycaemia leads to an alteration in vasoactive hormones production (primarily angiotensin II but also endothelin-1), formation of advanced glycation end-products (AGE), hemodynamic changes, and activation of various secondary metabolic pathways leading to oxidative stress, protein kinase C activation and increased polyol production[159]. All of which are ultimately associated with increased local TGF-β production and activity. Conversely, neutralizing anti-TGF-β antibodies ameliorate renal hypertrophy and the overexpression of matrix protein mRNA in diabetic animal models[160]. Antagonism of TGF-β using monoclonal antibodies virtually abolishes high glucose induced matrix production *in vitro*[161].

1.3.2 Latent and active TGF-β

All three isoforms of TGF-β are synthesized as large precursor proteins that are 390-412 amino acids in size that are modified intracellularly prior to secretion. The proteolysis yields two products that assemble into dimmers. The N-terminal pro-regions form a 65-74 kDa dimer, referred to as the latency-associated peptide (LAP), which contains a mannose 6-phosphate moiety, while the 25 kDa dimer from the C-terminal region is called the mature TGF-β or active TGF-β [78]. There are 3 cysteine groups in each TGF-β1-LAP in positions 33, 223 and 225, which are linked by disulfide bonds. When the cysteine groups in position 223 and 225 are replaced by a serine groups, active TGF-β1 is released. When TGF-β1-LAP is associated with another protein called the latency binding protein (LTBP), it is referred to as large L-TGF-β1. When unassociated with LTBP, it is known as small L-TGF-β1. Both large and small L-TGF-β1 cannot interact with their

receptors and therefore have no biological effects. Large L-TGF-β1 facilitates its sequestration within the extracellular matrix[162].

The regulation of TGF-β1 activity may occur at level of transcription and translation of TGF-β1. However, the most important regulator of TGF-β activity is determined by factors that convert latent to biologically active protein. Since TGF-β1 has been reported to have numerous biological effects, the regulation of TGF-β1 action is critical to both the maintenance of normal physiological function and the pathogenesis of numerous diseases. We have learned from animal studies that complete blocking of TGF-β1, by either a pan-neutralizing TGF-β1 antibody or a TGF-β receptor ablation antibody, results in severe cytotoxicity and unacceptable side effects, which are probably due to the role of TGF-β1 in maintaining cell survival and limiting inflammation[163, 164]. In addition to that, recent reports using transgenic mice overexpressing latent TGF-β1, were found to have substantially reduced fibrosis in both unilateral ureteric obstruction (UUO) and anti-GBM nephritis models of fibrosis[165, 166]. This highlights the complex activation of latent TGF-β1, which if dysregulated may play a more significant role in its pro-fibrogenic actions. Hence targeting the activation of latent to biologically active TGF-β1 may have therapeutic potential.

1.3.3 Activation of latent TGF-β1

The secretion and storage of TGF-β1 is a complex and restricted biological process. As already stated, one of the most important means of controlling the biological effects of TGF-β1 is the regulation of the conversion of LTGF-β1 to active TGF-β1 [167]. The release

of TGF-β1 from the latent complex permits TGF-β1 to be bound by its ubiquitously expressed cell surface tyrosine kinase type I and type II receptors that initiate its signalling cascade. *In vitro* activation of TGF-β1 can be achieved by extreme pH (such as 2 or 8), heat (100°C), chaotropic agents such as SDS and urea. Other known physiological activators include serine protease, plasmin, endoglycosidase F, sialidase, neuraminidase, cathepsins B and D, caplain, and thrombospondin-1[168-173]. The isoform most often described to be susceptible to the aforementioned *in vitro* activation, is TGF-β1. It is unclear which of the above agents can activate other isoforms of TGF-β.

1.3.3.1 Plasminogen/ plasmin proteolytic system

Antonelli-Orlidge *et al*[174], and Sato *et al.*[175] first described this physiological system of activation of L-TGF-β_1. Plasmin is a serine protease derived from enzymatic cleavage of plasminogen by urokinase plasminogen activator (uPA) or tissue-type plasminogen activator (tPA). Even though plasmin is better known for its role in fibrinolysis, it is also known for its role in cell migration and fibrosis[176]. In fibrosis, plasmin activates L-TGF-β1 by removing the LAP from the latent complex; and activates several proMMPs, which can modulate ECM deposition and degradation[177, 178]. tPA-mediated plasminogen activation is mainly involved in the dissolution of fibrin in the circulation. uPA activation requires binding to surface receptors known as urokinase plasminogen activator receptors (uPAR) resulting in enhanced activation of cell-bound plasminogen. Plasminogen activator-1 inhibitor (PAI-1) is the major inhibitor in this proteolytic activation system (Figure 1.3.3.1.1).

When exposed to angiotensin II, renal mesangial cells[179], proximal tubular cells (PTCs)[180] and aortic vascular smooth muscle cells[181], have been shown to have increased activation of L-TGF-β1 as well as increased in total TGF-β1 production. Release of active TGF-β1 by PTCs and mesangial cells occurs in an autocrine manner, leading to cellular hypertrophy and ECM synthesis[179, 180]. Furthermore, exposure to high concentrations of glucose[161], thromboxane[182], and cyclical stretching[183] have a similar induction and activation of TGF-β1 in renal cells. Studer *et al.* speculate that the mechanism of activation of L-TGF-β1 in these cells is through protein kinase C which induces tPA, leading to the generation of plasmin and subsequent activation of TGF-β1[184].

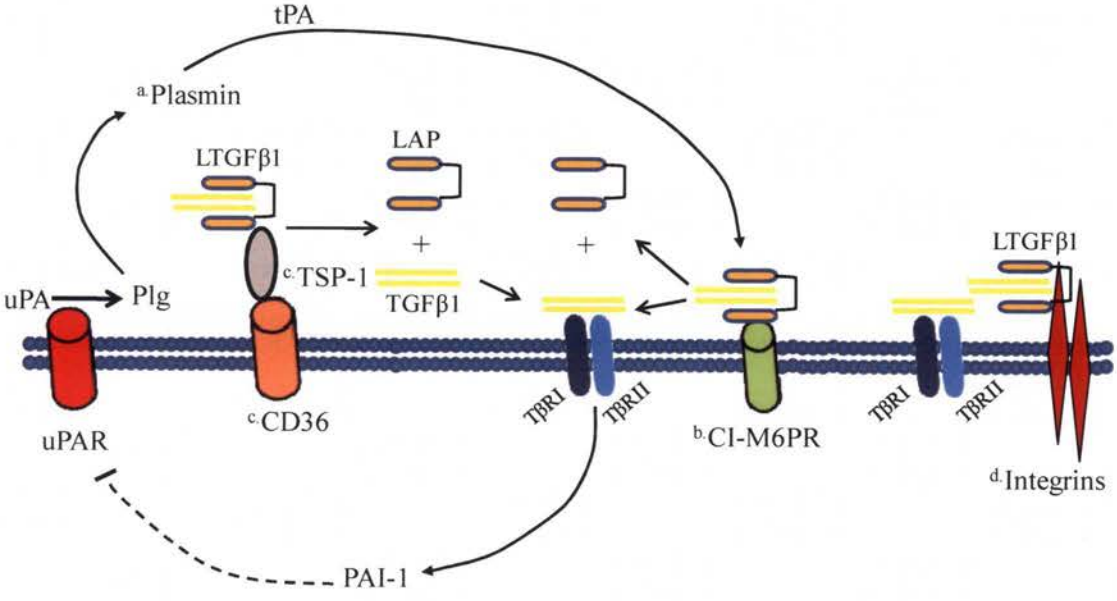

Figure 1.3.3.1.1 Mechanisms of activation of L-TGFβ1.

Plasminogen/ plasmin proteolytic activation (a). Plasmin is released from plasminogen (Plg) by the enzymatic action of urokinase plasminogen activator (uPA) or tissue-type plasminogen activator (tPA). uPA couples with urokinase plasminogen receptor (uPAR) which is present on the cell surface. L-TGF-β1 can either bind with Cation independent

mannose-6-phosphate receptor (CI-M6PR) (b) or thrombospondin-1 (TSP-1) (c), which is associated with the TSP-1 receptor (CD36), to release the active TGF-β1. In addition, the direct association of L-TGF-β1 with integrins (d) on epithelial cells leads to a structural conformation of LAP such that TGF-β1 can interact with its adjacent receptors. TGF-β1 is a strong inducer of Plasminogen activator inhibitor (PAI-1) which inhibits uPAR expression thus preventing the uPA from activating plasminogen to complete a feedback loop.

1.3.3.2 Cationic mannose-6-phosphate receptors (CI-M6PR)

It is observed that the cell surface localization of L-TGF-β1 is important for activation. This is dependent on the interaction of the mannose-6-phosphtae (M6P) moieties on the LAP with M6P receptors (M6PRs), which are ubiquitously located on the cell surface. There are two mannose 6-phosphate (M6P) receptors – the 46kDa cation-dependent M6PR (CD-M6PR) and the ~300-kDa cation-independent M6PR (CI-M6PR)/ insulin-like growth factor-II (IGF-II) receptor. The CI-M6PR is a multifunctional receptor that mediates several processes that are essential for normal cellular function[185]. One such process which is shared with the CD-MPR, is the delivery of newly synthesized acid hydrolases from the trans-Golgi network to endosomes for their subsequent transfer to lysosomes. In addition, the CI-MPR has been implicated in several other physiological processes. Of relevance to the present thesis, it facilitates the activation of the latent precursor of TGF-β1. This direct interaction of L-TGF-β1 and CI-M6PR at the cell

membrane is thought to be a natural process of concentrating L-TGF-β1 to a limited surface area thus allowing a more efficient way of activation[167].

In addition to direct interaction with the L-TGF-β1, CI-M6PR also plays a role in another process involved in L-TGF-β1 activation, the plasminogen/ plasmin system and uPA. Using an elegant *in vitro* model, Godar *et al.* demonstrated that the full length of uPAR and plasminogen both interact with the N-terminus of repeat 1 of the CI-M6PR, which is situated on the opposite side of the carbohydrate-binding sites, suggesting a M6P independent activated process[186]. Thus it is possible that the CI-M6PR binds simultaneously to both uPAR/ plasminogen and a M6P-oligosaccharide[187]. Subsequent studies have proposed that such binding may modulate TGF-β_1 activation, cell surface uPAR expression, and uPAR-mediated functions on cell adhesion, fibrinolysis, migration and fibrosis [186, 188-190].

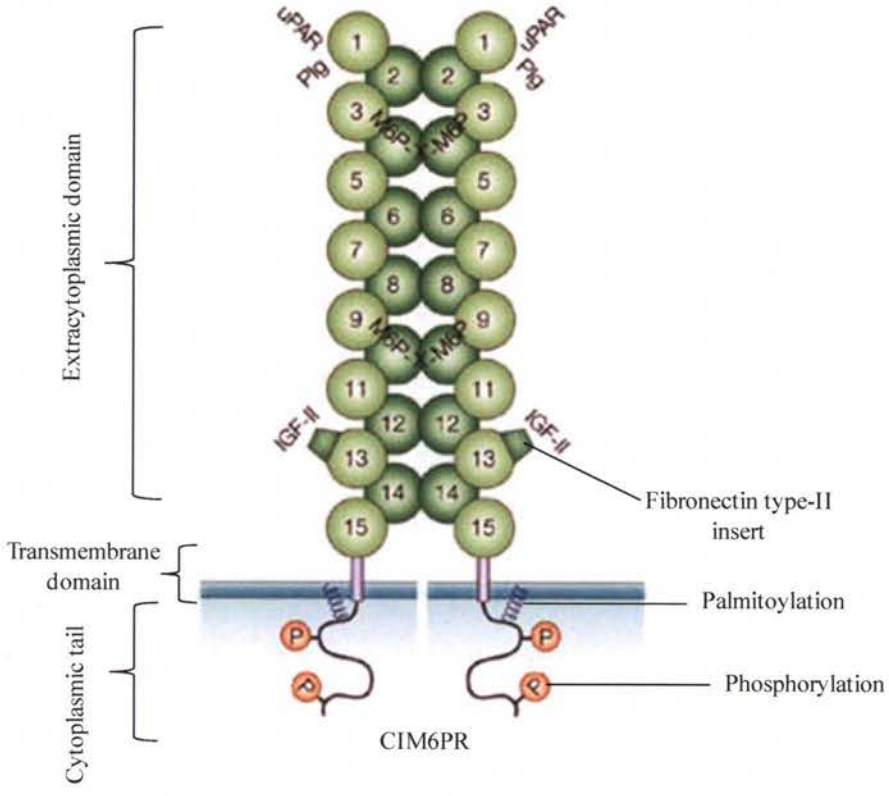

Modified from Ghosh et al. 2003 *Nature review/ Molecular cell biology*

Figure 1.3.3.2.1 Structure of cation-independent mannose-6-phosphate receptor.

CI-M6PR exists as dimers on the cells membrane. Receptor dimerization allows for high-affinity binding of ligands. The extracytoplasmic domain contains two distinct M6P-binding sites and a single IGF-II-binding site. The cytoplasmic tails contain numerous sorting signals, which are modified by phosphorylation or palmitoylation[185]*. Plg: plasminogen, uPAR: urokinase plasminogen activator receptors, IGF-II: insulin-like growth factor.*

1.3.3.2.1 Synthetic CI-M6PR analogues and their therapeutic potential

Over the years, analogues have been synthesized to target the CI-M6PR. Synthetic analogues must be isometric to M6P and need only to contain one single negative charge to allow stable and efficient binding, interestingly, the phosphorous atom is not necessary to ensure recognition[187]. Roche *et al.* have shown that association of antifibrotic agents with human serum albumin, which contain the M6P moiety, allow selective delivery to liver stellate cells. They showed that with this approach they can efficiently target these cells via the CI-M6PR and reduce the fibrotic response[191, 192]. Others have shown in animal models that these analogues can efficiently reduce the size of scars during the wound healing processes [193]and the improve the range of motion after tendon injury[194].

CI-M6PR analogues have been proposed to have therapeutic potential in enzyme replacement therapy in the treatment of lysosomal diseases by increasing the specificity and efficiency of enzyme delivery[195, 196]. In many solid tumours such as breast cancer, CI-M6PR is over-expressed. Therefore, the delivery of cytotoxic drugs via CI-M6PR is considered to more specifically target cytotoxic drugs to lysosomes[197, 198]. Other applications of CI-M6PR analogues, such as their role in L-TGF-β_1 activation, hence modifying wound healing and fibrotic process require further exploration. This competitive inhibition could also apply to other pathological processes, which is mediated through CI-M6PR interactions. Finally, the CI-M6PR analogues may also be used to target drugs or nano-particles to lysosomes to delivery of photo-sensitive, or pH sensitive drugs for imaging in cancers that express high levels of CI-M6PR.

1.3.3.3 Thrombospondin-1 (TSP-1) activation of L-TGF-β_1

Thrombospondin is a glycoprotein that exists in five isoforms, of which TSP-1 is the most extensively studied[199]. TSP-1 can be derived from platelets, endothelial cells, mesangial cells and fibroblasts. Recent studies have highlighted the ability of TSP-1 to activate L-TGF-β1 in human mesangial and PTCs after exposure to high concentrations of glucose[200, 201]. Murphy-Ulrich *et al.* has demonstrated that TSP-1 can interact with the L-TGF-β1 peptide directly[171]. Using a rat alveolar macrophage model, Yehualaeshet *et al.* showed that the TSP-1/L- TGF-β1 complex requires binding to the TSP receptor (CD36) on macrophages before cleavage by the plasmin (Figure 1.3.3.1.1)[202]. The exact role and mechanism by which TSP-1 activates L-TGF-β1 in other cells, as well as *in vivo*, remains controversial.

1.3.3.4 Activation of L-TGF-β1 by reactive oxygen species

Ionizing radiation generates a number of ROS and hydroxyl radicals. Ionizing radiation has been shown to activate recombinant human L-TGF-β1 to level comparable to that achieved by plasmin activation. It is proposed that these ROS affect the cysteine or methionine residues in the LAP, resulting in altered stability, changes in structural conformation and exposure of the TGF-β1 receptor binding sites[203]. Kidney tissues from rats fed with antioxidant deficient diet showed increased expression of TGF-β1 mRNA and Collagen I, III and IV, suggesting that ROS may play a role in TGF-β1 regulation and hence kidney fibrosis [204].

1.3.3.5 Integrin mediated activation of L-TGF-β1

Munger *et al.* first described the direct binding of L-TGF-β1 with integrins on epithelial cells. This interaction leads to conformational change in the L-TGF-β1, such that the mature TGF-β1 binds to the TGF-β1 receptor located in close proximity without releasing the LAP [205]. Hence, unlike other mechanisms of yielding biologically active TGF-β1, it is a non proteolytic activation mechanism. The integrins that have been reported to bind with L-TGF-β1 include αvβ6, αvβ1,αvβ8, αvβ3, and more weakly, αvβ5[206]. Recent evidence suggests that this binding plays an important role in maintaining polarity of kidney epithelial cells and the epithelial barrier[207].

1.3.4 Termination of the activation of TGF-β1

Plasminogen activator-1 inhibitor (PAI-1) is the major inhibitor of the plasminogen/ plasmin proteolytic activation system. PAI-1 achieves this through induction of internalization of PAI-1/uPAR/uPA complex which results in diminished generation of plasmin[208]. Interestingly, TGF-β1 is a potent inducer of PAI-1 suggesting that the activation of L-TGF-β1 is a self limiting rather than self perpetuating process[209] (Figure 1.3.3.1.1). PAI-1 expression is also upregulated by inflammatory cytokines (e.g. IL-6, TNF), angiotensin II and aldosterone suggestive of a negative feedback regulatory mechanism. Inactivation of TGF-β1 can also be achieved by removal of the stimuli such as pH change, restoration of hypoxia etc. It has been shown, active TGF-β1 can bind with specific proteins such as decorin[210], betaglycan[211], LAP or α2-macroglobulin[212] and becomes biologically inactive. Down regulation of the TGFβ receptors can also lead to

down regulation of the TGF-β1 activity which has been explored as a therapeutic potential in renal fibrosis [213].

1.3.5 Circulating TGF-β1 and relationship to CKD

Suthantiran and others have shown that African Americans with hypertension and ESKD have higher circulating levels of TGF-β1 as compared to the Caucasian population[214, 215]. The proposed explanation, in addition to the conventional genetic and lifestyle risk factors, includes difference in the bidirectional activities of TGF-β1 and the renin angiotensin system (RAS) in the induction of TGF-β1 activation[216-219]. Recently, a cross sectional study reported a positive association between the circulating TGF-β1 and a variety of established risk factors for CKD progression. Peripheral blood TGF-β1 protein levels positively correlated with plasma renin activity (PRA), systolic blood pressure, diastolic blood pressure, body mass index (BMI), and the presence of metabolic syndrome in African American but not in whites[220]. In the same study, these investigators reported TGF-β1 protein levels were predictive of microalbuminuria in African Americans when compared to the Caucasian population. However, importantly, recent multicenter cohort study demonstrated that most African Americans with CKD due to hypertension continued to progress despite being treated with RAS inhibitors[221]. Hence, further investigation into whether there is consistent association between circulating TGF-β1 and the various risk factors for CKD is required. Subsequently, the potential role of combining anti-TGF-β1 strategies and RAS inhibitors in CKD should also be explored.

The EURODIAB follow up study has demonstrated that circulating and urinary TGF-β1 correlates with proliferative retinopathy and nephropathy in type I DM[222]. In type II diabetes mellitus, circulating total TGF-β1 has been shown to be elevated as compared to the non-diabetic population[223]. Hellmich *et al.* has documented a higher level of circulating active TGF-β1 in those diabetic patients with nephropathy compared to those without nephropathy[224], which correlated with the urinary albumin excretion. However, the sample size of this study was too small to ascertain whether the circulating TGF-β1 could be used as a biomarker to predict patients at risk of diabetic nephropathy.

1.3.6 Signaling pathways in kidney fibrosis

In the setting of CKD, it is conceivable that three major TGF-β1 signalling pathways namely, TGF-β1/ Smad, integrins/ ILK, and Wnt/ β-catenin signalling are essential for kidney fibrosis. These pathways are intricately connected and integrated at different levels, and together they control a host of transcriptional regulators and signalling mediators that are required for renal fibrosis.

1.3.6.1 TGF-β/ Smad signaling

Given the universal upregulation of TGF-β1 expression in the fibrotic kidney, its signalling pathways are particularly relevant to the pathogenesis of kidney fibrosis. TGF-β1 membrane receptor complex comprises two families of proteins with serine/ threonine kinase activity, namely type II (TβRII) and type I (TβRI) receptors. TβRI includes activin

like kinase (ALK) receptors. Typically, TGF-β_1 first binds with TβRII, a 73-kDa serine threonine receptors that is constitutively phosphorylated. TβRII then recruits TβRI to form a tight complex, leading to phosphorylation and activation of a group of small protein known as small mothers against decapentaplegic (Smad) proteins. The Smad family include receptor Smad (R-Smad), common Smads (Co-Smads) and inhibitory Smads (I-Smads). The TGFβ/TβR complex phosphorylates R-Smad 2 and Smad 3. Phosphorylated Smads then heteroligomerize with the common partner Smad 4 (Co-Smad) and translocate into the nucleus, where they control the transcription of TGF-β-responsive genes through interaction with specific *cis*-acting elements in the regulatory regions[225, 226] (Figure 1.3.6.1.1). Of interest, many of the EMT related genes are the targets of TGF-β/ Smad signalling such as connective tissue growth factor (CTGF), ILF, PINCH-1, β1-integrin, Wnt, Snail, Id1, α-SMA, Collagen IA2 and MMP-2[227-230].

While the relative functional roles of Smad 2 and Smad 3 remain to be fully elucidated, recent studies using the unilateral ureteral obstruction (UUO) model in Smad 3 knockout mice, suggests that the majority of TGF-β target genes are controlled through Smad 3-dependent transcriptional regulation[231]. Consistent with this, primary tubular epithelial cells from Smad 3 null mice are resistant to EMT and kidney fibrosis[231, 232]. Targeting Smad 7 (I-Smad)[233, 234] and administration of the endogenous TGF-β inhibitors, HGF and BMP-7, which are considered to by modulate the Smad signalling, have been mechanistically linked to reduced renal fibrotic lesions[80, 235]. Several Smad-independent TGF-β signalling pathways have been implicated in the regulation of kidney fibrosis. These non-Smad pathways include RhoA[236, 237], p38 mitogen-activated protein kinase (MAPK)[238, 239] and phosphatidylinositol-3-kinase/Akt[240].

1.3.6.2 Integrin-linked kinases (ILK) signaling

ILK is an intracellular serine/ threonine protein kinase that interacts with the cytoplasmic domains of the β-integrins and mediates integrin signalling in diverse types of cells. ILK expression is found to be upregulated in a wide variety of CKD in experimental and clinical settings[241, 242]. Furthermore, ILK is identified as a key mediator of podocyte dysfunction and proteinuria in many proteinuric kidney diseases[243]. ILK can elicit its biological effect by functioning as a scaffolding protein which interacts with integrins and PINCH, or as a protein kinase which phosphorylates Akt or dephosphorylates GSK-3β, leading to stabilization of β-catenine[244]. This in turn controls the expression of an array of genes involved in EMT and inhibition of ILK attenuates renal interstitial fibrosis[245]. ILK expression is upregulated in a wide variety of CKDs[241, 242]. Interestingly, many component of the ILK signalling such as ILK, PINCH-1 and β1-integrin are induced simultaneously by TGF-β1 in a Smad dependent manner (Figure 1.3.6.1.1).

1.3.6.3 Wnt/β-catenin signaling

Wnt proteins belong to a highly conserved family of secreted growth factors that play an essential role in organogenesis, tissue homeostasis, and tumour formation[246]. Wnt proteins transmit their signal across the plasma membrane by interacting with the Frizzles receptor and the co-receptor LDL receptor-related protein-5/6. This induces a series of downstream signalling events resulting in dephosphorylation and stabilization of β-catenin. Accumulation of β-catenin in the cytoplasm leads to its nuclear translocation where it binds

to T-cells factor/lymphoid enhancer-binding factor-1 (LEF1) to stimulate the transcription of Wnt target genes such as Twist, Jagged1, Snail, LEF-1,c-myc and fibronectin[247] (Figure 1.3.6.1.1). The role of this pathway is well understood in organ development and tumour metastasis but is less well established in the setting of CKD[248]. Nonetheless, Wnt genes are induced in the fibrotic kidney after obstructive injury[249]. Consistent with that, inhibition of Wnt/β-catenin pathway ameliorates renal fibrosis after obstructive injury *in vivo*[250].

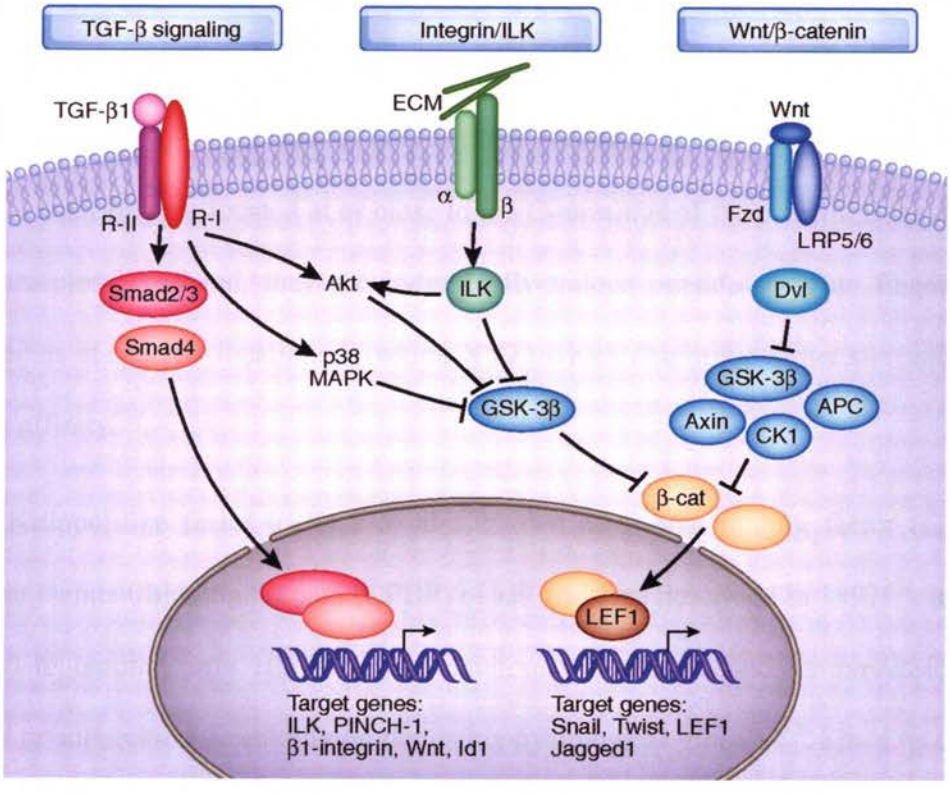

Figure 1.3.6.1.1 Simplified schematic shows major intracellular signalling involved in the regulation of EMT in kidney fibrosis [99].

Fzd: Frizzled receptors, LRP5/6: LDL-receptor-related protein 5/6, CK1: casein kinase-1, APC: adenomatosis polyposis coli, Dvl: Dishevelled, LEF1: lymphoid enhancer-binding factor-1

1.4 Krüppel-like factor family and Krüppel-like factor-6

Krüppel-like transcription factors (KLFs) are a 17 member family of DNA binding transcriptional regulators that play diverse roles during differentiation and development- with each functioning as an activator of transcription, a repressor or both. They form a subset of the broad class of proteins containing zinc fingers and are so named because of their homology to the *Drosophila melanogaster* protein, Krüppel. The zinc finger contains a single zinc atom, which serves as a critical structure of the finger motif. The KLFs contain 3 such fingers, located at or close to the C-terminus of the protein. Even though the KLFs are closely related, they are individually unique outside the zinc fingers, with 3 amino acids at specific locations (position XYZ) which determine target site selection and binding affinity[251].

Krüppel-like factor-6 (KLF-6) also known as G-box binding factor (GBF), core promoter element-binding domain (CPBP) or zf9 was first described in 1997[252]. It was then assigned to chromosome 10p15. It is ubiquitously expressed and its expression can be induced or suppressed depending on the pathophysiological process[253]. Since its discovery, KLF-6 has been recognized to play a significant role in embryogenesis, carcinogenesis,

inflammation and fibrosis. Its embryological expression is restricted to the excretory system such as Wolffian duct and the ureteric bud, and is thought to play a role in development and differentiation of the collecting duct systems[254]. While most commonly described in terms of its role as a tumour suppressor gene[255-258], KLF-6 has also been shown to act as an immediate-early gene *in vivo* models of hepatic fibrosis[259]. Of the growing list of target genes directly or indirectly regulated by KLF-6 include collagen α1[260], leucotriene C3 synthase[261], uPA[262], TGF-β1 and TβRI and TβRII[259] and the E-cadherin promoter[263].

1.4.1 KLF-6 and kidney fibrosis

Even though KLF-6 mRNA is known to be expressed in the embryonic kidney, its expression in the mature adult kidney is minimal. Recently, KLF-6 has been identified as one of the genes whose expression is markedly upregulated (>10 fold) within the first few hours of renal ischemia-reperfusion injury in mice, with the expression of TGF-β1 mRNA and protein following a pattern similar to that of KLF-6 both *in vivo* and *in vitro*[264]. Our laboratory has demonstrated marked induction of renal proximal tubular KLF-6 expression in STZ-induced diabetic Ren-2 rats as early as 8 weeks. Upregulation of KLF-6 mRNA was also seen in renal proximal tubular cells (HK-2) exposed to high glucose (30 mM) condition for 11 days. The induction of KLF-6 mRNA parallels the induction of TGF-β1 mRNA by high glucose. Using silencing techniques, induction of KLF-6 by high glucose is confirmed to be mediated through TGF-β1. Cells overexpressing KLF-6 have lower E-cadherin and higher vimentin suggestive of a role in EMT, which is not seen in KLF-6

silenced cells[265]. We have recently confirmed that KLF-6 can bind to the promoter regions of thioredoxin-interacting protein (Txnip), which is a critical regulator of cellular glucose homeostasis[266]. Txnip is markedly induced in mesangial cells and proximal tubular cells exposed to high glucose, resulting in ECM accumulation. KLF-6 silenced cells attenuated high glucose induced Txnip. Collectively, these observations suggest that KLF-6 may play a key role in the development of diabetic nephropathy.

1.5 Bone morphogenetic proteins

Bone morphogenetic proteins (BMPs), also known as osteogenic proteins (OPs), are secreted signalling molecules that belong to the TGF-β-superfamily of growth factors. The first BMPs were originally identified by their ability to induce ectopic bone formation when implanted under the skin of rodents[267]. Since then more than 30 BMPs have been identified. It has become rapidly evident that their pattern of expression, as well as their physiological functions, are not restricted to skeletal development but include cell proliferation, cell differentiation apoptosis and organogenesis[268]. In 2002 the FDA approved the clinical use of two products containing rhBMP-2 and rhBMP-7 in spinal fusion and in the non-unions of long bones. In a recent review, Reddi proposed the re-naming of BMPs as 'body morphogenetic proteins', due to their extensive role in various tissues and organs beyond that of bone[269].

BMPs, as all members of the TGF-β-superfamily, are homo or heterodimer linked by disulphide bridges[270]. These large precursor polypeptide chains contain a long hydrophobic, poorly conserved N-terminal pro-region sequence and a mature domain with

a highly conserved C-terminal region. The N-terminal not only varies among the different BMPs it controls the stability of the processed mature protein[271]. Enzymatic proteolytic cleavage gives rise to form mature proteins. BMPs are biologically active in homodimer and heterodimer conformation. Crystallographic studies reported that BMP-2,-7[270],-9 and -14 have a similar polypeptide core to that of TGF-β[272, 273]. The differences in the hydrophobic core amongst these BMPs are responsible for the different affinities to the various receptors and possibly for its different physiological roles[274].

1.5.1 BMP members and their function

Table 1.5.1.1 BMP members and their functions

BMP	Nomenclature	Ch. Location	Main physiological functions
Bone morphogenetic proteins			
BMP-1		8p21	Not a BMP member but a metalloproteinase involves in cartilage development[275]
BMP-2	BMP-2a	20p.12	Cartilage, bone and heart morphogenesis[276, 277]
BMP-3	Osteogenin	4pq14-q21	Lung and kidney development[278]. Negative regulator for bone morphogenesis[279]
BMP-3b	GDF-10	10q11.2	Negative regulator for bone morphogenesis[279]
BMP-4	BMP-2b	14q22-q23	Cartilage, bone and kidney morphogenesis[280-282]
BMP-5	-	6q12.1	Limb development and bone morphogenesis[283, 284]
BMP-6	Vrg1, Dvr6	6p24-p23	Hypertrophy of cartilage and oestrogen mediated bone morphogenesis[285, 286]
BMP-7	OP-1	20q13	Cartilage and bone morphogenesis and kidney formation[287-290]
BMP-8a	OP-2	1p34.3	Bone morphogenesis and spermatogenesis
BMP-9	GDF-2	10q11.22	Bone morphogenesis, cholinergic neuron development and glucose metabolism[276, 291]
BMP-11	GDF-11	12q13.2	Axial skeleton, eyes, kidney and pancreas development[292-294]
Cartilage-derived morphogenetic proteins			
BMP-12	CDMP-3GDF-7	2p24.1	Ligament, tendon and sensory neuron development[295, 296]
BMP-13	CDMP-2, GDF-6	8q22.1	Cartilage development and hypertrophy[295]
BMP-14	CDMP-1, GDF-5	20q11.2	Chondrogenesis and angiogenesis[297, 298]
Others			
BMP-8b	OP-3	1p35-p32	Spermatogenesis[299]
BMP-10	-	2p13.3	Heart morphogenesis[300]
BMP-15	GDF-9b	xp11.2	Ovary physiology[301]
BMP-16	Nodal		Embryonic development
BMP-17	Lefty		Embryonic development
BMP-18	Lefty		Embryonic development

Summary of BMP members in humans with their acceptable abbreviation, other nomenclature, chromosomal location and their main physiological functions. BMPs currently approved for clinical use are underlined

1.5.2 Bone morphogenetic protein-7 (BMP-7)

BMP-7, also known as osteogenic protein-1 (OP-1) is one of the many currently known BMPs. It is of particular interest to the nephrology community not only because of its role in kidney development, but also due to the recent evidence suggesting that BMP-7 has a critical role in cell growth regulation, cell differentiation, chemotaxis and apoptosis in various cell types, especially kidney epithelial cells[302]. BMP-7 is highly conserved and shared 98% amino acid homology between human and mice. It is synthesized as a large precursor and cleaved by proteolytic reaction to release mature biological active BMP-7, which is a glycosylated disulphide-linked homodimeric protein of 36kDa[303]. BMP-7 is widely expressed in developing tissues and is important for the normal morphogenesis of kidney, eye, bone and limbs. In the adult, its expression is limited to kidney, cartilage and bone. In adult kidney, BMP-7 is expressed in the epithelial cells of distal tubules, collecting ducts and podocytes[302]. Bioavailability studies using radioactive labelled I125-BMP-7 shows that exogenous administration of rhBMP-7 has a half life of about 30 minutes, and that radioactive labelled BMP-7 is predominantly found in the kidney cortex and medulla shortly after intravenous administration[304].

1.5.3 BMP receptors

There are three BMP type I receptors (BMPR-IA/ activin receptor-like kinase-3(ALK-3), BMPR-IB/ ALK-6 and ALK-2) and three BMP type II receptors (BMPR-II, activin type IIA receptor and activin type IIB receptor)[305]. At embryonic day 12.5 to 14.5 of mouse kidney development, BMPR-IA, -IB and BMPRII are expressed in the tips and

body of the branching ureter and comma shaped body. However, only BMP type I receptors but not type II receptors are expressed in the body of ureteric bud until embryonic day 17.5[306]. This observation suggests that BMPs regulate epithelial-mesenchymal interaction and ureteric branching by differential receptor expression during kidney morphogenesis.

The distribution of type I receptors within the adult kidney itself varies. High affinity BMP-7 type I receptors ALK-2 and BMPR-IA but not BMPR-IB are expressed in human podocytes and mesangial cells. However, all type I receptors are found in kidney tubules [307]. It is suggested that these cells are capable of responding to BMP-7 in a paracrine-like manner[308]. The affinity of BMPs for type II receptors is much weaker than for the type I receptors, and the different BMPs bind to these receptors with different affinities. For example, BMP-4 preferentially binds BMPR-IA and -IB. BMP-7 binds BMPR-IA with a higher affinity than BMPRI-IB [309]. A mutation in the GS domain of the BMPR-IA/ ALK-3 can lead to constitutive activation of the receptor, and such an activated receptor mimics the effects of the entire receptor-ligand complex in the absence of BMP-7 and the type II receptor [80, 310]. These findings suggest the specificity of intracellular signals is mainly determined by type I BMP receptors[311].

1.5.4 BMP-7 signalling

Receptors are able to bind ligands independently, but the heterodimerisation of the type I and type II receptor chains is required for signalling. BMP-7 binds to the low affinity type II receptors and the type I receptors are activated by the transphosphorylation of the

glycine-serine (GS)-rich domain of these receptors, which leads to phosphorylation of cytosolic Smad proteins[312]. Smad 1, Smad 5 and Smad 8 are the known R-Smad involved in BMP-7 signalling. Activated R-Smad forms a complex with Smad 4 (Co-Smad), which is translocated into the nucleus and modulates gene transcription with other transcriptional factors (Figure 1.5.4.1). BMP-activated Smads bind preferentially to the transcriptional factors with a GCCGnCGC sequence and only weakly to AGAC or GTCT gene sequences, which are bound by TGF-β- or activin-activated Smads[313]. Some of these transcriptional factors are Runx, osteorix, Id proteins, Hoxc-8, MyoD, SIP1 amongst others. Smad 6, the inhibitory Smad which preferentially inhibits BMP signalling acts by preventing the activation of type I receptors upon binding to its ligands and also by preventing the formation of R-Smads with Smad 4[314, 315]. BMP-7 signalling is also modulated by Smad ubiquitin regulatory factors (Smurfs) which induce the ubiquitination and degradation of Smads thus controlling the signallings of BMPs[315]. Even though the BMP-7 and TGF-β1 signalling are known to be distinctly unique in their signalling pathways, it is interesting to note that Smurfs can enhance the responsiveness to Smad 2, which mediates TGF-β1 signalling. Hence Smurfs have an opposite effect to that of the BMPs[316].

It has been reported that MAPK pathways can modulate BMP/Smad signalling. Observations in *Xenopus* show that activation of MAPK pathways promotes the termination of Smad-mediated BMP signalling[317]. This is achieved by interaction with the MH1 and MH2 domains in the Smads. The MH1 domain is involved in DNA binding and the MH2 domain in binding to cytoplasmic retention factors, activated receptors, nucleoporin and DNA-binding cofactors, coactivators and corepressors in the nucleus. Recently, Motazed *et al.* have reported an inverse relationship of BMP-7 concentration

with p38/MAPK stimulation in human PTCs. The group demonstrated that a low concentration (7.5 ng/ml) of rhBMP-7 induces p38/MAPK signalling but a high concentration of rhBMP-7 stimulated Smad 1 dependent signalling in association with inhibition of p38/MAPK. The net effect of a high concentration of rhBMP-7 accounts for its antifibrotic properties [318].

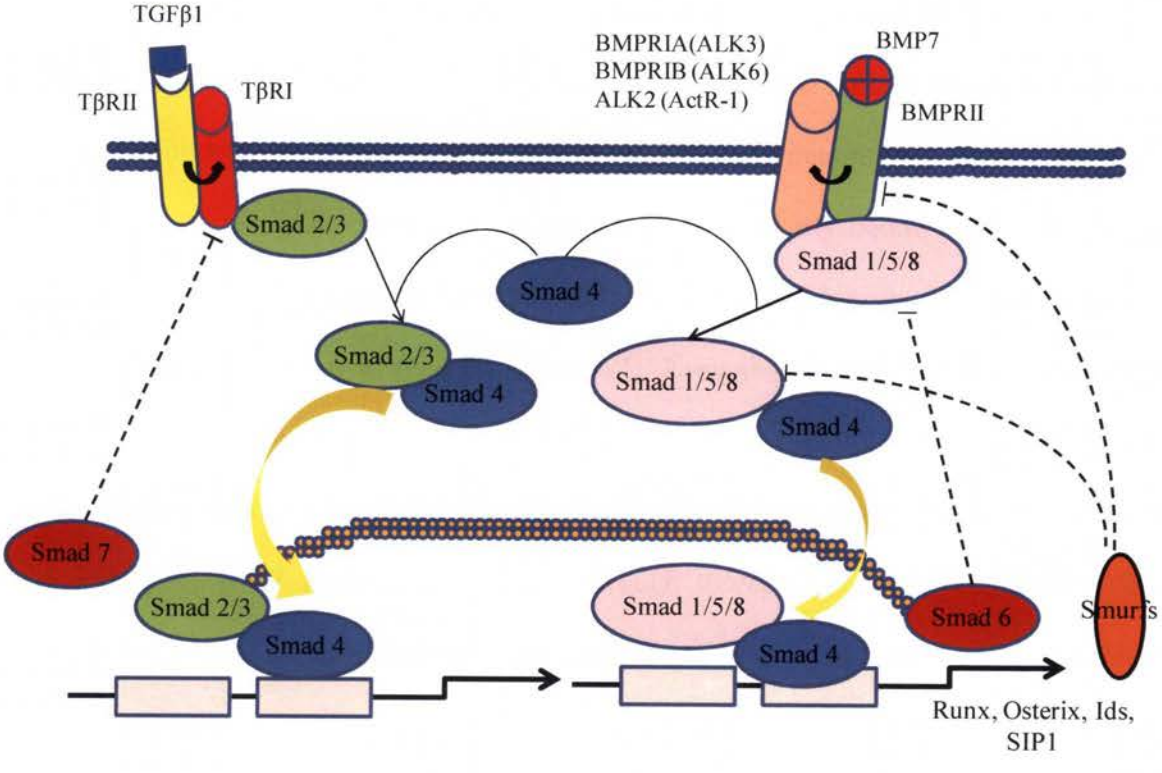

Figure 1.5.4.1 Schematic representation of BMP-7 and TGF-β1 signalling pathways.

1.5.5 Regulation of BMP-7 in the kidney

The biological activity of BMP-7 appears to be controlled by at least three different mechanisms namely, A) Local BMP-7 concentration and its receptors, B) Binding of BMP-7 to extracellular matrix, and C) Agonist and antagonists. Studies which utilized I^{125}-labeled BMP-7 have suggested that the BMPRII is constitutively expressed on PTCs, whilst expression of the type I BMP receptors may be regulated in disease states[319]. Zeisberg *et al.*, using models which overexpressed BMPR-IA/ ALK-3 receptors in murine PTCs, demonstrated a regulatory role of BMP receptors in determining BMP-7 activity[80]. BMP-7 is secreted as a complex of homodimer non-covalently bound with a pro-peptide chain which has high affinity to fibrillin-1 in the kidney[320]. Vukicevis *et al.* has previously shown that BMP-7 binds to type IV collagen[321]. Even though little is known about how BMP-7 is mobilized from the ECM and how the pro-peptide is cleaved, several extracellular molecules have been identified acting as agonists or antagonists to BMP-7 in the kidney[322]. BMP antagonists function through direct association with BMPs, thus prohibiting the BMPs from binding to their cognate receptors. Such extracellular inhibitors include noggin, Gremlin, vertebrate chordin, CRIM1, DAN/Cerebrus and uterine sensitization-associated gene-1 (USAG-1) [323]. The expression of Gremlin in adult kidney is almost undetectable in the healthy state, but its expression increases in many CKD models, including diabetic nephropathy, UUO and cisplatin induced nephropathy. In these models, BMP-7 expression is markedly suppressed. In contrast, BMP-7 activity is enhanced by increased binding to the receptor of an extracellular protein, kielin/chordin-like protein (KCP) [324] . Overall, the relevance of an altered presence of BMP receptors, the agonists

and antagonists which are involved in the regulation of BMP-7 in PTCs is not entirely clear.

Studies by Lund *et al.* suggested that decreased BMP-7 levels directly correlate with a loss of viable renal mass[325]. This implies quantification of circulating BMP-7 and its protein expression may serve as a biomarker for CKD. However, this may have limited value due to the complexity of BMP-7 regulation and the lack of a sensitive assay. With the availability of more reliable assays for BMP-7, the possibility of measuring circulating BMP-7 as a biomarker for CKD is likely to be further explored.

1.5.6 BMP-7 and kidney development

BMP-7 deficient homozygous mice die soon after birth due to dysplastic kidneys which appear arrested in development[326]. BMP-7 is detected in the ureteric bud as it emerges from the Wolffian duct at 11 days post-conception (dpc) and its expression is maintained in this region throughout the development[327]. Its presence is crucial after 14.5 dpc in metanephric mesenchymal condensation, branching and differentiation of the ureteric epithelial structures. Mutant mice kidneys show massive apoptosis with undifferentiated mesenchymal cells, suggesting that BMP-7 is important for cell proliferation, differentiation and survival[328]. Furthermore, in concert with fibroblast growth factor-2 (FGF-2), BMP-7 acts as a survival factor to promote differentiation of the stromal progenitor cells adjacent metanephric mesenchyme (which will give rise to glomeruli and most parts of the tubular apparatus), through a process known as mesenchymal-epithelial transition (MET). It is thought that BMP-7 is expressed by the undifferentiated stromal

cells and exerts its action in an autocrine manner[321]. Even though it is challenging to delineate specific functions of other BMPs which also have a role in kidney development, namely BMP-2[329], BMP-4[330] and BMP-5[331], various studies have established that BMP-7 is one of the most important mediator of the morphogenesis of the ureteric buds[332].

1.5.7 BMP-7 and kidney fibrosis

Distal tubular BMP-7 expression decreases in several acute and chronic kidney disease models and pre-emptive administration of exogenous BMP-7 can ameliorate injury in models of ischemic nephropathy, UUO, lupus nephritis, nephrotoxic serum nephritis and diabetic nephropathy [333]. Its protective role has also been confirmed in various cell types including PTCs [80], podocytes [334], mesangial cells [335], fibroblasts [336] and endothelial cells [337]. The proposed protective mechanisms in proximal tubule cells include direct inhibition of TGF-β1 production, decrease of pro-inflammatory genes and chemoattractants, and epigenetic regulation [338, 339] . A summary of the *in vivo* and *in vitro* evidence of the protective value of recombinant human BMP-7 (rhBMP-7) in a number of acute and chronic kidney injury models, are listed in Table 1.5.7.1.

Table 1.5.7.1 **Summary of published therapeutic effects of BMP-7 in renal diseases**

Model/ Cells	**Stimulated Human conditions**	**Time of BMP-7 administration**	**BMP-7 dosage**	**Effects of BMP-7**
Ischemic-reperfusion (rat) [304]	ATN	At the time of insult	250μg/kg	↓injury, ↑ regeneration
Unilateral urethral obstruction (UUO) (rat)[340]	Obstructive uropathy	Pre-procedure	300μg/kg	↓ tubular atrophy & interstitial fibrosis
MRL $^{lpr/lpr}$ (mouse)[341]	Lupus nephritis	Early disease state	300μg/kg	↓ tubular atrophy & interstitial fibrosis
COL4A3$^{-/-}$ (mouse)[341]	Alport's syndrome	Early disease state	300μg/kg	↓ tubular atrophy & interstitial fibrosis
Nephrotoxic nephritis (mouse)[336]	Acute anti-GBM GN	3 weeks post induction	300μg/kg	Regression of tubulointerstitial injury
STZ-induced DM (rat)[342]	Diabetic nephropathy	16 weeks of onset of DM	300μg /kg	Reverses kidney hypertrophy, improved glomerular lesion & GFR
STZ- induced DM in human BMP7 transgenic mice[343]	Diabetic nephropathy		300-500μg /kg	Id-1, ↓PAI-1, ↓fibrogenesis, preserves podocyte number, ↓albuminuria
Human Mesangial cells[335]	IgA nephropathy	1 hour pre-incubation	250 ng/ml	↓TNFα, IL-6, TGFβ1, NF-κB, -Smad 6 & Smad 7
Human PTCs[308]	Basal & TNF-α stimulated conditions	24 hours treatment	100 ng/ml	↓ pro-inflammatory cytokines
Podocytes (mouse)[334]	High glucose	Concurrent exposure for 7 days	300 ng/ml	Preserves synapotopodin and podocin expression

TGF-β1 induces EMT in renal tubular epithelium and disrupts the tubular polarity. Conversely, BMP-7 has been reported to limit these consequences of TGF-β as demonstrated by re-induction of E-cadherin, a key epithelial cell adhesion molecule[80]. It has been shown in murine mesangial cells that BMP-7 can reduce TGF-β1-induced ECM production such as type IV collagen, and elaboration of profibrotic cytokines like TSP-1 and connective tissue growth factor (CTGF)[344]. BMP-7 maintains the level and activity of MMP-2 and prevents TGF-β1 dependent upregulation of PAI-1. In addition, BMP-7 reduces the nuclear accumulation of Smad 3 and blocks the transcriptional upregulation of the TGF-β1/ Smad 3 target, CAGA-lux, in mesangial cells. Recent evidence suggests that BMP-7 induces the inhibitory I-Smads, Smad 6 and Smad 7 in both PTCs and mesangial cells[335, 345]. Smad 7 interferes with the TGF-β1signalling through inhibition of the phosphorylation of Smad 2/3 whereas Smad 6 suppresses the transcriptional activity of glucocorticoid and mineralocorticoid receptors via its C-terminal MH2 domains by attracting histone deacetylase-3[346]. Smad 7 also limits Smad 1/5/8 phosphorylation, hence completing the negative feedback loop of BMP-7 signalling. Immunohistochemistry has also suggested upregulation of nuclear Smad 1 in tubular epithelium suggestive that BMP-7 counteracts TGF-β1 action through direct antagonism involving the Smad pathways[80]. Moreover, BMP-7 represses basal and TNF-α stimulated expression of proinflammatory cytokines in PTCs, which includes IL-6, IL-1β, IL-8, MCP-1, and the vasoconstrictor endothelin-2 (ET-2)[308]. *In vivo* BMP-7 also represses the expression of pro-inflammatory genes and thus reduces the recruitment of macrophages and other inflammatory cells[304]. Emerging pre-clinical evidence suggests that exogenous administration of rhBMP-7 can at

least partially resolve the glomerular and interstitial injury in experimental diabetic nephropathy[342, 343].

However, the antifibrotic effects of BMP-7 were at best modest in a rat protein-overloaded model in the absence of significant tubular epithelial cell apoptosis and EMT[347]. In most published studies using animal models, exogenous administration of BMP-7 was given either "pre-insult" or at an early time point in the establishment of pathology. There is emerging evidence to suggest its ability to reverse TGF-β1 induced EMT in established human kidney disease is limited. Dudas *et al.* have recently shown that BMP-7 fails to attenuate TGF-β1 induced EMT in two different human proximal tubular cell lines[348]. Therefore the antifibrotic value of BMP-7 in human kidney disease remains controversial.

1.6 Nuclear hormone receptors

Nuclear hormone receptors are transcription factors comprised of four main functional domains: the N-terminal transcriptional activation domains, which contain the activation function (AF1) domains, the action of which is independent of presence of ligands; the DNA-binding domains which binds the receptor's target genes; the ligand-binding domains; and the C-terminal, ligand-dependent activation function (AFs) domains, which are located in the carboxyl terminus of the ligand binding domains and modulates receptor activity in response to the interaction with receptor agonist[349]. Some of the nuclear receptors known to be involved in the pathogenesis of renal disease include vitamin D receptor (VDR), peroxisome-proliferator associated receptors (PPARs), farnesoid X

receptor (FXR) and hepatocyte nuclear factor 4α (HNF4α). Nuclear receptors are well known for their involvement in various metabolic processes such as glucose and lipid metabolism, inflammation, oxidative stress and fibrosis[350]. Nuclear hormone receptors regulate their physiological effects by controlling the transcription of a myriad of genes through diverse mechanisms; for examples, nuclear hormone receptors can regulates their own expression level. The function of nuclear hormone receptors is regulated by ligand activity and level, by the action of coregulatory proteins, as well as by post-translational modification[351, 352].

A total of 48 human and 49 mouse genes that encode nuclear receptors have been identified [353, 354]. The first nuclear hormone receptors were discovered in an effort to define the mechanism of action of vitamin A, vitamin D, thyroid hormone, steroidal glucocorticoids, mineralocorticoid hormones and sex hormones. Estrogen receptors and VDRs have promising effects in the context of diabetic nephropathy. A number of 'orphan receptors' were subsequently discovered, which were nuclear hormone receptors for which physiological function and identity of activating ligands were unknown. Some of these receptors were found to have physiologic ligands derived from dietary lipid and metabolites, such as bile salts, fatty acids and eicosanoids. These receptors are now called 'adopted orphan receptors', and of these the PPARs and FXR have been shown to have a major role in the prevention of diabetic nephropathy [32, 33]. Nuclear hormone receptors are well established targets for small molecule modulators therefore, both biomedical and pharmaceutical researchers have strived to develop synthetic ligands that selectively modify nuclear hormone receptors function. The approach is currently under investigation

as a strategy for the treatment of endocrine and metabolic disease, such as diabetic nephropathy [34].

1.6.1 Farnesoid X receptors

FXR which is better known as the bile acid receptor has recently being associated with metabolic syndrome and kidney fibrosis[355]. FXR is also known as NR1H4, is an adopted orphan nuclear receptor named after farnesol, an intermediate in the mevalonate biosynthetic pathway which was found to weakly activate FXR at supraphysiological concentrations [356, 357]. It is located in Chromosome 12q23.3. FXR was first discovered to have a critical role in regulation of bile acid metabolism. Chenodeoxycholic acid (CDCA) and its conjugated forms, which are hydrophobic, are the most potent endogenous ligands of FXR, whereas the hydrophilic bile acids ursodeoxycholic acid (UDCA) and muricholic acid do not activate this receptor[358-360]. The main physiological role of FXR is to function as a bile acid sensor in enterohepatic tissues. FXR activation regulates the expression of various transport proteins and biosynthetic enzymes crucial to the physiological maintenance of cholesterol and bile acid homeostasis. In addition, activation of FXR lowers plasma triglycerides and glucose levels through a mechanism that involves both the repression of key regulatory genes in the liver and the modulation of insulin sensitivity in peripheral tissues, including kidneys. With the availability of FXR-deficient mice, increasing evidence suggests that FXR agonists do not just play an important role in bile acid, cholesterol, triglycerides and glucose metabolism but have been shown to have a role in liver regeneration[361], tumorigenesis[362, 363], and to possess antifibrotic and anti-

inflammatory properties. Because of this, FXR has been described as a multipurpose nuclear receptor[364], a metabolic regulator and a cell protector[355]. Currently potent synthetic FXR agonists that have been identified include GW4064, 6-ehtylchenodeoxycholic acids (6-ECDCAs) and fexaramine.

FXR is highly expressed in the liver, intestine, adrenal gland and kidney, but with lower expression in fat and heart [365]. There are two FXR genes, FXRα (NR1H4) and FXRβ (NR1H5) in mammals. FXRβ is a lanosterol sensor that encodes a functional protein in rodents, rabbits, and dogs but is a pseudogene in human[366]. A single FXRα gene encodes four isoforms which are expressed in a tissue-dependent manner [367]. FXRα1 and α2 are predominantly found in ileum and adrenal gland, whereas α3 and are abundantly expressed in ileum and kidney but also found at low levels in stomach duodenum and jejunum (Table 1.6.1.1).

FXR shares the common modular structure of all members of the metabolic-nuclear receptor superfamily, which includes a highly DNA-binding domain in the N-terminal region and a moderately conserved ligand binding domain in the C-terminal region. The ligand-independent activation function-1 (AF-1) and ligand dependent activation function-2 (AF-2) are located in N-terminal and C-terminal regions, respectively. Activation of FXR has an important role in maintaining glucose, lipid, and bile acid homeostasis in the enterohepatic system [368, 369]. The diseases have been linked with FXR are cholestasis, diabetes mellitus, atherosclerosis, cholesterol gall stone disease, liver regeneration and inflammation, and liver, breast and colonic cancer[355].

Table 1.6.1.1 **Summary of FXR related information**

Gene	NR1H4 (FXR)
Expression	Liver Small intestine Kidney Adrenals Vascular smooth muscle Adipose tissue Breast cancer
Natural agonists	**Primary bile acid:** CA, CDCA **Secondary bile acid:** LCA, DCA **Polyunsaturated fatty acids:** arachidonic acid; docosahexaenoic acid, and linolenic acid **Bile acid metabolites:** 26- or 25-hydroxylated bile alcohols **Oxysterols:** oxysterol 22(R)-hydroxysholesterol **Androsterone** (very weak activity) **The order of potency of these ligands:** 26- or 25-hydroxylated bile alcohols=CDCA>LCA=DCA>CA
Synthetic agonists	GW4064 (high-affinity agonist), 6ECDCA (semisynthetic bile acid), AGN29, AGN31 **The potency of these ligands:** GW4064 and 6ECDCA are more potent than the bile acids AGN29 and AGN31 are FXR-selective ligands and 25-fold more potent than naturally occurring ligands
Antagonists	Guggulsterone, lithocholate, AGN34
Response elements	**IR-1:** GAGTTAaTGACCT GGGTGAaTAACCT GGGACAtTGATCCT AGGTCAaGTGCCT GGGTCAgTGACCC **DR-1:** AGAGCAnAGGGGA **ER-8:** TGAACTcttaaccaAGTTCA **Monomer binding site:** GATCCTTGAACTCT TGAACT

CDCA: chenodeoxycholic acid, DCA: Deoxycholic acid, LCA: Lithocholic acid, CA: Cholic acid

Wang et al. 2008 Cell Research[355]

1.6.2 FXR and its target genes

FXR regulates the expression of a wide variety of target genes by binding either as a monomer or as heterodimer with its obligate partner, 9-cis-retinoic acid receptor (RXR), to the FXR response elements (FXREs). Typical FXREs consist of an inverted repeat of AGGTCA[370]. FXR regulates human intestinal bile acid binding protein (IBABP), small heterodimer partner (SHP)[371], bile salt export pump (BSEP), Bile acid-CoA: amino acid N-acetyltransferase (BAT) and phospholipid transfer protein (PLTP), with varied affinities[372]. By binding to the FXREs, FXR alters the expression of groups of genes involved in bile acid homeostasis. FXR activates SHP, which in turn inhibits cholesterol 7α-hydroxylase (CYP7A1) expression, hence repress bile acid synthesis[373]. However, the significance of this process in organs other than liver and intestines remains unclear.

Studies of FXR knock-out animals have shown that FXR regulates genes that participate in lipoprotein and triglyceride metabolism. These include genes for phospholipid transfer proteins (PLTP), the very low density lipoprotein receptor (VLDL-R) and apolipoprotein C-II and apolipoprotein E[374, 375]. In addition, activation of FXR leads to repression of the sterol regulatory element-binding protein-1c (SREBP-1c), a transcription factor which plays a crucial role in fatty acid and triglyceride synthesis[376]. The close intrinsic interaction between lipid and glucose metabolism is through FXR regulation on phosphoenolpyruvate carboxykinase (PEPCK), which is key enzymes in the catalytic pathway of hepatic gluconeogenesis[377].

Upon ligand binding, FXR undergoes conformational changes to release corepressors such as nuclear corepressors and recruit coactivators such as steroid receptors

coactivator-1 (SRC-1), protein arginine (R) methyl transferase-1 (PRMT-1), coactivator-associated arginine(R) methyltrasnferase-1 (CARM-1), peroxisome-proliferator-receptors (PPAR)-γ coactivator-1α (PGC-1α) and vitamin-D-receptor-interacting protein-205 (DRIP-205)[355]. The mechanism and relevance of regulation by these coactivators by FXR ligands is still unknown.

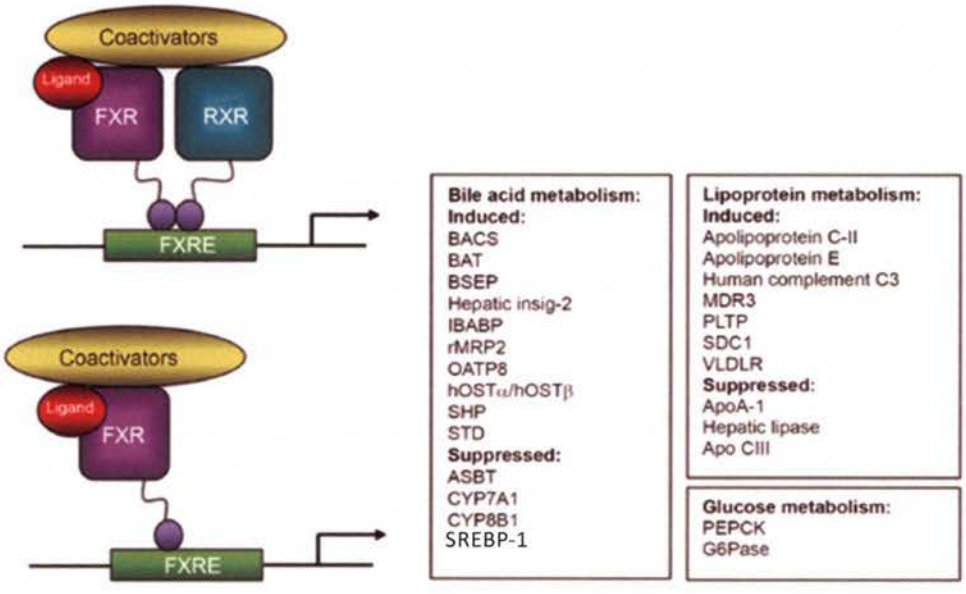

Figure 1.6.2.1 Ligand binding of FXR and targets genes regulated by FXR.

FXR regulates a large number of target genes involved in bile acid, lipoprotein and glucose metabolisms. FXR binds to DNA either as a heterodimer with RXR or as a monomer to regulate the expression of various genes[355]

1.6.3 Role of FXR in kidney fibrosis

The antifibrotic role of FXR agonist was first demonstrated in a model of hepatic fibrosis. Fiorucci *et al.* has demonstrated that FXR activation prevents rat liver fibrosis induced with porcine serum or bile duct ligation [378] and atherosclerosis in *Ldlr*-knockout mice and *ApoE*-knockout mice [379, 380]. In mouse kidney, FXR expressed in both isolated glomeruli and proximal tubules. The expression levels of FXR in the proximal tubule cells are approximately 5 times more than that of the glomeruli[33]. FXR was also found to be expressed in both cultured mouse mesangial cells and podocytes [33]. Levi's group have also demonstrated a protective role of FXR activation in the kidney of db/db mice with type 2 diabetes and in DBA/2J mice fed with a 'western diet' as a model of diet-induced obesity and insulin resistance[381]. These experimental models of disease showed improvements in proteinuria, glomerulosclerosis, tubulointerstitial fibrosis and macrophages infiltration with FXR activation. It is postulated that the renoprotective effects are mediated by effects on lipid metabolism, oxidative stress, and on the production of proinflammatory cytokines and profibrotic cytokines. In addition, deletion of the gene that encodes FXR in mice with STZ-induced type I diabetes which leads to increased renal injury compared with wild-type mC57BL/6 mice with STZ-induced type I diabetes. The evidence suggests that modulation of FXR could be a promising therapeutic avenue for treatment of diabetic nephropathy.

The first synthetic FXR agonist is GW4064, which is a high affinity non-steroidal agent that has been tested in rodent studies and *in vitro* cell cultures [368, 369]. However, the poor bioavailability of GW4064 has limited its clinical development. The high affinity, semi synthetic, bile acid derived FXR agonist, INT 747 (6α-ethyl-chenodeoxycholic acid) was subsequently developed and has exhibited anticholestatic and antifibrotic properties in

rodent model of liver disease. A clinical trial is in progress to examine the physiological effect of FXR activation by INT 747 in humans with non-alcoholic fatty liver disease.

1.6.4 Sterol regulatory element-binding proteins (SREBPs)

Sterol regulatory element-binding proteins (SREBPs) are members of the basic helix-loop-helix leucine zipper family of transcription factors. SREBPs are synthesized as 2,150-amino acid precursor proteins that remain bound to the endoplasmic reticulum. Upon sterol deprivation, the precursor protein undergoes a sequential two-step cleavage process to release the NH2-terminal portion. This NH2-terminal, mature segment then enters the nucleus and activates the transcription of genes involved in cholesterol and fatty acid synthesis by binding to sterol regulatory elements or to the E-boxes within their promoter region[382]. Currently, there are three isoforms of SREBPs namely SREBP-1a, SREBP-1c and SREBP-2. SREBP-1a and SREBP-1c are derived from a single gene. SREBP-1a is the more common isoforms found in cultured cells and is a stronger activator of transcription than SREBP-1c. SREBP-2, which derived from a different gene and is known to be involved in the transcription of cholesterogenic enzymes. All cultured cells exclusively express SREBP-2 and the -1a isoforms, whereas most organs including the liver, express predominantly SREBP-2 and -1c isoforms of SREBP-1[383].

SREBP-1 is involved in transcriptional regulation of lipid and cholesterol synthesis. Genes regulated by SREBPs include the low density lipoprotein receptors, 3-hydroxy-3-methylglutaryl-CoA synthase, acetyl-CoA carboxylase, fatty acid synthase (FAS), stearoyl-CoA desaturase-1 and -2 (SCD), ATP citrate lyase (ACL), S14, and glycerol-3-phosphate

acyltransferase. Activation of FXR suppresses SREBP-1 expression through an indirect mechanism. The potential involvement of SREBP-1 in kidney disease has been described in transgenic mice overexpressing SREBP-1a, and in diet-induced or obesity-related diabetic mice[384, 385]. Overexpression of renal SREBP-1a resulted in triglycerides accumulation associated with increased expression of profibrotic factors (TGF-β1, PAI-1, vascular endothelial growth factor (VEGF)), enhanced mesangial expansion, increased ECM accumulation and proteinuria[386]. In contrast, SREBP-1c knock-out prevented high fat diet induced lipid-induced nephropathy[387]. Recently, PEPCK-promoter transgenic mice which overexpressed nuclear SREBP-1c, exhibited characteristic histological findings that mimic diabetic nephropathy, despite the absence of hyperglycemia or hyperlipidemia, suggesting that SREBP-1c activation in the kidney could contribute to the emergence or progression of diabetic nephropathy[388]. However, the exact role of SREBP-1 in renal fibrosis remains unclear.

1.6.5 Interaction of FXR and PPARγ nuclear receptors

Other nuclear receptors known to be involved in the pathogenesis of CKD, particularly diabetic nephropathy, are VDR, PPARα, PPARγ, PPARδ, Liver X receptors (LXR) and estrogen-related receptors (ERR)[350]. Of these, PPARs have been most widely reported to have a complex interaction with FXR in fibrosis.

FXR ligands used in a hepatic fibrosis model can induce PPARγ in transdifferentiated hepatic stellate cells and effectively inhibit αSMA and collagen Iα synthesis, and TGF-β1. The antifibrotic effect is potentiated by the addition of

rosiglitazone, a potent PPARγ agonist, suggesting a synergistic effect of these two nuclear receptors[389]. Mencarelli *et al.* using ApoE$^{-/-}$ mice fed with high fat diets discovered that a synthetic FXR agonist reduced the extent of atherosclerotic plaque in a dose-dependent manner. This protective effect was comparable to that exerted by rosiglitazone. The expression of FXR and SHP in the aorta of ApoE$^{-/-}$ mice is endogenously upregulated. On the contrary, PPARγ expression is markedly suppressed in this animal model. The pathogenic relevance in this model is unclear, but the group has shown that FXR ablation in this model increases the tendency towards development of severe atherosclerotic disease[390]. This evidence suggests that FXR and PPARγ both have an independent yet interdependent relationship, in protection against atherosclerotic plaque formation. In another study, peroxisome proliferator-activated receptor-γ coactivator 1α (PGC-1α) was found to regulate triglyceride metabolism through a FXR-dependent pathway by increasing FXR mRNA and its target genes, via coactivation of PPARγ and HNF4α[391]. More recently, diverse PPARγ agonists have been shown to have a differential modulatory effect on FXR. Troglitazone, but not rosiglitazone or pioglitazone can potently antagonize bile acid-mediated activation of FXR and affect its downstream target genes[392]. This suggests that the relationship of FXR and PPAR family is much more complex and may involve both conventional and unconventional signalling pathways. The mechanistic interaction of these nuclear receptors in the pathogenesis of human kidney disease remains largely unclear. Therefore, the synergistic effects of FXR and PPARγ ligands on CKD remain an important area of investigation.

1.7 The aims of this thesis

Despite of all the beneficial interventions implemented in patients with CKD, such as blood pressure control, blockade of the renin-angiotensin-aldosterone system and tight glycaemic control in the case of patients with diabetes mellitus, functional decline occurs in most patients with CKD. Additional treatment modalities that target novel pathogenetic pathways involved in CKD are urgently needed to slow its progression.

The central aim of this thesis is to dissect the mechanisms involved in CKD and to explore the therapeutic potential of available agents in models mimicking CKD and/or diabetic nephropathy. The therapeutic agents studied in this thesis include rhBMP-7, PXS-25, a CI-M6PR inhibitor and GW4064, a selective FXR agonist.

By using HK-2 cells, the antifibrotic properties of BMP-7 is first confirmed either by using exogenous administration of rhBMP-7 or overexpression studies. The specificity of intracellular signalling of BMP-7 is mainly determined via type I BMP receptor signalling. Our group has previously demonstrated a parallel transcriptional induction of KLF-6 in PTCs exposed to TGF-β1. Hence the interaction between TGF-β1, KLF-6, BMP-7 and its receptors, and their roles and interrelationships in the development of EMT is studied.

One of the most important means of controlling the biological effects of TGF-β1 is the regulation of its activation. Hyperglycaemic and/or hypoxic conditions are the dual environments of the diabetic milieu, which are known to induce tubulointerstitial fibrosis. By using a selective CI-M6PR inhibitor, PXS25, we aimed to address the therapeutic potential of this agent by using an *in vitro* model of proximal tubular cell line cultured in

either or both of these conditions. Unlike TGF-β1 neutralizing antibodies and other non-selective inhibitors of TGF-β1, PXS25 is a selective CI-M6PR inhibitor which prevents the CI-M6PR-mediated $TGF\beta_1$ activation but still allows active $TGF\beta_1$ formation via CI-M6PR independent pathways.

Studies in humans with type I and type II diabetes mellitus and in diabetic animal models have reported an accumulation of lipids in the kidney, even in the absence of abnormalities in serum lipid levels, which is correlated with the development of tubulointerstitial fibrosis. Nuclear receptors are known to regulate lipid and glucose metabolism in kidney cells. Using GW4064 and PPARγ agonists, we aim to study the effect of high glucose on FXR expression, FXR regulation of ECM accumulation and inflammation, and to compare the effects of PPARγ and FXR agonists in human tubular cells.

Finally, we explore the potential of circulating TGF-β1 and BMP-7 as biomarkers for progression of diabetic nephropathy. The Action in Diabetes and Vascular Disease: Preterax and Diamicron Modified Release Controlled Evaluation (ADVANCE) Collaborative Group study, is a factorial randomised, double blinded controlled trial conducted at 215 collaborating centres in 20 countries from Asia, Australasian, Europe, and North America, involving 11,140 patients with type 2 diabetes, assigned to either standard glucose control or intensive controlled arms (HbA1C <6.5%). Primary end points were composites of major macrovascular events (death from cardiovascular causes, nonfatal myocardial infarction, or nonfatal stroke) and major microvascular events (new or worsening nephropathy or retinopathy), with a median follow up period of 5 years. The study was reported in 2008, and concluded that intensive glucose control, yielded a 10%

relative reduction in the combined outcome of major macrovascular and microvascular events, primarily as a consequence of a 21% relative reduction in nephropathy.

With appropriate ethics approval, we were provided with the opportunity to utilize the serum samples collected at the study entry point from ADVANCE study, who develop a renal endpoint (defined as doubling of serum creatinine to at least 200umol/l, need for renal replacement therapy, or death due to renal disease). We studied the circulating profibrotic and anti-fibrotic cytokines of 64 patients who have a major renal outcome, using an appropriate number of patients who did not develope adverse outcome as the control. Firstly, we aim to assess the baseline circulating value of TGFβ-1 and BMP-7 in people with Type II diabetes mellitus. Secondly, to assess whether baseline circulating levels of TGF-β1, BMP-7 and their ratio are related to the risk of progressive diabetic nephropathy and whether any relationships identified are independent of other baseline clinical parameters.

CHAPTER 2: Materials and methods

2.1 *In vitro* Model

2.1.1 Human kidney-2 (HK-2) cells

Human kidney-2 cells (HK-2) cells from American Type Cell Collection (ATCC, USA) were used as the primary model for studies undertaken in this thesis. First described in 1994, they are derived from a primary proximal tubules cell (PTC) culture from normal adult human renal cortex exposed to a recombinant retrovirus containing the human papillomavirus (HPV16). E6/E7 genes resulted in a cell line which has grown continuously in serum free media for more than a year. The E6/E7 genes of HPV are able to immortalise different types of epithelial cells without significantly altering the functional characteristics of the cells [393, 394]. HK-2 cell growth is epidermal growth factor (EGF) dependent and the cells retain a phenotype indicative of well-differentiated PTCs (positive for alkaline phosphatase, gamma glutamyl transpeptidase, leucine aminopeptidase, acid phosphatase, cytokeratin, $\alpha 3\beta 1$ integrin, and fibronectin; negative for factor VIII-related antigen, 6.19 antigen and CALLA endopeptidase) [395]. Furthermore, HK-2 cells retain functional characteristics of proximal tubular epithelium (Na^+ dependent/ phlorizin sensitive sugar transport; adenylate cyclase responsiveness to parathyroid, but not to antidiuretic hormone). The cell line is well-differentiated on the basis of its histochemical, immune cytochemical and functional characteristics, and it can reproduce experimental results obtained from freshly isolated PTCs. It has been used extensively in *in vitro* experimentation [265, 396, 397].

2.1.2 Cell culture conditions

HK-2 cells were grown in keratinocyte-serum free medium (KSFM) (Invitrogen, USA) supplemented with 5ng/ml recombinant epidermal growth factor (EGF) (Gibco, NY, USA) and 0.05ng/ml bovine pituitary extract on 10cm petri dishes (BS Biosciences, USA). Cells were incubated at 37°C, in a humidified 5% CO_2 and 95% air. Medium was refreshed every 48-72 hours until confluent. Trypsin-EDTA solution containing 0.25% (w/v) trypsin (Invitrogen, USA) was used to mobilise cells from their petri dishes. Cells were then centrifuged at 2000 rpm and subsequently washed three times in KSFM to remove trypsin-EDTA. Cells were either resuspended in KSFM for immediate experimental use or frozen and stored in liquid nitrogen.

2.1.3 Hypoxic cell culture conditions

Cells were grown in 6 well dishes (Sarstedt, Germany) at 37°C, 5% CO_2 and 95% air until they reached ~70-80% confluence. Once the cells were ready, they were transferred to the hypoxic chamber (Coy Laboratory Inc, USA) with conditions set at 37°C, 5% CO_2 and 1% O_2, and incubated overnight 24 hours prior to the treatment while the medium was equilibrated to hypoxia (1% O_2). Concurrently with the hypoxic condition experiment, similar passage cells cultured in normal oxygen concentration (normoxic) as previously described were used as a control. Cells were collected in the same manner for both hypoxic and normoxic treated conditions.

2.1.4 Primary culture of human proximal tubular cells (PTCs)

Using previously well described methods, segments of macroscopically and histologically normal renal cortex were obtained under aseptic conditions from patients undergoing nephrectomy for small (<6cm) tumours [398, 399]. Patients with known renal disease or systemic disease affecting tubulointerstitial pathology were excluded from the study. Written informed consent was obtained from each patient prior to surgery, and ethics approval for the study was obtained from the Royal North Shore Hospital (RNSH) Research Ethics Committee.

The kidney cortex was dissected from the medulla. Part of the cortex was kept for immunohistochemistry, and the remaining cortex was finely minced using a razor blade on ice. The minced tissue was washed twice in PBS and then digested by 1mg/ml collagenase (383 IU/mg from Worthington, USA) for 15 min at 37°C. The digested mixture was then passed through a μm mesh. Collagenase was removed by washing the filtrate three times in PBS. The filtrate was resuspended in 50ml of 45% Percoll (Pharmacia, Uppsala, Sweden) and centrifuged at 20,000 rpm at 4°C for 30min. The lowermost tissue band containing highly purified PTCs was carefully removed and washed. The PTCs were washed separately three times in phosphate buffered saline (PBS). The fragments of PTC pellets were resuspended in serum-free hormonally defined media consisting of 1:1 (vol/vol) Dulbecco's modified Eagle's media (Trace, Australia) supplemented with 10ng/ml (1.64nM) epidermal growth factor, 5mg/ml human transferrin, 5mg/ml (0.87mM) bovine insulin, 0.05mM hydrocortisone, 50mM prostaglandin E1, 50nM selenium and 5pM tri-iodothyronine (all from Sigma Aldrich, USA). Medium was changed every three days until the cells became confluent. Passage 2 cells were used for all experiments. The

ultrastructure, growth and immunohistochemistry of PTCs have been well characterized in the laboratory and shown to reproducibly reflect the biology and physiology of their in vivo counterparts [400, 401].

2.2 *In vivo* model

2.2.1 Diabetic transgenic (mRen-2)27 rat

(mRen-2)27 diabetic rat is a well established model of diabetic nephropathy. These rats developed severe renal impairment and histologic injury, resembling human diabetic nephropathy. In the transgenic (mRen-2)27 rat, the mouse *Ren-2 gene* is inserted into the genome of a Sprangue-Dawley rat such that over-expression of renin occurs at sites of normal physiological expression. This model displays hypertension and develops progressive nephropathy with the induction of STZ diabetes, displaying an amplified tissue renin angiotensin system (RAS) which is likely responsible for the classic glomerular and tubulointerstitial changes [402]. This progressive renal disease is partially prevented by ACE inhibitor treatment [403] . These diabetic animals have elevated tissue TGF-β1, rendering them an appropriate model for our study [404]. Female rats were chosen because of their reduced likelihood of developing malignant hypertension, which can also cause pathological changes in the kidney.

Eight-week-old female, homozygous (mRen-2)27 rats (St. Vincent's hospital Animal House, Melbourne, VIC, Australia)weighing 170 ± 20gm were randomised to receive either 55mg/kg of streptozotocin (STZ) (Sigma, St Louis, MO, USA) diluted in 0.1M citrate buffer pH 4.5 or citrate buffer only (control non-diabetic animals) by tail vein

injection following using an AMES glucometer (Bayer Diagnostics, Melbourne, VIC, Australia) and only the STZ-treated animals with blood glucose >20mmol/L were considered diabetic. Every 4 weeks, systolic blood pressure was determined in pre-heated conscious rats via tail-cuff plethysmography using a non-invasive blood pressure controller and Powerlab (AD instrument, NSW, Australia). All animals were housed in a stable environment maintained at 22 ± 1°C with a 12 hours light and dark cycle commencing at 6 am, and allowed free access to tap water and standard rat chow containing 0.25% Na^+ and 0.76K^+ (GR2; Clark-King & Co., Gladesville, NSW, Australia). Diabetic rats received twice weekly injections of insulin (2 to 4units intraperitoneally; Humulin NPH, Eli Lilly and Co., Indianapolis, USA) to reduce mortality and to promote weight gain. Experimental procedures adhered to the guidelines of the National Health and Medical Research Council of Australia's Code for the Care and Use of Animals for Scientific Purposes, and were approved by the Bioethics Committee of the University of Melbourne.

Rats were anaesthetised (Nembutal 60mg/kg body weight i.p. Boehringer-Ingelheim, Australia) at week 16, and the abdominal aorta cannulated with an 18G needle. Perfusion-exsanguination commenced at systolic blood pressure 180-220 mmHg via the abdominal aorta with 0.1M PBS, pH 7.4 (20-50mls) to renal circulating blood, and the inferior vena cava adjacent to the renal vein was simultaneously severed, allowing free flow of the perfusate. After clearance of circulating blood, 4% paraformaldehyde in 0.1< phosphate buffer, pH 7.4 was perfused for a further 5 min (100-200mls of fixative). Kidneys were then excised, decapsulated, sliced transversely, immersed in 4% paraformaldehyde in 0.1M phosphate buffer for overnight fixation and then paraffin-embedded for subsequent light microscopic evaluation.

2.2.2 Human kidney biopsy specimens

Paraffin-embedded tissue blocks from biopsies of renal biopsy specimens with diabetic glomerulosclerosis were randomly retrieved from the files of the Department of Pathology, RNSH between Jan 2007 to December 2009. Each patient was contacted and verbal informed consent was obtained. Diabetic changes were confirmed by light microscopy on examination by a RNSH pathologist, and only established diabetic nephropathy specimens were selected for our study. Patients' characteristics and biochemistry were retrospectively traced from the laboratory computer systems or medical records. Controls consisted of histologically normal kidneys obtained with informed consent from patients undergoing nephrectomy for small (<6 cm) kidney tumours. Ethics approval for the study was obtained from the RNSH Human Research Ethics Committee. The kidney cortex (with the tumour removed) was fixed overnight in 10% neutral buffered formalin (Fronine, Taren Point, NSW, Australia) at 4°C followed by embedding in paraffin for subsequent light microscopic evaluation.

2.3 Immunohistochemistry

2.3.1 Tissue preparation and immunohistochemical staining

For immunohistochemistry staining, four micron sections paraffin section were placed into xylene to remove the paraffin wax, and rehydrated in graded ethanol. Antigen retrieval was performed by incubation in a citrate buffer bath, pH 6, for 20mins at boiling

temperature. Slides were then left to cool at room temperature before being washed with excessive running distilled water, marked and then washed once with 0.01% tween in 0.1mol/L PBS, pH 7.4. Endogenous peroxidase was removed by incubation with 3% hydrogen peroxide for 5 minutes. After one wash with wash buffer, slides were blocked with serum free blocking solution (Dako cytochemistry, USA). Sections were then incubated in primary antibody with PBS/ antibody diluents (Dako Cytochemistry, USA) either overnight at 4°C, or for 1 hour at room temperature. Sections were thoroughly washed with wash buffer (2x 5 minute) before incubation with equal volume of Envision dual linked system (EDL) (Dako Cytochemistry, USA) for 30 minutes. Following rinsing with PBS (2x5 minute), localisation of the peroxidase conjugates was achieved by using diaminobenzidine tetrahydrocholoride (DAB) as a chromogen for 10 minutes. Sections were rinsed in tap water for 5 minutes to stop the reaction and then counterstained in Mayer's haematoxylin followed by washing with tap water, then dehydrated with grade ethanol, cleared and mounted in Dako glycerol mounting medium (Dako, USA). Slides were blinded, and analysed using the Olympus digital microscope (Olympus, Tokyo, Japan).

To confirm the specificity of the antibody stained, Genecard system was first used to check the tissue or organ in which the protein of interest is most abundantly expressed. Initial screening of proteins of interest was performed using normal atlas biopsy core specimens generously provided by Ms Sanaz Maleki and Dr. Kerrie McDonald from the Cancer Genetics Group of the Kolling Institute of Medical Research. These biopsy specimens included normal tissue from kidney, liver, brain, breast, ovary, uterus, placental, prostate, tonsil, colon, parotid gland, testis, muscle and pancreas. Screening was initially

performed using various dilutions of primary antibody. Sections were also incubated with comparable dilution of non-specific IgG or with the primary antibody omitted to serve as positive and negative controls.

2.3.2 Semiquantitative morphometry analysis

Two methodologies were used to semiquantify histological changes. The first method involves categorising histological changes from 0 to 3. By visually examining several non-overlapping areas at 200x magnificent with special stains (periodic acid-Schiff (PAS) or Masson's trichrome stains), each area was graded as follows: 0 = normal; 1= 1 to 25% pathological lesion; 2= 26 to 50% pathological lesion and 3 > 50% pathological lesions. The sum of the total score divided by the number of non-overlapping field studied was used as the final score. This method was used for glomerulosclerosis and tubulointerstitial scores. The second methodology involved the use of the automated cellular imaging system (ACIS III) (Dako, USA). Slides were loaded into a microscope scanner connected to the ACIS III computer, which captured and saved a high resolution composite image of each section in its entirety. Each glomerulus was marked carefully using a hands-free mode, and the volume of each glomerulus was calculated and expressed as μm^2 (Figure 2.3.2.1). Thresholds for brown (e.g. pink color in PAS staining, Figure 2.3.2.2a) or blue (nuclear staining, Figure 2.3.2.2b) were predetermined, and these colour threshold settings was applied to all images to ensure consistency. The software can isolate the predetermined colour threshold and express this area in μm^2. Using a simple calculation, the percentage of the area of predetermined colour over the volume of glomeruli can be easily determined. This method was used to determine glomerular volume (GV), mesangial sclerosis per glomerular volume (Mes/G) and the volume of mesangial

cells per glomerular volume (MC/G). All the analysis was scored by at least two blinded assessors.

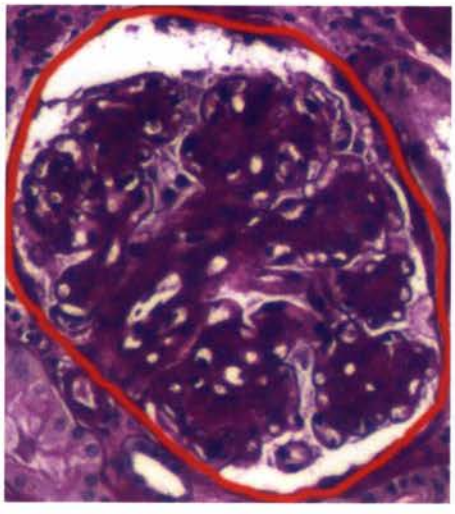

Figure 2.3.2.1 Semiquantitation of glomerular volume.

Using freehand mode, the outline of a glomerulus is traced and using the software ACIS III version 3.2.2, the area of each glomerulus can be calculated and expressed in μm^2.

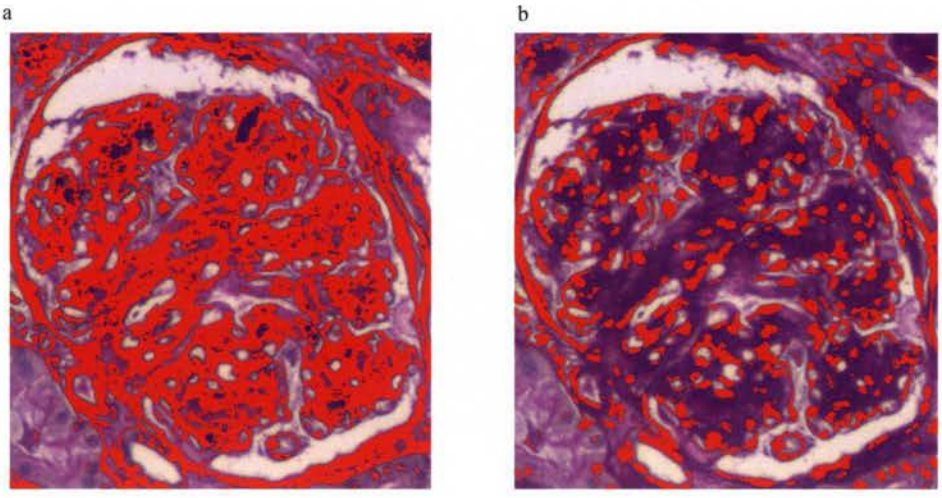

Figure 2.3.2.2 Determination of colour threshold for mesangial sclerosis and nuclei.

ACIS III allows predetermination of the colour threshold on scanned high resolution composite image of each section. A threshold for brown (i.e. pink colour in PAS staining) representing the mesangial sclerosis area or blue (representing the cells nuclei) were predetermined and these colour threshold settings. This is an operator-dependent area; however, the predetermined setting is applied to all images to ensure consistency. Since all special staining was performed in the same batch and with the same setting, variability is expected to be minimal. By using a simple calculation, mesangial sclerosis/ glomerular area (Mes/Glom) and Mesangial cells/ glomerular area (MC/Glom) can be estimated.

2.4 Immunofluorescence (IF)

Immunofluorescence was performed in paraffin embedded kidney sections and cultured cells.

2.4.1 Paraffin embedded tissue sections

Four micron paraffin kidney sections using similar antigen retrieval techniques described as above (2.3.1). Specific primary antibody in appropriate dilution was incubated overnight at 4°C followed by the secondary anti-rabbit Alexa Fluor® 488 antibody in its appropriate dilution three washes. Slides were then counterstained with 4',6-diamidino-2-phenylindole (DAPI) (Invitrogen, CA, USA) and were visualised using the Olympus immunofluorescence microscope (Olympus, Tokyo, Japan) or a Confocal microscope (Leica Microsystem, CA, USA).

2.4.2 Cells

HK-2 cells were cultured on glass coverslips to 70-80% confluence and experimental conditions were applied accordingly. Conditioned medium was discarded and cells fixed with 4% paraformaldehyde after three washes with ice-cold PBS. The cell membranes were permeabilised with ice-cold methanol for 10 minutes, followed by incubation with the primary antibody for one hour. Secondary anti-rabbit Alexa Fluor® 488 antibody in its appropriate dilution (Invitrogen, USA) was applied after three washes, counterstained with DAPI, mounted on glass slides and visualised using Olympus

immunofluorescence microscope (Olympus, Japan) or Confocal microscope (Leica Microsystem, CA, USA).

2.5 Western blotting

2.5.1 Cell lysates preparation

Standard Western immunoblotting was performed to detect the presence and change in levels of expression of specific proteins. Cells were collected and the cell pellet resuspended in cell lysis buffer containing 50mM Tris-HCl, 150mM NaCl, 5mM EDTA (pH 7.4), 1% Triton-X100 and protease inhibitor (Roche Diagnostic, Mannheim, Germany). Just before use, 1mM Dithiothreitol (DTT), 1mM sodium orthovanadate, 10μg/ml Leupeptin, 10μg/ml Aprotinin and 1mM Phenylmethylsulphonyl Fluoride (PMSF) was added fresh. Cells were lysed in ice cold cell lysis buffer for 45 minutes. If the nuclear fraction was required, samples were sonicated (Sonics Vibracell, CT, USA) on ice for 5 minutes (2.5s alternating with 1.5s break) to release the nuclear proteins. The lysate was again centrifuged at 12,000 rpm, 4°C for 10min. The pellet was discarded and the supernatant collected was used for protein analysis. The extracted protein was stored at -80°C for future use.

2.5.2 Protein assay and SDS-PAGE

Total protein concentrations were determined using the Bio-Rad SmartSpec ™ 3000 (Bio-Rad, CA, USA). Depending on the protein molecular weight, 7.5% or 10% Tris

glycine sodium dodecyl sulphate polyacrylamide gel (SDS-PAGE) gels were used (H_2O, 30% acrylamide, 1.5M Tris pH 8.8, 10% SDS, 10% ammonium persulfate (APS) and tetramethylethylenediamine (TEMED)) for protein electrophoresis. As polymerisation occurred almost instantly, these chemicals were added at the terminal phases of experimentation. The resolving solution was poured into an assembled Bio-Rad gel apparatus and a layer of isopropanol was poured on top to prevent oxygen from entering the setting gel, which inhibits polymerisation. Once the gel set, the isopropanol was removed and a stacking gel, (30% acrylamide, 1.0M Tris pH 6.8, 10% APS and TEMED) was poured onto the top of the set resolving gel, with a gel comb inserted.

For reducing conditions, 50-70µg of total cell protein was mixed with 6x denaturing buffer containing 0.35M Tris pH 6.8, 10% SDS, 30% glycerol, 0.175mM Bromophenol Blue and 6% (v/v) β-mercaptoethanol, and was then heated at 95°C for 10 minutes before electrophoresis. This linearised the proteins and exposed the site for primary antibody binding. The protein samples were then loaded onto the gel and electrophoresis was conducted at 120V for approximately 1.5 to 2 hours in Tris gylcine buffer (144g/L Glycine, 29g/L Tris base, 10g/L SDS). Prestained molecular markers (FERMENTAS page ruler, Quantum Scientific, QLD, Australia) were added to give an estimate of protein size. Proteins were then transferred onto a Hybond ECL nitrocellulose membrane (Amersham Pharmacia Biotech, Buck, UK) in the transfer buffer (25mM Tris base, 192mM Glycine, 20% methanol) by electroblotting at 100V for 120minutes. For phosphorylated protein, 0.1mM of sodium orthovanadate was added in the transfer buffer to preserve the phosphorylation of proteins of interest by inhibiting endogenous phosphatases present in the cell lysate mixture. Non specific binding sites were blocked for

1 hour (0.2% Tween-20 in Tris-buffered saline (TTBS) in 5% skim milk, pH 7.4) after which the membrane was exposed to the respective primary antibodies overnight at 4°C. Following 3x washing with 0.2% TTBS (2.42g/L Tris base, 29.2g/L 0.2M NaCl, pH7.4), the membrane was incubated with the respective peroxidase labelled secondary antibody (Anti-mouse or Anti-rabbit, Amersham Pharmacia Biotech, Buck, UK) for 1 hour at room temperature, and again washed 3 times. Protein was visualised with enhanced chemiluminescence (ECL) detection system (Amerhsam Pharmacia Biotech, Buck, UK). Chemiluminescence images were captured by LAS 4000 (Fujifilm, NJ, USA). Alternatively, X-Ray film (GE, Amersham Pharmacia Biotech, Bucks, UK) was used. The resultant X-rays were scanned and the relative band intensities were measured using Image J software or Multigauge software version 3.0 (Fujifilm, NJ, USA). Probed membranes normally had the antibodies stripped and re-probed for β-actin or tubulin to confirm equal loading of proteins. The moist nitrocellulose membranes were submerged in stripping buffer (62.5mM Tris-HCl (pH6.7), 2% sodium disulphide, H2O and 100m β-mercaptoethanol) and incubated at 50°C for 30 minutes with gentle agitation. Membranes were then rinsed with water and washed twice for 10 minutes in 50ml 0.2%TTBS. Membranes were then ready for re-probe with primary antibody.

Table 2.5.2.1 **Antibodies used for western blotting**

Antibody	Company	Dilution	Band (kDa)
Anti-E-cadherin	BD Transduction Laboratories™, CA, USA	1:1000	120
Anti-phospho Smad 2	Cell signalling, MA, USA	1:1000	58
Anti-phospho Smad 1/5/8	Cell signalling, MA, USA	1:1000	56
Anti-fibronectin	NeoMarkers, CA USA	1:100	220
Anti-collagen IV	Abcam Ltd, Cambridge, MA, USA	1:5000	250
Anti-α tubulin	Sigma, MO, USA	1:5000	50
Anti- KLF6	Santa Cruz Biotechology, CA, USA	1:250	43
Anti- PPARγ	Santa Cruz Biotechology, CA, USA	1:100	50
Anti-β-Actin	Santa Cruz Biotechology, CA, USA	1:300	42
Anti-NR1H4 (FXR)	Abcam Ltd, Cambridge, MA, USA	1: 2000	54
Anti-SREBP-1	Milipore, MA, USA	1:1000	126
Anti-BMPR-IA	Abcam Ltd, Cambridge, MA, USA	1: 1000	60

2.6 Gelatin zymography

After an appropriate length of treatment, the culture supernatants were collected at times specified by the experimental protocol and centrifuged at 1,000 rpm for 5 minutes at 4°C to remove cellular debris. Equal volumes of samples were mixed with sample buffer and loaded onto a 10% non-reducing SDS-PAGE containing 1mg per ml of gelatin (Sigma, MO, USA), and subjected to electrophoresis for up to 2 hours at 4°C. After electrophoresis the gels were washed in re-naturing buffer (50mM Tris, 2.5% TritonX-100). The gels were incubated for a further 24 hours in developing buffer (50mmol/L Tris-HCl, 100mmol/L NaCl, 10mmol/L $CaCl_2$, 0.02% NaN_3, pH 7.5) at 37°C with gentle agitation. Next, the gels were stained for 15 minutes with Coomassie Blue 250 (Bio-Rad, CA, USA) dissolved in 50% ethanol and 10% acetic acid and de-stained in 30% ethanol and 10% acetic acid. The identity of each band was confirmed based on the molecular weight determined by prestained molecular markers. The lytic bands representing matrix metalloproteinases-2, MMP-2 (72 kDa) and MMP-9 (92kDa) activity were quantified using Multigauge software V3.0 (Fujifilm, NJ, USA). At the same time, equal volumes of all samples of interest were loaded onto another 10% non-reducing SDS-PAGE without gelatin, and subjected electrophoresis in similar conditions. After electrophoresis, gels were immediately stained with Coomassie blue and de-stained as described. The relative band intensities of the total protein were measured using Multigauge software V3.0 (Fujifilm, NJ, USA). The results of MMP-2 and MMP-9 were normalized to the results of total protein bands studied.

2.7 Cell viability studies

Cell proliferation or cytotoxicity was measured by an assay based on the reduction of yellow tetrazolium compound, 3-(4,5-dimethylthiazol-2-yl)-5-(3-carboxy-methoxy-methoxy-phenyl)-2-(4-sulfophenyl)-2H-tetrazolium, known as MTS. The MTS tetrazolium compound is bio-reduced by metabolically active cells, presumably by NADPH by into a coloured formazan product that is soluble in tissue culture medium. CellTiter 96® AQ_{ueous} One Solution Cell proliferation Assay (Promega, Madison, WI, USA) was used in our studies. HK-2 cells were seeded at 1x104 cells/well in a 96-well plate. At 50% confluence the cells were treated for 48- 72 hours in quadruplicate, as per experimental protocol. 20µl of CellTiter 96® AQ_{ueous} One solution Reagent were added into each well containing 100µl of culture medium. The cells were then incubated for 1-4 hours at 37°C in a tissue culture incubator as per manufacturer's instruction. To measure the soluble formazan produced by cellular reduction of the MTS, the absorbance at 490nm was read using a 96-well microplate reader.

2.8 Flow cytometric analysis

Cells harvested by trypsinisation at the end of the 24 hour period after transfection were spun to obtain a cell pellet. The cell pellet was washed in ice-cold phosphate buffered saline (PBS), then fixed in 70% ice-cold ethanol in drops before stored at -20°C until for future use. To study plasmid transfection efficiency, GFP-labelled plasmid was used, so no further staining was needed. For cell cycle analysis, cells were washed again in cold PBS, then resuspended in BPS containing 0.1% Triton-x100 and kept on ice for 30 minutes. The

cell pellet was then resuspended in 1 ml of fluorochrome solution containing propidium iodide (PI) 50µg.ml (Sigma, MO, USA), RNAse A 50µg/ml (Sigma, MO, USA), 0.25µM EDTA and 0.001% Triton X-100 and left for at least 1 hour in the dark. This suspension was filtered using a 50-micron mesh prior to scanning. Flow cytometry was performed using a FACScan flow cytometer (Becton Dickinson, CA, USA). The PI fluorescence of individual nuclei and the forward and side scatter were all measured using identical instrument settings with a minimum of 20,000 events. DNA contents in apoptosis and each phase of cell cycle were measured.

2.9 Enzyme linked immunosorbent assay (ELISA)

2.9.1 Transforming growth factor-β1 (TGF-β1) ELISA

Supernatant collected at the time of cell harvesting as per experimental protocol which was centrifuged and stored at -80°C for future used was first thawed on ice. TGF-β1 levels were determined with an immunoassay system (Promega, WI, USA) as per manufacturer's instructions. Briefly, flat-bottom 96-well plates (Nunc™, Roskilde, Denmark) were coated with TGF-β1monoclonal antibody overnight at 4°C, which binds with soluble TGF-β1. After blocking with TGF-β1 block for 35 minutes at room temperature, 200µl supernatant samples were applied in triplicate. A standard curve was prepared using the TGF-β1standard provided by the manufacturer in 1: 2 serial dilutions. Samples were incubated for 1.5 hours with shaking at (500 ± 100 rpm), and washed 5 times with TBST. 100µl of Anti-TGF-β1 pAb was added in each well and the samples were incubated for 90 minutes with shaking. This was followed by 5 more washes and then the

addition of TGF-β1HRP conjugate, 100µl per well, for another 2 hours at room temperature with shaking. Colour development was achieved after five washes with TMB One solution for 15 minutes. The absorbance readings at 450nm were read using a 96-well microplate reader. This system is linear between 15.6 -1000pg/ml. Samples were acid treated, then neutralized to convert the latent form to the bioactive form of TGF-β1 in order to measure total TGF-β1. Cell lysate protein concentration was determined using Bio-Rad Protein assay and TGF-β1levels were corrected for protein content per well.

2.9.2 Human BMP-7 ELISA

Conditioned media of HK-2 cells over-expressing BMP-7 were collected at the end of 72 hours, centrifuged and stored at -80°C for future analysis. BMP-7 levels were determined with an immunoassay kit assay (R & D, MN, USA) as per manufacturer's instruction, and read using a microplate reader at 450nm. Cell lysate protein concentration was determined using Bio-Rad Protein assay, and BMP-7 levels were corrected for protein content per well. For human circulating BMP-7, blood was collected, after informed consent had been obtained, from healthy volunteers or ESKD patients on hemodialysis, and immediately spun to separate the cellular component and serum. Serum was collected and stored at -80°C for future use. A serial 1: 2 dilution of serum samples was first performed to determine the dilution need for human circulating BMP-7 study. As per manufacturer's instruction, circulating BMP-7 was measured as described above and the absorbance at 450nm was recorded and plotted against the standard to determine the circulating level of BMP-7.

2.9.3 MCP-1 ELISA

HK-2 cells were seeded to 50% confluence in 10cm petri dishes. After 48 hours of treatment as per experiment protocol, supernatants were collected, spun and stored at -80°C until MCP-1 levels were determined with an immunoassay kit assay (Biosource International, CA, USA) as per manufacturer's instruction, and read using a microplate reader at 450nm. Cell lysate protein concentration was determined using Bio-Rad Protein assay and MCP-1 levels were corrected for protein content per well.

2.10 Reverse transcription polymerase chain reaction (RT-PCR)

Total RNA was extracted using RNAeasy Mini kit (Qiagen, USA) according to manufacturer's instructions. RNA quality assessment consisted of electrophoresis through an agarose gel to detect distinct ribosomal bands, and measurement of 260/280 absorbance using Nanodrop 1000 Version 3.7.1 (Thermo Scientific, DE, USA). Acceptable $A_{260/280}$ ratios fell in the range of 1.6 to 1.9 in H_2O.

2.10.1 DNasing RNA

For each RNA sample, 1 to 2 µg RNA, 2 µl 10x DNase I buffer (Invitrogen, USA), 2 µl DNase I (Invitrogen, USA) were added into a RNase-free Eppendorf tube. RNase-free water was then added to make the reaction volume up to 20 µl, followed by incubation at 37°C for 15 min in a heating block (Thermoline, Australia) and subsequently by the addition of 2 µl of 25 mM EDTA and incubation at 65°C for 5 min to inactivate the DNase

I. DNased RNA was then placed on ice for at least 1 min and stored at -80°C for RT-PCT use.

2.10.2 Semiquantitative polymerase chain reaction (PCR)

2.10.2.1 One step reverse transcription (RT) and PCR

Synthesis of cDNA and PCR were accomplished using a single step technique using the SuperScript™ III One-Step RT-PCT System with Platinum® *Taq* High Fidelity (All component from Invitrogen, USA unless otherwise specified). The system consists of two major components: SuperScript™ III RT/ Platinum® *Taq* High Fidelity enzyme mix and 2X reaction mixture. Because SuperScript™ III RT is not significantly inhibited by ribosomal and transfer RNA, it can be used to synthesize cDNA from total RNA, at a temperature range of 45-60°C. The 2X reaction Mix consists of a proprietary buffer system optimized for reverse transcription and PCR, and includes Mg^{2+}, deoxyribonucleotide triphosphates (dNTPs), and stabilizers.

The following components were added to 2 µl of DNased RNA at a concentration of 5ng/ µl in a 0.2ml, nuclease-free, thin-walled PCR tube on ice:

Component	Volume
2X Reaction Mix	25 µl
Sense primer (10 µM)	1µl
Anti-sense primer (10 µM)	1µl
Superscript™ III RT/ Platinum® Taq enzyme mix	2µl

RNase free water 19µl

The samples were mixed and cDNA synthesis/ RT-PCR performed on a MJ Thermal-Cycler PTC-200 (Bio-Rad, Hercules, CA, USA). The program was set as follow:

A: cDNA synthesis ad pre-denaturation

1 cycle of 50C for 30min, followed by 94°C for 2 min

B: PCR amplification (cycling for 26-34 cycles)

Denaturation: 94°C for 30sec

Annealing: x °C for 45 sec

(Annealing temperature adapted for specific primer set used)

Extension: 72°C for 1 min

C: Final extension: 72°C for 10 min

Twenty µl of amplification product was mixed with 1 µl Bluejuice DNA sample loading buffer (Invitrogen, USA), loaded onto a 1.5% agarose gel and run concurrently with a DNA ladder at 80 mA for 1 hour. The amplification product was visualized by ethidium bromide or GelGreen™ Nucleic Acid Stain (Biotium Ltd, CA, USA). Bands were imaged using the GelDoc XR system (Bio-Rad, Hercules, CA, USA) and quantitated by densitometry using Quantity One software (Bio-Rad, Hercules, CA, USA). β-Actin was used as an internal control for normalization of samples. The primer sequences, annealing temperature and cycles numbers used for the specific genes of interest are included in the relevant chapters.

2.10.2.2 Two step PCR

Two step PCR was also used in some experiments, particularly for genes with low mRNA expression. It consists of breaking down into two components namely Reverse transcription (RT) and PCR.

A) cDNA synthesis by reverse transcription (RT)

Synthesis of cDNA was achieved by two methodologies, using either Superscript ™ III or SuperScript ® VILO cDNA synthesis kits(All components from Invitrogen, CA, USA).

For the former, 9 µl of RNase free water, 1 µl of Random primer, 1 µl of dNTP and 1-5 µl of DNase RNA was prepared for each sample. The above components were added together and heated to 65° for 5 minutes then placed on ice. The following components were then added: 4 µl of 5x Strand Buffer, 2 µl of 0.1M DTT and 1 µl of RNase Out. These were mixed gently and incubated at 42°C for 2 minutes. One µl reverse transcriptase Superscript ™ III was added to the samples, and an equal amount of water was added to the negative controls. The samples were then incubated at 25°C for 10 minutes, 42°C for 50 minutes, 70°C for 15 minutes, and cooled rapidly to 4°C. One µl RNAse H was then added to remove RNA templates, and the sample was incubated at 37°C for 20 minutes and subsequently stored at -20°C until next use.

In some of the experiments, especially for real time PCR, cDNA was synthesized using SuperScript ® VILO™ cDNA synthesis kit. One micrograms of DNased RNA were

used This formulation provides enhanced cDNA synthesis efficiency, and can be used with very low and very high amounts of input RNA (up to 2.5 µg total RNA) in a 20 µl reaction. For a single reaction, 4 µl of 5X VILO™ Reaction Mix, 2 µl of 10X SuperScript® Enzyme Mix is made up with DEPC-treated water to 20 µl. The mixture is gently mixed and incubated at 25°C for 10 minutes, then at 42°C for 60 minutes. The reaction was terminated at 85°C at 5 minutes. The synthesized cDNA was stored at -20°C until use.

B) PCR

The following components were added to 2 µl of RT product in a nuclease-free, thin-walled PCR tube on ice:

Component	Volume
10X PCR Buffer	5 µl
10 mM dNTP	1 µl
50 mM $MgCl_2$	1.5 µl
Sense primer (10 µM)	0.5 µl
Anti-sense primer (10 µM)	0.5 µl
Platinum Taq DNA enzyme	0.2µl
RNase free water	(to make up to 48 µl in total)

The samples were mixed and spun before subjecting to PCR on a MJ Thermal-Cycler PTC-200 (Bio-Rad, Hercules, CA, USA). The program was set as follows:

PCR amplification (cycling for 26-34 cycles)

Denaturation: 94°C for 30sec

Annealing: x °C for 45 sec

(Annealing temperature adapted for specific primer set used)

Extension: 72°C for 1 min

C: Final extension: 72°C for 10 min

D: 4°C before storage at -20°C

Subsequent steps are similar to that of one step PCR.

2.11 Real time PCR

Real time PCR was performed using either Brilliant® SYBR® Green Single-Step qRT-PCR Master Mix (Stratagene, La Jolla, CA, USA) or TaqMan® probe-based gene expression Assay with TaqMan® Gene Expression Master Mix (Applied Biosystems Inc. Foster City, CA, USA).

2.11.1 Brilliant® SYBR® green single-Step qRT-PCR

The following components were added to 1 µl of DNased RNA at a concentration of 90.91ng/ml in a 0.2ml, nuclease free, 96 well PCR plate (Bio-Rad, Hercules, CA, USA) on ice:

Component	Volume
2X Master Mix	11 µl
Sense primer (1 µM)	2.2 µl

Anti-sense primer (1 μM)	2.2 μl
RT/ RNase Block Enzyme Mixture	0.00625 μl
Fluorescein (1 μM)	0.26 μl
RNase free water	4.278 μl

The samples were mixed gently and real time PCR performed on a Bio-Rad iCycler iQ system (Bio-Rad, Hercules, CA, USA). The program was set as follows:

A: cDNA synthesis and pre-denaturation

1 cycle of 50°C for 30 min, followed by 95°C for 10 min

B: PCR amplification (cycling for 40 cycles)

Denaturation: 95°C for 30 sec

Annealing: x °C for 1 min

(Annealing temperature adapted for specific primer set used)

Extension: 72°C for 39 sec

C: Final extension: 72°C for 2 min

The fluorescence threshold value was calculated using the iCycler iQ system software. When the reaction product amplification exceeded the threshold value, the corresponding cycle number was termed C_T. The calculation of relative change in mRNA was performed using the delta-delta method [405]. β-actin or TATA binding protein (TBP) were used as an internal control for sample normalization. The primer sequences, annealing temperature and cycle numbers used for the specific genes of interest are included in the relevant chapters.

2.11.2 *TaqMan*® probe-based gene expression Assay

Two microlitres (50ng) of cDNA were used as templates in a 20 µl PCR reaction. The mixture contained 10 µl of 2X *TaqMan*® Gene Expression Master Mix (Applied Biosystem, CA, USA), 1 µl of *TaqMan*® gene expression assay probe (Applied Biosystem, CA, USA) and DEPC treated water. TaqMan® Gene Expression Assay probe is a gene-specific expression assays containing two unlabelled PCR primers and one FAM dye-labeled *Taqman*® MGB prove (Applied Biosystem, CA, USA). Robotic arm epMotion 5070 (Eppendorf, Hamburg, Germany) was used for transferring, mixing and pipetting using maximum retrieval epT.I.P.S Motion 1 tips (Eppendorf, Hamburg, Germany) into either 96-well or 384-well MicroAmp® Fast optical plates with barcode (Applied Biosystem, CA, USA) to minimize mechanical pipetting error. Quantitative real-time PCR was performed using an ABI Prism 7900 HT Sequence Detection System (Applied Biosystem, CA, USA) for 95°C for 10 minutes followed by 40 cycles repeat of 95°C for 15 seconds and 60°C for 1 minute. One of the advantages of using Probe-label gene expression assay is that the annealing temperature is fixed for all genes of interest at 60°C. The reaction was performed at least in triplicate, and analyzed via relative quantitation with data presented as average fold change using delta delta method, as compared to control after normalization with either β-actin or TATA Binding Protein (TBP). Analysis of data was performed using RQ Manager Version 1.2 (Applied Biosystem, CA, USA). *TaqMan*® gene expression Assay probes used in this PhD thesis are as Table 2.10.2.1

Table 2.11.2.1 ***Taqman*® gene expression assay probe**

Gene Name	Assay ID	Amplicon length
Fibronectin 1	Hs01549976_m1	81
E-cadherin	Hs01013953_m1	65
Vimentin	Hs00958116_m1	70
FXR (NR1H4)	Hs00231968_m1	85
SHP1 (NR0B2)	Hs00222677_m1	87
SREBP1c	Hs01088691_m1	90
MCP-1 (CCL-2)	Hs00234140_m1	101
TGF-β1	Hs00998133_m1	57

Endogenous control	Part ID
Human β-Actin	4333762F
Human TATA Binding protein (TBP)	4333762F

FXR:Farsenoid X receptor, NR1H4 (Nuclear Receptor Subfamily 1, group H, member 4,
SHP: Short heterodimer protein, NR0B2: Nuclear Receptor Subgroup 0, group B, member 2
SREBP1c: Sterol Regulatory Element Binding Transcription Factor 1, Isoform c.

2.12 Plasmid construction

2.12.1 Construction of plasmid

Full length cDNA of human BMP-7 was isolated from HK-2 cells using Genomic cDNA extraction kit (Invitrogen CA, USA). Full length BMP-7 was synthesized by semi-quantitative RT-PCR using SuperScript III (Invitrogen CA, USA) and PfuUltra^{TM} High-Fidelity DNA Polymerase (Stratagene, USA) using BMP-7 cloning primers for pcDNA3.1/Hygro (Invitrogen, CA, USA) as follows: Forward primer ATGCTAGCATGCACGTGCGCTCACTG and reverse primer,

GCGGATCCTACTAGTGGCAGCCACAGGC. After purification using PCR purification kits (Qiagen, CA, USA), restriction enzyme digestion was performed to assure the identity of the genomic DNA. One third of the total purified PCR product was cut using restriction enzymes *BstX I, Bgl I* and *EcoR I* (New England Biolabs, MA, USA) buffered in water containing at least 1% of bovine serum albumin (BSA) in a 100 µl reaction. The mixture was incubated at 37°C overnight (or the appropriate temperature for the specific enzymes). BlueJuice (Invitrogen, CA, USA) was added to the samples, which were then run on a 1.5% agarose gel (Bio-Rad, CA, USA) in 1x TAB buffer (4.84 h Tris Base, 1.14ml glacial acetic acid, 2 ml 0.5M EDTA pH 8) containing GelGreen™ Nucleic Acid Stain (Biotium Ltd, CA, USA) for approximately 30 minutes at 90 volts. Number of fragments and their base pair can be estimated depending on the sites of enzymatic digestion. A DNA ladder (Roche Applied Science, Indianapolis, USA) and uncut control were run in separate lanes to confirm the size of the insert (Figure 2.11.1.1). Another two third of the purified PCR product was subjected to restriction enzymes cutting at *Nhe I* and *BamH I* (New England Biolabs, MA, USA) to obtain a linear BMP-7 cDNA. A linear BMP-7 cDNA should correspond to its expected base pair (~1.3kb). The product was purified and measured using NanoDrop 1000 Version 3.7.1 (Thermo Scientific, DE, USA).

The mammalian expression vector pcDNA3.1/Hygro (5.6kb) (Invitrogen, CA, USA) was linearised by incubating with *Nhe I* and *BamH I*, then extracted on a 1.5% agarose gel and purified using a gel extraction kit. The full length cDNA of BMP-7 was then dephosphorylated by shrimp alkaline phosphatase, 1U/ µl (Roche, USA) and then ligated with linearised pCDNA3.1/Hygro in a mixture of DEPC water, 5x ligase buffer, T4 ligase (Invitrogen, USA), BMP-7 cDNA and pcDNA3.1/Hygro vector in a ratio of 1:3.

Another set of vectors without cDNA insertion was used as control. To determine the optimal condition of vector cDNA ligation, one set of the mixture was kept at room temperature and another set was incubated at 4°C overnight.

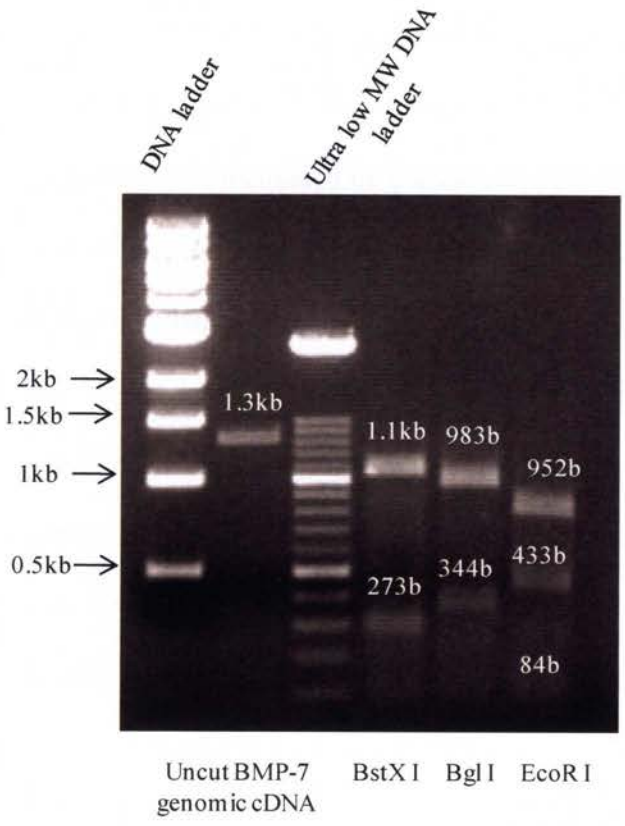

Figure 2.12.1.1 linear BMP-7 cDNA and fragments with restriction enzymatic digestion.

Genomic cDNA of human BMP-7 extracted from HK-2 cells has a molecular weight of 1.3kb. Restriction enzyme digestion by BstX I and Bgl produced two fragments whereas EcoR I produced three fragments. This suggested that the linear cDNA obtained corresponds to the human BMP-7 cDNA.

Library Efficiency DH5α Competent Cells (Invitrogen, CA, USA) were thawed on ice and 100 µl was transferred to a microtube. One to two microlitres of ligated product was added, and the mixture was incubated on ice for 30 minutes. The competent cells were then heat-shocked for 45 seconds at 42°C and placed back on ice for 2 minutes. 0.9 ml of room temperature Super Optimal Catabolite repression (S.O.C) broth (0.5% Yeast extract, 2% tryptone, 10mM NaCl, 2.5mM KCl, 10mM $MgCl_2$, 20mM Mg SO_4, 20 mM glucose) was added to the tube, which was incubated on a shaker at 225 rpm for 1 hour at 37°C. The transformed cells were then spread on Luria-Bertani agar plates containing 100 µg per ml ampicillin. The plate was incubated overnight at 37°C. Each plate was marked carefully as control vector (C) at either room temperature or 4°C and insert vector (I) at room temperature or 4°C (Figure 2.12.1.2). Single colonies were picked the next day, and put into 100ml of Lysogeny broth (LB) media (10gm per L tryptone, 5 gm per L yeast extract, 10 g per L NaCl) with 100 µg of ampicillin, and shaken at 225 rpm 14-16 hours at 37°C. The plasmid vector was then extracted using PureYield™ Plasmid Midiprep System (Promega, USA), and the concentration of each sample was measured.

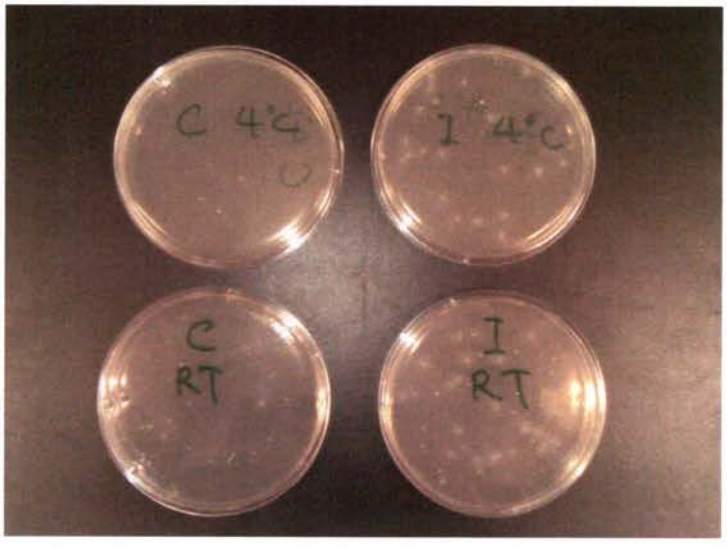

Figure 2.12.1.2 Colonies of pcDNA3.1/Hygro.BMP-7 ligated product.

Ligation of BMP-7 and vector was performed at room temperature (RT) or 4°C to obtain the optimal condition. At the same time, ligation without BMP-7 insert (I) was performed in the same experimental condition to serve as a control. The ligated products were then grown in SOC media, spread onto LB Agar plate and incubated overnight at 37°C. Figure 2.11.1.3 first row, showed minimum number of colonies in both room temperature and 4°C (Control). Many colonies were seen in the insert group especially those in which the ligation occurred at RT. A ratio of 10:1 colonies in the insert vector vs. control usually indicates a successful ligation process.

2.12.2 DNA quantification and verification

DNA was quantified using NanoDrop 1000 Version 3.7.1 (Thermo Scientific, DE, USA). Part of the purified product was subjected to restriction enzyme digestion to assure the identity of the plasmid. Plasmid inserts were cut using *BamH I* and *Nhe I*. The mixture was incubated at 37°C overnight then run on an agarose gels containing GelGreen™ Nucleic Acid Stain. A DNA ladder and supercoiled uncut plasmid were run at the same time. Successful insertion and ligation of BMP-7 sequence was based on the ability of these restriction enzymes to cut circular DNA into linear DNA at points of insertion. Linear DNA runs slower than circular DNA on the gel (Figure 2.12.2.1A). One µl of 10 µM sequencing primer for pcDNA3.1/ Hygro 5'AAGCAGAGCTCTCTGGCTAACT (Sigma Aldrich, MO, USA) was added into 15 µl of plasmids in 10mM TrisHCl (pH 8.3). The sequences and orientation of the constructed human BMP-7 in pcDNA3.1/Hygro plasmid were then confirmed by sequencing in the DNA Core Facility, SUPAMAC (University of Sydney, Australia).

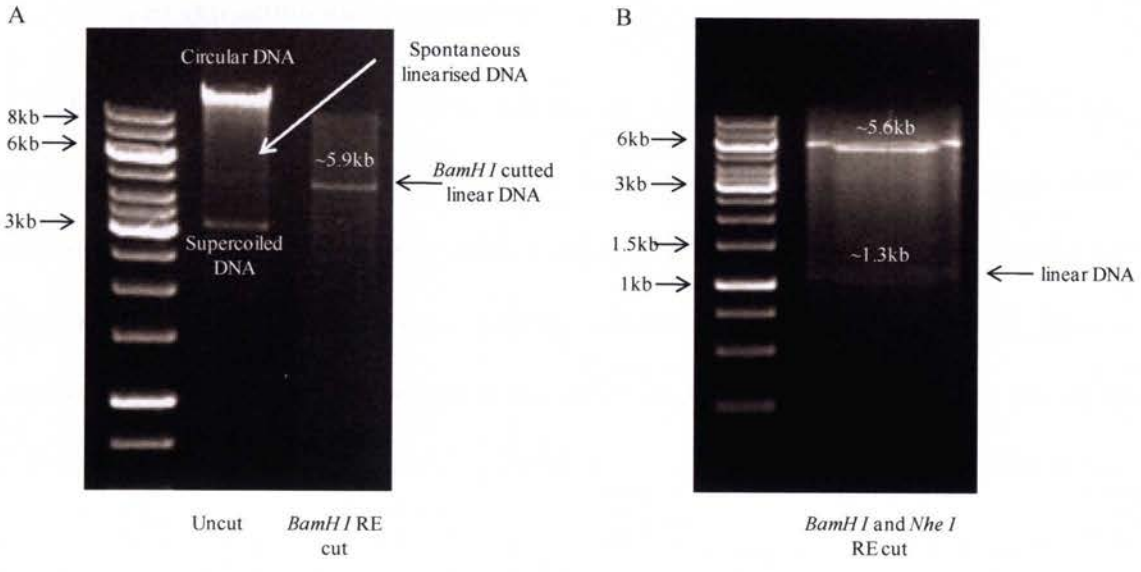

Figure 2.12.2.1 Restriction enzyme digestion by *BamH I* and *Nhe I.*

This is used to ensure identity of the plasmid. Uncut DNA plasmids have multiple bands. Supercoiled DNA plasmid runs faster than spontaneous linearised DNA. The most prominent band represents the circular DNA which migrate the slowest (A). BamH I restriction enzyme linearised DNA into one single band (A). Nhe I RE further cut the linearised DNA into two bands i.e. vector band and the inserted BMP-7 cDNA band (B). The base pair did not equate to the initial molecular weight of pcDNA3.1/ Hygro or BMP-7 cDNA because during previous RE digestion, part of the base pairs have been removed therefore the molecular weight is usually less than the initial molecular weight.

2.12.3 Plasmid extraction and purification

Once clones were confirmed by sequencing, Library Efficiency DH5α Competent Cells (Invitrogen, CA, USA) were used for transformation to increase plasmid yield. Experimental DNA that was free of phenol, ethanol, protein and detergents was used for maximum transformation efficiency. One µl plasmid was incubated with ice thawed competent cells for 30 min, then heat shocked for 45 sec at 42°C. Cells were placed in S.O.C media (Invitrogen, CA, USA) at 37°C on a shaker at 225 rpm for 1 hour. After overnight incubation in LB media (QBiogene, USA) containing 100 µg/ml ampicillin (Sigma, USA) at 37°C at 225 rpm, cells were spin down at 10,000 g for 10 min. The wizard plus midi-prep DNA purification system (Promega, WI, USA) was used for plasmid preparations according to the manufacturer's instructions. The 100 ml of culture was centrifuged at 10,000 x g for 10 minutes at 4°C. The pellet was then resuspended in Cell Resuspension Solution. Three ml of cell lysis solution was added and the solution was mixed by inverting gently and incubated at room temperature for 3 minutes before addition of 5 ml of neutralization solution. The above homogenate was poured into the clearing column (placed above the binding column) and a vacuum was applied for filtration. Once the solution passed through the column, 5 ml of endotoxin removal wash was passed through the column. The vacuum was continued for 20 seconds after the liquid had passed through the column. To elute DNA from the membrane, 600 µl nuclease free water was placed in the column and centrifuged at 1500 *g* for 5 minutes at room temperature. The collected filtrate was quantified using a nanodrop 1000 Version 3.7.1 (Thermo Scientific, DE, USA).

2.12.4 Plasmid transfection

To enforce BMP-7 expression in HK-2 cells, cells were seeded into a 6-well plate (Sarstedt, Germany) at 80-90% confluence for plasmid transfection. For each transfection sample 250 µl Opti-MEN (Invitrogen, CA, USA) and 6 to 8 µl of lipofectamine 2000 (Invitrogen, CA, USA) was mixed and incubated at room temperature for 5 min. Concurrently, 250 µl of Opti-MEM was added to 4 to 6 µg of KLF6 or BMP-7 plasmids and were mixed and incubated at room temperature for 30 minutes. Each well was first washed with Opti-MEN and 300 µl were added to each well to avoid drying of the cells. This is followed by 500 µl of lipofectamine-plasmid complex in each well. In parallel, cells were transfected with specific empty vector plasmid to serve as a negative control, or by lipofectamine reagent alone to serve as "mock transfection". Transfection medium was removed after 6 hours of incubation at 37°C, 5% CO_2 and 95% air, and replaced with 2 ml complete keratinocyte growth medium overnight. The following day the cells were exposed to appropriate treatment conditions. Both mRNA and protein were used to verify the transfected gene expression levels.

2.13 RNA interference

RNA interference (RNAi) technology was used to determine the differential role of KLF-6 in mediating the expression of TGF-β1 induced EMT and BMP receptors. Short interfering RNAs (SiRNA) are an intermediate component in the RNA interference pathway, the process by which double-stranded RNA silences homologous genes.

There are currently five methods for generation of siRNA: chemical synthesis, *in vitro* transcription, digestion of long dsRNA by an RNase III family enzyme (eg. Dicer, RNase III), expression in cells from a siRNA expression plasmid or viral vector, and expression in cells from PCR-derived siRNA expression cassette. The first three methods involve *in vitro* preparation of siRNA that is then introduced directly into mammalian cells by transfection, electroporation or other means. The last two methods rely on the transfection of DNA-based vectors and cassettes that express siRNA within the cells. The KLF-6 silencing model undertaken as part of the work in this thesis was chemically synthesized. The general principle of RNA interference used in this project is summarized as below:

27-mer double –stranded RNA molecules were chemically synthesized (Ambion, USA). The complementary oligonucleotides were 2'-deprotected, annealed, and purified by the manufacturer. The sequence specifically targeting human KLF-6 (accession no NM_001008490) was 5' AAGCCAGGTGACAAGGGAAATGGCGAT-3'. Non-specific siRNA was used as control.

2.13.1 siRNA transfection

HK-2 cells were plated in 6-well tissue culture plates and grown to 60-70% confluence. The next day, they were transfected with KLF-6 siRNA using Lipofectamine 2000 (Invitrogen, CA, USA). Briefly, for each transfection samples 250 µl Opti-MEN (Invitrogen, CA, USA) and 6 µl of lipofectamine 2000 (Invitrogen, CA, USA) were mixed and incubated at room temperature for 5 min. Concurrently, 250 µl of Opti-MEM were

added to 80 nM/L of KLF6 siRNA and was mixed and incubated at room temperature for 30 minutes. Each well was first washed with Opti-MEN and 300 µl were added to each well to avoid drying of the cells. This was followed by 500 µl of lipofectamine-plasmid complex in each well. In parallel cells were transfected with No-specific siRNA to serve as a negative control. This was followed by 6 hours of incubation at 37°C, 5% CO_2 and 95% air. Unlike plasmid transfection, the medium was not removed after 6 hours. Instead, 2 ml of fresh keratinocyte growth medium were added and kept overnight. The following day the medium was removed and the cells were exposed to appropriate treatment conditions. RNA and cell lysates were prepared for western blotting and RT-PCR to evaluate KLF-6 expression at a protein and RNA level.

2.14 Statistic analysis

Each experiment was performed independently a minimum of five times. Results for normally distributed data were expressed as mean ± S.D. For non-parametric data, they were expressed as median, (interquartile range, IQR). Statistical comparisons between two groups were made by *t*-test and by analysis of variance (ANOVA) for multiple group comparisons. The Wilcoxon test was used for non-normally distributed data and the *Chi-square* test used for categorical data. All Analyses except chapter 6, were performed using the software package Statview, version 4.5 (Anacus Concepts Inc, Berkeley CA, USA). Other statistical analyses were described separately in individual chapters. P values <0.05 were considered significant.

CHAPTER 3: Transforming growth factor-β1 (TGF-β1) and Krüppel-like factor-6 (KLF-6) impede bone morphogenetic protein-7 (BMP-7) renoprotection, via downregulation of bone morphogenetic protein receptor-IA (BMPR-IA) in renal proximal tubule cells.

3.1 Specific background and review

Most chronic nephropathies share pathogenic mechanisms that contribute to disease progression, independent of the original cause or disease. As discussed in Chapter 1, renal fibrosis represents a failed wound-healing process of renal tissue, typically characterised by consistent histopathological features of glomerulosclerosis and interstitial fibrosis, which implies a 'final common pathway' of injury. This process is typically progressive and irreversible, and the most important predictor of the rate of progression of chronic kidney disease [406].

Convincing evidence now exists to suggest the proximal tubular epithelial cell (PTC) also plays an important role in the deposition of extracellular matrix (ECM) in the kidney. PTCs which are mesenchymal in origin, appear capable of reverting to a mesenchymal phenotype via a process known as epithelial-mesenchymal transition (EMT) in response to certain physiological stresses. EMT is characterized by a highly regulated process driven predominantly by the pleiotropic cytokine transforming growth factor-β1 (TGF-β1) [71].

The transcription factor KLF-6 as previously defined in chapter 1.4.1 plays a diverse role during differentiation and development, capable of functioning as activators of transcription, repressors, or both. The list of cellular 'target' genes of KLF-6 includes collagen α1 [260], urokinase plasminogen activator (uPA) [262], TGF-β1 and types I and II TGF-β1 receptors [259]. It also directly regulates the E-cadherin promoter [263]. Our group has previously demonstrated that exposure of proximal tubule cells to TGF-β1 induces EMT, with parallel transcriptional induction of KLF-6. KLF-6 over-expression significantly promotes a phenotype transformation consistent with EMT. In addition to that, animal models of diabetic nephropathy showed increased proximal tubular KLF6 expression in parallel with features of EMT [265]. These findings collectively suggest that KLF6 plays a role in mediating TGFβ1-induced EMT in proximal tubule cells.

Bone morphogenetic protein-7 (BMP-7) is one of the members of the BMP/TGF-β-superfamily, which is best known for its role during embryonic development, but is also known to regulate growth, differentiation, chemotaxis and apoptosis in various adult cell types. BMP-7 is most abundantly present in adult kidney, bone and cartilage. In the adult kidney, BMP-7 is endogenously expressed in the epithelial cells of distal tubules, collecting ducts and podocytes [302]. Tubular BMP-7 expression decreases in several acute and chronic kidney disease models and pre-emptive administration of exogenous BMP-7 can ameliorate injury in models of ischemic nephropathy, unilateral ureteral obstructive nephropathy, lupus nephritis, nephrotoxic serum nephritis and diabetic nephropathy [333]. Its protective role has also been confirmed in various cell types including proximal tubular cells [80], podocytes [334], mesangial cells [407], fibroblasts [408] and endothelial cells [337]. The proposed protective mechanisms in proximal tubule cells include direct inhibition of TGF-

β1 production, decrease in pro-inflammatory genes and chemoattractants, and epigenetic regulation [338, 339] . However, the evidence suggesting it can reverse TGF-β1-induced EMT in established human kidney disease is limited. In most published studies using animal models, exogenous administration of BMP-7 was given either "pre-insult" or at an early time point in the establishment of pathology. Dudas *et al* [348] have recently shown that BMP-7 fails to attenuate TGF-β1 induced EMT in two different human proximal tubular cell lines. Therefore the antifibrotic value of BMP-7 remains controversial.

The biological activity of BMP-7 in the kidney is controlled at various levels. At the site of the target cells, signal transduction in the BMP-7 in general is initiated by ligand binding to its receptor complex. There are three BMP type I receptors (BMPR-IA/ activin receptor-like kinase-3 (ALK-3), BMPR-IB/ ALK-6 and ALK-2) and three BMP type II receptors (BMPR-II, activin type IIA receptor and activin type IIB receptor). In contrast to the expression of BMP-7, BMP receptor expression is reported in both proximal and distal tubular cells. This suggests that these cells are capable of responding to BMP-7 in a paracrine-like manner [308]. Receptors are able to bind ligands independently, but the heterodimerisation of the type I and type II receptor chains is required for signalling. Cytosolic signalling starts generally when the constitutively active type II receptor kinase transphosphorylates the type I receptor at a regulatory element, the GS domain. The latent type I kinase is thereby activated, with downstream phosphorylation of Smad proteins which, after migration into the nucleus, function in concert with other proteins as transcription factors for the regulation of responsive genes [312]. A mutation in the GS domain of the type I receptor can lead to constitutive activation of the receptor, and such an activated receptor mimics the effects of the entire receptor-ligand complex in the absence

of BMP-7 and the type II receptor [310]. This evidence suggests that the type I receptor is the primary transducer of this pathway, establishing an important regulatory step for BMP-7 signalling. Therefore, BMP-7 activity in healthy and diseased states is likely to be regulated by the availability of its type I receptors.

The distribution of type I receptors within the kidney itself varies. High affinity BMP-7 type I receptors ALK-2 and BMPR-IA but not BMPR-IB are expressed in human podocytes and mesangial cells. However, all type I receptors are found in kidney tubules [307]. The affinity of BMPs for type II receptors is much weaker than for the type I receptors, and the different BMPs bind to these receptors with different affinities. For example, BMP-4 preferentially binds BMPR-IA and -IB. BMP-7 binds ALK2 and BMPR-IA with a higher affinity than BMPRI-IB [309].

Several extracellular molecules have been identified that bind to BMP-7, acting as agonists or antagonists in the kidney. BMP antagonists function through direct association with BMPs, thus limiting the BMPs from binding to their cognate receptors. Such extracellular inhibitors include noggin, gremlin, vertebrate chordin and uterine sensitization-associated gene-1 (USAG-1) [323]. In contrast, BMP-7 activity is enhanced by increased binding to the receptor of an extracellular protein, kielin/chordin-like protein (KCP) [324] . Overall, the relevance of altered presence of BMP receptors, its agonists and antagonists or BMP-7 itself on CKD progression has not been definitely established. The aim of the present study was to determine the interaction of TGF-β, KLF-6, BMP-7 and its receptors, and their roles and interrelationships in the development of EMT.

3.2 Material and methods

3.2.1 Cell culture

HK-2 cells, a human proximal tubular cell line from American Type Cell Collection (ATCC, USA), were used in this study as outlined in Chapter 2 and previously described [396]. HK-2 cells were 70% confluent when seeded onto a six-well plate, and cells were maintained in keratinocyte serum-free medium (Invitrogen, Carlsbad CA,USA) supplemented with bovine pituitary extract 20-30 μg/ml and epidermal growth factor 0.1-0.2 ng/ml (Gibco, Grand Island, NY, USA), containing 5 mmol/L or 30 mmol/L D-glucose, for a total of 48 or 72 hours. Cells were also grown in 5 mmol/L D-glucose medium containing TGF-β1 (Sigma-Aldrich, St Louis, MI, USA) at 0.5 ng/ml, which is the determined optimal dose for EMT induction in HK-2 cells. 5mM D-glucose and 25 mmol/L L-glucose was used as the osmotic control. These cells were grown at 37^0C in a humidified 5% CO_2 incubator. Recombinant BMP-7 (BioVision, Mountain View CA, USA) was used at a concentration of 1 μg/ml in an attempt to reverse EMT after 24 hours exposure to TGF-β1. Cell culture media were changed every 48 hours and studies were undertaken up to 72 hours after exposure to the experimental conditions. Primary cultures of proximal tubular cells, obtained from nephrectomised kidneys using previously well described methods, were used to confirm human BMP-7 and BMP receptor expression [398].

3.2.2 KLF-6 and BMP-7 plasmid construction and transfection

Fragments of human KLF-6 (NM_001300) and BMP-7 cDNA (NM_001719) were cloned into pCMV6-XL5 (Origene, Rockville MD, USA) and pcDNA.hygro3.1

(Invitrogen, Carlsbad CA, USA) vectors respectively. DNA sequencing confirmed the cDNA had been cloned into the vector. Each of these plasmids was purified using a PureYield Plasmid Midiprep system (Promega, Madison WI, USA). HK-2 cells at 70% confluence when seeded onto a six-well plate were used for plasmid transfection. Six micrograms of either KLF-6 or BMP-7 plasmid were introduced into HK-2 cells using Lipofectamine 2000 according to manufacturer's instructions. In parallel, cells were transfected with an empty pCMV6-XL5 or pcDNA.hygro3.1 vector containing non-targeting sequence and transfection reagent only which both served as controls. Both mRNA and protein were used to verify the transfected gene expression levels.

3.2.3 Flow cytometric analysis

To study plasmid transfection efficiency and to determine the optimal amount of lipofectamine to be used, GFP-labelled plasmid transfected HK-2 cells were harvested by trypsinisation at the end of the 24 hour period after transfection, and spun to obtain a cell pellet. The cell pellet was washed in ice-cold phosphate buffered saline (PBS), then fixed in 70% ice-cold ethanol in drops before stored at -20°C for future use. Flow cytometry was performed using a FACScan flow cytometer (Becton Dickinson, CA, USA). The PI fluorescence of individual nuclei and the forward and side scatter were all measured using identical instrument settings with a minimum of 20,000 events.

3.2.4 Gene Silencing by Small Interfering RNA (siRNA)

27-mer double-stranded RNA molecules were chemically synthesized (Ambion, Austin TX, USA). The complementary oligonucleotides were 2'-deprotected, annealed, and purified by the manufacturer. The sequence specifically targeting human KLF-6 (accession no. NM_001008490) was 5'-AAGCCAGGTGACAAGGGAAATGGCGAT-3'. HK-2 cells grown at 50-60% confluence plated in a six-well plate were used in this experiment. Eighty nmol/L of KLF-6 siRNA was introduced into HK-2 cells using Lipofectamine 2000 according to manufacturer's instructions. In parallel, cells were transfected with a non-specific siRNA which served as control. Silencing was confirmed by knock-down of mRNA and protein expression. A knock down of 60 to 80% was achieved in all experiments. BMP receptor mRNA and protein expression were measured using real time PCR and western blot analysis respectively.

3.2.5 Real-time reverse transcription polymerase chain reaction (real time RT-PCR)

RNA was extracted using RNAeasy mini kit (Qiagen, Valencia, CA, USA) according to manufacturer's instructions. Both water blank and non-reverse transcribed RNA samples were used as negative controls. Briefly, total RNA (1 μg) was treated with DNase I (Invitrogen, Carlsbad CA, USA), and then cDNA was synthesized using reverse transcriptase Superscript II RT (Invitrogen, Carlsbad CA, USA). Real-time PCR was performed using Brilliant® SYBR® Green Single-Step QRT-PCR Master Mix (Stratagene, La Jolla, CA, USA) to assess transcript levels of BMPR-IA, BMPR-IB, ALK-2, BMPR-II, KLF-6, Id-2, BMP-2, BMP-4 and BMP-7. Primer specificity in real time was first

confirmed using RT-PCR. Primer sequences are shown in Table 3.2.1.Real-time quantitation was performed on the Bio-Rad iCycler iQ system (Hercules CA, USA). The fluorescence threshold value was calculated using the iCycler iQ system software. The calculation of relative change in mRNA was performed using the delta-delta method [405], with normalization for the housekeeping gene β-actin or 18s. Primers for E-cadherin and vimentin were validated for RT-PCR and calculated as a percentage of the change after normalization for β-actin gene expression.

Table 3.2.5.1 **RT-PCR Primers**

Gene Name	Accession No.	Sense	Antisense	Size (bp)
BMPR-IA/ ALK-3	NM_004329	5' TCAGACTCCGACCAGAAAAAGT	5' TGGCAAAGCAATGTCCATTAGTT	151
BMPR-IB/ ALK-6	NM_001203	5' GAAGGCTCAGATTTTCAGTG	5' GGACCAAGAGCAAACTACAG	199
ALK-2	NM_001105	5' AAAGGCTGCTTCCAGGTTTATG	5' CCGTGATGTTCCTCTTACACC	113
BMPR-II	NM_001204	5' GCAGAGGCTCGGCTTACT	5' GTTTCAGGGCTGGGGATT	348
BMP-7	NM_001719	5' GCTACGCCGCCTACTACT	5' GACGGAGATGGCATTGAG	161
KLF-6	NM_001008490	5' TCCACGCCTCCATCTTCT	5' CATCGCATTTCCCTTGT	136
E-cadherin	NM_004360	5' TCTTCAATCCCACCACG	5' TCTCCAAATCCGATATGTTA	461
Vimentin	NM_003380	5' GGACTCGGTGGACTTCTC	5' CGCATCTCCTCCTCGTAG	221
Id-2	NM_002166	5' GACCCGATGAGCCTGCTATAC	5' AATAGTGGGATGCGAGTCCAG	167
BMP-2	NM_001200	5' ACTACCAGAAACGAGTGGGAA	5' ATCTGTTCTCGGAAAACCTGAAG	111
BMP-4	NM_130851.2	5' TGGTCTTGAGTATCCTGAGCG	5' GCTGAGGTTAAAGAGGAAACGA	130
β-Actin	AY582799	5' ATCGTGCGTGACATTAAG	5' ATTGCCAATGGTGATGAC	135
18s	NR 003286.1	5' TCGAGGCCCTGTAATTGGAAA	5' CCCTCCAATGGATCCTCGTT	61

3.2.6 Western blot analysis

Supernatant was collected and centrifuged at 3000 rpm, 4°C for 5 mins to remove cell debris. Protein lysates were extracted as previously described [397]. In brief, cells were lysed in ice cold cell lysis buffer (50 μM Tris-HCl, 150 mM NaCl, 5 mM EDTA, 50 μl Triton-X 100 per 10 ml and Proteinase Inhibitor Cocktail (Roche Diagnostics, Mannheim, Germany) one tablet per 10 ml, pH 7.4). The lysate was centrifuged at 12,000 rpm, 4°C for

10 mins. The pellet and the supernatant were discarded, and the cell lysate was collected and stored at -80°C. Protein assays (Bio-Rad, CA, USA) were done to determine the protein concentration of the cell lysates. Thirty micrograms of total cell protein was mixed with 6x Laemmli sample buffer containing mercaptoethanol, and heated to 95°C for 10 min. Samples were then analysed by SDS-PAGE in 7.5% or 10% gel and electroblotted to Hybond nitrocellulose membranes (Amersham Pharmacia Biotech, Bucks, UK). Membranes were blocked in Tris-buffered saline containing 0.2% Tween 20 (TTBWS) in 5% skim milk for 2 hours, incubated overnight at 4°C with BMPR-IA 1:1000 (Abcam Ltd, Cambridge, UK), KLF-6 1:500 (Santa Cruz Biotechnology, Santa Cruz, CA, USA), E-cadherin 1:1000 (BD Transduction Laboratories™, CA, USA), fibronectin 1:100 (NeoMarkers, CA USA), collagen IV 1:5000 (Abcam Ltd, Cambridge, UK) in TTBS (Tris buffered saline with 0.2% Tween) containing 5% skim milk. Membranes were washed with TTBS and incubated with horseradish peroxidase (HRP)-conjugated secondary antibody. Proteins were visualized using the enzymatic chemiluminescence (ECL) detection system (Amersham Pharmacia Biotech, Bucks, UK). The bands corresponding to BMPR-IA (60 kDa), KLF-6 (43 kDa), E-cadherin (120 kDa), fibronectin (220kDa), collagen IV (250kDa) and phosphorylated Smad 1/5/8 (pSmad1/5/8 (56kDa) were captured using LAS 4000 (Fujifilm, Tokyo, Japan). All membranes were reprobed with β-actin 1:1000 (Santa Cruz Biotechnology, Santa Cruz CA, USA) and results were corrected for β-actin as a loading control and analysed using Multigauge system (Fujifilm, Tokyo, Japan). Equal volumes of supernatant media (30μl) run in SDS-PAGE gel and counterstained with Coomassie blue were used to quantify total supernatant protein. Secreted fibronectin and collagen IV were normalised to the total protein measured by Coomassie blue.

3.2.7 Gelatin zymography

The conditioned media collected at the end of 72 hours were centrifuged at 1,000RPM for 10 minutes at 4°C to remove cellular debris. Equal volumes of samples were mixed with sample buffer and loaded onto a 10% non-reducing sodium disulphide-polyacrylamide gel containing 1mg per ml of gelatin, and subjected to electrophoresis for up to 2 hours at 4°C. After electrophoresis the gels were washed in re-naturing buffer (50mM Tris, 2.5% Triton X-100). The gels were then incubated at 37°C overnight in developing buffer (50mmol/L Tris-HCl, 100mmol/L NaCl, 10mmol/L CaCl2, 0.02% NaN3, pH 7.5). The gels were then stained for 15 minutes with Coomassie Blue R-250 (Bio-Rad, CA, USA) dissolved in 50% ethanol and 10% acetic acid and de-stained in 30% ethanol and 10% acetic acid. MMP-9 and MMP-2 were confirmed by their molecular weight. The lytic bands representing matrix metalloproteinases-2 (MMP-2, 72kDa) and -9 (MMP-9, 92kDa) protein levels were quantified using Multigauge software V3.0 (Fujifilm, NJ, USA).

3.2.8 Cell proliferation and cytotoxicity study

Cytotoxic and proliferative effects of rhBMP-7 on HK-2 cells were assessed using CellTiter 96® AQ_{ueous} One Solution Cell proliferation Assay (Promega, Madison, WI, USA). Subconfluent HK-2 cells were passaged onto 96 well plates. Cells were incubated with rhBMP-7 at concentrations of 150 ng/ml, 250 ng/ml, 500 ng/ml 1000 ng/ml and 2000 ng/ml for 72 hours. The absorbance of the formazan released in each samples was recorded

at 490nm using a 96 well plate reader. The results were standardised to the untreated control group. The levels of formazan in the culture supernatant reflect mitochondrial activity, and thus a reduction in formazan levels released by confluent cells represents a cytotoxic effect [409].

3.2.9 *In vivo* studies in diabetic transgenic (mRen-2)27 rats

mRen-2 diabetic rats were used as a well established model of diabetic nephropathy, displaying an amplified tissue renin angiotensin system (RAS) and exhibiting classical glomerular and tubulointerstitial changes [402]. These diabetic animals have elevated tissue TGF-β1, rendering them an appropriate model for the present study [404]. Kidney tissues (n=5) were obtained from 16 weeks post streptozotocin (STZ)-treated homozygous (mRen-2)27 rats (St. Vincent's Hospital Animal House, Melbourne, Australia) with established diabetes at the time of sacrifice as previously described [403]. Using the perfusion-exsanguination method, ice-cold saline was used to perfuse kidneys via abdominal aortic cannulation. Kidneys were excised, decapsulated, sliced transversely and snap-frozen in liquid nitrogen. RNA was extracted from homogenised kidney tissue according to manufacturer's instructions (Qiagen, Valencia, CA, USA). mRNA expression of BMPR-IA, ALK2 and BMP-7 were studied in these animal with appropriate control animals (n=5), using real time PCR.

3.2.10 Human kidney tissue preparation and immunohistochemistry (IHC)

Paraffin-embedded tissue blocks from biopsies of five renal biopsies (n=5) with diabetic glomerulosclerosis were randomly retrieved from the files of the Department of Pathology, Royal North Shore Hospital (RNSH). Each patient was contacted and informed consent was obtained. Controls consisted of histologically normal kidneys obtained, with informed consent, from patients undergoing nephrectomy for small (<6 cm) kidney tumours (n=5). Ethical approval for the study was obtained from the Royal North Shore Hospital Human Research Ethics Committee. The kidney cortex (removed from the tumour) was fixed overnight in 10% neutral buffered formalin (Fronine, Taren Point, NSW, Australia) at 4°C followed by embedding in paraffin for subsequent light microscopic evaluation. Four-micrometer-thick paraffin sections were stained with periodic acid-Schiff and Masson trichrome reagent.

For BMP-7 and KLF-6 immunohistochemistry (IHC) similar staining protocols were used. Initial screening of BMP-7 was performed using normal atlas biopsy core blocks provided by Ms Sanaz Maleki from the Cancer Genetics group of the Kolling Institute of Medical Research. The normal body atlas contained core biopsy specimens from normal tissue of kidney, liver, brain, breast, ovaries, uterus, placental, prostate, tonsil, colon, parotid gland, testis, muscle and pancreas. Briefly, after heat treatment for antigen retrieval, endogenous peroxidase was quenched with 3% hydrogen peroxide for 5 mins (Dako Cytochemistry, Tokyo, Japan). Tissues were incubated with the primary polyclonal anti-BMP-7 (1:250 dilutions, Abcam Ltd, Cambridge, UK) and KLF-6 (1:100 dilution, Santa Cruz, CA) at 4°C overnight. This was followed by exposure to equal volumes of Envision dual linked system (Dako Cytochemistry, Tokyo, Japan) for 30 minutes. After two 5 minute

washes, staining was developed with 3.3 diaminobenzidine tetrahydrochloride (Dako Cytochemistry, Tokyo, Japan) for 10 minutes before counterstaining with Mayer's haemotoxylin stains. Sections incubated with anti-rabbit IgG instead of the primary antiserum served as the negative controls. All staining was performed in a same batch on the same day by the same individual.

3.2.11 Immunofluorescence (IF)

IF was performed in paraffinized kidney sections and in cells grown on glass coverslips and fixed in 4% paraformaldehyde in phosphate buffered saline (PBS). For kidneys sections, deparaffinization, rehydration, antigen retrieval and blocking were performed as detailed above. BMPRIA antibody (1:25 dilation, Abcam Ltd, Cambridge, UK) was then incubated with either kidney sections or cells at 4°C overnight, secondary anti-rabbit Alex Fluor® 488 (1:300 dilution, Invitrogen, Australia) was applied after three washes. Slides were then counterstained with DAPI (Invitrogen, CA, USA), mouthed in IF mouthing solution (DAKO, USA) followed by visualization using an Olympus immunofluorescence microscope (Olympus, Japan).

HK2 cells were cultured on glass coverslips to 70-80% confluent and were treated according to experimental protocols. Conditioned media was discarded and cells were fixed with 4% paraformaldehyde after three washes with ice-cold PBS. The cell membranes were permeabilised with ice-cold methanol for 10 minutes and were incubated with the primary anti-BMPIRA (1:25 dilution, Abcam Ltd, Cambridge) for one hour after 30 minutes blocking. Secondary anti-rabbit Alexa Flour® 488 (1:300 dilution, Invitrogen, Australia)

was applied after three washes, counterstained with DAPI, mounted on glass slides and visualised using Olympus immunofluorescence microscope (Olympus, Japan).

3.2.11 Quantitation of immunohistochemistry

The first 10 non-overlapping glomeruli from each sample stained with PAS were selected for analysis. Glomerulosclerosis was scored from 0 to 3; 0 = normal; 1 = 1 to 25% sclerosis; 2 = 26% to 50% sclerosis and 3 = >50% sclerosis. The Automated Cellular Imaging System (ACIS III) (Dako, USA) was used to quantitatively evaluate the glomerular volume (GV), mesangial sclerosis per glomerular volume (Mes/G) and mesangial cell volume per glomerular volume (MC/G) as described in details in Chapter 2. Using Masson's trichrome staining, ten non-overlapping cortical areas at 200x magnification was assessed for tubulointerstitial fibrosis (IF) score; 0 = Normal; 1 = 1 to 25% IF; 2 = 26% to 50% IF and 3 >50% IF. The average of 10 non-overlapping cortical IF scores was used for analysis. Tubular BMP-7 expression was scored by calculating the number of positive-staining tubules in the cortex examined under 200x magnification HFPs. All the analyses were scored by at least two blinded assessors.

3.2.12 BMP-7 ELISA assay

Blood specimens from healthy volunteers and patients with diabetic end stage renal patients on dialysis were collected with consent and immediately spun at 1500rpm for 15 min at 4°C. Serum was collected and stored at -80°C. Similarly, conditioned media from

HK-2 cells transfected with BMP-7 plasmid was collected at the end of 72 hours and centrifuged at 3000 rpm for 10 minutes to remove cell debris and then stored at -80°C. Both human sera and cell supernatant were used for measurement of BMP-7 protein using enzyme-linked immunosorbent assay (R&D Systems, Minneapolis, MN, USA) as per manufacturer's instructions. This assay recognizes recombinant and natural human BMP-7, with no significant cross-reactivity with other BMPs. The recommended minimal detectable concentration (MDD) of BMP-7 was 0.79 pg/ml.

3.2.13 Statistical analysis

Each experiment was performed independently a minimum of five times. Real-time PCR results are expressed as fold change compared with the control value. RT-PCR data are expressed as percentage of control value. Results are expressed as mean ± SEM. Statistical comparisons between groups were made by analysis of variance (ANOVA), with pairwise multiple comparison by Fisher's protected least-significant difference test. Analyses were performed using the software package Statview, version 4.5 (Anacus Concepts Inc, Berkeley CA, USA). P values <0.05 were considered significant.

3.3 Results

3.3.1 BMP-7 and BMP receptor expression in HK-2

RT-PCR confirmed the presence of all BMP receptors' mRNA, namely BMPR-IA, BMPR-IB, ALK-2 and BMPR-II receptors in both HK-2 and primary culture of human PTC (Figure 3.3.1.1A & B). Each of the primers was amplified at 30 cycles. BMP-7 mRNA was easily detected in human kidney cortex. However, no basal BMP-7 mRNA or protein was detected in either HK-2 cells or PTC (Figure 3.3.1.1C). IHC confirmed membrane and cytoplasmic staining for BMP-7 in distal tubules and/or collecting duct epithelial cells. No staining was observed in proximal tubules or glomeruli (Figure 3.3.1.1D)

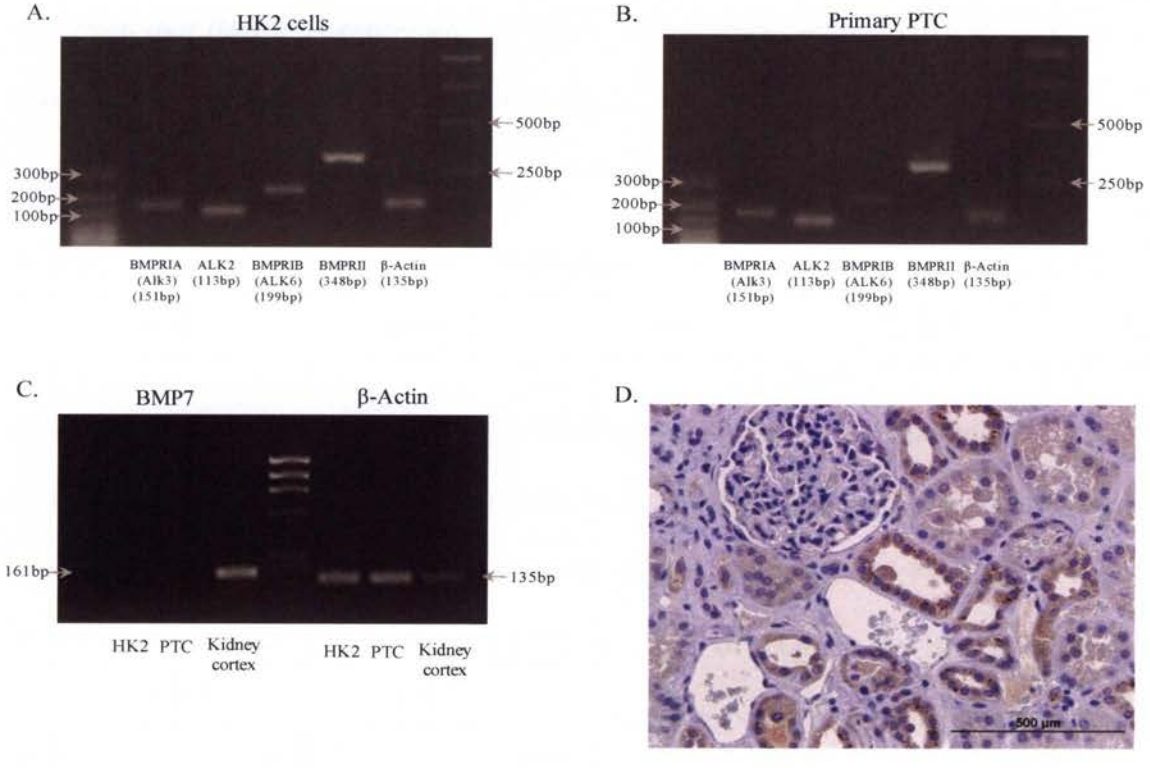

Figure 3.3.1.1 Type I and type II BMP receptors expression in human proximal tubular cells.

The human proximal tubular cell line (HK-2) possesses both type I and type II BMP receptors namely, BMPR-IA, also known as activin receptor-like kinase-3 (ALK-3) (151bp), BMPR-IB/ ALK-6 (199bp), ALK-2(113bp) and BMPR-II (348bp). BMPR-II is ubiquitously expressed (A). mRNA of all these receptors is similarly detected in primary proximal tubular epithelial cells (PTC). However, BMPR-IB mRNA is minimally expressed in PTC as compared to HK-2 cells (B). β-Actin was used as the endogenous internal control gene. BMP-7 mRNA (161bp) is abundantly expressed in the kidney cortex. However, BMP-7 mRNA could not be detected in HK-2 cells or in proximal tubular cells in primary culture (C). Immunohistochemistry of normal adult human kidney cortex confirmed that BMP-7 is expressed only in the distal tubules or collecting duct, but is not found in the proximal tubules or glomeruli (D).

3.3.2 BMP receptor expression inTGF-β1 treated HK-2 cells

Exposure of HK-2 cells to 0.5 ng/ml TGF-β1 significantly suppressed BMPR-IA mRNA expression at 48 hours to 0.5 ± 0.1-fold ($p \leq 0.01$) and at 72 hours to 0.8 ± 0.0-fold ($p<0.01$) as compared to control (Figure 3.3.2.1A). BMPR-IA protein expression was also significantly suppressed after exposure to TGF-β1 for 72 hours to 37.9 ± 7.8% of control ($p<0.05$) (Figure 3.3.2.2A). The suppressive effect of TGF-β1 on BMPR-IA protein expression was dose dependent. Twenty-four hours exposure to 0.2ng/ml, 0.5 ng/ml, 1 ng/ml or 2 ng/ml TGF-β1 significantly reduced BMPR-IA protein expression to 71.2 ± 12.5% ($p<0.05$), 38.8 ± 3.3% ($p<0.01$), 28.6 ± 3.9% ($p<0.01$) and 19.65 ± 6.0% ($p<0.01$) of

the control value respectively (Figure 3.3.2.2B). Subsequently, 0.5 ng/ml TGF-β1 was chosen for experimental studies, due its suppressive effect on BMPR-IA and its ability to induce EMT.

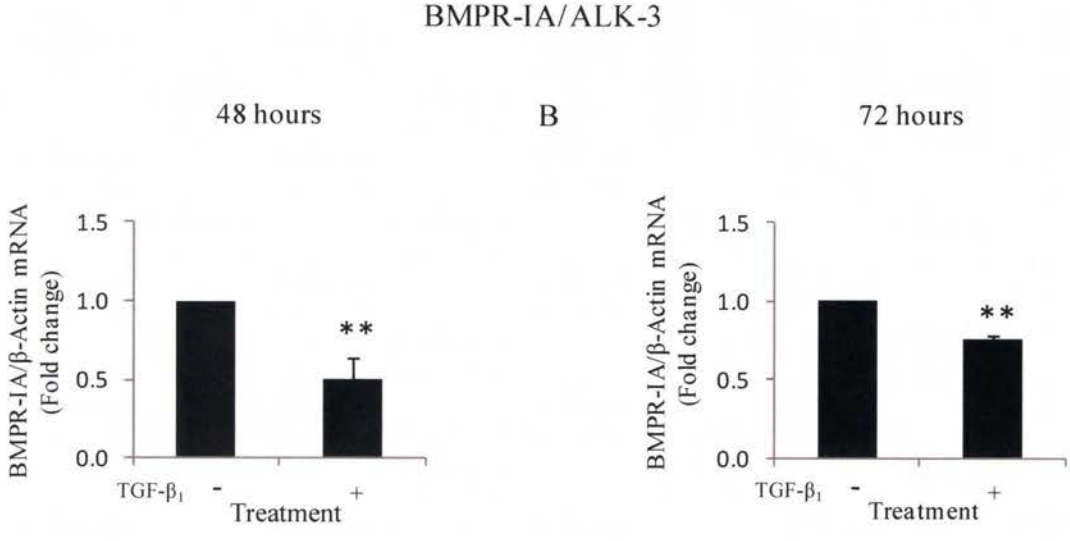

Figure 3.3.2.1 Effect of TGF-β1 on BMPR-IA mRNA and protein expression.

Exposure of HK2 cells to 0.5ng/ml of recombinant human TGF-β1 (rhTGF-β1) suppresses BMPR-IA mRNA expression at both 48 and 72 hours (A & B). All cells were cultured in 5mM D-Glucose unless otherwise specified. All data were expressed in mean ± SEM *(**$p<0.01$ vs. Control, $n=5$).*

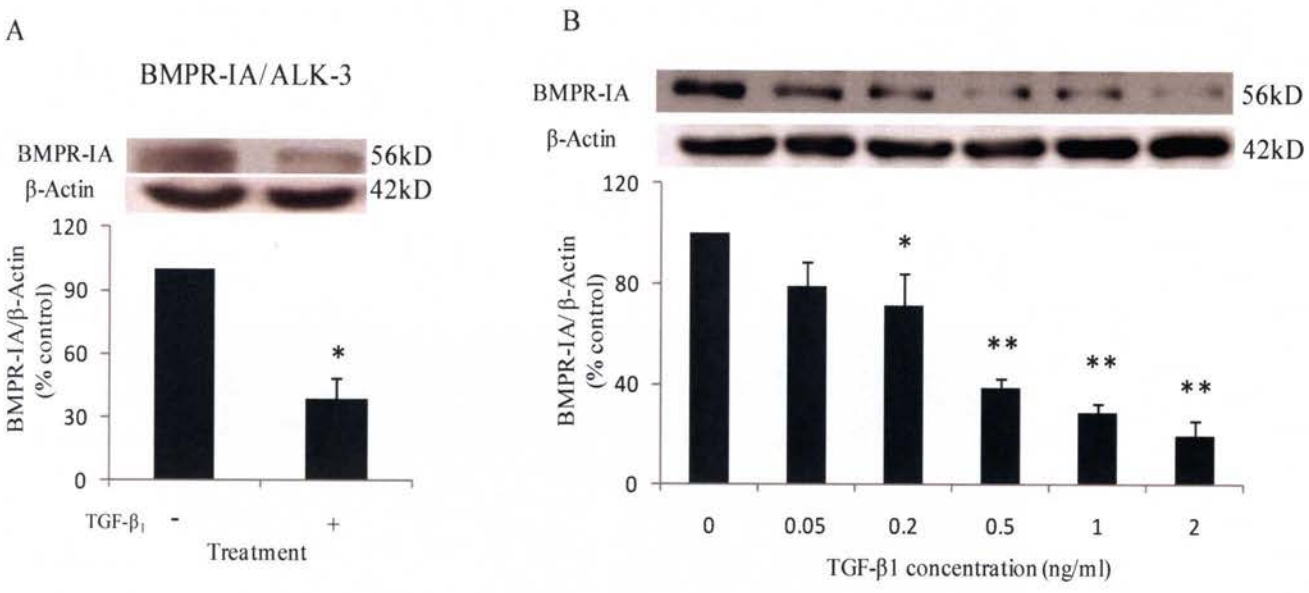

Figure 3.3.2.2 Effects of TGF-β1 exposure on BMPR-IA protein expression.

*Down-regulation of BMPR-IA protein expression is TGF-β1 dose dependent, and is also significantly suppressed by at 72 hours (A). The suppressive effect of BMPR-IA protein expression is TGF-β1 dose dependent and reaches statistical significance with 0.2ng/ml of rhTGF-β1 (B). Results are expressed as mean ± SEM, *$p<0.05$, ** $p<0.01$ vs. Control, $n=3$)*

0.5ng/ml TGF-β1 is sufficient to induce EMT in HK-2 cells as shown in Figure 3.3.2.3. Cells exposed to TGF-β1 also showed lower expression of BMPR-IA expression as compared to the controls.

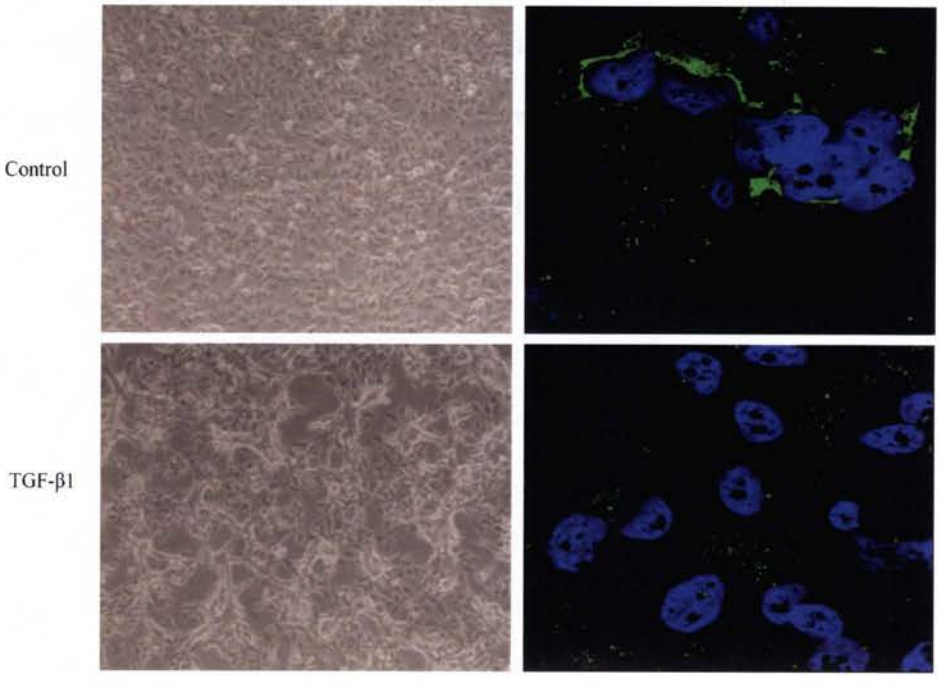

Figure 3.3.2.3 EMT and BMPR-IA expression in HK-2 cells.

Twenty four hours exposure of 0.5 mg/ml of rhTGF-β1 changed the normal appearance of cobble stone-like HK-2 cells (Left upper panel) to elongated, spindle shape-like myofibroblastic cells, suggestive of EMT (Left lower panel). When these cells were stained using Immunofluorescence techniques for BMPR-IA, control HK-2 cells exhibit higher amount of membrane BMPR-IA staining (Green, Right upper panel) as compared to the HK-2 cells exposed to TGF-β1 (Right lower panel). DAPI was used to stained nuclei (Blue).

Conversely, TGF-β1 paradoxically increased ALK-2 and BMPR-IB mRNA expression. BMPR-IB mRNA expression was increased to 1.5 ± 0.1-fold at 48 hours ($p<0.05$) and to 2.0 ± 0.3-fold at 72 hours ($p<0.05$) when compared to the control (Figure 3.3.2.4A). Similarly, ALK-2 mRNA expression increased upon exposure to TGF-β1 to 2.0 ± 0.2-fold at 48 hours ($p<0.05$) and to 2.2 ± 0.3-fold at 72 hours ($p<0.05$) when compared to the control (Figure 3.3.2.4B). TGF-β1 also induced BMPR-II mRNA expression to 1.6 ±.0.1-fold ($p<0.05$), but not at the 72 hour time point (Data not shown).

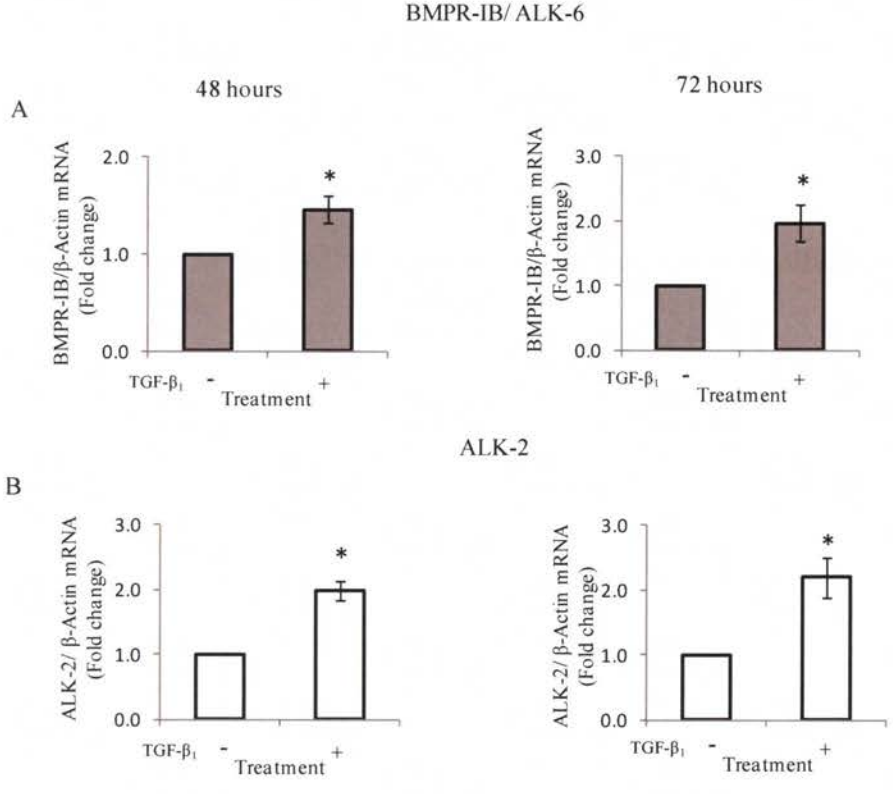

Figure 3.3.2.4 Effect of TGF-β1 on BMPR-IB and ALK-2 mRNA expression.

*Unlike its effect on BMPR-IA expression, TGF-β1 up-regulates BMPR-IB and ALK-2 mRNA expression at both time points (A & B). Results are expressed as mean ± SEM, *$p<0.05$ vs. Control, $n=5$).*

3.3.3 TGF-β1 suppression of BMPR-IA in HK-2 cells is reversible

To assess if the suppressive effect of TGF-β1 on BMPR-IA expression is reversible, HK-2 cells were exposed to 0.5ng/ml of TGF-β1 for 24 hours following which TGF-β1 was removed and replaced with normal conditioned media, labelled as without (W/O) TGF-β1. Concurrently, another group of HK-2 cells were continuously exposed to 0.5ng/ml of TGF-β1, labelled as with TGF-β1 (*Figure 3.3.3.1*). Cell lysates were collected at various time points indicated. HK-2 cells not exposed to TGF-β1 at 96 hours were used as the positive control. Both groups showed comparable reduction in BMPR-IA protein expression 24 hours post initial exposure to TGF-β1. The W/O TGF-β1 groups demonstrated recovery of the BMPRIA which reached statistical significance at 72 hours ($p<0.01$) and 96 hours ($p< 0.001$). However, the recovery of BMPR-IA was not observed in the ongoing presence of a low concentration of TGF-β1. No BMP-7 mRNA expression could be detected in the control and TGF-β1 treated groups (data not shown).

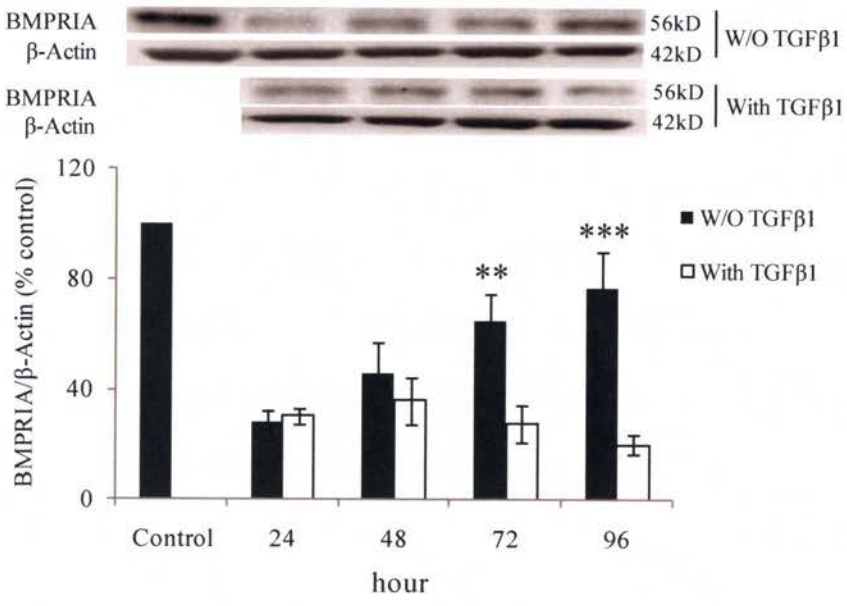

Figure 3.3.3.1The suppressive effect of TGFβ-1 on BMPR-IA protein expression was reversible.

*HK-2 cells were exposed to 0.5ng/ml of TGF-β1 for 24 hours following which TGF-β1was removed and replaced with normal conditioned media (W/O TGF-β1). Concurrently, another group of HK-2 cells were continuously exposed to 0.5ng/ml of TGF-β1 (With TGF-β1). Cell lysates were collected at various time points indicated; the control being HK-2 cells in the absence of TGF-β1 at 96 hours. Both groups exhibited similar amount of BMPR-IA protein expression at 24 hours post exposure to TGF-β1 (27.8 ± 4.7% (W/O TGF-β1) vs. 30.2 ± 3.1% (With TGF-β1). The W/O TGF-β1 groups demonstrated recovery of the BMPR-IA which reached statistical significance at 72 hours (64.4 ± 10.3% (W/O TGF-β1) vs. 27.5 ± 6.8% (With TGF-β1), ** $p<0.01$) and 96 hours (77.1 ± 13% (W/O TGF-β1) vs.20.4 ± 3.6% (With TGF-β1), *** $p< 0.001$). However, the recovery of BMPR-IA was not observed in the ongoing presence of a low concentration TGF-β1. All experiments were done in at least triplicate at all time points.*

3.3.4 BMP receptors expression on exposure to 25mM D-Glucose

Thirty mM of D-glucose (high glucose) had no effect on the mRNA expression of any BMP receptor subtype: namely BMPR-IA, 1.02 ± 0.0-fold; BMPR-IB, 1.1 ± 0.2-fold and ALK-2, 0.9 ± 0.4-fold at 72 hours when compared to 5 mM glucose (Figure 3.3.4.1A, B & C). Data as shown is for the 72 hours time point. Similar results were seen at all time points namely 24, 48 and 72 hours by RT-PCR (data not shown). Exposure to independent osmotic stress similarly did not affect the expression level of these receptors. No BMP-7 mRNA expression could be detected in HK-2 cells exposed to TGF-β1 or high glucose exposed HK-2 cells.

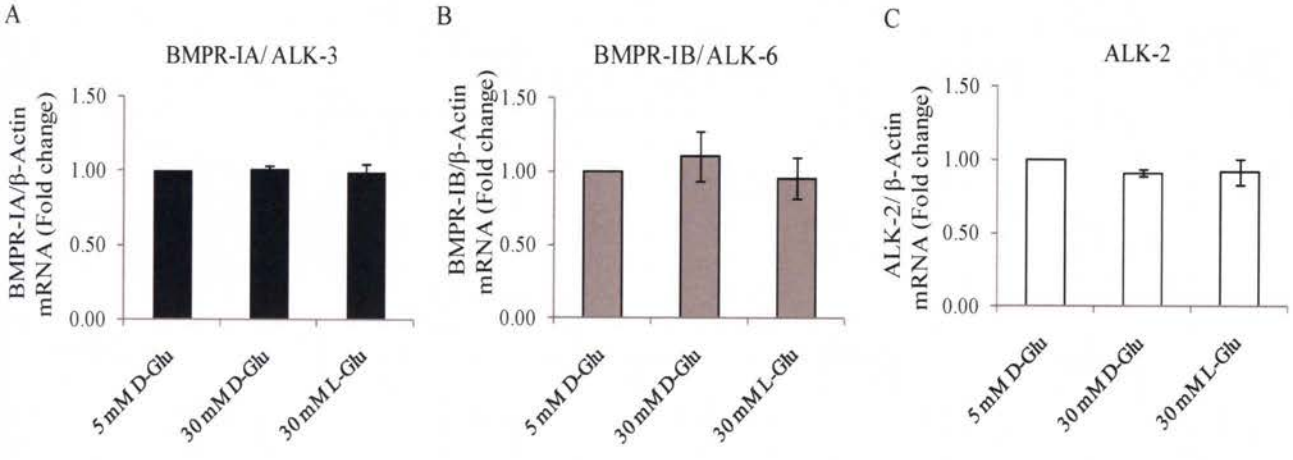

Figure 3.3.4.1 Effect of 30 mM D-Glucose on BMP receptor expression.

When HK-2 cells were cultured in 30 mM D-Glucose (high glucose) for 24, 48 and 72 hours, BMP receptors' mRNA expression was not changed in the presence of high glucose. 72 hours' real time PCR data are shown (A, B & C). Five mM D-Glucose and twenty-five mM L-Glucose were used as an osmotic control. Similarly no regulation of BMP receptor mRNA expression was observed. Results are expressed as mean ± SEM, (n=5).

3.3.5 BMP receptor expression in KLF-6 over-expressing HK-2 cells

The optimal concentration of 8µl per well of cells of Lipofectamine 2000 was determined using flow cytometric analysis, to achieve ≥ 90% of transfection efficiency as shown in Figure 3.3.5.1.

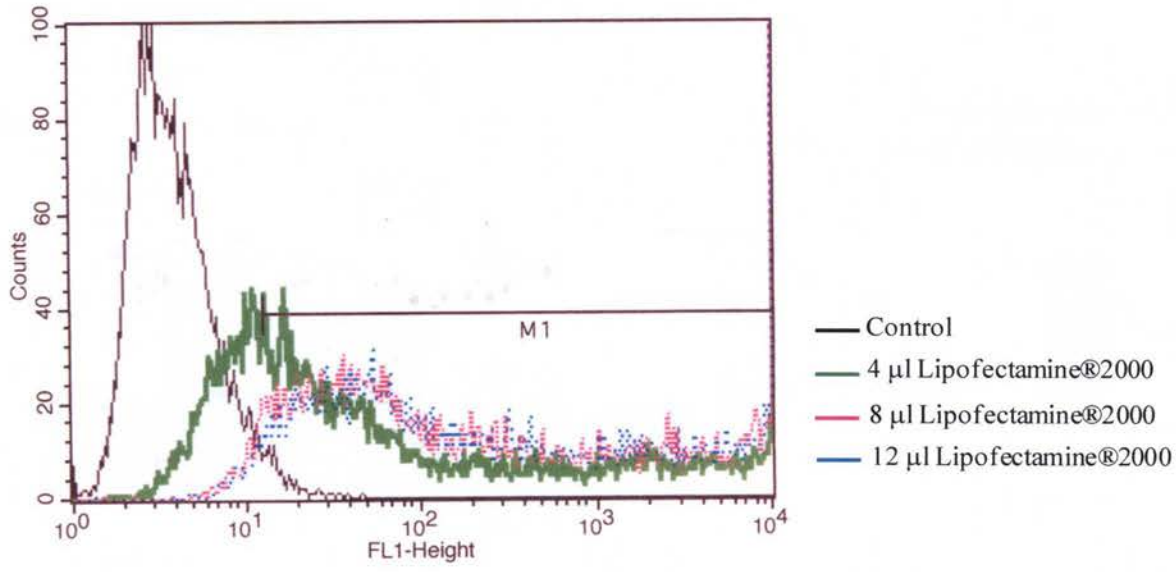

Figure 3.3.5.1 Determination of optimal concentration of transfection reagent using a GFP labelled plasmid.

The background fluorosence was first analysed using no GFP-labelled plasmid as a baseline. Almost 70% of the HK-2 cells were GFP positive when 4 µl of Lipofectamine®2000 was used as the transfection agent (___). When 8 µl (___) of transfecting agent was used, 97% of the cells were labelled and 93% when 12 µl (___) of lipofecatimine®2000 was used. Hence, 8 µl of transfecting agent was subsequently used for all over-expression experiments.

KLF-6 plasmid transfection increased KLF-6 mRNA expression by 9 fold ($p<0.01$) (Figure 3.3.5.2A). This was reflected in a 239.4 ± 29.7% ($p<0.01$) greater amount of KLF6 protein expression when compared to the empty vector (EV) control cells (Figure 3.3.5.2B). Mock transfection (transfection agent alone) did not increase KLF-6 protein level (data not shown).

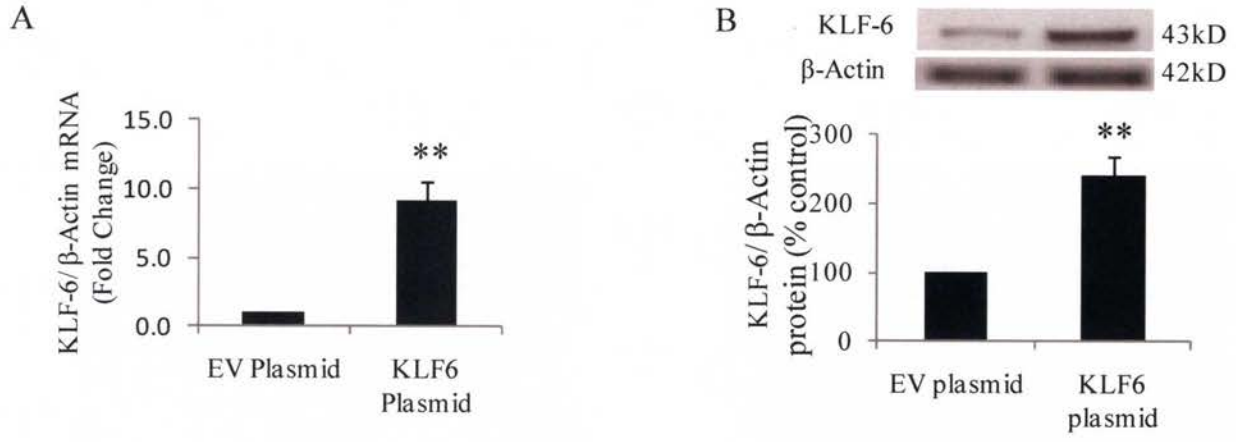

Figure 3.3.5.2 KLF-6 plasmid transfection.

*KLF-6 plasmid transfection was confirmed by markedly increased KLF-6 mRNA and protein analysis as compared to empty vector (EV) transfection (A & B)(**p<0.01 vs. Control, n=5).*

In addition to the western blot studies, the efficiency of KLF-6 transfection was assessed by immunofluorescence techniques using polyclonal anti-KLF-6 antibody. More than 60% HK-2 cells were stained positively for KLF-6 (Figure 3.3.5.3B) in their nuclei when compared to cells transfected with empty vector (EV) as shown in Figure 3.3.5.3A.

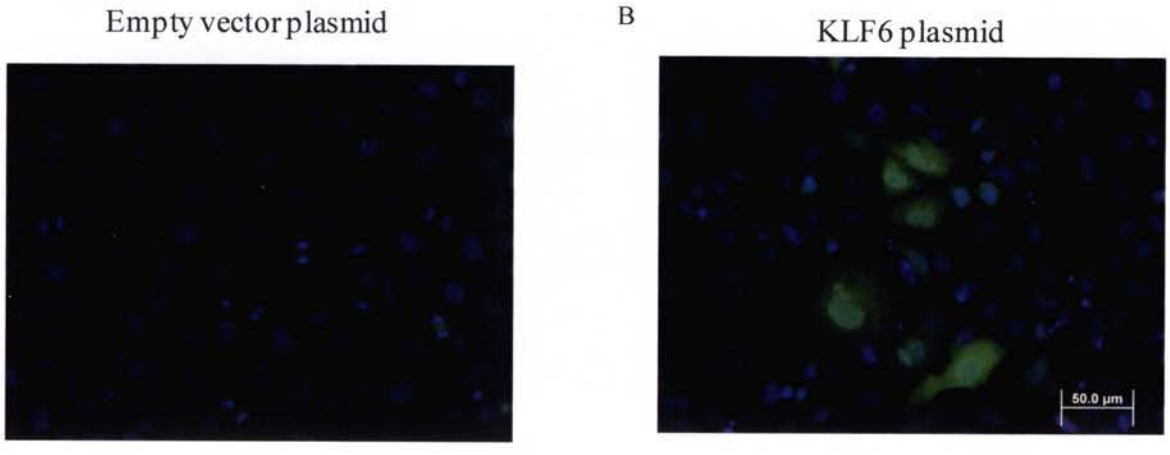

Figure 3.3.5.3 Confirmation of HK-2 cells over-expressing KLF-6 by immunofluorescence.

Using Immunofluorescence technique, KLF-6 was detected in the nuclei of HK-2 transfected with KLF-6 plasmid (Green, Alexa Fluor 488) (B) when compared with HK-2 cells transfected empty vector (EV) (A) which showed negligible KLF-6 nuclear staining.

When BMP receptors were examined in these KLF-6 over-expressing cells, BMPR-IA, BMPR-IB and ALK-2 receptors were found to be significantly suppressed as compared to the control, 0.7 ± 0.1 ($p<0.01$), 0.4 ± 0.1 ($p<0.05$) and 0.7 ± 0.1 ($p<0.01$) (Figure 3.3.5.4A, C & D). BMPR-IA protein expression was also significantly suppressed to 56.8 ± 7.5% as compared to the control cells ($p<0.01$) (Figure 3.3.5.4B). The suppressive effect of KLF-6 on BMPR-IA expression is further confirmed by BMPR-IA IF staining (Figure 3.3.5.5).

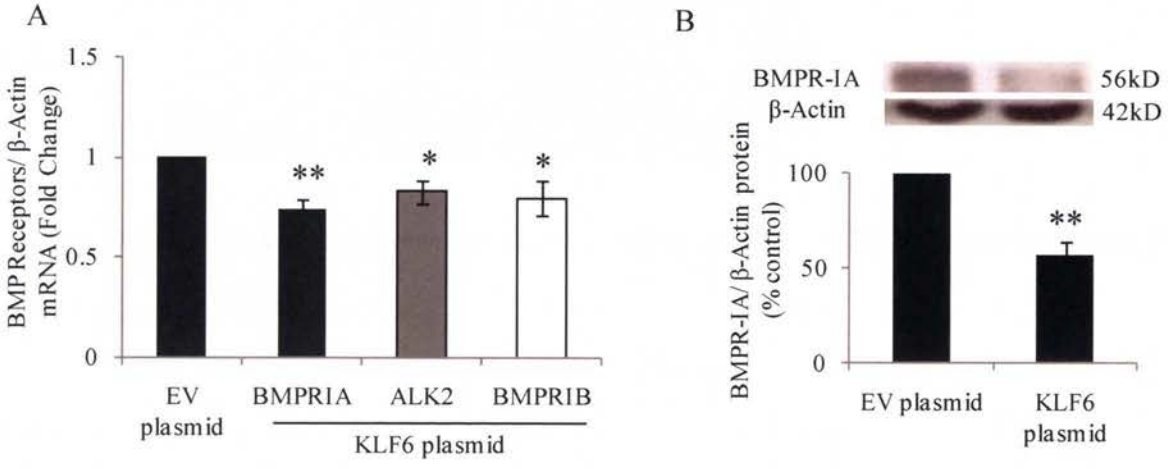

Figure 3.3.5.4 KLF-6 over-expression suppresses the expression of all type I BMP receptor subtypes.

*Cells over-expressing KLF-6 exhibit significantly lower mRNA expression of all type I BMP receptors subtypes. KLF-6 plasmid transfection most significantly suppressed BMPR-IA and ALK-2 (A & D). BMPR-IA protein expression is significantly suppressed at 72 hours in HK-2 cells over-expressing KLF-6 (B). Results are expressed as mean ± SEM ** $p<0.01$, * $p<0.05$ vs. Control ($n=5$).*

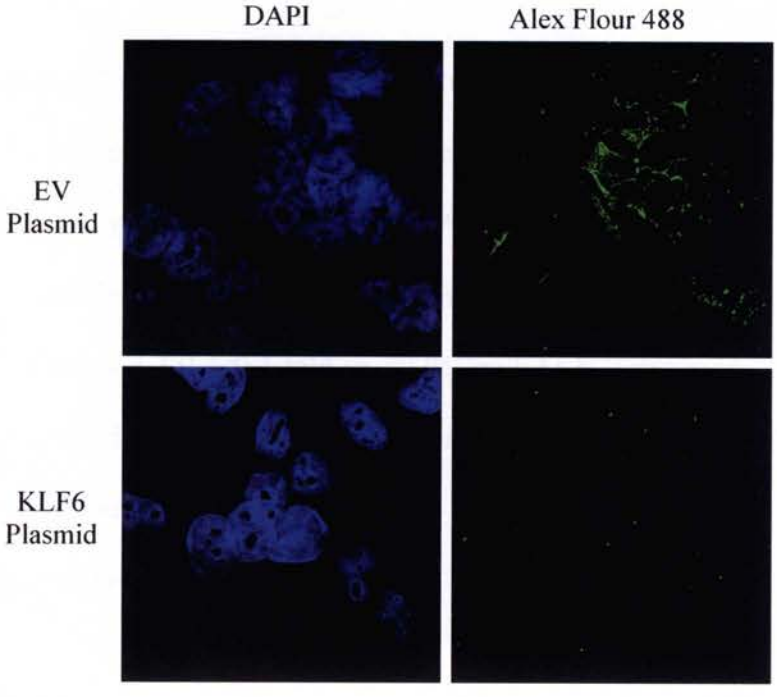

Figure 3.3.5.5 Immunofluorescence staining of BMPR-IA in KLF-6 over-expressing HK-2 cells.

HK-2 cells cultured on glass cover slips to achieve 70-80% confluence, and were followed by KLF-6 plasmid transfection. Twenty four hours later, these cells were fixed, blocked and stained with BMPR-IA (1:25 dilution). Nuclei of these cells were counter stained with DAPI (Blue). Upper panel shows HK-2 cells transfected with an empty vector (EV) plasmid have high basal expression of BMPR-IA (green). The BMPR-IA expression was markedly down regulated in KLF6 over-expressing cells (lower right panel).

3.3.6 BMP receptor expression in KLF6 siRNA treated cells

KLF-6 mRNA expression was silenced using siRNA specifically targeting KLF-6 (Figure 3.3.6.1A, $p<0.0001$), which translated to a reduced protein expression of 12.9 ± 1.5% of control ($p<0.0001$) (Figure 3.3.6.1B). KLF-6 silenced HK-2 cells exhibited significantly greater BMPR-IA mRNA expression, 2.1 ± 0.2-fold ($p<0.01$) as compared to non specific (NS) siRNA treated cells (Figure 3.3.6.2A). BMPR-IB receptor mRNA was also increased 1.9 ± 0.2-fold ($p <0.05$) and ALK-2 receptors mRNA increased 1.8 ± 0.1-fold ($p<0.05$) as compared to cells transfected with a non-specific siRNA (Figure 3.3.5.2B & C). These data confirm that KLF-6 plays a regulatory role in BMP receptor mRNA and protein expression.

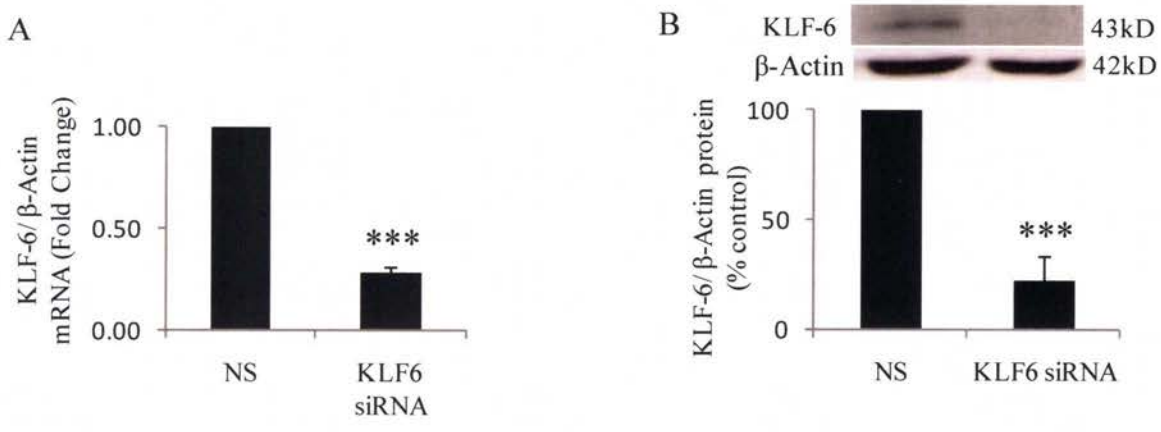

Figure 3.3.6.1 KLF-6 Silenced HK-2 cells.

*Silencing of KLF-6 using siRNA techniques. KLF-6 knock-down is achieved by transfecting HK-2 cells with siRNA specific for KLF-6. Knock-down of KLF-6 is confirmed by mRNA and protein analysis compared to results in transfected cells with non specific (NS) siRNA (A & B). Results are expressed as mean ± SEM, ***p <0.0001 vs. Control, (n=5).*

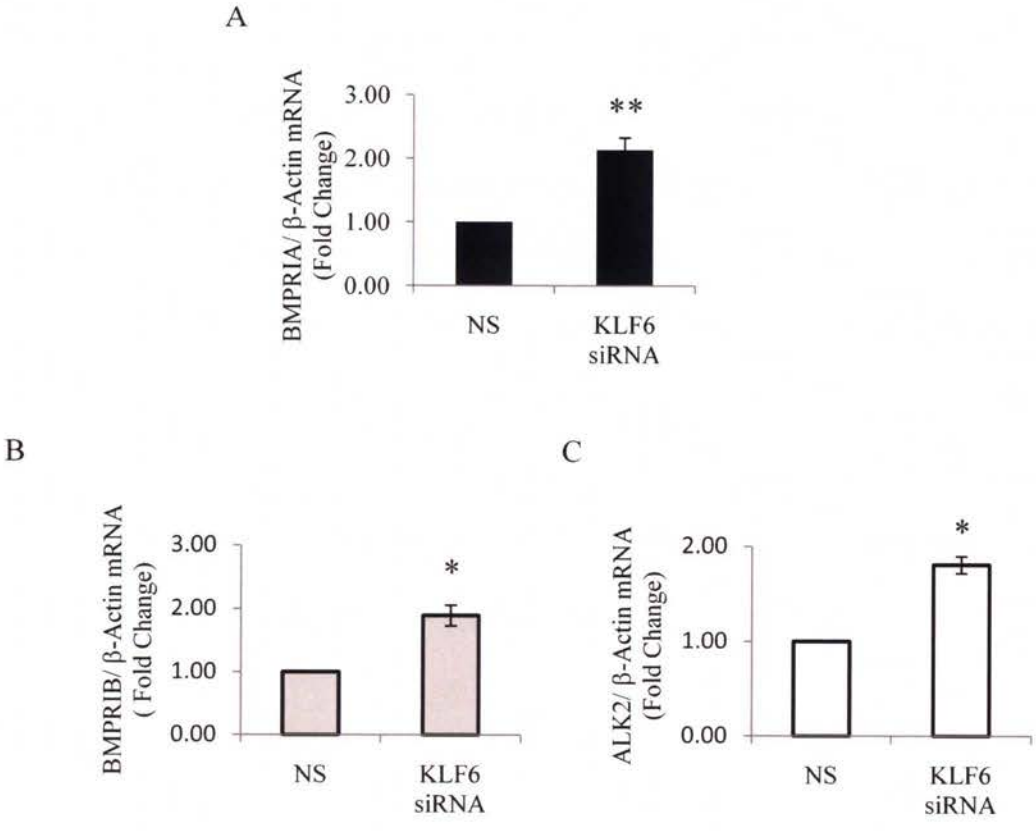

Figure 3.3.6.2 Effects of KLF-6 silencing on BMP receptors mRNA expression.

*BMPR-IA mRNA expression is significantly increased in KLF-6 knock-down cells (A). KLF-6 knock-down also increased BMPR-IB and ALK-2 mRNA expression (C & D). These results confirm that KLF-6 has a regulatory role on type I BMP receptor expression. Results are expressed as mean ± SEM ** $p<0.01$, *$p<0.05$ vs. control, (n=5).*

3.3.7 KLF-6 silencing rescued TGF-β1 induced BMPR-IA suppression

We have shown HK-2 cells exposed to 0.5 ng/ml of TGF-β1 suppressed BMPR-IA mRNA and protein expression (section 3.3.2). We have also demonstrated that KLF-6 silenced HK-2 cells exhibited significantly greater BMPR-IA mRNA (Figure 3.3.6.2A). Figure 3.3.7.1 shows that KLF-6 silenced HK-2 cells have greater BMPR-IA protein expression, 149.8 ± 10% as compared to the control. When HK-2 treated with NS siRNA were exposed to 0.5ng/ml of TGF-β1 for 24 hours, BMPR-IA is significantly suppressed to 65 ± 3.2% as compared to the control groups ($p<0.01$). However, when KLF-6 silenced cells were exposed to 0.5ng/ml of TGF-β1 for similar duration, BMPR-IA expression is 110.1 ± 6.4% vs. control. These data confirm that silencing of KLF-6 in HK-2 cells is able to rescue TGF-β1 suppression on BMPR-IA expression and strongly suggests that KLF-6 has a regulatory role in BMPR-IA expression.

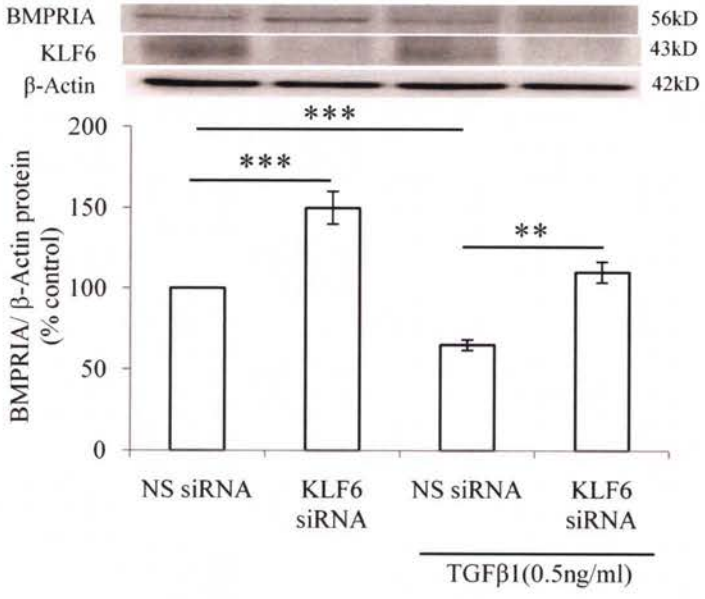

Figure 3.3.7.1 KLF-6 knock-down rescues TGF-β1-induced suppression on BMPR-IA in HK-2 cells.

*KLF-6 knock-down HK-2 exhibits greater BMPR-IA protein expression as compared to the control. When HK-2 cells treated with NS siRNA were exposed to 0.5 ng/ml of TGFβ1 for 24 hours, BMPRIA expression was markedly down regulated. However the suppressive effect of TGFβ1 on BMPRIA expression was not seen in KLF6 silenced cells (***p< 0.0001, **p<0.01, n=4).*

3.3.8 BMPR-IA, ALK2 and BMP-7 mRNA expression in diabetic Ren-2 rat kidney

Diabetic animals (n=5) exhibited an elevated blood sugar and HbA1c, 32.8 ± 0.19mmol/L ($p<0.0001$) and 11.4 ± 0.38% ($p<0.0001$) as compared to their non-diabetic counterparts, 5.8 ± 0.29mmol/L and 3.8 ± 0.05% respectively. These animals have increased urinary albumin excretion, 81 ± 1.3 vs. 14 ± 1.2mg/day ($p<0.05$) (Table 3.3.8.1). We have previously demonstrated that KLF-6 is up-regulated in the kidneys of diabetic Ren-2 rats at 16 weeks.

Table 3.3.8.1. **Animal characteristics**

Group	n	Body weight (gm)	Blood glucose (mmol/L)	HbA1c (%)	AER (mg/24hours)	SBP (mmHg)
Control (Ren-2)	5	294 ± 11.5	5.8 ± 0.29	3.8 ± 0.05	14 ± 1.2	155 ± 1
Diabetic (Ren-2)	5	272 ± 11.9	32.8 ± 0.18***	11.4 ± 0.38***	81 ± 1.3*	188 ± 7

Values are expressed as means ± SEM
*$p<0.05$ versus Ren-2 control
***$p<0.0001$ versus Ren-2 control

BMPR-IA mRNA was significantly reduced in the kidney cortex of the STZ-induced diabetic rats, 0.7 ± 0.1-folds ($p< 0.05$) as compared to the non-diabetic rats (Figure 3.3.8.1A). ALK-2 mRNA expression was more markedly attenuated to 0.5 ± 0.1-fold ($p<0.01$) (Figure 3.3.8.1B). Anti-BMPR-IA antibody used in western blotting was not suitable for immunohistochemistry in rat kidneys. Kidney cortex BMP-7 mRNA was significantly reduced in these diabetic rats, 0.9 ± 0.0-fold ($p<0.05$) (Figure 3.3.8.1C). Even though the *in vitro* data suggests that TGF-β1 has differential stimulatory and inhibitory role on BMP receptors expression in human proximal tubule cells, the *in vivo* data suggests a longer term net suppressive effect of TGF-β1 on BMP-7 and all of its receptors in an

endogenously TGF-β1-rich animal model. Together with our previous published data, we conclude that both KLF-6 and TGF-β1 have a regulatory role on BMP receptors.

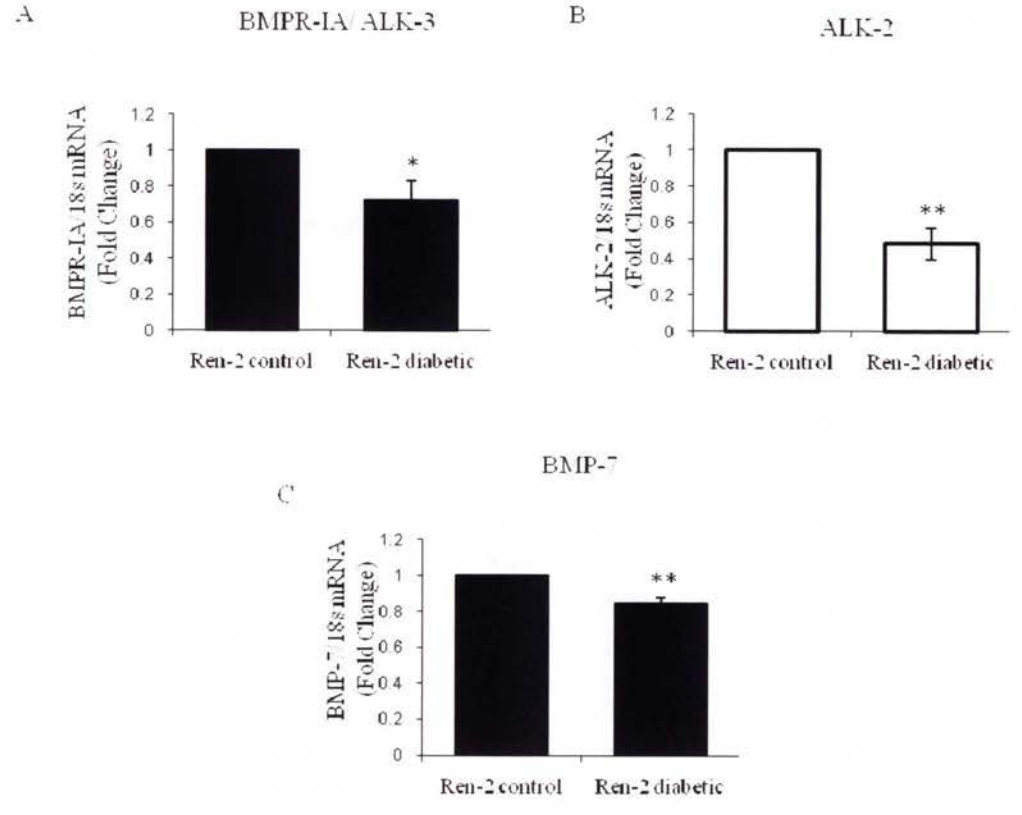

Figure 3.3.8.1 BMP-7 and BMP receptors mRNA expression in the Ren-2 diabetic rat.

*Ren-2 diabetic rats sacrificed at 16 weeks post streptozotocin-induced diabetes exhibit significantly lower expression of BMPR-IA and ALK-2 mRNA as compared to the control animals (n=5, A & B). These animals also exhibit significantly lower BMP-7 mRNA as compared to their non-diabetic counterpart (C). Results are expressed as mean ± SEM, ** $p<0.01$, * $p<0.05$ vs. Control, n=5 each groups.*

3.3.9 Effect of rhBMP-7 on EMT

To ascertain the effect of BMP-7 on EMT and fibrosis, we initially used recombinant human BMP-7. Cell proliferation studies using various concentrations of rhBMP-7 demonstrated no proliferative or cytotoxic effect on HK-2 cells, even at supraphysiological concentrations of 2000 ng/ml (Figure 3.3.9.1) at 72 hours. 1000ng/ml of rhBMP-7 was used for subsequent experiments to reverse TGF-β1 induced EMT.

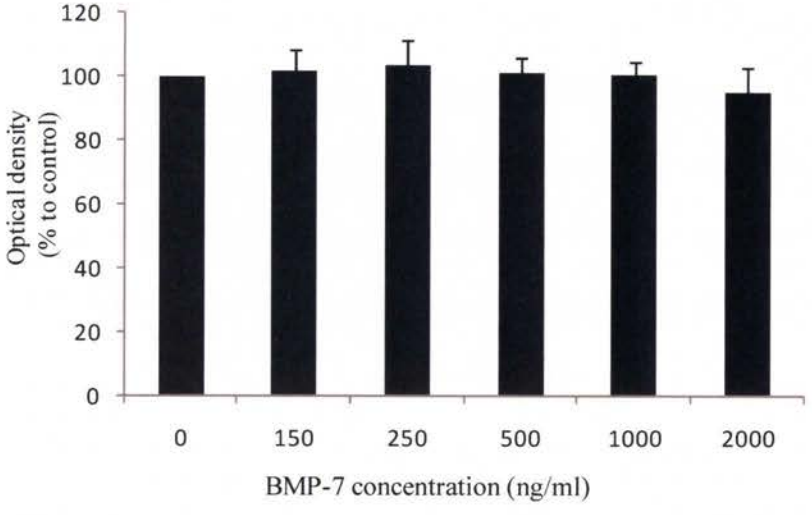

Figure 3.3.9.1 Effect of recombinant human BMP-7 on HK-2 cell proliferation and cytotoxicity.

Subconfluent HK2 cells grown in 96-well plates were incubated with various concentrations of rhBMP7 for 72 hours. Media were changed at 48 hours. rhBMP7 exerted no cytotoxic or proliferative effects on HK-2 cells, even at the high concentration of 2000ng/ml.

E-cadherin is a Ca^{2+}-dependent cell adhesion molecule that plays an important role in the development and maintenance of renal epithelial polarity. Loss of E-cadherin expression is considered to be one of the earliest changes in EMT. We have established the minimum required dose of 0.5ng/ml of rhTGFβ1 to induced EMT in HK2 (Figure 3.3.9.2). We have demonstrated that exposure to 0.5 ng/ml of TGF-β1 for 72 hours significantly suppressed E-cadherin mRNA expression to 32 ± 2.4% as compared to cells not exposed to TGF-β1 (Figure 3.3.9.3A, lane 2, $p<0.0001$), and this was associated with increases in the mesenchymal marker vimentin mRNA, to 128 ± 5.5% of the control (Figure 3.3.9.3B, lane 2, $p<0.05$). The suppressive effect on E-cadherin mRNA expression by TGF-β1 was seen despite removal of TGF-β1 from the media after 24 hours of exposure, 40 ± 5.5% (Figure 3.3.9.2A, lane 4, $p<0.0001$). Co-incubation of TGF-β1 and BMP-7, even at the supraphysiological dose of 1000 ng/ml, failed to restore TGF-β1-induced E-cadherin loss (44 ± 5.9%, Figure 3.3.9.2A, lane 3, $p<0.0001$). However, if TGF-β1 was removed after 24 hours and the cells were subsequently exposed to 1000 ng/ml of BMP-7, E-cadherin mRNA expression was significantly restored to 70 ± 7.9% (Figure 3.3.9.2A, lane 5, $p<0.01$). In parallel, the increased vimentin mRNA expression was reversed towards baseline; 104 ± 10.1% (Figure 3.3.9.2B, lane 5, $p<0.05$). These data suggest any therapeutic effect of BMP-7 is limited in the presence of TGF-β1.

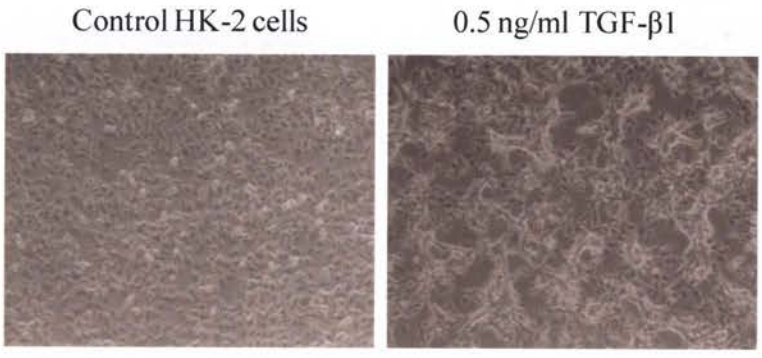

Figure 3.3.9.2 TGF-β1 induces EMT in HK-2 cells.

HK-2 cells are monolayer, cuboidal epithelial cells (Left). After 24 hours exposure to 05 ng/ml of TGF-β1, these cells acquired a phenotype of elongated, spindle shape, occasional clumped, myofibroblastic-looking cell indicated EMT (Right).

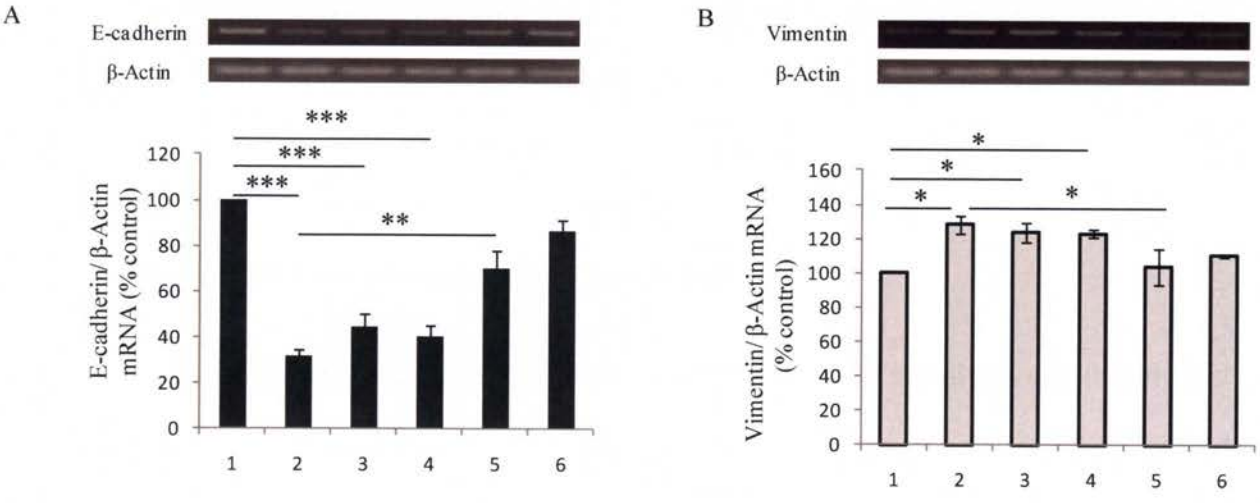

Figure 3.3.9.3 BMP-7 was able to reverse EMT only in the absence of TGF-β1.

Lane 1= Normal standard medium; Lane 2 = TGF-β1 (0.5ng/ml) only for 72 hours; Lane 3 = TGF-β1(0.5ng/ml) and BMP-7(1000ng/ml) for 72 hours; Lane 4 = TGF-β1(0.5ng/ml) for first 24 hours followed by standard medium for another 48 hours; Lane 5 = TGF-β1(0.5ng/ml) for first 24 hours followed by BMP-7(1000ng/ml) for next 48 hours ; Lane 6 = BMP-7 (1000ng/ml) only.

*Twenty-four hours' exposure to 0.5 ng/ml of TGF-β1 is sufficient to induce EMT in HK-2 cells, as indicated by loss of E-cadherin and induction of vimentin (Figure 3.3.9.1A & B, Lane 2). HK-2 cells exposed to TGF-β1 alone, TGF-β1 for the first 24 hours or both TGF-β1 and BMP-7 (lane 2, 3 & 4), all exhibit lower E-cadherin expression as compared to control (***$p<0.0001$) and significantly increased vimentin mRNA expression (*$p<0.05$). Removal of TGF-β1 from the media alone did not restore markers of EMT to normal. However, removal of TGF-β1 from the media followed by exposure to high dose BMP-7 (1000 ng/ml) significantly restored the TGF-β1 induced loss of E-cadherin (**$p<0.01$) and*

*gain of vimentin (*p<0.05) (Figure 3.3.9.1.A & B, Lane 5). Results are expressed as mean ± SEM, ***p<0.0001, ** p<0.01, *p<0.05 vs. Control, n=4.*

3.3.10 rhBMP-7 and phosphorylated Smad1/5/8

Smad proteins are essential components of TGF/ BMP signalling that link ligand/ receptor signals to transcriptional control. All members possess two highly conserved MAD homology domains in the amino (MH1) and carboxyl (MH2) terminus that are connected by a proline-rich non-conserved region. Stimulation of cells with BMP-7 leads to phosphorylation of endogenous Smad1/5/8 which associates with co-factor Smad4 before translocating into the nucleus to induce the promoter of the target gene. On the other hand, Smad 2/3 are the downstream signalling pathway for TGF-β1. There is no cross-reactivity between TGF-β1 and BMP-7 other than their common involvement with Smad 4, which both these cytokines require for nuclear translocation. We first demonstrated that phosphorylation of Smad1/5/8 occurred as early as 15 minutes after exposure to rhBMP7, and peaked at 2 hours post exposure. A significant elevation was only observed up to 2 hours post exposure to rhBMP-7. Subsequently, pSmad 1/5/8 levels remained between peak and control values for up to 24 hours then declined to baseline by 48 hours (Figure 3.3.10.1). Phosphorylation of Smad1/5/8 is dependent on the concentration of rhBMP-7 to which the HK-2 cells were exposed. The higher the concentration of rhBMP-7, the more pSmad1/5/8 was recruited (Figure 3.3.10.2). When cells were exposed to 500 ng/ml and 1000ng/ml of BMP-7 for 2 hours, pSmad1/5/8 was significantly increased to 243.4 ± 55.3% ($p<0.05$) and 368 ± 33.3% ($p<0.01$) compared to baseline values.

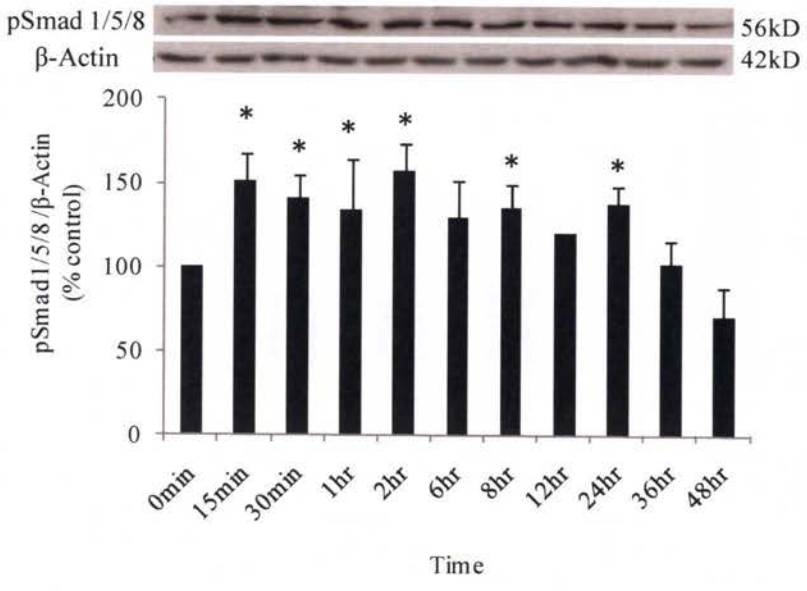

Figure 3.3.10.1 Phosphorylation of Smad1/5/8 after exposure to rhBMP7.

*HK-2 cells were exposed 1000ng/ml of rhBMP-7, and cell lysates were collected at fixed time points for western blot analysis of pSmad1/5/8. Recruitment of pSmad1/5/8 occurred early at 15 minutes and peaked at 2 hours. Subsequently, pSmad 1/5/8 levels remained between peak and control values for up to 24 hours then declined to baseline by 48 hours. Results are expressed as mean ± SEM, *p<0.05 vs. Control, n=3. hr = hour, min= minute.*

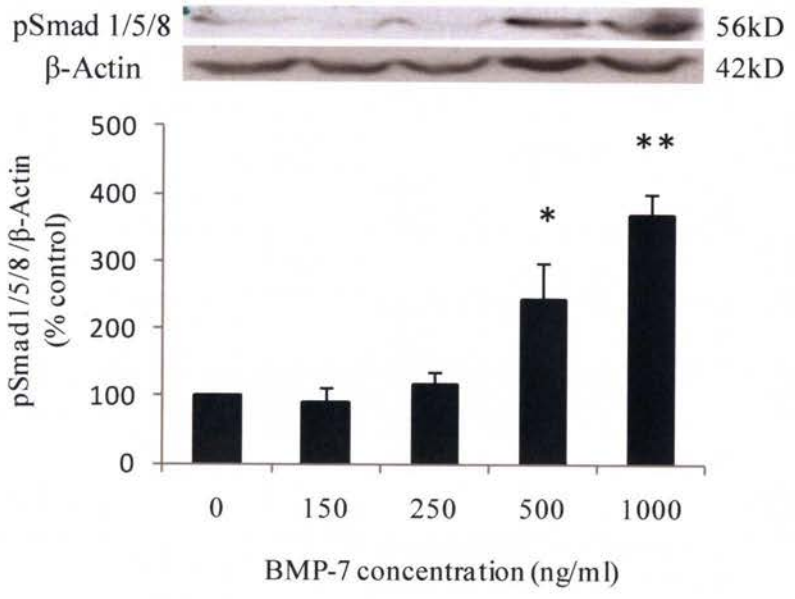

Figure 3.3.10.2 Recruitment of pSmad1/5/8 is dependent on the concentration of rhBMP-7.

*HK-2 cells were exposed to incremental concentration of rhBMP-7 and all sample cell lysates were collected 2 hours after exposure to rhBMP-7. Higher the concentration of rhBMP-7, the more pSmad1/5/8 was recruited. Significant increased in pSmad1/5/8 were seen with 500 and 1000ng/ml of rhBMP-7. Results are expressed as mean ± SEM, ** $p<0.01$, * $p<0.05$ vs. Control, n=3.*

3.3.11 Effect of KLF-6 on BMP-7 and TGF-β1 downstream signalling

We have now shown that KLF-6 has a regulatory effect on BMPR-IA mRNA and protein expression. To assess the relationship of KLF-6 with TGF-β1 and BMP-7 and their

respectively downstream signalling, pSmad 1/5/8 and pSmad2 were studied in KLF-6 over-expressing and silenced HK-2 cells. KLF-6 over-expressing HK-2 cells have a basal level of pSmad 1/5/8 expression similar to that of the empty vector (EV) plasmid transfected cells. However, when these cells were exposed to 1000ng/ml of BMP-7, pSmad 1/5/8 was markedly increased in the EV to 155.9 ± 15.4%, $p<0.05$. However, this increase in pSmad 1/5/8 was not seen in the KLF-6 over-expressing cells, 108.9 ± 14.6, $p<0.05$ (Figure 3.3.11.1).

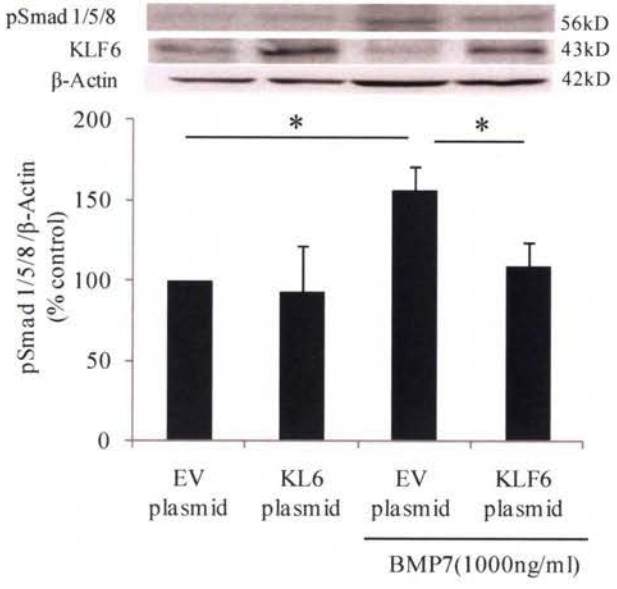

Figure 3.3.11.1 Phosphorylated Smad 1/5/8 in KLF-6 over-expressing HK-2 cells.

*Cells exposed to BMP-7 had an increase in pSmad 1/5/8 as compared to control (bar 3, *p<0.05). KLF-6 overexpressing cells had a significantly reduced pSmad 1/5/8 expression compared to cells transfected with a non specific plasmid vector. Results are expressed as mean ± SEM, *p<0.05 vs. Control, n=3.*

In KLF-6 silenced cells, basal pSmad 1/5/8 expression was similar in the cells treated with non specific siRNA (NS). When control cells were exposed to 1000 ng/ml of rhBMP7, pSmad 1/5/8 signalling increased to 168.9 ± 4.8%, $p<0.01$. A further increase in pSmad 1/5/8 was seen in the KLF-6 silenced cells to 214.3 ± 12.3%, $p<0.01$ (Figure 3.3.11.2).

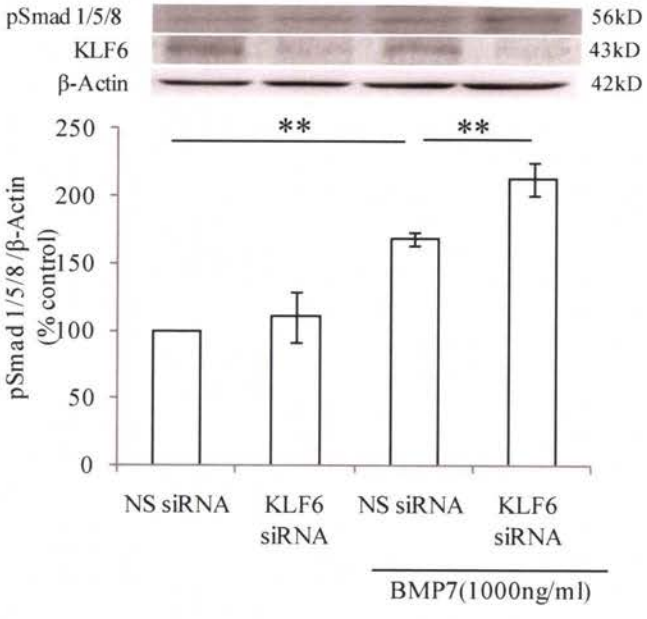

Figure 3.3.11.2 Phosphorylated Smad 1/5/8 expression KLF-6 silenced cells.

Successful KLF-6 silencing was confirmed by western blot analysis. There was no difference in the basal level of pSmad 1/5/8 between the KLF-6 silenced cells vs. the control. When HK-2 cells transfected with these transfected cells were exposed to 1000 ng/ml of rhBMP7, pSmad 1/5/8 signalling was higher in the KLF6 silenced cells

To assess whether the synergistic effects of TGF-β1 and KLF-6 were mediated through pSmad 2, KLF-6 over-expressing cells were exposed to 0.5ng/ml of TGF-β1. Basal pSmad 2 was similar in the EV and KLF-6 plasmid transfected groups (Figure 3.3.11.3) suggesting that TGF-β1 and pSmad 2 are upstream of KLF-6. Following 24 hours of exposure to 0.5ng/ml of rhTGF-β1, pSmad 2 signalling significantly increased to 392.4 ± 24.9% ($p<0.0001$) in the EV plasmid transfected cells, and further increased in cells over-expressing KLF-6. The potentiating effects of KLF-6 on TGF-β1 was clearly demonstrated by a further increment of pSmad 2 to 628.8 ± 66.6%, $p<0.0001$ (Figure 3.3.11.3). This strongly suggests KLF-6 potentiates TGF-β1 via a Smad 2 dependent pathway and also confirms that KLF-6 is downstream of TGF-β1/ Smad 2.

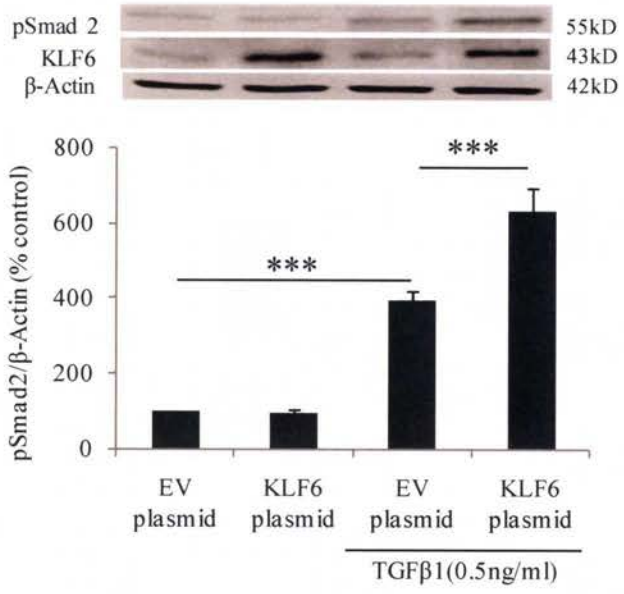

Figure 3.3.11.3 Phosphorylated Smad 2 in KLF-6 over-expressing cells exposed to TGF-β1.

*Basal pSmad 2 was not affected by KLF-6 overexpression. Twenty four hours exposure to TGF-β1 significantly increased pSmad 2 expression in EV plasmid transfected cells, with a further increment in pSmad 2 expression in KLF-6 overexpressing cells. All experiments were done in triplicate at each time points and all data were expressed in mean ± SEM, ***$p<0.0001$, $n=3$.*

3.3.12 BMP-7 plasmid transfection

Transfection with the BMP-7 plasmid resulted in significant BMP-7 mRNA expression (Figure 3.3.12.1A). The supernatant of these cells contained 408.7± 32.7 ng/ml of BMP-7 (Figure 3.3.12.1B) as compared to cells transfected with an empty vector (EV) plasmid in which BMP-7 expression was not detected.

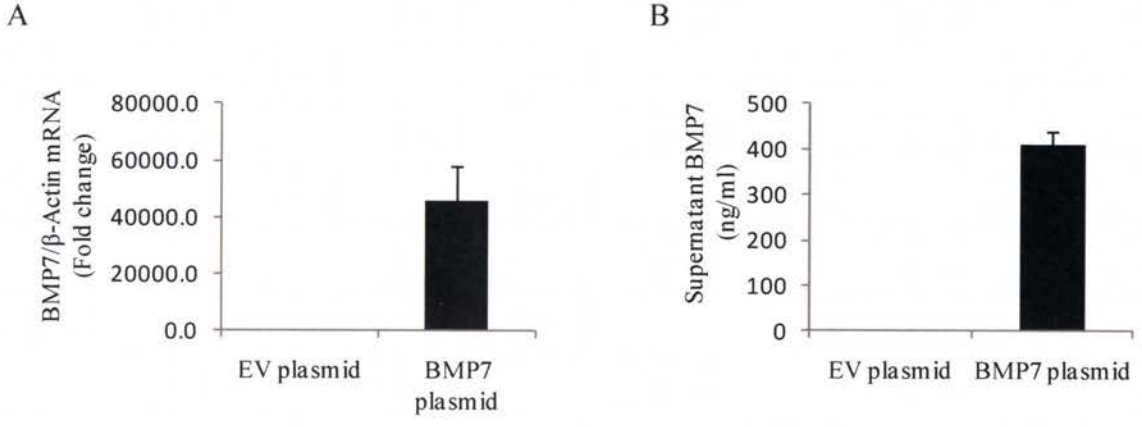

Figure 3.3.12.1 BMP-7 over-expression in HK-2 cells.

*Transfection of the BMP-7 plasmid resulted in significant expression of BMP-7 mRNA (A). BMP-7 protein overexpression was confirmed by ELISA (B). Downstream signalling was confirmed by increased pSmad1/5/8 (C, **$p<0.01$ vs. control). All experiments were done in triplicate at each time points and all data were expressed in mean ± SEM, ***$p<0.0001$, $n=3$.*

The BMP-7 over-expressing cells also significantly expressed pSmad1/5/8, 522± 54.9%, ($p<0.01$) as compared to empty vector plasmid control at 72 hours post transfection (Figure 3.3.12.2). There appears to be basal pSmad 1/5/8 expression in the EV transfected cells which is probably due to the cross reactivity of the antibody used with Smad 1/5/8. However, the phosphorylation of Smad 1/5/8 is almost 5-folds more in the BMP-7 over-expressing cells compared to the EV transfected HK-2 cells.

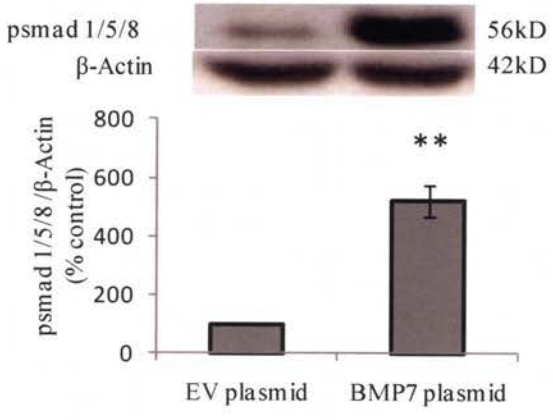

Figure 3.3.12.2 Phosphorylated Smad 1/5/8 expression in BMP-7 over-expressing cells.

*Overexpression of BMP-7 increased BMP-7 protein expression and downstream signalling activity, confirmed by increased pSmad 1/5/8. All experiments were done in triplicate at each time points and all data were expressed in mean ± SEM, **$p<0.01$, $n=3$.*

It has been recently shown that expression of inhibitors of DNA binding/ differentiation 2 (Id2), which antagonizes basic helix-loop-helix transcription factors, is increased by BMP-7, and ectopic expression of Id2 and Id3 renders epithelial cells refractory to TGF-β1 induced EMT [410, 411]. Id2 mRNA was up-regulated by 2.2 fold in BMP-7 over-expressing cells ($p < 0.01$) (Figure 3.3.12.3A). Since BMP-2 and BMP-4 share the same pSmad1/5/8 downstream signalling as BMP-7, their mRNA was examined to ensure specificity of the transfection for BMP-7.ross-reactivity. Figure 3.3.12.3B and 3.3.12.3C confirm that BMP-7 transfected cells showed no increase in BMP-2 and BMP-4 mRNA compared to baseline control values.

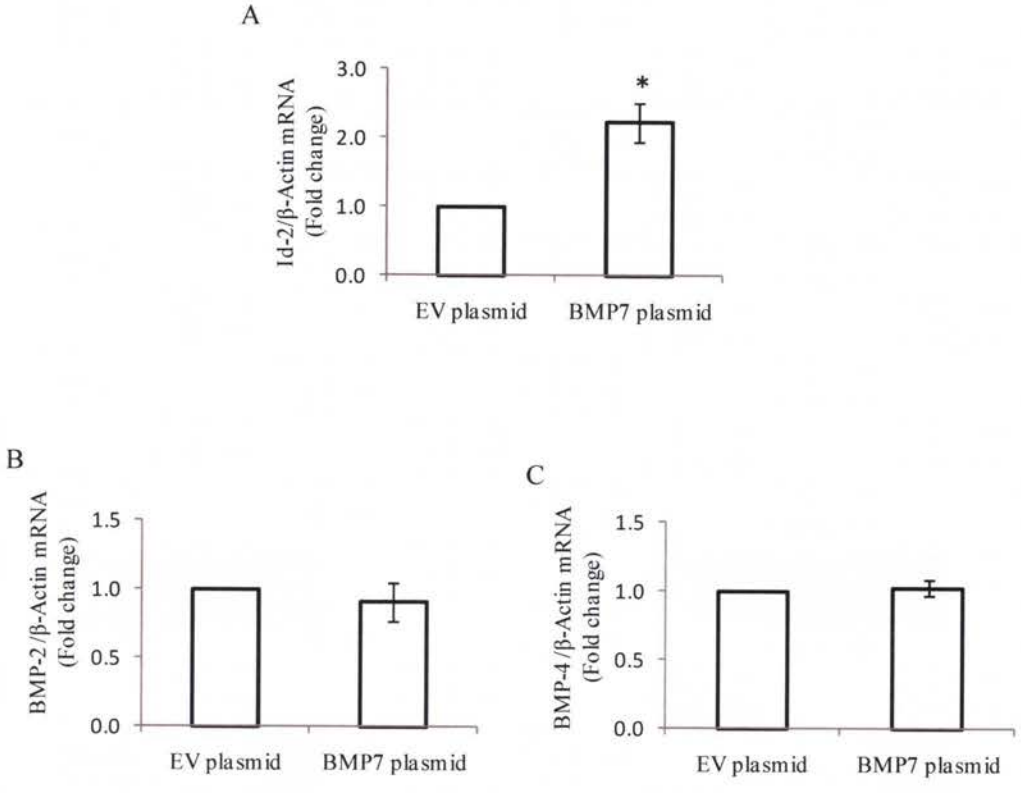

Figure 3.3.12.3 Increased in Id-2 mRNA expression in BMP-7 over-expressing cells.

*Real-time relative quantitation of Id-2 mRNA, a downstream target gene of BMP-7which is known to be induced by BMP-7, was found to be significantly elevated in BMP-7 transfected cells (A). To ensure that there was no non-specific transfection of other BMP isoforms, namely BMP-2 and BMP-4 were examined. BMP-2 and BMP-4 mRNA were not found to be elevated, indicating the specificity of transfection for BMP-7 (B & C). Results are expressed as mean of fold change ± SEM. All experiments were done in at least three replicates, *p<0.05 vs. control, n=3.*

3.3.13 BMP-7 plasmid transfection and EMT markers

Cells over-expressing BMP-7 demonstrated significantly increased E-cadherin, to 121± 4.1% ($p<0.01$) and significantly reduced vimentin, to 85.1±1.7% ($p<0.01$) as compared to control (Figure 3.3.13.1A and B). This further supports the fact that BMP-7 plays a protective role in the prevention of EMT.

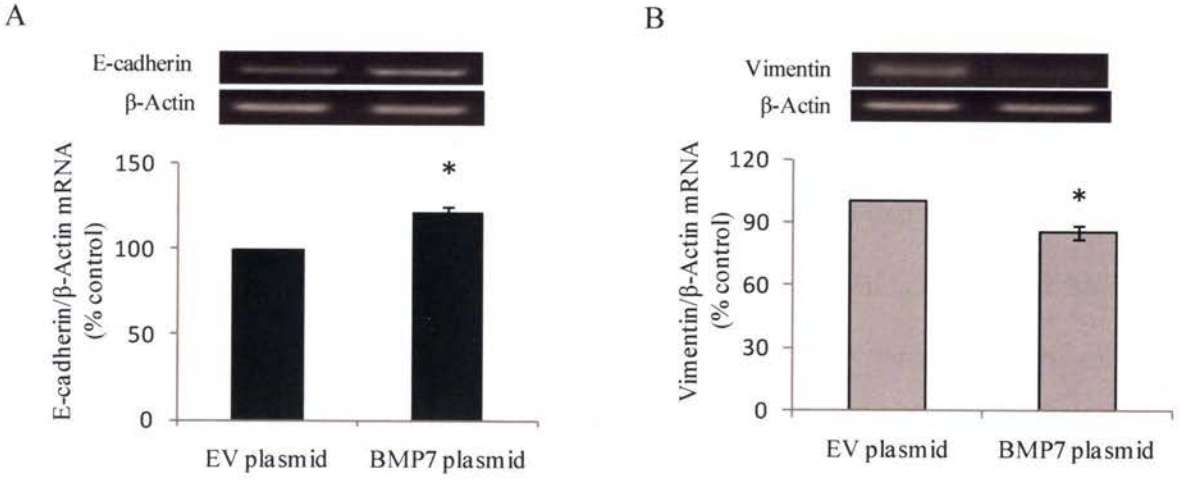

Figure 3.3.13.1 Over-expression of BMP-7 on EMT markers.

*BMP-7 transfected cells exhibited significantly higher E-cadherin mRNA (A) and lower vimentin mRNA (B) suggestive of a protective role of BMP-7 in the development of EMT. All experiments were performed in at least 4 different sets (n=4). Results are expressed as mean ± SEM, * $p<0.05$ vs. control.*

We repeated the previous experiments by exposing these BMP-7 over-expressing cells to the lowest concentration of TGF-β1 that was demonstrated to induce EMT in HK-2 cells, i.e. 0.5ng/ml. Western blotting confirmed that BMP-7 over-expressing cells had significant up-regulation in E-cadherin protein expression, 122.9 ± 5.6% ($p<0.05$) as compared to the control (Figure 3.3.13.2A). TGF-β1 significantly down-regulated E-cadherin protein expression in both empty vector plasmid transfected cells, 61.4 ± 2.6%, $p<0.05$ as well as in BMP-7 plasmid transfected cells, 60.9 ± 14.1%, ($p<0.05$). The preservation of E-cadherin by cells over-expressing BMP-7 was not observed in the presence of TGF-β1. Phosphorylated Smad1/5/8 was markedly increased in cell over-expressing BMP-7, 175 ± 19.2%, $p<0.01$, which was down-regulated to 86.5 ± 8.1%, $p<0.01$ when exposed to TGF-β1 (Figure 3.3.13.2B). The fact that pSmad1/5/8 suppression by TGF-β1 was not different between the empty vector plasmid control and BMP-7 over-expressing cells suggested that TGF-β1 itself does not interfere with pSmad1/5/8 signalling, but its suppressive effects are likely mediated through its suppression of BMP receptors, ultimately mitigating against the protective effects of BMP-7. This observation further confirms that TGF-β1 and its associated up-regulation of KLF-6 suppresses BMP receptor expression which is essential for BMP-7 downstream signalling, and its protective effect in limiting EMT.

A

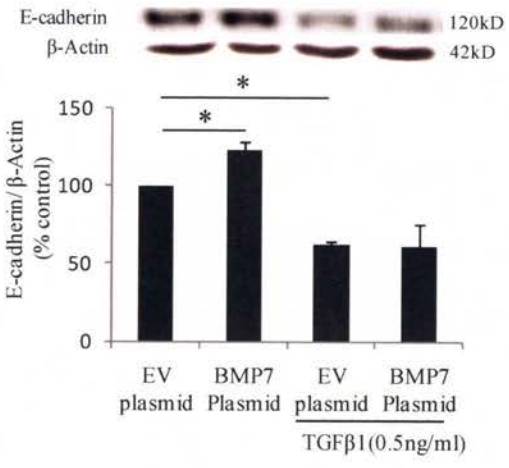

B

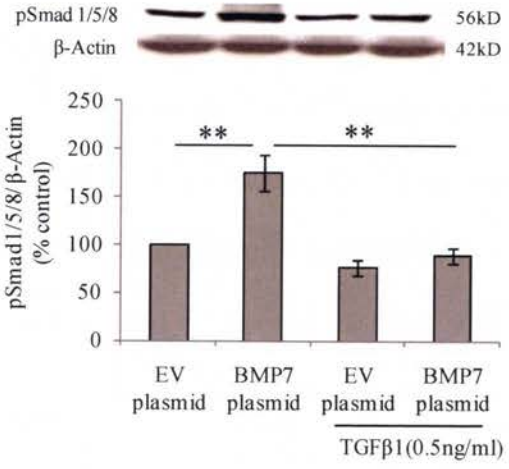

Figure 3.3.13.2 Cells over-expressing BMP-7 failed to up-regulate E-cadherin protein expression in the presence of TGF-β1.

Western blotting confirmed that up-regulation of E-cadherin mRNA is associated with increased E-cadherin protein expression in cells that over-express BMP-7 (A). However, in the presence of low dose TGF-β1 (0.5 ng/ml), the lowest concentration of TGF-β1 that was pre-determined to induce EMT in HK-2 cells, E-cadherin was equally suppressed in the empty vector and in BMP-7 overexpressing cells (A). Phosphorylated Smad1/5/8, which was markedly elevated in cells in which BMP-7 was over-expressed, was significantly suppressed by exposure to TGF-β1 for 72 hours (B). All cells were harvested for analysis 72 hours post transfection. Results are expressed as mean ± SEM, $**p<0.01$, $*p<0.05$ vs. control, $n=3$.

3.3.14 BMP-7 plasmid transfection on extracellular matrix (ECM) markers

The protein expression of two extracellular matrix proteins accumulated in renal fibrosis, namely fibronectin and collagen IV was determined in HK-2 cells transfected with empty vector and BMP-7 plasmids. Since these proteins are involved in the formation of extracellular matrix, the secreted form in the conditioned medium was measured. The secreted protein was normalised with total protein measured by Coomassie blue. BMP-7 transfected cells had a slight increase in secreted fibronectin, 119 ± 17.7%, which failed to reach statistical significance (Figure 3.3.14.1A). Exposure to low dose TGF-β1 significantly increased fibronectin secretion to 145 ± 11.9%, $p< 0.01$ as compared to the control, after normalizing to the total protein content in the supernatant measured by Coomassie blue (Figure 3.3.14.1A). However, BMP-7 over-expressing cells did not reverse TGF-β1 induced fibronectin secretion, 138 ± 23.8%. Collagen IV was similarly up-regulated by exposure to TGF-β1 in cells transfected with both the empty vector and the BMP-7 plasmid, 173 ± 30.2% and 184 ± 35.9 respectively (Figure 3.3.14.2B). Hence BMP-7 appears to have no inhibitory effect on TGF-β1 induced extracellular matrix production.

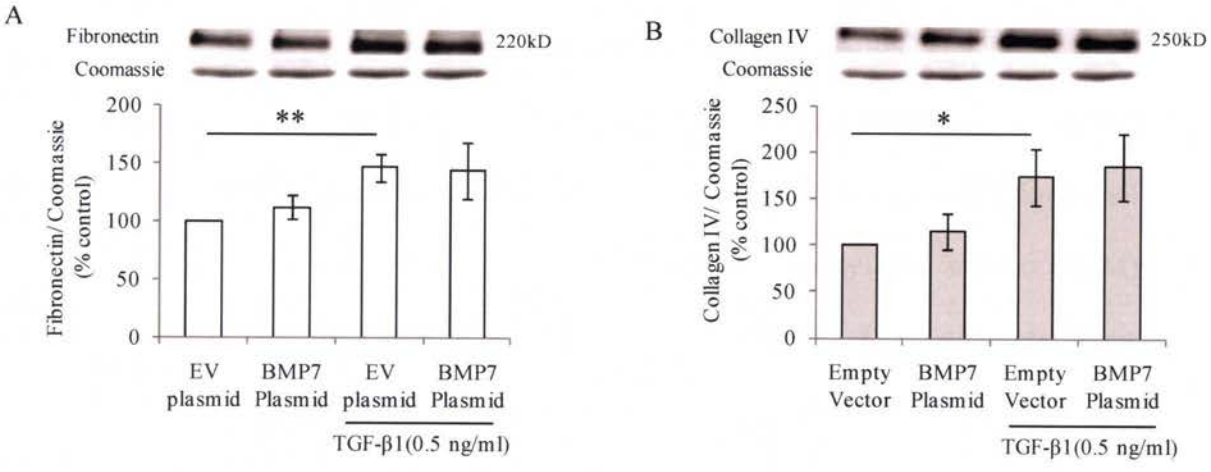

Figure 3.3.14.1 BMP-7 over-expression and its effects on fibronectin or collagen IV production in HK-2 cells.

*Thirty microlitres of conditioned medium with 6x samples of non-reducing sample buffer were analysed using two separate 7.5% SDS-PAGE gels. These gels were analysed using the same settings and identical conditions. One of the gels was then transferred to a western blot membrane for fibronectin or collagen IV analysis. The remaining gel was stained with Coomassie blue. BMP-7 over-expression has no effect on fibronectin (A) and collagen IV (B) production. TGF-β1 induced secretion of both fibronectin and collagen IV in HK-2 cells, and this was not modified by over-expression of BMP-7, either in the basal state or with concurrent exposure to TGF-β1. All experiments were done in triplicate at each time points and all data were expressed in mean ± SEM, **$p<0.01$, * $p<0.05$ vs. control $n=3$.*

3.3.15 BMP-7 over-expression on matrix metalloproteinase-9 and -2 (MMP-9 and MMP-2)

MMPs are a large family of zinc-dependent matrix-degrading enzymes, which include the interstitial collagenases, stromelysins, gelatinases and elastases which are secreted, as well as being membrane-bound. MMPs share several structural and functional properties and synergistically degrade a broad range of extracellular matrix (ECM) compounds. There are two gelatinases, MMP-2 and MMP-9. They differ by their molecular mass: 72-kD gelatinise (MMP-2) and 92kD gelatinase (MMP-9). TGF-β1 has been shown to play a pivotal role in regulating ECM production in models of tubulointerstitial injury via its effects on matrix regulatory enzymes [412]. BMP-7 over-expressing cells did not affect basal MMP-2 or MMP-9 production (Figure 3.3.15.1A & B). Seventy-two hours' exposure to TGF-β1 significantly increased both MMPs. BMP-7 did not affect production of these MMPs in either basal or TGF-β1 stimulated conditions.

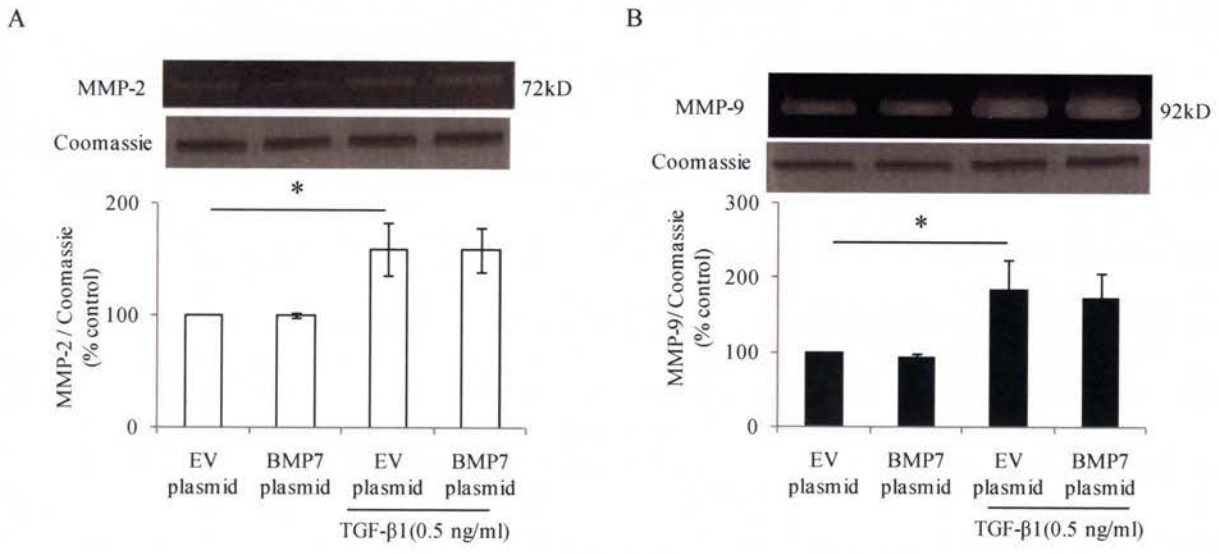

Figure 3.3.15.1 BMP-7 over-expression and its effects on MMP-2 and MMP-9 expression in HK-2 cells.

*Basal expression of MMP-2(A) and MMP-9(B) in the supernatant is comparable between the HK-2 cells transfected with EV and BMP-7 over-expressing cells. TGF-β1 significantly increased both MMP-2 and MMP-9 expression. BMP-7 did not affect the production of these MMPs in TGF-β1 stimulated condition. All experiments were done in at least triplicate at each time points and all data were expressed in mean ± SEM, * $p<0.05$ vs. control $n=4$.*

3.3.16 Glomerulosclerosis and tubulointerstitial fibrosis in human kidney biopsy specimens

Renal biopsies from five diabetic patients were evaluated. The patients' ages ranged from 40 to 66 years: three were women and two were men. All patients had long standing type 2 diabetes of at least 10 years' duration. All biopsies were reviewed by two pathologists. On light microscopy all showed advanced glomerular lesions, with characteristic Kimmelsteil-Wilson nodules with diffuse or nodular thickening of the glomerular basement membrane (Figure 3.3.16.1) and marked interstitial fibrosis (Figure 3.3.16.2). Demographic data are shown in Table 3.3.16.1

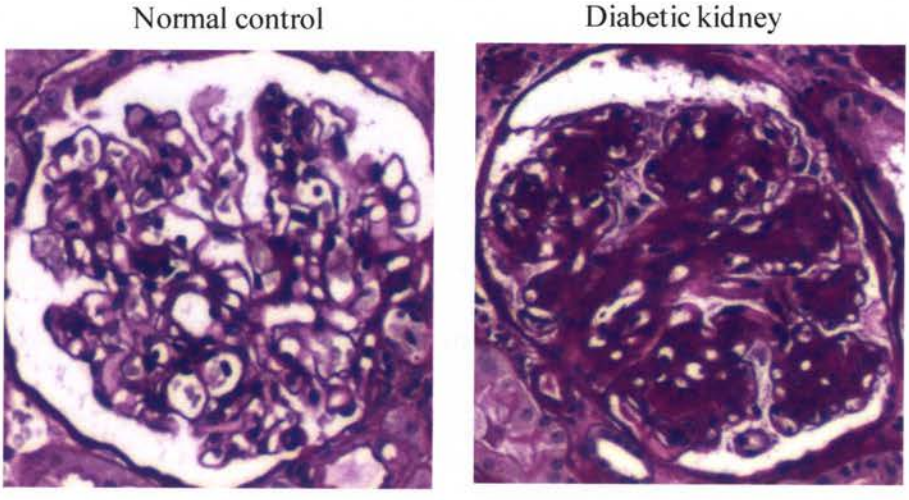

Figure 3.3.16.1 Typical diabetic nephropathy changes demonstrated by periodic acid-schiff (PAS) staining.

Glomeruli show a diffuse increase in mesangial matrix and nodular sclerosis. These nodules have the classical appearance of Kimmelstiel-Wilson nodules (Diabetic kidney). The mesangial matrix shows positive staining with a PAS stain which is negative for Congo

red. The mesangial sclerosis per glomerular area is significantly higher in diabetic individuals as compared to normal controls.

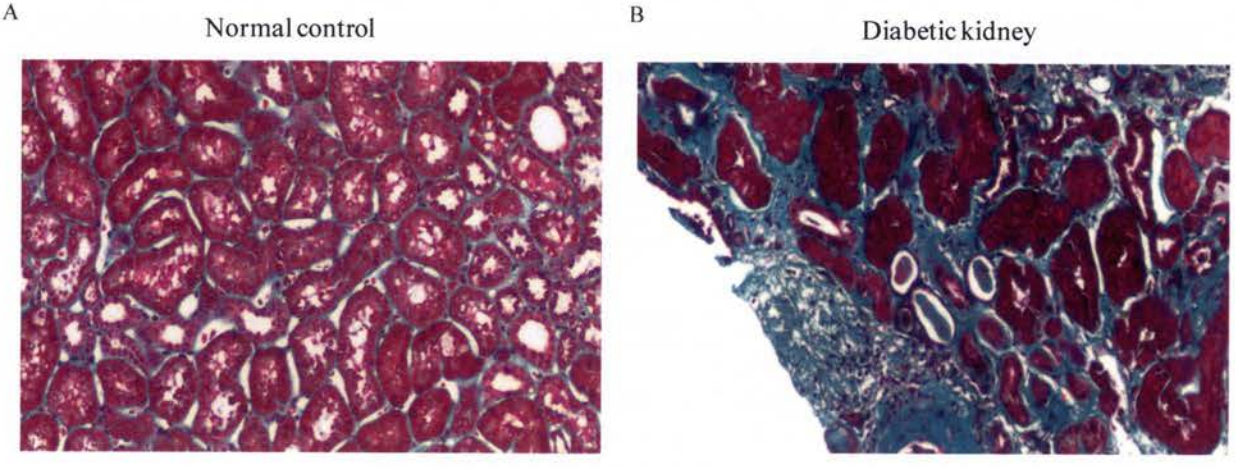

Figure 3.3.16.2 Masson trichrome staining of diabetic kidney tissues.

A marked increase in interstitial fibrosis and tubular atrophy is seen in diabetic (B) but not in normal kidney (A). Many atrophic tubules have thickened basement membranes. Tubular epithelial cells show vacuolation in keeping with proteinuria. The tubular lumens have numerous hyaline and granular casts. There is also patchy interstitial inflammation. The infiltrate consists mostly of lymphocytes. The interstitial fibrosis score is significantly higher in diabetic individuals as compared to tissue from normal kidney.

Table 3.3.16.1 **Baseline characteristics**

sex/ Age (y)	Sr creat (μmol/L)	eGFR (ml/min/ 1.73m^2)	U. prot/ creat (mg/mmol)	HbA1c (%)	Co-morbidity	Light microscopy
1.♀/ 66	117	27	300	9.2	DM,HPT	Nodular sclerosis, Kimemenstiel-wilson nodules, thickened basement membrane, advanced diabetic nephropathy.
2.♀/ 53	594	10	250	7.1	DM,HPT, IHD	diffuse and nodular lesion, Kimmenstiel-wilson nodules,
3.♂/ 44	260	23	41	6.1	DM	4/10 glomeruli sclerosed, increased mesangial matrix consistent with diabetic changes
4.♂/ 40	365	17	119	5.8	DM,HPT, IHD	Increase mesangial matrix with nodular and diffuse changes, early diabetic nephropathy
5.♀/ 56	274	22	450	8.4	DM, TIA	Advance diabetic nephropathy

♀, Female; ♂, Male; HPT, Hypertension; DM, diabetes mellitus; IHD, ischemic heart disease; TIA, Transient ischemic attack

eGFR, estimated glomerular filtration rate (MDRD calculation); sr.creat, serum creatinine; u.Prot/creat, urinary protein creatinine ratio.

Five normal specimens of kidney tissue from patients who had undergone nephrectomy for tumour, were used as the control for morphometric semiquantitative analysis as summarised in *Table 3.3.16.2* As expected, the diabetic individuals had significantly increased glomerular volume 22487.2 ± 1815.0 μm^2 vs. 4381.5 ± 1959.5μm^2, $p<0.05$ compared with non diabetic individuals. They also had increased glomerulosclerosis, as indicated by higher glomerulosclerosis scores, 2± 0.3 vs. 0.6± 0.2, $p<0.05$ and a higher percentage of mesangial sclerosis volume over glomerular volume, 43.0 ± 5.5% vs. 29.0 ± 2.9%, $p<0.05$. However, the mesangial cellularity was not different between the two groups, probably due to advance glomerulosclerosis in the diabetic group.

Table 3.3.16.2. **Semiquantative morphometry analysis**

	n	GS	GV(μm^2)	Mes/G(%)	MC/G(%)	TI	BMP7 positive tubules
Control	5	0.6 ± 0.2	22487.2±1815	29.0±2.9	4.0±0.3	0.4 ± 0.2	5.2 ± 0.86
Diabetic	5	2.0± 0.3*	4381.5±1959.5*	43.0±5.5*	3.0±0.6	2.0 ± 0.2*	1.0 ± 0.32*

* $p<0.05$ versus normal nephrectomised kidney
Values are expressed as means ± SEM
GS, glomerulosclerosis score; GV, glomerular volume; Mes/G, mesangial sclerosis/glomerular volume
MC/G, Mesangial cell/glomerular volume; TI, tubulointerstitial fibrosis score

3.3.17 BMP-7, KLF-6 and BMPR-IA in human kidney

The cortical tubular BMP-7 expression in the kidney specimens from patients with type 2 diabetes was significantly reduced, 1 ± 0.32, as compared to the normal kidney, 5.2 ± 0.86 tubules per high power field ($p<0.05$, Table 3.3.16.2*)*. Figure 3.3.17.1 demonstrates that in BMP-7 positive tubules are found in abundance in normal kidney specimens (A) but are significantly down regulated in kidney biopsy specimens from patients with diabetic nephropathy (B). Interestingly, reduced BMP-7 staining was seen not only in areas with significant tubular damage or atrophy, but also in areas with well preserved glomeruli, tubular structures and minimal fibrosis. This observation suggests that in patients with diabetic nephropathy tubular BMP-7 is down-regulated before established fibrosis and significant loss of kidney mass are seen.

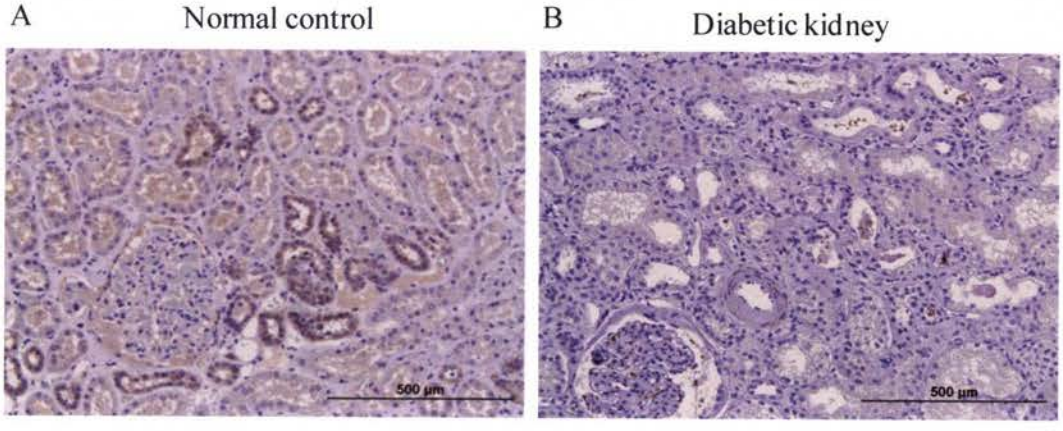

Figure 3.3.17.1 Immunohistochemistry of BMP-7 in human kidneys with diabetic nephropathy.

BMP-7 was positively stained in distal tubules and collecting duct, but not in proximal tubules and glomeruli (A) of control kidney specimens from patients who underwent nephrectomy for tumour, and compared with kidney biopsy specimens from patients with long standing diabetic nephropathy (B).

KLF-6 was seen in nuclei of proximal tubules, occasionally seen distal tubules and collecting ducts. Glomerular mesangial cells were occasional positive for KLF-6 however; no podocytes stained positively for KLF6. In normal kidney tissues, (Figures 3.3.17.2A) KLF-6 positively stained nuclei were less in number and intensity when compared with diabetic biopsy specimens (Figure 3.3.17.2B).

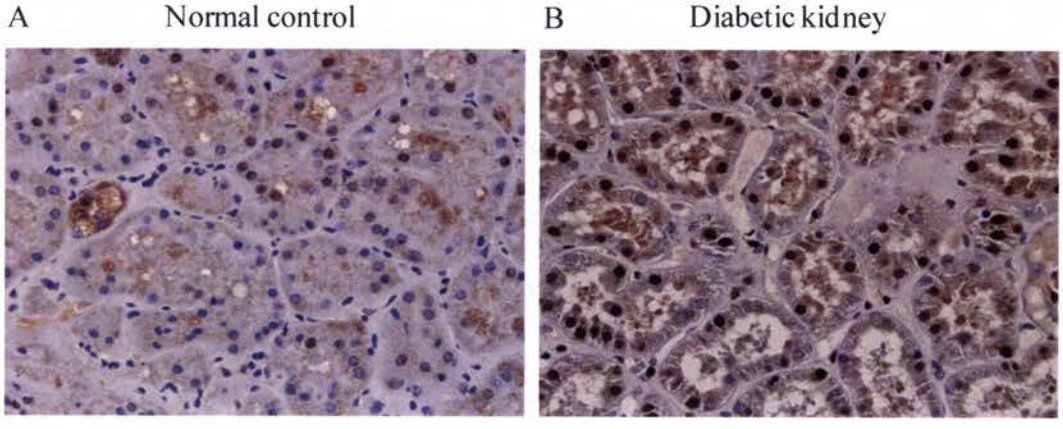

Figure 3.3.17.2 KLF-6 expression in human kidneys.

KLF-6 positive nuclei were seen in tubules, glomeruli and mesangium normal kidney specimens (A). In kidney biopsy specimens with established diabetic nephropathy, the number and intensity of KLF-6 positive nuclei markedly increased. This increase was most prominently seen in proximal tubules (B).

Immunofluorescence techniques were used to stain BMPR-IA. BMPR-IA was detected in membrane and cytoplasm of epithelial cells of proximal and distal tubules. No glomerular or mesangial BMPR-IA was detected. BMPRIA was abundantly expressed in healthy kidney specimens (Figure 3.3.17.3A) which was markedly suppressed in biopsy specimens of individual with diabetic nephropathy (Figure 3.3.17.3B).

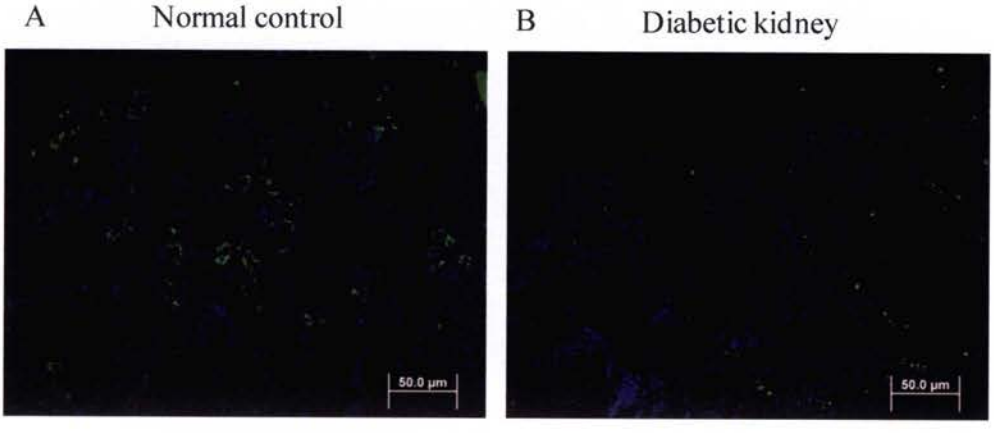

Figure 3.3.17.3 Immunofluorescence staining of BMPR-IA.

Paraffin embedded 3µm sections were used. BMPR-IA staining was seen in proximal and distal tubules in kidney tissues of normal subjects (A). However, glomerular and mesangial BMPR-IA could not be detected. BMPR-IA staining was markedly reduced in kidney biopsy specimens with established diabetic nephropathy (B). Since paraffin embedded sections were used, localization of the stained tubules was possible.

3.3.18 Circulating BMP-7 is markedly reduced in patients on hemodialysis

Using a sensitive sandwiched ELISA technique, circulating BMP-7 from serum obtained from five healthy volunteers was found to be in the range 138.27 to 380.85ng/ml (mean value of 207.2 ± 45pg/ml) as compared to patients with end stage renal disease (ESRD) having 11.85 to 41.84 ng/ml (mean value of 35.2 ± 5.1pg/ml, $p<0.01$). Of the 5 ESRD patients on hemodialysis, 3 had long standing type II diabetes.

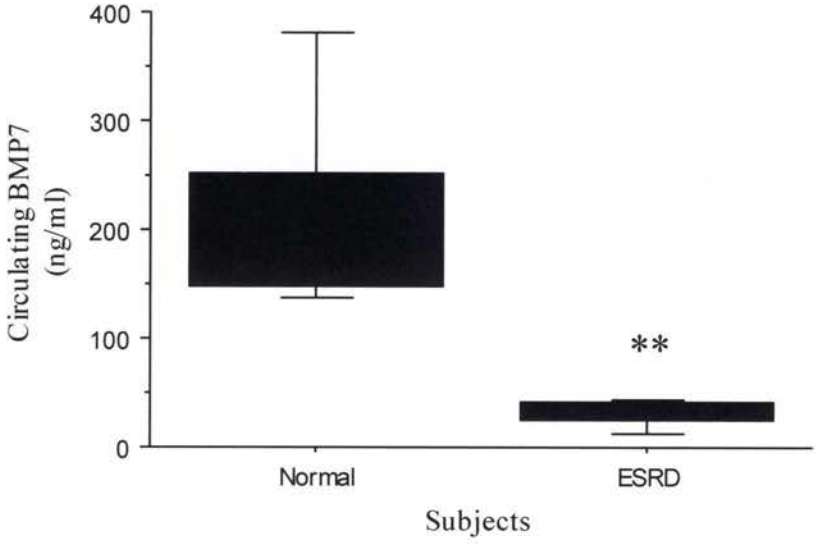

Figure 3.3.18.1 Circulating BMP-7 in ESRD patients on haemodialysis.

*Normal healthy volunteers have a significantly higher level of circulating BMP-7 in comparison. n=5, Results are expressed as mean ± SEM, **p<0.01 vs. control.*

3.4 Discussion

Bone morphogenetic protein-7 is widely expressed throughout embryonic development. Its critical importance in nephrogenesis has been clearly demonstrated in the inductive interaction between ureteric bud and metanephric mesenchyme resulting in mesenchymal-to-epithelial transformation (MET) [413]. In the adult, the kidney is the main site of BMP-7 synthesis in the thick ascending limb of the loop of Henle, distal convoluted tubules, medullary collecting duct, podocytes, urothelium, ureter and adventitia of renal arteries. Although BMP-7 is found in abundance in the distal tubules, our observations in both HK-2 cells and PTC cell cultures have confirmed other reports that BMP-7 is not expressed in the human proximal tubule [345]. The three main BMP type I receptors for BMP-7 ALK-2, BMPR-IA and BMPR-IB, are detected in proximal tubular cells. Hence, its action in segments where it is not expressed suggests that BMP-7 acts via a paracrine manner or through systemic delivery. Its likely function is to maintain tubular epithelial differentiation and prevent apoptosis. The importance of BMP receptors in the developing kidney is highlighted by reports demonstrating that deficiency of BMPR-IA in the ureteric bud results in renal malformation, associated with a decreased number of collecting ducts and their progenitor branches [414].

TGF-β1 has long been recognized as a pivotal driver of EMT both in *in vivo* and *in vitro* studies [415]. Because of the role of BMP-7 in driving MET, it has been considered that BMP-7 may be a 'natural' antagonist to TGF-β1 induced EMT, which has been confirmed by several *in vivo* and *in vitro* studies [416, 417]. However, administration of rhBMP-7 in these models was usually performed before the establishment of significant renal disease. In most studies rhBMP-7 was administered immediately before [340] or at the point of insult [304];

early in the disease [341, 408], or using a transfection methodology or transgenic animal to over-express BMP-7 at an early stage of the disease [80, 343] . More recent *in vitro* evidence suggests that BMP-7 does not attenuate TGF-β1 induced EMT [348, 418]. The question is therefore raised as to the effectiveness of BMP-7 as an antifibrotic agent in established renal disease. The present study demonstrates mechanistically the reasons underpinning the failure of BMP-7 to impact on TGF-β1 induced EMT; namely, that TGF-β1 transcriptionally regulates BMPR-IA, the major BMP receptor interacting with BMP-7 in a dose dependent manner [80], resulting in receptor down-regulation and a reduction in BMP receptor/ ligand interactions. Our results suggest that BMP-7 is unlikely to be of therapeutic efficacy as its inherent actions mitigating against EMT are only effective if TGF-β1 is removed, which is unlikely to be the case in established renal disease. This observation is further supported by the failure of cells over-expressing BMP-7 to up-regulate E-cadherin in the presence of TGF-β1.

The present study further demonstrates that KLF-6 over-expression in the proximal tubule further suppresses expression of all type I BMPR-IA, lowers E-cadherin expression and increases vimentin expression. Conversely, BMPR-IA expression was increased and E-cadherin was increased in HK-2 cells in which KLF-6 was silenced. We have previously shown in *in vitro* studies that exposure to high glucose for 11 days leads to an increase in KLF6 expression in HK-2 cells, and that this increase is mediated by TGF-β1 [265]. Furthermore, in animal models of diabetic nephropathy proximal tubular KLF expression is increased in parallel with features of EMT. In the present studies we found a significant reduction of BMPR-IA and ALK-2 receptor mRNA expression in cortical tissues of the diabetic Ren-2 rat at 16 weeks. This was further supported by the evidence of reduction of

BMPR-IA staining in kidney biopsy specimens of diabetic nephropathy individuals. Although long-term exposure to high glucose is known to up-regulate KLF-6, this study failed to demonstrate any suppressive effect of short term exposure to high glucose on type I BMP receptor expression. As TGF-β1 was demonstrated to have stimulatory effects on BMPR-IB and ALK-2 at 48 and 72 hours, we consider that TGF-β1 is likely to directly inhibit BMPR-IA expression, and in the longer term, induction of KLF6 by TGF-β1 further reduces all type I BMP receptors as observed in *in vivo* studies.

The local concentration of BMP-7 is controlled not only by the precise regulation of its receptors expression, but also by BMP antagonists. BMP antagonists function through direct binding to BMP-7 thus limiting BMPs from binding their cognate receptors [322]. Chordin is not detectable in the kidney, and follistatin mRNA has been found not to be different in control and disease groups [419]. Conversely, gremlin has been shown to be markedly up-regulated by TGF-β1 or exposure to high glucose in HK-2 cells [420]. USAG-1, which is thought to be the antagonist most abundantly found in the kidney, is primarily located in the distal tubules and not found in proximal tubules [322]. Although the role of BMP-7 antagonists was not specifically studied, we used supraphysiological concentrations of BMP-7 and over-expression strategies to limit the effect of regulatory antagonists that may have confounded our observations. Despite high local concentrations of BMP-7, EMT was not reversed, suggesting that local regulation of antagonists is not responsible for the lack of a renoprotective effect of BMP-7 in the presence of TGF-β1.

Our human studies further suggest a reduction in distal tubular expression of BMP-7 in the kidneys of humans with established diabetic nephropathy, indicating a reduction in both ligand and receptor expression *in vivo*. The reduction of BMP-7 is seen not only in

areas of interstitial fibrosis, but also in healthy tubules with no significant glomerulosclerosis or tubulointerstitial fibrosis. Although, BMP-7 is known to induce BMPR-IA mRNA expression [348], the above studies where BMP-7 was used in supraphysiological doses and over-expressed with no significant mitigating effect on markers of EMT suggest that reduced BMP-7 expression is not primarily responsible for its lack of effect in the presence of TGF-β1.

Even though much of the role of BMP-7 during development is understood, its exact function and its high concentration in the adult kidney remain unclear. Since BMP receptors to which BMP-7 binds are expressed in areas that do not produce BMP-7, such as the proximal tubular cells and other organs, this suggests the intriguing scenario that BMP-7, which is produced abundantly in the kidney, is constantly released into the circulation, functioning at distant sites in a hormone-like manner. Lund et al suggested that decreased BMP-7 levels directly correlate with a loss of viable renal mass, and BMP-7 expression is decreased in renal injury [325]. We confirmed that circulating BMP-7 level is significantly reduced in end stage renal patients on haemodialysis. This raises the possibility of measuring circulating BMP-7 as a marker for chronic renal fibrosis.

In summary, the present study has demonstrated that the expression of proximal tubular BMPR-IA is limited in diabetic nephropathy due to increased expression of TGF-β1 and KLF-6. This is likely to limit any therapeutic potential of BMP-7 in mitigating against EMT in chronic nephropathies.

CHAPTER 4: Cationic Independent Mannose 6- Phosphate Receptor Inhibitor (PXS-25) Inhibits Fibrosis in Human Proximal Tubular (HK-2) Cells by Inhibiting Conversion of Latent to Active Transforming Growth Factor-β1

4.1 Specific background and review

Tissue fibrosis is a maladaptive accumulation of ECM and a common endpoint in organs that sustain chronic injury. It is the result of a multifaceted, multilayered cellular response ultimately leading to the destruction of tissues and irreversible loss of normal tissue function. In nephropathy complicating both Type 1 and Type 2 DM, chronic hyperglycemia is the primary cause of the injury [421], although it is recognized that multiple injurious mediators, including advanced glycated end products and generation of reactive oxygen species arise as a consequence of hyperglycaemia. Despite glomerular lesions being characteristic of diabetic nephropathy, it is now recognized that pathology within the tubulointerstitium is ultimately more predictive of the renal outcome [422]. Renal epithelial cells contribute significantly to the development of renal fibrosis, as they increase and remodel ECM when stimulated either by cytokines or their microenvironment, or when they transition into myofibroblasts as a result of a process known as EMT. As discussed in prior chapters, the most prominent cytokine in the development of diabetic nephropathy is the profibrotic cytokines TGF-β1. Accumulated evidence establishes a crucial role for TGF-β1 in mediating fibrosis. Given the universal upregulation of its expression in the fibrotic kidney, TGF-β1 and its role in the pathogenesis of renal fibrosis is unarguable.

More recently, peritubular capillary loss and reduced blood flow limiting oxygen supply to the renal interstitium leading to chronic interstitial and tubular cell hypoxia, is recognized to play an active role in the progression of chronic renal disease, including diabetic nephropathy [84, 423]. This is evident in renal biopsy samples from patients with CKD, which typically display loss of peritubular capillaries in areas of tubulointerstitial fibrosis [424]. Key mediators of global cellular adaptation to hypoxia are Hypoxia-Inducible Factors, HIF-1 and HIF-2 being the most extensively studied. The role of HIF in renal fibrosis is complicated and may involve a functional interaction with HIF-dependent and HIF-independent signalling pathways such as the TGF-β [425, 426] or the Notch pathway [427]. Hypoxia can drive fibrogenesis through a direct transcriptional increase in collagen genes or gene products that are directly involved in the regulation of ECM turnover. Hypoxia is known to induce collagen I, tissue-inhibitor of metalloproteinases-1 (TIMP-1) and connective tissue growth factor (CTGF) [428], whilst decreasing matrix metallopeptidase-2 (MMP-2) [429] in renal epithelial cells. Hypoxia is also known to induce plasminogen activator inhibitor-1 (PAI-1) which is an important regulator of the activation of latent TGF-β1 [430].

The TGF-β families are synthesized as precursor proteins that are modified intracellularly prior to secretion. One of the most relevant intracellular modifications is the cleavage of the N-terminal pro-region from the C-terminal portion of the protein. The N-terminal pro-region is referred to as the latency-associated peptide (LAP) which contains the mannose 6-phosphate moiety, while the C-terminal region is called the mature TGF-β1 or active TGF-β1 [78]. When the mature TGF-β1 is associated with the LAP it is called L-TGF-β1 and cannot interact with its receptor and has no biological effect. In addition, L-

TGF-β1 frequently is covalently bound to latent TGF-β-binding protein (LTBP), which facilitates its sequestration within the extracellular matrix [162]. The secretion and storage of TGF-β1 is a complex and restricted biological process. However, one of the most important means of controlling the biological effects of TGF-β1 is the regulation of the conversion of LTGF-β1 to active TGF-β1 [167]. The release of TGF-β1 from the latent complex, which is referred to as activation, permits TGF-β1 to be bound by its ubiquitously expressed cell surface tyrosine kinase type I and type II receptors that initiate its signalling cascade. Since TGF-β1 has been reported to have numerous biological effects, the regulation of TGF-β1 action is critical to both the maintenance of normal physiological functions and the pathogenesis of numerous diseases. We have also recognised that blocking TGF-β1, by either a pan-neutralizing TGF-β1 antibody or TGF-β receptor ablation antibody, results in severe cytotoxicity and unacceptable side effects, which is probably due to the role of TGF-β1 in maintaining cell survival and limiting inflammation [431, 432].

Activation of TGF-β1 is known to occur via the Cationic Independent Mannose 6-phosphate receptor pathway. There are two mannose 6-phosphate (M6P) receptors – the 46 kDa cation-dependent M6PR (CD-M6PR) and the ~300-kDa cation-independent M6PR (CI-M6PR)/ insulin-like growth factor-II (IGF-II) receptor. The CI-M6PR is a multifunctional receptor that carries out several tasks that are essential for normal cellular function. One such task, which is shared with the CD-MPR, is the delivery of newly synthesized acid hydrolases from the trans-Golgi network to endosomes for their subsequent transfer to lysosomes. In addition, the CI-MPR has been implicated in several other physiological processes. Of relevance to the present study, it facilitates the activation

of the latent precursor of TGF-β1. Using an elegant *in vitro* model, Godar *et al.* demonstrated that the CI-M6PR forms a complex with the urokinase (plasminogen activator receptor (uPAR) through a binding site on the extracellular domain 1 of the CI-M6PR. Urokinase bound to uPAR then converts plasminogen to plasmin, which mediates the release of active TGF-β1. Subsequently, several groups have reported similar mechanisms that involve binding of the TGF-β_1 precursor to the cell-surface CI-M6PR [186, 188]. Another major mechanism of TGF-β1 activation is through the matrix glycoprotein thrombosphondin-1[433]. However, the contribution of the CI-M6PR pathway in the activation of latent TGF-β1 relative to the other known mechanisms of activation is unclear [185]. In the present study, by using a selective CI-M6PR inhibitor, PXS-25, we aimed to address this by using an *in vitro* model of proximal tubular cells cultured in either a high glucose or the combination of hypoxia and high glucose conditions, mimicking the early and later stages of the diabetic milieu. Being a selective CI-M6PR inhibitor, PXS-25 prevents the CI-M6PR-mediated TGF-β1 release but still allows active TGF-β1 formation via CI-M6PR independent pathways. Therefore we hypothesized that PSX-25 could potentially prevent or ameliorate tissue fibrosis without compromising the physiologic effects of TGF-β1.

4.2 Materials and methods

4.2.1 Cell culture

HK-2 cells, a human proximal cell line from American Type Cell Collection (ATCC, USA), were used in this study as outlined in Chapter 2 and previously described

[396]. HK-2 cells were 70-80% confluent when seeded onto a six-well plate, and cells were maintained in Keratinocyte serum-free medium (Invitrogen, Carlsbad CA, USA) containing 5 mM or 30 mM D-glucose (25 mM plus 5 mM in media), for a total of 72 hours. These cells were grown at 37^0C in a humidified 5% CO_2 incubator. Cationic-independent Mannose 6-phosphate Inhibitor (PXS-25), courtesy of Pharmaxis Ltd, was used at a concentration of 100 ng/ml in all experimental conditions. Cell culture media was changed every 48 hours and studied after 72 hours exposure to the experimental conditions. At the same time cells from the same passage were grown in another 6 well dishes (Sarstedt, Germany) initially at 37°C, 5% CO_2 and 95% air until they reached 70-80% confluence. Once the cells were ready for experimentation, they were transferred to the hypoxic chamber (Coy Laboratory Inc, USA) with a set condition 37°C, 5% CO_2 and 1% O_2. Media containing 5 mM and 30 mM D-Glucose with or without PXS-25 was equilibrated to hypoxia (1% O_2) by incubation overnight in the hypoxic chamber 24 hours prior to experimentation. 25mM L-glucose plus 5 mM D-glucose was used as the osmotic control.

4.2.2 Cell proliferation and cytotoxicity studies

Cytotoxic and proliferative effects of PXS-25 on HK-2 cells at concentrations of 1 μM, 10 μM, 100 μM, 200 μM, 500 μM and 1000 μM for 48 and 72 hours were assessed using CellTiter 96® AQ_{ueous} One Solution Cell proliferation Assay (Promega, Madison, WI) as previously described [409].

4.2.3 Transforming growth factor-β1 (TGF-β1) ELISA

Supernatant collected at the time of medium change at 48 hours and at the time of cell harvesting at 72 hours was merged as per the experimental protocol. Minimal medium was used to avoid dilution of produced TGF-β1 and at the same time to ensure cell viability. The supernatant was centrifuged and stored at -80°C. Active TGF-β1 levels were determined with an immunoassay system (Promega, WI, USA) as per the manufacturer's instructions. Total TGF-β1 were obtained by 1N hydrochloric acid treatment for 15 minutes, and then neutralized with 1N sodium hydroxide. The absorbance readings at 450nm were read using a 96-well microplate reader. This system is linear between 15.6 - 1000pg/ml. It has a less than 3% cross reactivity with TGF-β2 and TGF-β3. Total cell lysate protein content was determined using the Bio-Rad Protein assay. TGF-β1 levels were corrected for total cellular protein content (pg TGF-β1/μg protein) and were expressed as a percentage of control value.

4.2.4 Relative quantitative real-time reverse transcription polymerase chain reaction

RNA was extracted using the RNAeasy mini kit (Qiagen, Valencia, CA, USA) according to manufacturer's instructions as described in Chapter 2. cDNA was generated by reverse transcribing 1 μg of total RNA in a reaction volume of 20ul using VILO cDNA synthesis kits (Invitrogen Carlsbad, CA, USA). One microlitres (50ng) of cDNA was used as the template in 20μl PCR reactions. Quantitative real-time PCR was performed using an ABI Prism 7900 HT Sequence Detection System (Applied Biosystems, Foster City, CA,

USA) with Taqman Gene Expression Master Mix (Applied Biosystems) and gene-specific expression assays containing two unlabelled PCR primers and fibronectin (Hs01549976_m1) FAM dye-labeled Taqman MGB probe (Applied Biosystems). Reactions were performed in at least triplicate and analyzed by relative quantitation using RQ Manager software, Version 1.2 (Applied Biosystems). All data is presented as the fold change compared to control after normalization to TATA Binding Protein (TBP) for hypoxic conditions or β-Actin for normoxic conditions. Water blank was used as the negative template control.

4.2.5 Western blot analysis

Supernatant was collected and centrifuged at 3000 rpm, 4°C for 5 mins to remove cell debris. Protein lysates were extracted as previously described [397]. In brief, cells were first lysed in ice cold cell lysis buffer and then centrifuged at 12,000 rpm, 4°C for 10 mins. The cell lysate supernatant was collected and stored at -80°C. Thirty micrograms of total cell protein with 6x Laemmli sample buffer were analysed by SDS-PAGE in 7.5% or 10% gel and electroblotted to Hybond nitrocellulose membranes (Amersham Pharmacia Biotech, Bucks). After one hour blocking with 5% skim milk, membranes were incubated overnight at 4°C with fibronectin 1:100 (NeoMarkers, CA, USA), collagen IV 1:5000 (Abcam Ltd, Cambridge, USA) and pSmad 2 1:1000 (Cell Signalling, CA, USA). Membranes were then incubated with the appropriate washed horseradish peroxidase (HRP)-conjugated secondary antibody. Proteins were visualized using the enzymatic chemiluminescence (ECL) detection system (Amersham Pharmacia Biotech, Bucks). The

bands corresponding to fibronectin (220kDa), collagen IV (250kDa) and pSmad 2 (56kDa) were captured using LAS 4000 (Fujifilm, Tokyo, Japan). All membranes were reprobed with α-tubulin 1:10,000 (Sigma Aldrich, CA, USA) and results were corrected for α-tubulin as a loading control and analysed using Multigauge system (Fujifilm, Tokyo, Japan). Equal volumes of supernatant media (30μl) run in SDS-PAGE gel and counterstained with Coomassie blue were used to quantify total supernatant protein. Secreted fibronectin and collagen IV were normalised to the total protein measured by Coomassie blue.

4.2.6 Gelatin zymography

The culture supernatants were collected at 72 hours and centrifuged at 1,000 rpm for 5 minutes at 4°C to remove cellular debris. Equal volume of samples was mixed with sample buffer and loaded onto a 10% non-reducing sodium disulphide polyacrilamide gel (SDS-PAGE) containing 1mg per ml of gelatin (Sigma, MO, USA) and subjected to electrophoresis. The electrophorised gels were washed in re-naturing buffer (50mM Tris, 2.5% TritonX-100) then incubated for a further 24 hours in developing buffer (50mmol/L Tris-HCl, 100mmol/L NaCl, 10mmol/L $CaCl_2$, 0.02% NaN_3, pH 7.5) at 37°C. The gels were stained for 15 minutes with Coomassie Blue 250 (Bio-Rad, CA, USA) followed by de-staining. The lytic bands representing matrix metalloproteinases-2, MMP-2 (72 kDa) and MMP-9 (92kDa) activity were quantified using Multigauge software V3.0 (Fujifilm, NJ, USA). At the same time, equal volume of all samples of interest were loaded onto another 10% non-reducing SDS-PAGE without gelatin and subjected to similar conditions

of electrophoresis. The relative band intensities of the total protein were measured using Multigauge software V3.0 (Fujifilm, NJ, USA). The results of MMP-2 and MMP-9 were normalized to the results of total protein bands studied.

4.2.7 Statistical analysis

Each experiment was performed independently three to five times. Real-time PCR results are expressed as fold change compared with the control value. RT-PCR data are expressed as a percentage of control values. Results are expressed as mean ± SEM. Statistical comparisons between groups were made by analysis of variance (ANOVA), with pairwise multiple comparison made by Fisher's protected least-significant difference test. Analyses were performed using the software package Statview, version 4.5 (Abacus Concepts Inc, Berkeley CA). p values <0.05 were considered significant.

4.3 Results

4.3.1 High glucose and hypoxia induce total and active TGF-β1 production

When HK-2 cells were grown in 30 mM D-glucose for 72 hours, total TGF-β1 production increased to 133.1 ± 4.1% ($p < 0.05$), compared to cells cultured in 5 mM D-glucose (Figure 4.3.1.1). Similarly, cells exposed to hypoxic conditions (represented by white bars) had a higher amount of total TGF-β1 at 128.6 ± 6.8%, $p < 0.05$ as compared to cells cultured in 20% oxygen (represented by solid black bars). In both cases the incremental increase in total TGF-β1 was associated with a specific increase in its active

form. Both high glucose and hypoxia independently induced active TGF-β1 release to 138.3 ± 13.7%, ($p < 0.01$) and 154.8 ± 10.9% ($p<0.01$) of control values respectively. When HK-2 cells were cultured in both hypoxic and high glucose conditions, the total and active TGF-β1 was increased to 124.6 ± 6.8% and 149.3 ± 16.9%, respectively, which was no different to the TGF-β1 production seen in cells cultured in either high glucose or hypoxic conditions alone.

When PXS-25 (100μM) was added to the medium, active TGF-β1 production induced by high glucose was significantly reduced to 102.4 ± 14.2% of control values ($p<0.01$; Figure 4.3.1.2). PXS-25 did not modify hypoxia induced increases in active TGF-β1 production. In combined hypoxic and high glucose conditions, TGF-β1 production was not modified by the concurrent presence of PXS-25. These observations suggest that both high glucose and hypoxic conditions independently increase total and active TGF-β1 production in human proximal tubular HK-2 cells with differential regulation by PXS-25. The combined presence of high glucose and hypoxia did not induce additive effects, suggesting that both individual insults may be sufficient to maximally stimulate cellular production of total and active TGF-β1 albeit through different mechanisms. The results suggest that high glucose induces active TGF-β1 release through a CI-M6PR dependent pathway, whereas hypoxia induces active TGF-β1 through CI-M6PR independent pathways which dominate in the combined presence of hypoxia and hyperglycemia.

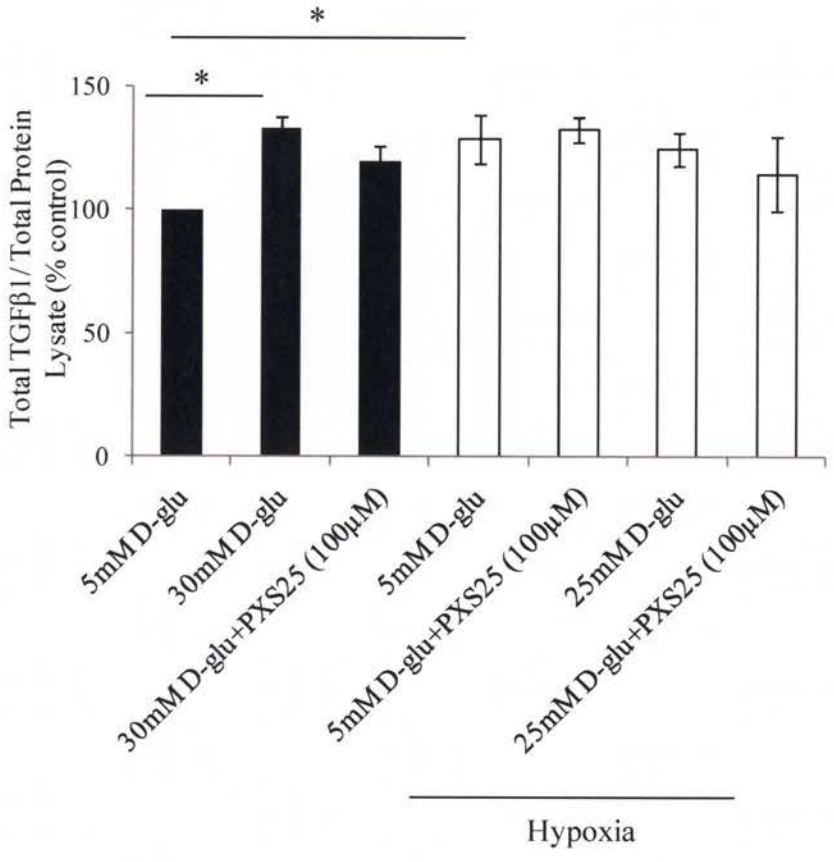

Figure 4.3.1.1 Total TGF-β1 in HK-2 cells in conditioned media.

(Normoxic conditions were represented by black bars and hypoxic with white bars). The baseline value of total TGF-β1 under normal glucose normoxic conditions was 65.1 ± 8.8 pg/μg and active TGF-β1is 6.3 ± 1.1 pg/μg of protein lysates. The active TGF-β1 constituted slightly less than 10% of the total TGF-β1. These bar charts were expressed as a percentage of the baseline readings. Exposure to 30 mM of D-glucose (high glucose) for 72 hours increased total TGF-β1 production, as did exposure to hypoxia ($p<0.05$). Total TGF-β1 was measured after acid hydrolysis to release all latent TGF-β1. Results are expressed as mean ± SEM (n=5).*

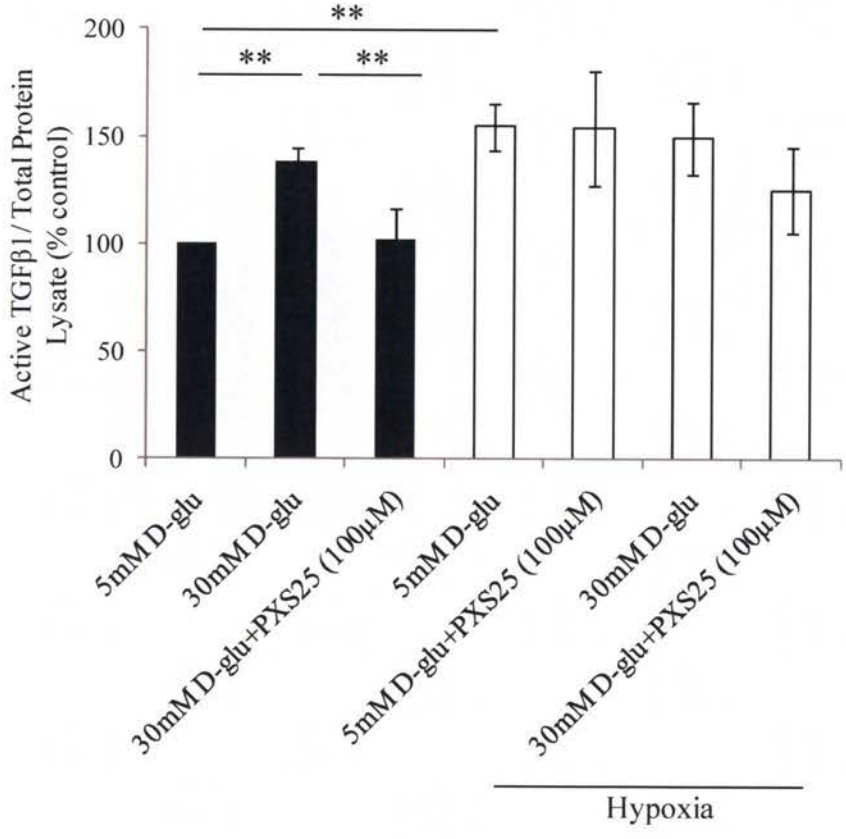

Figure 4.3.1.2 Active TGF-β1 in HK-2 cells in conditioned media.

*(Normoxic conditions are represented by the black bars and hypoxia by the open bars): Active TGF-β1, which reflects the bioactivity of TGF-β1, is induced by high glucose, and this induction is suppressed by treatment with the CI-M6PR inhibitor, PXS25 (** $p<0.01$). Hypoxia also increased active TGF-β1 formation, but high glucose did not have an additive effect on the activation of latent TGF-β1. Treatment with PXS-25 in hypoxic conditions alone did not modify the activation of TGF-β1. This is similarly seen in combined hypoxic and high glucose conditions. PXS-25 had only a modest effect on the activation of latent TGF-β1 which did not reach statistical significance. Results are expressed as means ± SEM (n=5).*

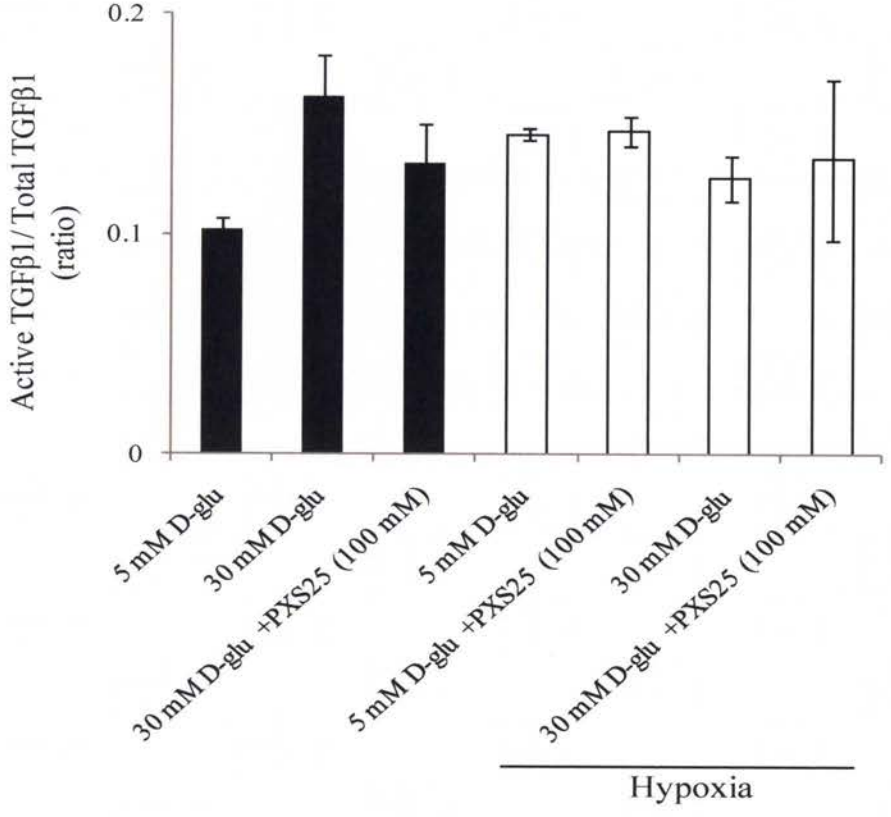

Figure 4.3.1.3 Active TGF-β1 and total TGF-β1 ratio.

The ratio of active total TGF-β1 corrected to the total protein content of each well showed similar trends of results which were comparable to that of the active TGF-β1 however none of the groups achieved statistical significance probably because very low level of active TGF-β1 is required to exert any physiological effects. Furthermore the proportion of the active TGF-β1 was very small as compared to the total TGF-β1. In many instances the active TGF-β1 was lower than 10%. Results are expressed as means ± SEM (n=5).

4.3.2 PXS-25 does not have cytotoxic effects on HK-2 cells

To ensure the suppression of TGF-β1 by PXS-25 is not due to a cytotoxic effect, CellTiter 96® AQ_{ueous} One Solution Cell proliferation Assay (Promega, Madison, WI) was used to assess cell toxicity as described in Chapter 2. The results were standardized to the untreated control group and expressed as percentage of control. In normoxic conditions, PXS-25 did not have any cytotoxic effect on HK-2 cells at both 48 and 72 hours time points (Figure 4.3.2.1A & B). PXS-25 is clearly a stable and non toxic product as even at very high concentrations of PXS-25 (1000μM) there was no cytotoxic effects on HK-2 cells. This observation is similarly seen when the HK-2 cells were cultured in hypoxic conditions with increasing concentration of PXS-25 at both time points. (Figure 4.3.2.2 A & B). Subsequently, all experiments were designed for 72 hours exposure to 100μM of PXS-25.

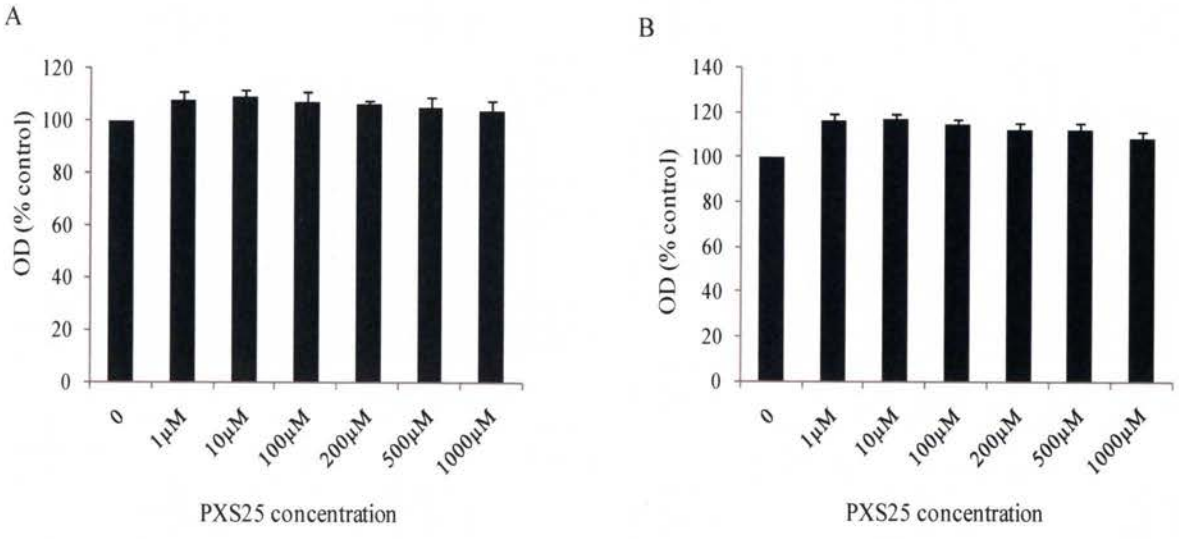

Figure 4.3.2.1 Effect of PXS-25 and cell toxicity in normoxic condition.

Exposure to various concentrations of PXS-25 did not affect cell proliferation or cell toxicity at 48 hours (A) or at 72 hours (B). Results are expressed as means ± SEM (n=3).

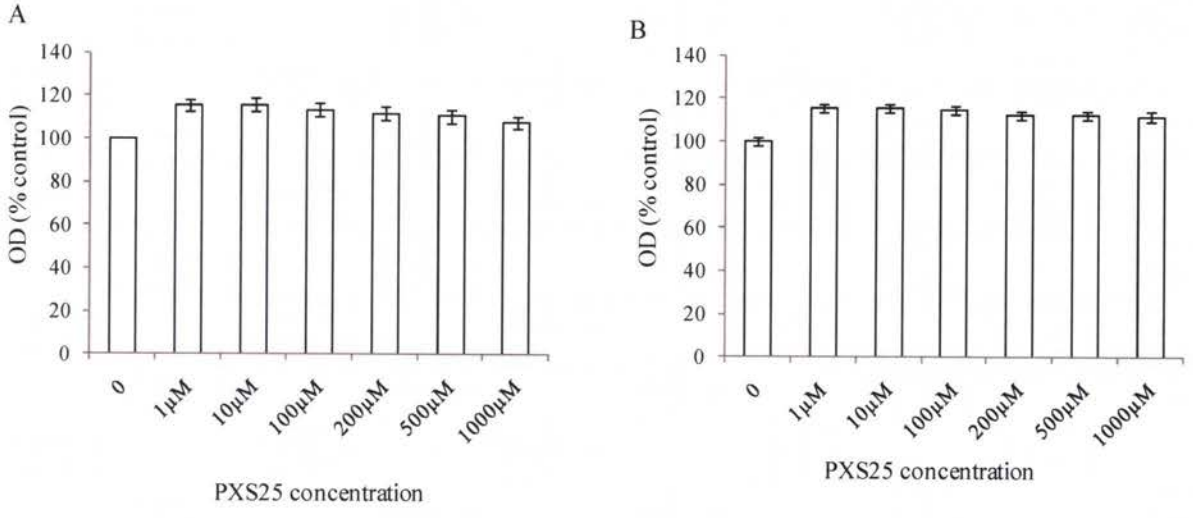

Figure 4.3.2.2 Effect of PXS-25 on cell proliferation in hypoxic conditions.

Similarly PXS-25 has no cytotoxic effects on HK-2 cells at 48 (A) and 72 hours (B) at various concentrations under hypoxic conditions. Results are expressed as means ± SEM (n=3).

4.3.3 High glucose induced phosphorylated Smad 2 which is suppressed by CI-M6PR inhibitor

Smad proteins are the key mediators of TGF-β1 signalling. Upon stimulation by TGF-β1, the transmembrane type II TGF-β receptor forms tight complexes with the type I receptor, leading to phosphorylation and activation of Smad 2 and Smad 3 [434]. Phosphorylated Smads then hetero-oligomerize with the common partner Smad4 and translocate into the nucleus, where they control the transcription of TGFβ-responsive genes through interaction with specific *cis*-acting element in the regulatory regions. Figure 4.3.3.1 shows that phosphorylated Smad 2 is significantly induced in HK-2 cells when

exposed to hyperglycemia for 72 hours to 125.8 ± 5.4%, $p < 0.01$, as compared to the control cells cultured in media containing 5 mM D-glucose. This effect is not seen in cells exposed to L-glucose which was used as an osmotic control (data not shown). Concurrent exposure to PXS-25 significantly reduced the pSmad 2 to 107.4 ± 2.6%, $p<0.01$, of the control value. These results confirm that hyperglycemia induces active TGF-β1 release via a CI-M6PR dependent-pathway, PXS-25 prevents the conversion of latent to active TGF-β1 and thus causes a reduction in pSmad 2 levels.

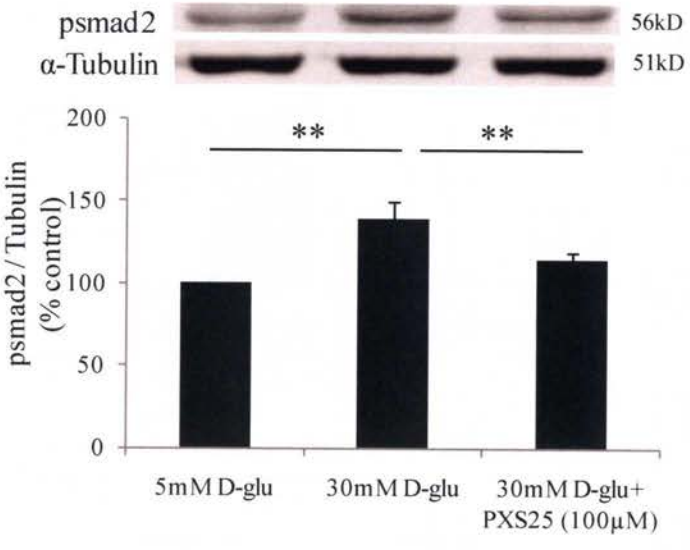

Figure 4.3.3.1 Phosphorylated Smad 2 expression in high glucose with or without PXS-25.

*Exposure to high glucose for 72 hours induced pSmad 2 activation (** $p<0.01$). PXS-25 is able to suppress pSmad 2 activation by preventing activation of latent TGF-β1. Results are expressed as means ± SEM (n=4).*

Hypoxia in cells cultured in 5 M D-glucose also effectively induced pSmad 2 to 175.9 ± 7.8% of control values ($p<0.01$, Figure 4.3.3.2). Indicating that hypoxia alone can too effectively induce activation of latent TGF-β1

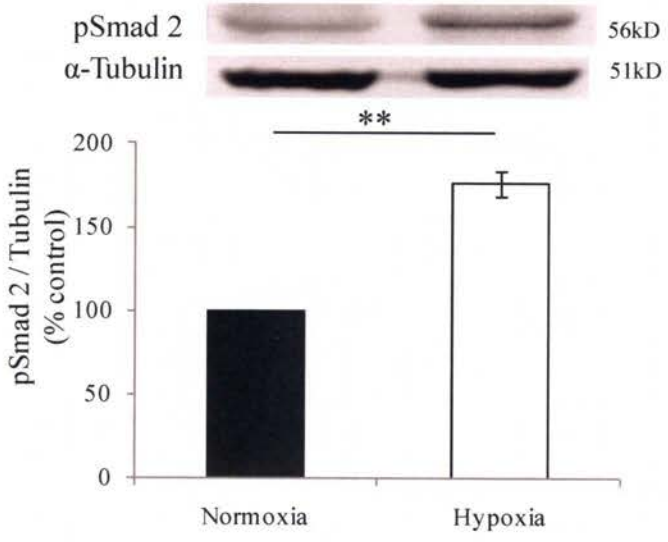

Figure 4.3.3.2 Phosphorylated Smad 2 in normoxic vs. hypoxic conditions.

*pSmad 2 was significantly increased in cell cultured under hypoxic vs. normoxic conditions (**$p<0.01$). Results are expressed as means ± SEM (n=4).*

Conversely, the combination of high glucose and hypoxia did not induce pSmad 2 to a greater extent than was observed in cells exposed to hypoxia alone (Figure 4.3.3.3). However, no significant reduction in pSmad 2 was observed when cells exposed to high glucose and hypoxia were simultaneously exposed to PXS-25. This evidence supports the above data suggesting that TGF-β1 activation by high glucose is dependent on CI-M6PR,

whereas in hypoxia it is predominantly via a CI-M6PR independent pathway. The addition of high glucose to hypoxic conditions did not further increase the active TGF-β1 production and its downstream Smad signalling. The concurrent presence of PXS-25 only marginally suppressed pSmad 2.

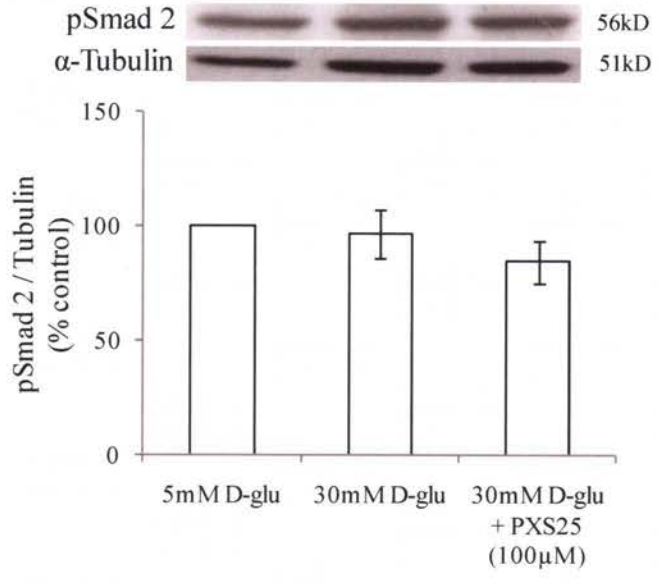

Figure 4.3.3.3 Phosphorylated Smad 2 in hypoxic and / or high glucose conditions.

In combined hypoxia and high glucose no increase in pSmad 2 was evident. Addition of PXS-25 has no effect on TGF-β1 downstream pSmad 2 signalling. Results are expressed as means ± SEM (n=4).

4.3.4 Suppression of fibronectin mRNA by PXS-25 is dose dependent

Fibronectin is one of the target genes regulated by TGF-β1 in renal proximal tubular cells [397]. We therefore looked into the suppressive effect of PXS-25 in fibronectin production at the transcriptional level. Results depicted in Figure 4.3.4.1 clearly show that high glucose induced fibronectin mRNA to 1.18 ± 0.04 fold of control values, $p<0.05$. Increasing concentrations of PXS-25 suppressed fibronectin mRNA in a dose dependent manner, ranging from 0.1 μM, 1 μM, 10 μM and 100 μM, to 0.93 ± 0.08 fold-change, $p<0.05$; 0.87 ± 0.06 fold-change, $p<0.05$; 0.76 ± 0.08 fold-change, $p<0.01$; and 0.61 ± 0.08 fold change, $p<0.0001$. Because of this, the concentration of 100 μM was determined to be the concentration to be used in all experiments.

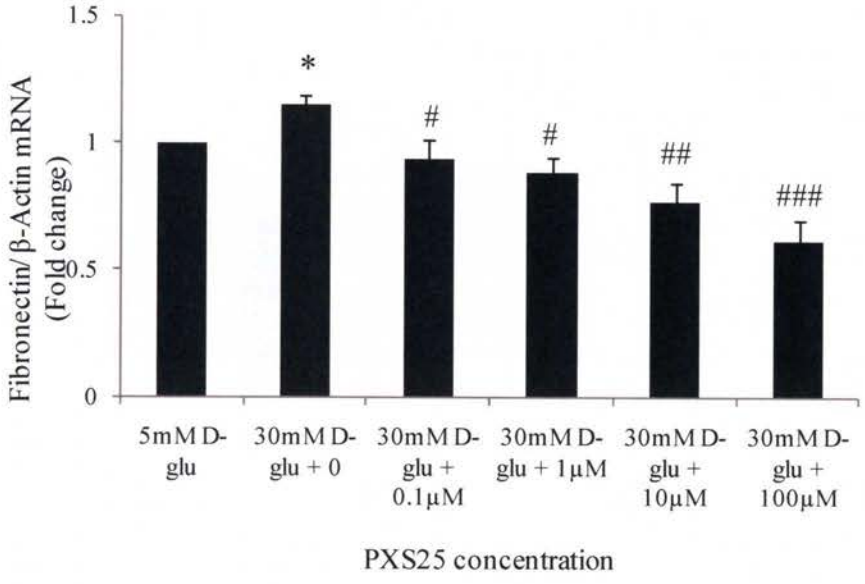

Figure 4.3.4.1. Effect of PXS-25 on fibronectin mRNA expression.

*High glucose induced fibronectin mRNA expression, which was suppressed by PXS-25 most effectively at 100 μM concentration (5 mM vs. 30 mM D-glucose; *p<0.05, 30 mM D-glucose vs. 30 mM D-glucose + PXS-25, #p<0.05, ##p<0.01 and ###p<0.0001, (n=4).*

Cells exposed to hypoxic conditions alone had increased fibronectin mRNA expression, 1.23 ± 0.1 fold-change compared to control, $p<0.01$ (Figure 4.3.4.2) and when combined with high glucose, there was a further increase in fibronectin mRNA expression to 1.6 ± 0.2 fold-change, $p<0.05$ vs. hypoxia alone. However, exposure to PXS-25 had little effect on fibronectin expression in combined hypoxic and high glucose conditions.

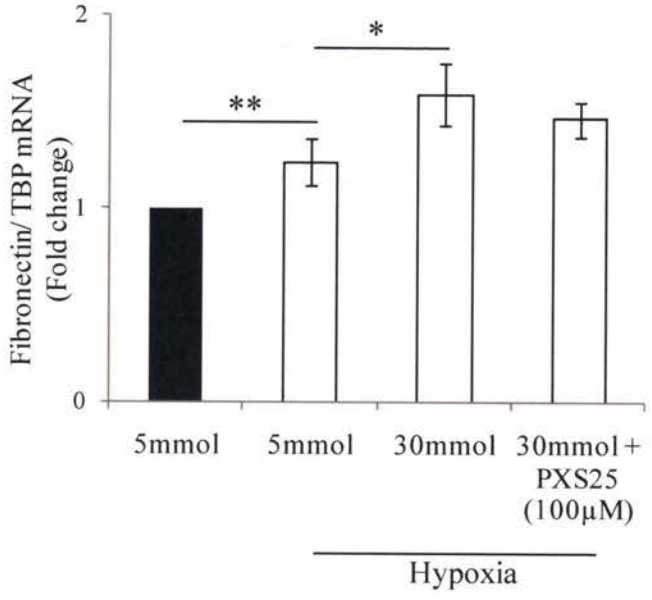

Figure 4.3.4.2. Fibronectin mRNA expression in hypoxic high glucose conditions.

*Fibronectin mRNA was induced by hypoxia, and its expression was further induced by high glucose, but this was not suppressed by PXS-25 (** $p<0.01$* $p<0.05$, $n=4$). Real-time PCR results were normalized to the housekeeping gene α-tubulin and shown as fold change compared to control.*

4.3.5 PXS-25 suppresses fibronectin and collagen IV production in HK-2 cells

TGF-β1 is well known to induce fibronectin and collagen IV production in renal proximal tubular cells. Figure 4.3.5.1A confirms that exposure to 30 mM D-glucose in normoxic conditions for 72 hours induced cellular fibronectin production to 157 ± 10% of control values ($p<0.01$). PXS-25 suppressed high glucose-induced fibronectin production to 127 ± 12% of control values ($p<0.05$ vs. high glucose). Similarly, cellular collagen IV production in HK-2 cells was increased by exposure to 30 mM D-glucose for 72 hours to 134.2 ± 10% of control values ($p<0.01$), and was decreased by PXS-25 to 111.2 ± 4% ($p<0.05$ vs. high glucose; Figure 4.3.5.2A). Since both of these ECM proteins are secreted proteins, the secreted form was also measured in the medium supernatant corrected to the total protein content measured by Coomassie staining. Figure 4.3.5.1B and 4.3.5.2B showed similar findings in the secreted forms of fibronectin and collagen IV in that the supernatant content increased to 134.8 ± 11% and 116.1 ± 3.2% of control values (both $p<0.05$), when exposed to 30 mM D-glucose for 72 hours. PXS-25 treatment reduced the secreted form of fibronectin to 99.1 ± 6% and of collagen IV to 103.2 ± 4% of control values (both $p<0.05$ when compared to high glucose). This result suggested that induction of fibronectin and collagen IV by high glucose is secondary to activation of latent of TGF-β1, which is dependent on CI-M6PR. This effect of hyperglycemia is independent of the osmotic effect of 30 mM D-glucose, and this was confirmed by exposing the HK-2 cells to the osmotic control in the same experimental settings (data not shown).

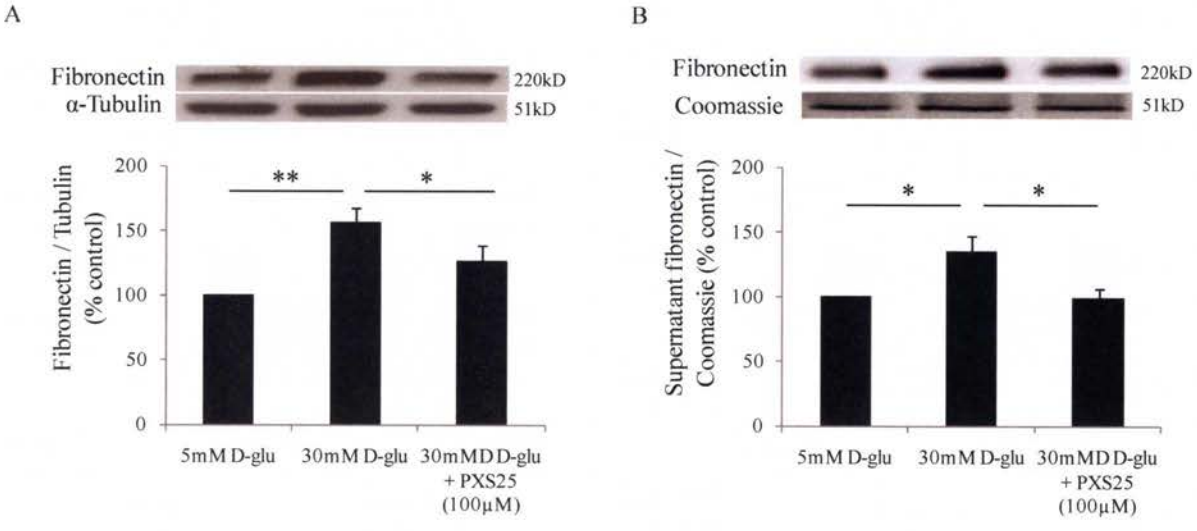

Figure 4.3.5.1. Fibronectin protein expression in HK-2 cells in normoxic high glucose conditions.

(Black bars indicate normoxic condition). High glucose induced both cellular (A) and secreted (B) fibronectin production in HK-2 cells. This effect was significantly suppressed by PXS-25 at 72 hours ($p<0.05$, ** $p<0.01$, $n=4$).*

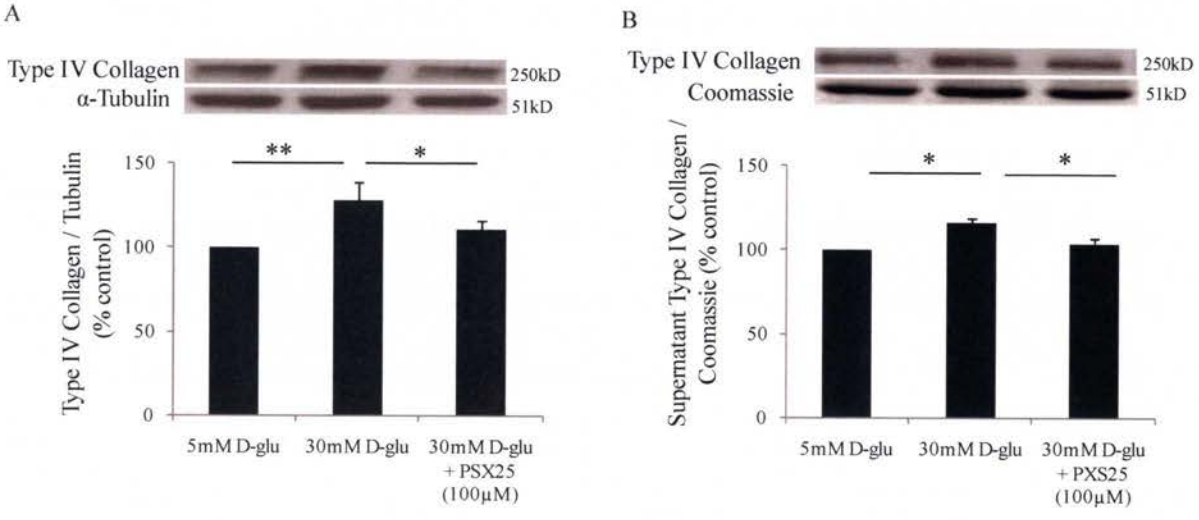

Figure 4.3.5.2. Type IV collagen expression in HK-2 cells in normoxic high glucose conditions.

(Black bars indicate normoxic condition). High glucose induced both cellular (A) and secreted (B) Type IV collagen production in HK-2 cells. This effect was significantly suppressed by PXS-25 at 72 hours ($p<0.05$, ** $p<0.01$, $n=4$).*

4.3.6 Fibronectin and collagen IV production in combined hypoxic high glucose conditions

Although we were not able to demonstrate an additive effect of combined high glucose and hypoxia in activating latent TGF-β1, high glucose further stimulated fibronectin and collagen IV production, beyond that observed when cells were exposed to hypoxia in 5 mM glucose. Cellular fibronectin increased to 123.9 ± 6% ($p < 0.01$; Figure 4.3.6.1A), and cellular collagen IV to 128 ± 12.1%, ($p < 0.05$; Figure 4.3.7.1C) of that observed in hypoxic conditions alone. Concurrent exposure to PXS-25 did not reduce these

two ECM proteins in the combined setting of high glucose and hypoxia. This pattern of results were similarly seen when the secreted forms of fibronectin and collagen IV were measured, as shown in Figures 4.3.6.1B and 4.3.6.1D. Again this data are again consistent with the previous data suggesting that in contrast to that observed in high glucose conditions, the activation of TGF-β1 in hypoxia, independent of the concurrent presence of high glucose is predominantly via a CI-M6PR independent pathway.

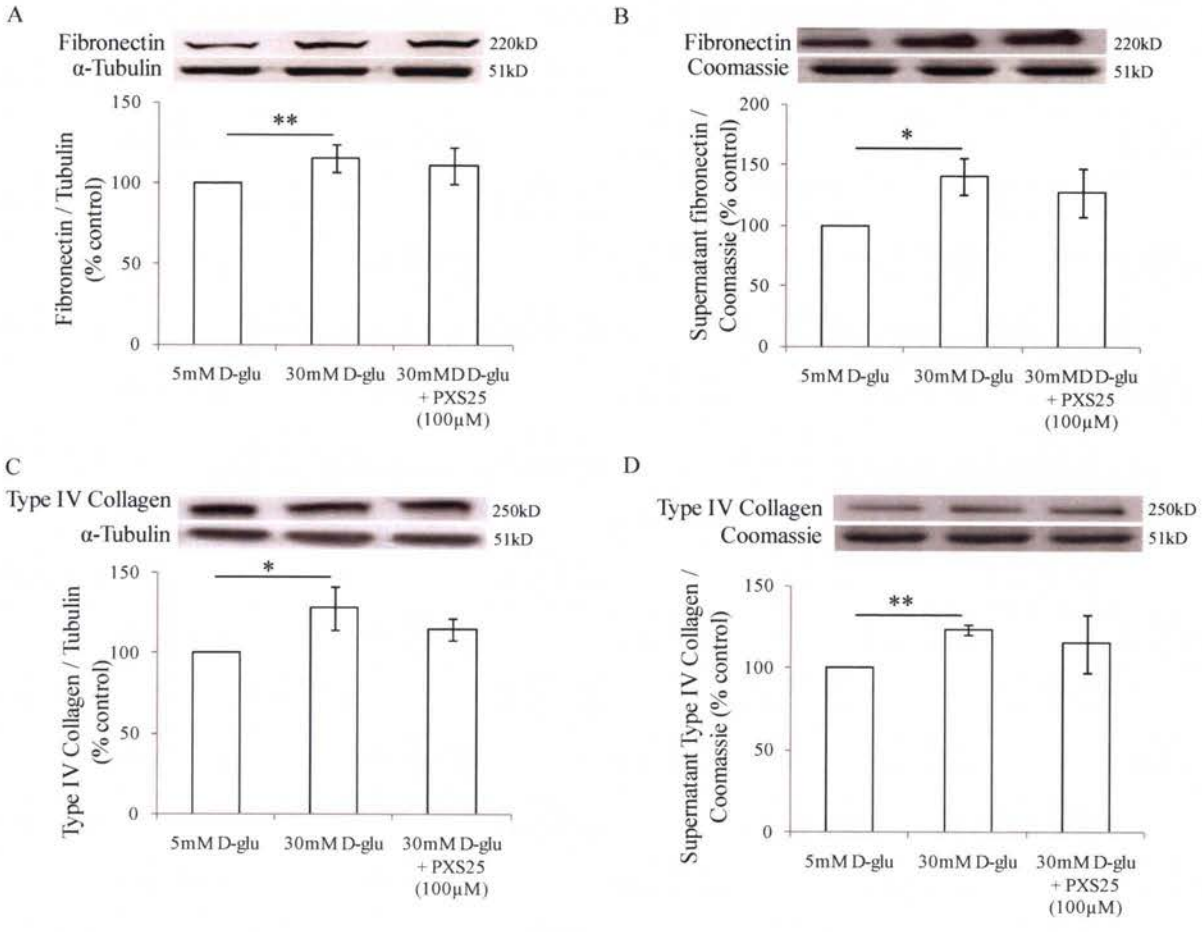

Figure 4.3.6.1. Fibronectin and collagen IV expression in HK-2 cells in hypoxic and high glucose conditions

*(All experiments in this figure were carried out under hypoxic conditions). In hypoxic conditions, high glucose was able to induce cellular and secreted forms of both fibronectin (A & B, *p<0.01) and collagen IV (C & D, *p<0.05, **p<0.01). However, concurrent exposure to PXS-25 failed to suppress the increase in these ECM proteins, suggesting that both hypoxia and high glucose can induce fibronectin or collagen IV through a TGF-β1 independent pathway. Results are expressed as means ± SEM (n=4).*

4.3.7 PSX-25 does not affect matrix metalloproteinases production

High glucose induced MMP-9 expression to 117.8 ± 3.2% of control under normoxic conditions ($p < 0.05$; Figure 4.3.7.1), whereas hypoxia had no influence (92.5 ± 3% of control; p=NS). Exposure to high glucose in the presence of hypoxia enhanced MMP production compared to that observed following exposure to hypoxia alone ($p<0.05$). However, this was no different to expression under control conditions. Exposure to PXS-25 in either high glucose or hypoxic conditions did not modify MMP-9 production. This implies that high glucose induces MMP-9 production independent of CI-M6PR activation of TGF-β1. Hence, the reduction of ECM proteins in PTC exposed to PXS-25 is unlikely to be due to secondary induction of gelatinases MMP-9. MMP-2 production is induced by high glucose to 106.6 ± 2% of control values ($p < 0.05$; Figure 4.3.7.2). Hypoxia alone or in combination with high glucose did not influence MMP-2 expression and PXS-25 did not modify MMP-2 expression under any experimental conditions.

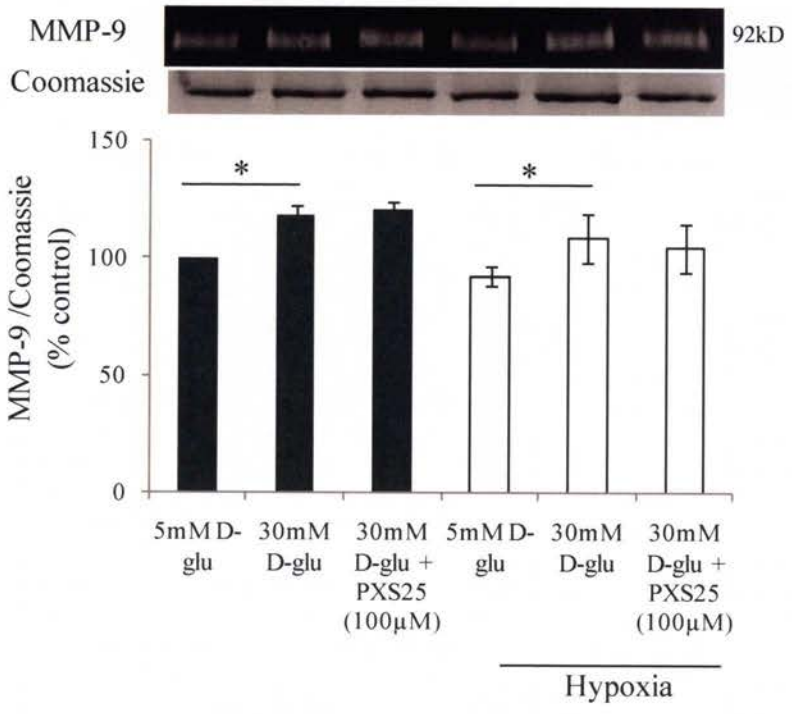

Figure **4.3.7.1. Effects of PXS-25 on MMP-9 production.**

*MMP-9 activity as measured by gelatin zymography was induced by 48 hours exposure to high glucose in both normoxia (Black solid bars) and hypoxia (white bars), but was not affected by PXS-25. Results are expressed as means ± SEM (n=4), *p<0.05.*

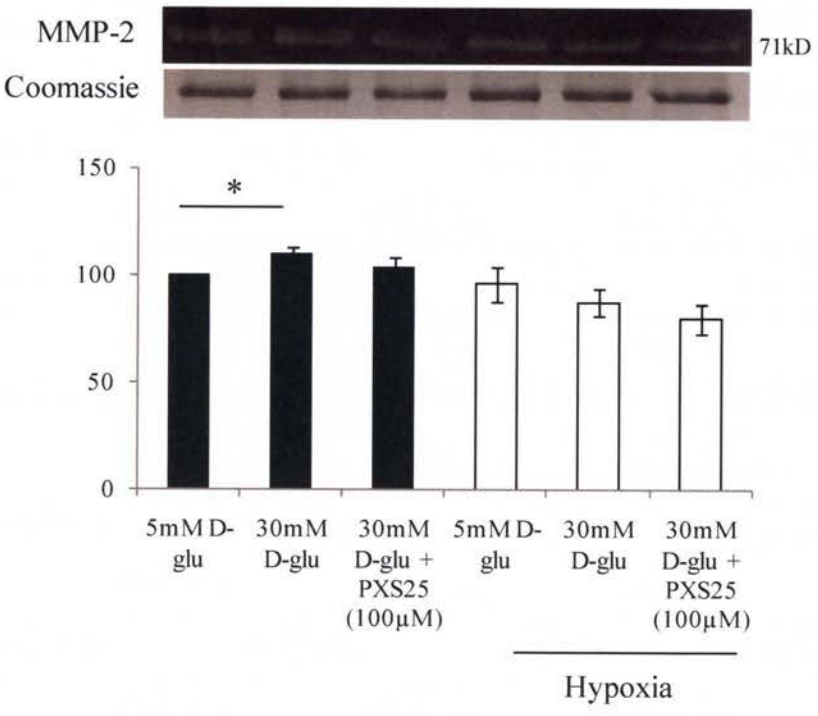

Figure 4.3.7.2. Effects of PXS-25 on MMP-2 production.

Forty eight hours exposure to high glucose induced MMP-2 activity in normoxic but not hypoxic conditions ($p<0.05$). Generally, MMP-2 activity is reduced in hypoxia, but this did not reach statistical significance. Results are expressed as means ± SEM (n=4).*

4.4 Discussion

These studies confirm the independent influences of high glucose and hypoxia on the generation of the fibrogenic cytokine TGF-β1, and the differing mechanisms that regulate the activation of TGF-β1 in the microenvironment that characterizes diabetic nephropathy. We have shown in the present study that activation of TGF-β1 by high glucose is CI-M6PR dependent, as the selective CI-M6PR inhibitor, PXS-25 blocks the

activation process and reduces downstream phosphorylated Smad 2 and downstream fibronectin and collagen IV production. It has also demonstrated that high glucose not only induces the activation of TGF-β1, it also induces the production of total TGF-β1, suggestive of an autocrine regulatory system. This is consistent with studies suggesting that TGFβ1 has been shown to amplify TGF-β1 production in a positive-feedback loop [161, 435]. Conversely, although hypoxia clearly induces activation of TGF-β1 and downstream induction of signalling and matrix proteins, it is through mechanisms independent of activation of the CI-M6PR. Our results clearly demonstrate that targeting treatment to limit high glucose induced cellular abnormalities is likely to be insufficient to yield significant benefits in limiting the progression of diabetic nephropathy.

It is increasingly recognized that hyperglycemia and hypoxia co-exist in the kidney in diabetic nephropathy. Brownlee *et al.* have suggested that intracellular hyperglycemia influences blood flow, microvascular cell loss leading to progressive capillary occlusion, and increased vascular permeability which with time, leads to progressive ischemia [436]. Hypoxia resulting from capillary loss and decreased blood flow has long been thought to play an active role in the progression of CKD and more recently, diabetic nephropathy has been considered as a disorder of oxygen metabolism [154]. Our results clearly demonstrate the importance of therapeutic targets that independently modify the deleterious effects of hyperglycemia and hypoxia. Alternatively, as tissue hypoxia is likely to be a consequence of long term tissue exposure to high glucose, blocking the cellular consequences of exposure to high glucose levels is likely to be of maximal benefit early in the course of diabetes prior to established pathology leading to tissue hypoxia.

The role of TGF-β1 in the pathogenesis of diabetic nephropathy is undisputed. Various groups have shown in different renal cells that exposure to high glucose [161], angiotensin II [179, 180], thromboxane [182], or cyclical stretch [183] results in increased transcription and activation of TGF-β1. Our laboratory has also shown that, in human tubular cells, high glucose increases activator protein (AP-1) binding, its downstream cytokine TGF-β1 and the downstream extracellular matrix protein fibronectin [397].

However, the post-transcriptional mechanisms that regulate TGF-β1 protein activation are less well characterized. Perhaps the most studied and well understood *in vitro* TGF-β1 activation system is the plasminogen/ plasmin proteolytic system. It is speculated that high glucose induces protein kinase C, leading to generation of plasmin, which releases mature TGF-β1 from L-TGF-β1 localized at the cell surface by the interaction of LAP with CI-M6P receptor. Our results support this view as blockade of the CI-M6P receptor with PXS-25 abolished activation of TGF-β1 in high glucose conditions

Activation of TGF-β1 in hypoxia is less clear. Higgins *et al.* have recently proposed that hypoxia promotes fibrogenesis in renal epithelial cells via mechanisms that are both dependent and independent of TGF-β1 and the hypoxia inducible proteins [85]. The likelihood that hypoxia and TGF-β1 act independently has been previously demonstrated in cultured fibroblasts [437]. Our data suggesting amplification of fibronectin production with hypoxia and high glucose support this hypothesis. More recently, hypoxia has been shown to be able to induce CTGF expression independent of high glucose by direct interaction of HIF-1 transcription factors with the CTGF promoter in PTCs [428]. Therefore, it is possible

that both hyperglycemia and hypoxia may independently induce profibrogenic properties through TGF-β1 dependent and independent pathways.

Tubulointerstitial fibrosis is caused not only by an increase in the rate of matrix synthesis, but also by the impaired degradation of matrix proteins. MMP-2 and MMP-9 whilst sharing the ability to degrade basement membrane collagens and gelatins their substrate specificity is not identical. MMP-2 degrades fibronectin and laminin, and has significantly less activity against type IV and V collagen than MMP-9 [87, 438]. TGF-β1 not only increases ECM synthesis, it is also able to interfere with proteolytic degradation of ECM proteins [439]. Orphanides *et al.* have also shown that human PTCs subjected to oxygen deprivation exhibited reduced MMP-2 activity and increased in TIMP-1 [429]. In our study, hyperglycemia induced production of both MMPs in normoxic conditions. However, under hypoxic conditions, high glucose induced only production of MMP-9, not of MMP-2. PXS-25 did not affect the level of MMPs produced in PTCs, suggesting that high glucose induction of MMPs is through a CI-M6PR independent pathway.

In conclusion, our study has clearly demonstrated the role of PXS-25 in the prevention of the early fibrotic response of PTCs to hyperglycemia. It has highlighted the potential for a CI-M6PR inhibitor to dampen ECM production in response to hyperglycemia. However, it has also highlighted that under the current experimental conditions mimicking the late stage of diabetic nephropathy, where hypoxia is present, activation of latent to active TGF-β_1 is less dependent on CI-M6PR, suggesting combination therapies may be required.

CHAPTER 5: Activation of Farnesoid X receptors inhibits extracellular matrix deposition in human kidney proximal tubular epithelial cells

5.1 Introduction

The initial chapters of this thesis have discussed several factors responsible for the development of nephropathy in DM and potential strategies to limit the development of diabetic nephropathy are needed. Studies in humans with type 1 and type 2 DM, and in animal models of this disease have reported an accumulation of lipids in the kidney, even in the absence of abnormalities in serum lipid levels – which is associated with the development of glomerulosclerosis, tubulointerstitial fibrosis, and the progression of diabetic renal disease [25]. Virchow first suggested the association between lipids and renal disease in 1858 [440]. There is now growing evidence that abnormal lipid metabolism is central to the development of renal disease.

More recently, the recognition of the metabolic syndrome further strengthens the link between glucose, lipids and renal disease. Although the exact mechanism is still poorly understood, several hormonal and metabolic factors have been shown to contribute to the pathogenesis of obesity-related renal disease. Peroxisome proliferator activated receptors (PPARs), a subfamily of the nuclear receptors have been recognized as key players in the pathogenesis of metabolic syndrome and its renal complications[441]. In recent years, much attention has been paid to PPARs and their synthetics agonists, particularly PPARγ agonists, as therapeutic targets in the treatment of diabetes mellitus and its renal complications.

Other nuclear receptors, better known as bile acid receptors or farnesoid X receptors (FXR or NR1H4), are also increasingly recognised as playing a role in metabolic disease and nephropathy. They are named after farnesol, an intermediate in the mevalonate biosynthetic pathway which has been found to weakly activate FXR at supraphysiological concentrations [356, 357]. FXR is highly expressed in the liver, intestine, adrenal gland and kidney, but with lower expression in fat and heart [365]. FXR alters the expression of groups of genes involved in bile acid homeostasis. One of the better known target genes is short heterodimer partner (SHP), which in turn inhibits cholesterol 7α-hydroxylase (CYP7A1) expression, hence represses bile acid synthesis in the liver[373]. Activation of FXR has an important role in maintaining glucose, cholesterol and lipid metabolism[368, 369]. However, the significance of this process in organs other than liver and intestine remains unclear. The diseases that have been linked to abnormal expression or regulation of FXR include cholestasis, DM, atherosclerosis, cholesterol gall stone disease, liver regeneration and inflammation, breast and colonic cancer[355]. Importantly, FXR agonists have been recently shown to limit renal fibrosis by modulating genes involved in lipid metabolism and ECM production in mouse mesangial cells and *in vivo* in an animal models of type I diabetic nephropathy [33].

FXR is also known for its role in the regulation of fatty acid metabolism by inhibiting sterol regulatory binding protein-1 (SREBP-1)[376, 391]. It has been shown in kidney mesangial cells that hyperglycemia induces mesangial NADPH oxidase (Nox) cytosolic protein p47phox, mediated by SREBP-1, which leads to a NADPH-mediated endogenous production of reactive oxygen species (ROS) [388] Sun *et al.* has shown using SREBP-1a transgenic mice, that its overexpression in the kidney causes lipid accumulation

and increased expression of profibrotic cytokines, ECM accumulation, mesangial expansion, glomerulosclerosis and proteinuria[386]. Conversely, in SREBP-1c knockout mice, a high saturated fatty acid diet failed to induce profibrotic responses with a lower expression of profibrotic cytokines and ECM accumlation[387]. These studies and many others suggest that alterations in renal lipid metabolism, mediated by SREBP-1, plays an important role in the pathogenesis and progression of renal disease in a variety of renal diseases, including nephropathy occurring in type 1 and type 2 diabetes[25, 385-387, 442].

As discussed in prior chapters, although glomerular lesions are characteristic of diabetic nephropathy, pathology within the tubulointerstitium is ultimately more predictive of the renal outcome [422]. Renal epithelial cells contribute largely to the development of renal fibrosis, as they increase and remodel ECM when stimulated either by cytokines or by their microenvironment. Although historically considered as a largely 'non-inflammatory' disease process, it has been recently demonstrated that inflammation plays a significant role in the development and progression of diabetic nephropathy [443, 444]. Studies in our lab have shown that TGF-β1 increases proinflammatory cytokines including MCP-1, macrophage inhibitory factor (MIF) and IL-8 production in human PTC [445].

FXR has been reported to interact with peroxisome proliferator-activated receptor γ (PPARγ) and Retinoid X receptor (RXR) in the liver. Mencarelli *et al.* using $ApoE^{-/-}$ mice fed with high fat diets, discovered that the expression of FXR and SHP in the aorta of $ApoE^{-/-}$ mice is endogenously upregulated. On the contrary, PPARγ expression is markedly suppressed in this animal model. Even though the pathogenic relevance of this is unclear, FXR ablation in this model accelerates the development of severe atherosclerotic disease[390]. In another study, peroxisome proliferator-activated receptor-γ coactivator 1α

(PGC-1α) was found to regulate triglyceride metabolism through a FXR-dependent pathway by increased FXR mRNA and its target genes, via coactivation of PPARγ and hepatocyte nuclear factor 4α (HNF4α)[391]. More recently, different PPARγ agonists have been shown to have differential modulatory effects on FXR. Troglitazone, but not rosiglitazone or pioglitazone can potently antagonize bile acid-mediated activation of FXR and affect its downstream target genes[392]. However, the mechanistic interaction of these nuclear receptors in the pathogenesis of human kidney diseases remains largely unknown. Our laboratory has previously shown that HK-2 cells exposed to short term elevations in glucose increased PPARγ expression with a parallel reduction in secreted MCP-1 [446]. We also showed that further upregulation of PPARγ with the use of an agonist further reduced MCP-1 expression. Hence in this study, we aimed to study the effect of high glucose on FXR expression, FXR regulation of ECM accumulation and inflammation, and to compare the effects of PPARγ and FXR agonists in human PTC.

5.2 Materials and methods

5.2.1 Cell culture

HK-2 cells, a human proximal cell line from American Type Cell Collection (ATCC, USA), were used in this study as previously described [396]. Cells were grown in 10 cm tissue culture dishes (Becton, Dickinson, NJ, USA), in Keratinocyte Serum-free Media (KSFM) supplemented with bovine pituitary extract and epidermal growth factor (GIBCO). These cells were grown at 37°C in a humidified 5% CO_2 incubator. The clinically available thiazolidinediones, pioglitazone (Cayman Chemical, MI, USA) and

rosiglitazone (Cayman Chemical, MI, USA) were used as PPARγ agonists. The FXR agonist used was GW 4064 (Sigma Aldrich, USA). Pioglitazone and rosiglitazone have a binding activity (IC_{50}) to the recombinant human PPARγ isoform of 3000nM. Our laboratory has previously undertaken the dose response experiments and the optimum concentration to induce PPARγ in PTCs for both pioglitazone and rosiglitazone is 10 μM. Initial 'dose response' experiments for GW4064 were undertaken to determine the concentration at which GW 4064 maximally stimulated FXR protein expression but were minimally cytotoxic. Exposure to 1 μM of GW 4064 showed no cell toxicity. When 60-70% confluent, cells were exposed to the following experimental conditions for 24 hours for determination of mRNA expression or 48 hours for protein expression unless otherwise stated:

1) 5 mM D-glucose +0.13% DMSO (vehicle control);

2) 30 mM D-glucose (ICN Biomedicals, Ohio, USA);

3) 10 μM pioglitazone;

4) 10 μM rosiglitazone;

5) 1 μM GW 4064;

6) 10 μM pioglitazone plus 30 mM D-glucose;

7) 10 μM rosiglitazone plus 30 mM D-glucose;

8) 1 μM GW 4064 plus 30 mM D-glucose and

9) 5 mM D-glucose + 25mM L-glucose as osmotic control (ICN Biomedicals, Ohio, USA). 0.13% DMSO was added as per the vehicle control.

5.2.2 Cell proliferation and cytotoxicity studies of GW 4064

$1.3x10^4$ cells were seeded in each of the 96-well plate. After 24 hours, they were then exposed to 5 mM D-glucose as the control, and 5 mM D-glucose plus 0.05 μM, 0.1 μM, 0.5 μM, 1 μM and 2 μM of GW 4064. Cells were then grown in standard culture conditions for a further 48 hours. The cytotoxic and proliferative effects of GW 4064 on HK2 cells were assessed using CellTiter 96® AQ_{ueous} One Solution Cell proliferation Assay (Promega, Madison, WI) as previously described [409].

5.2.3 Flow cytometric analysis for cell cycle

Cell cycle analysis was performed as per the methods detailed in Chapter 2. Briefly, cells were harvested by trypsinisation after 24 hours in the defined experimental conditions, spun, washed, then fixed in 70% ice-cold ethanol. The cell pellet was then resuspended in 1 ml of fluorochrome solution containing propidium iodide (PI) 50 μg/ml (Sigma, MO, USA), RNase A 50μg/ml (Sigma, MO, USA), 0.25μM EDTA and 0.001% Triton X-100 and left for at least 1 hour in the dark. Flow cytometry was performed using a FACScan flow cytometer (Becton Dickinson, CA, USA).

5.2.4 Relative quantitative real-time reverse transcription polymerase chain reaction

RNA was extracted using the RNAeasy mini kit (Qiagen, Valencia, CA, USA) according to manufacturer's instructions. cDNA was generated by reverse transcribing 1 μg of total RNA in a reaction volume of 20ul using VILO cDNA synthesis kits (Invitrogen, Carlsbad, CA, USA). One microlitre (50 ng) of cDNA was used as template in a 20μl PCR reaction. Quantitative real-time PCR was performed using an ABI Prism 7900 HT Sequence Detection System (Applied Biosystems, Foster City, CA, USA) with Taqman Gene Expression Master Mix (Applied Biosystems) and gene-specific expression assays containing two unlabelled PCR primers and FAM dye-labeled Taqman MGB probe (Applied Biosystems). Taqman probes used are listed in *Table 5.2.4.1.* Reactions were performed in at least triplicate and analyzed by relative quantitation using RQ Manager software, Version 1.2 (Applied Biosystems). All data are presented as fold change compared to control after normalization to β-Actin. A water blank was used as the negative template control.

Table 5.2.4.1. **RT-PCR Primers**

Gene Name	Assay ID	Amplicon length
FXR (NR1H4)	Hs00231968_m1	85
SHP(NR0B2)	Hs00222677_m1	87
SREBP-1c	Hs01088691_m1	90
Fibronectin	Hs01549976_m1	81
TGF-β1	Hs00998133_m1	57
MCP-1	Hs00234140_m1	101
Human β-Actin	4333762F	171

NR1H4, nuclear receptor, subfamily 1m group H, member 4

NR0B2, nuclear receptor, subfamily 0, group B, member 2

5.2.5 Western blot analysis

Cells were collected and the cell pellet was resuspended in cell lysis buffer as previously described in Chapter 2. The cell lysate was then sonicated to release nuclear proteins, spun at 12,000 rpm at 4°C and stored at -80°C. Protein lysate extraction and western blot was performed as previously described [397]. Briefly, thirty micrograms or seventy five micrograms (nuclear protein study) of total cell protein were mixed with 6X Laemmli sample buffer containing mercapto-ethanol and heated at 95°C for 10 min. Samples were then analyzed by SDS-PAGE in 7.5 to 10% gels and electroblotted to Hybond Nitrocellulose membranes (Amersham Pharmacia Biotech, Bucks, UK). Membranes were blocked in Tris-buffered saline containing 0.2% Tween 20 (TTBS) in 5

% skim milk for 2 hours and then incubated overnight at 4 °C with antibodies to PPARγ 1:300 (Santa Cruz, Biotechnology); FXR 1:1000 (Abcam. Ltd, Cambridge, USA); fibronectin 1:100 (NeoMarkers, CA); collagen IV 1:5000 (Abcam Ltd, Cambridge), and β-actin 1:300 (Santa Cruz, CA). Membranes were washed three times with TTBS and incubated with horseradish peroxidase-conjugated secondary antibody for 2 hours at room temperature and then washed three times with TTBS. The membranes were reprobed with β-Actin. Protein bands were visualized using the ECL detection system (Amersham Pharmacia Biotech). The bands corresponding to fibronectin (220kDa), collagen IV (250kDa), PPARγ (60kDa), FXR (54kDa) and β-Actin (42kDa) were captured using LAS 4000 (Fujifilm, Tokyo, Japan), corrected for β-actin as a loading control and analysed using the Multigauge system (Fujifilm, Tokyo).

5.2.6 Human kidney tissue preparation and immunohistochemistry (IHC)

Paraffin-embedded tissue blocks from renal biopsies from patients with diabetic nephropathy (n=3) were studied. Controls consisted of histologically normal kidneys obtained from patients undergoing nephrectomy for small kidney tumours (n=5). Ethics approval for the study was obtained from the Royal North Shore Hospital Human Research Ethics Committee. Four-micrometer-thick paraffin sections from the kidney cortex were used for immunohistochemistry for FXR. Tissue was incubated overnight at 4 °C with the polyclonal primary antibody anti-FXR (1:50 dilution, Abcam Ltd, Cambridge) followed by equal volume of Envision dual linked system (Dako Cytochemistry, Tokyo, Japan) for 30 minutes after two 5 minutes washes. Staining was developed with 3.3 diaminobenzidine tetrahydrochloride (Dako Cytochemistry, Tokyo, Japan) for 10 minutes before

counterstaining with Mayer's haemotoxylin stains. Images were visualised using an Olympus microscope (Olympus, Japan). Sections incubated with anti-rabbit IgG served as the negative controls.

5.2.7 Gene silencing by small interfering RNA (siRNA)

27-mer double-stranded RNA molecules were chemically synthesized (Shanghai GenePharma Co, Ltd, Shanghai, China). The complementary oligonucleotides were 2'-deprotected, annealed, and purified by the manufacturer. The sequence specifically targeting human FXR (NR1H4) (accession no. NM_005123) was 5'-GAUUGUUACUUCAACUCUATT-3', 5' UAGAAUUGAAGUAACAAUCTT 3'. HK-2 cells were grown in a 6-well plate. Eighty nmol/L of FXR siRNA was introduced into HK-2 cells using Lipofectamine 2000. In parallel, cells were transfected with a non-specific siRNA which served as a control. Twenty four hours after transfection, both the control and FXR silenced cells were exposed to 5 mM D-glucose or 30 mM D-glucose for 48 hours. Silencing was confirmed by knock-down of FXR mRNA and protein expression.

5.2.8 MCP-1 ELISA

Conditioned media were spun and stored at -80 °C until MCP-1 levels were determined by commercially available ELISA kits (Biosource International, CA, USA) as per manufacturer's instructions and read using a microplate reader at 450 nm. Cell lysate protein concentration was determined using the Bio-Rad protein assay, and MCP-1 levels were corrected for protein content per well.

5.3 Statistical analysis

Each experiment was performed independently a minimum of three times. Real-time PCR results are expressed as fold change compared with the control value. RT-PCR data are expressed as percentage of the control value. Results are expressed as mean ± SEM. Statistical comparisons between groups were made by analysis of variance (ANOVA), with pairwise multiple comparison made by Fisher's protected least-significant difference test. Analyses were performed using the software package Statview, version 4.5 (Anacus Concepts Inc, Berkeley CA). P values <0.05 were considered significant.

5.4 Results

5.4.1 High glucose down regulates FXR expression and regulates its target genes

Initial experiments were conducted to assess the effect of high glucose exposure on FXR expression and its downstream target genes. HK-2 cells were cultured in 5 mM D-glucose and 30 mM D-glucose at 24 and 72 hours to assess its early and later effects. Exposure to high glucose (30 mM D-glucose) significantly suppressed FXR mRNA expression to 0.5 ± 0.03-fold and 0.3 ± 0.1 fold-change at 24 and 72 hours respectively (Figure 5.4.1.1). This effect was not seen in cells cultured in 25 mM L-glucose +5 mM D-glucose which served as an osmotic control (data not shown).

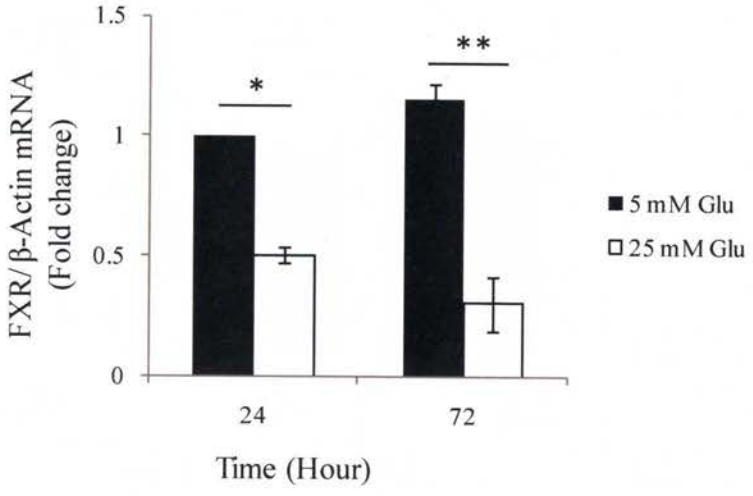

Figure 5.4.1.1 FXR mRNA and high glucose.

*High glucose down regulates FXR mRNA expression at 24 hours and further suppressed FXR mRNA at the 72 hour time point (*p < 0.05, **p < 0.01). All experiments were performed in at least triplicate for each time point and data are expressed as mean ± SEM (n=3).*

At 72 hours, exposure to high glucose was associated with down-regulation of SHP to 0.33 ± 0.2 fold-change, p <0.01 when compared the cells exposed to 5 mM D-glucose (Figure 5.4.1.2). At 24 hours, there was no difference in SHP mRNA expression, (1 vs. 1.1 ± 0.03 fold-change). This is in consistent with down regulation of the FXR gene expression observed after exposure to high glucose but the regulatory effects on downstream SHP expression was only observed at a later time point, in this case at 72 hours.

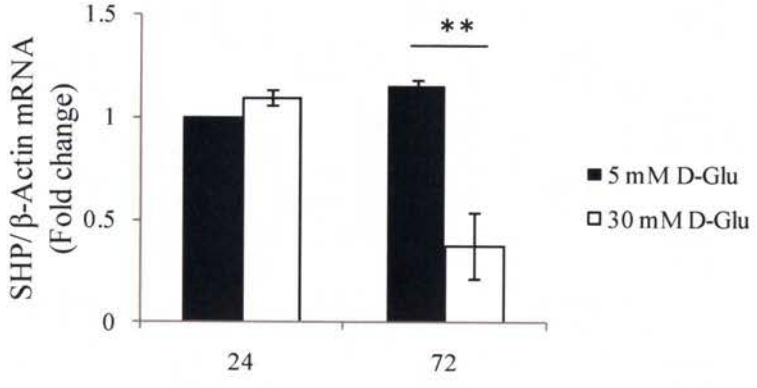

Figure 5.4.1.2 High glucose on short heterodimer protein (SHP).

*Even though SHP, the target gene directly regulated by FXR showed no difference in its mRNA expression at 24 hour post exposure to high glucose, its mRNA was suppressed after 72 hours exposure to high glucose (**$p < 0.01$). All experiments were performed in at least triplicate for each time point and data are expressed as mean ± SEM (n=3).*

Down regulation of FXR is associated with up-regulation of SREBP-1c mRNA, a target gene indirectly suppressed by FXR (Figure 5.4.1.3). At 72 hours, SREBP-1c mRNA was markedly up-regulated in the HK-2 cells exposed to high glucose, 2.4 ± 0.24 fold-change when compared to the cells exposed to 5 mM D-glucose, 1.15 ± 0.08 fold-change, $p < 0.001$.

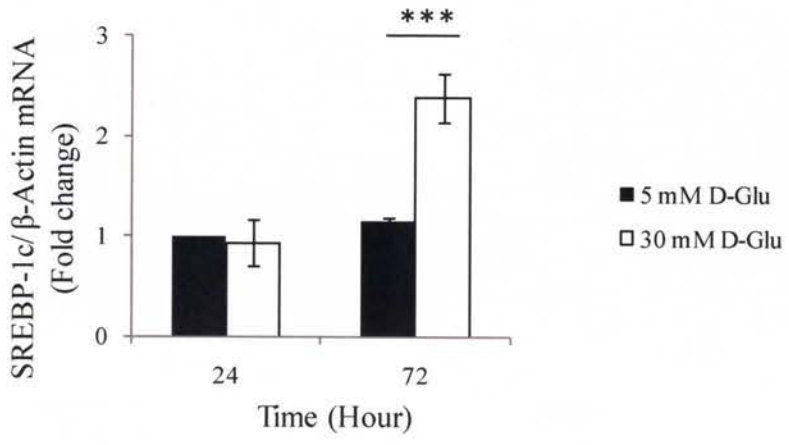

Figure 5.4.1.3 Sterol regulatory element-binding protein 1c mRNA expression on exposure to high glucose.

*SREBP-1c, a gene normally indirectly suppressed by FXR through fatty acid synthase inhibition, was up regulated at 72 hours post exposure to high glucose consistent with the observation of suppression of FXR in high glucose conditions. All experiments were performed in at least triplicate for each time point and data are expressed as mean ± SEM, ** $p < 0.01$, $n=3$.*

Immunohistochemistry confirmed nuclear staining of FXR in predominantly proximal and distal tubules of control nephrectomised kidney specimens. Mesangial cells occasionally stained positively for FXR. Reduction of nuclear FXR expression was seen in kidney biopsy specimen of individuals with diabetic nephropathy (Figure 5.4.1.4).

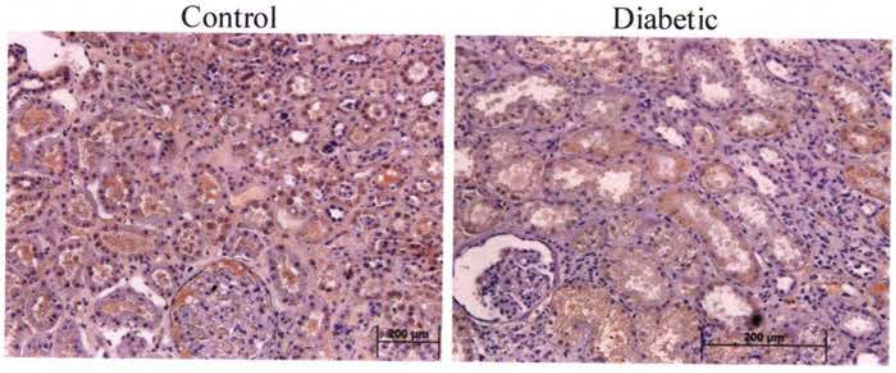

Figure 5.4.1.4 FXR expression in kidney biopsy specimens.

Kidney biopsy specimens from individuals with diabetic nephropathy showed a significant reduction in FXR nuclear staining (Right) compared to normal kidney tissue (Left). Predominant nuclear staining of FXR was detected in proximal, distal and collecting duct epithelial cells in normal kidney tissue. Podocytes and mesangial cells were occasionally positive for FXR staining.

5.4.2 Cell viability in the presence of GW 4064

Exposing HK-2 cells to GW 4064 had no effect on cell proliferation or cytotoxicity in the following concentration 0.05 μM, 0.1 μM, 0.5 μM and 1 μM. However, these cells demonstrated significant toxicity with 2 μM of GW 4064, 81.9 ± 1.8 % at 48 hours, compared to the control (Figure 5.4.2.1). Our laboratory has previously demonstrated exposure of high glucose does not affect HK-2 cell viability or proliferation [397].

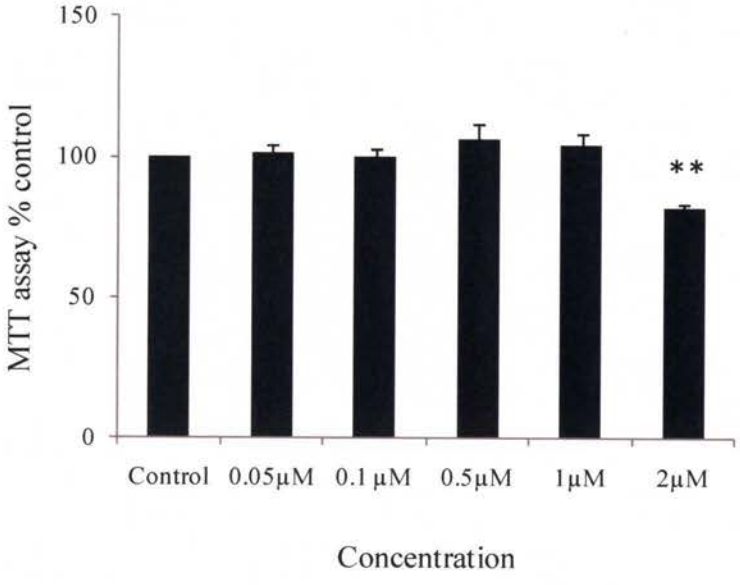

Figure 5.4.2.1 Effect of GW4064 on cell proliferation.

*HK-2 cells were incubated for 48 h with control media and media containing 0.05 μM, 0.1 μM, 0.5 μM, 1 μM and 2 μM of GW 4064. Cell proliferation and viability was assessed by CellTiter 96® AQ_{ueous} One Solution Cell proliferation Assay. Results were normalized to total protein content of each well and the normalized results are expressed as means ± SEM, n=3 (** $p < 0.01$ vs. Control).*

5.4.3 FXR agonists on cell cycle assessed by flow cytometry

These experiments were undertaken since our laboratory has previously demonstrated that the PPARγ agonist, L-805645 and pioglitazone both induce G1 phase arrest through a p21-mediated mechanism. One micromolar of GW 4064 had no effect on progression through the cell cycle. Cells exposed to 1 μM of GW 4064 showed a similar

percentage of cells in the G1 phase, 57.7±2.5% as compared to the control groups, 60.1±5.6% at 24 hours; 84.6±3.8% vs. 83.8±6.9% at 48 hours; and 90.9 ±10.1% vs. 92.4 ±9.4% at 72 hours. Together with the previous data, the concentration of GW 4064 used has minimal effect on viability or progression through the cell cycle [397].

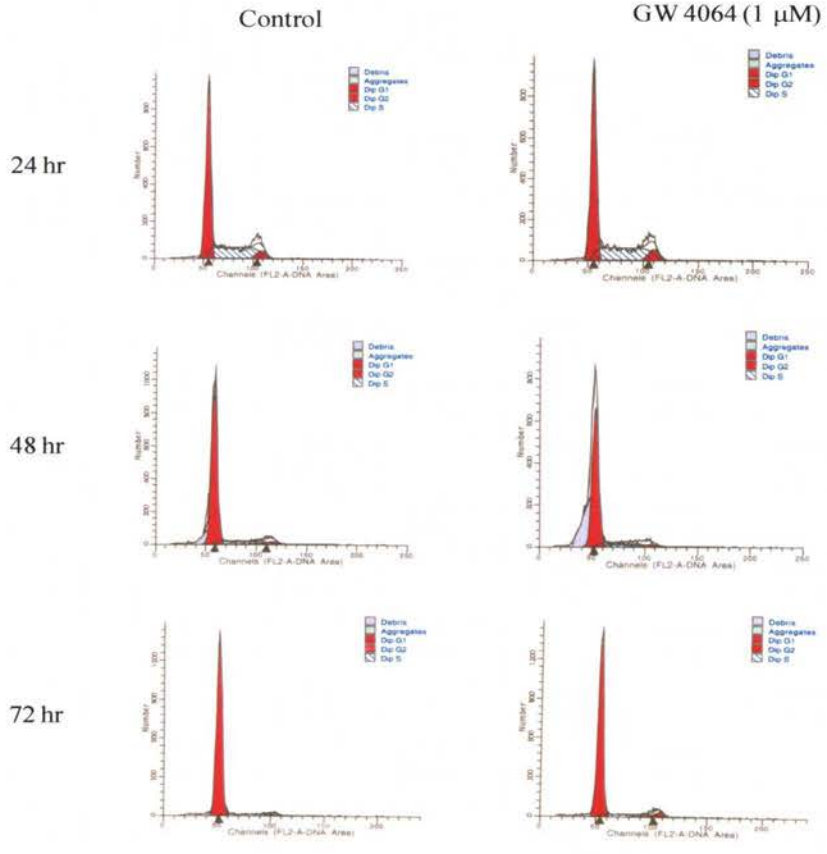

Figure 5.4.3.1 Effects of GW4064 on cell cycle progression.

One micro molar of GW4064 does not affect HK-2 cell cycle progression. All experiments were performed in at least triplicate for each time point and data are expressed as mean ± SEM, n=3.

5.4.4 PPARγ agonists and FXR agonists inhibit high glucose induced fibronectin expression

The protein expression of two extracellular matrix proteins accumulated in diabetic nephropathy, namely fibronectin and collagen IV was determined in the HK-2 cells. Fibronectin mRNA was found to be induced by 24 hours exposure to high glucose to 1.25 ± 0.05 fold-change, $p < 0.05$ as compared to the vehicle control (Figure 5.4.4.1). Both PPARγ agonists, pioglitazone and rosiglitazone were able to suppress high glucose induced fibronectin mRNA to 0.94 ± 0.04 fold-change, $p<0.01$, and 0.910 ± 0.06 fold-change, $p<0.01$ as compared to the high glucose exposed groups. GW 4064 was more effective in suppressing fibronectin mRNA to 0.63 ± 0.16 fold-change, $p < 0.001$. Fibronectin protein expression was induced to 177.1 ± 18% in cells exposed to high glucose for 48 hrs as compared to control ($p < 0.01$, Figure 5.4.4.2). Exposure to pioglitazone, rosiglitazone and GW 4064 alone did not alter fibronectin protein expression, being 115 ± 29%, 116 ± 27% and 140 ± 21%, respectively. However, all three agents suppressed high glucose-induced fibronectin production at 48 hrs to 102.4 ± 18%, 104% ± 17 and 83.4 ± 17% respectively when compared to control. Exposure to the osmotic control had no effect on fibronectin expression.

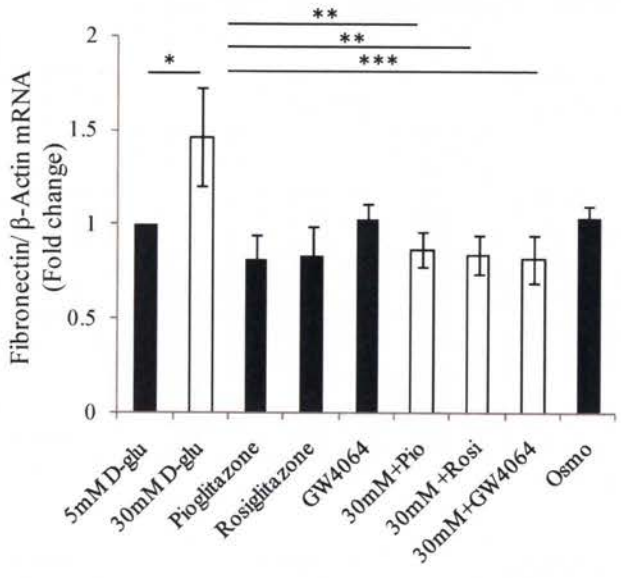

Figure 5.4.4.1 Effect of PPARγ and FXR agonists on fibronectin mRNA expression in high glucose conditions.

*HK-2 cells were incubated with the vehicle control media containing 5 mM D-glucose (solid black bars), 30 mM D-glucose (white bars), pioglitazone (10 μM), rosiglitazone (10 μM), GW 4064 (1 μM), pioglitazone (10 μM) + 30 mM D-glucose, rosiglitazone (10 μM) + 30 mM D-glucose, GW 4064 (1 μM) + 30 mM D-glucose, and 25 mM L-glucose + 5 mM D glucose in control media. RNA was collected at 24 hours and cell lysate was harvested at 48 hours. High glucose induced fibronectin mRNA expression which is not seen in the osmotic control (5mM D-glucose + 25 mM L-glucose). Both PPARγ agonists and FXR agonist are equally potent in preventing high glucose-induced fibronectin mRNA induction. All experiments were performed in at least triplicate for each time point and data are expressed as mean ± SEM, * $p<0.05$ vs. Control; ** $p < 0.01$ vs. Control; *** $p < 0.0001$ vs. Control, $n=3$.*

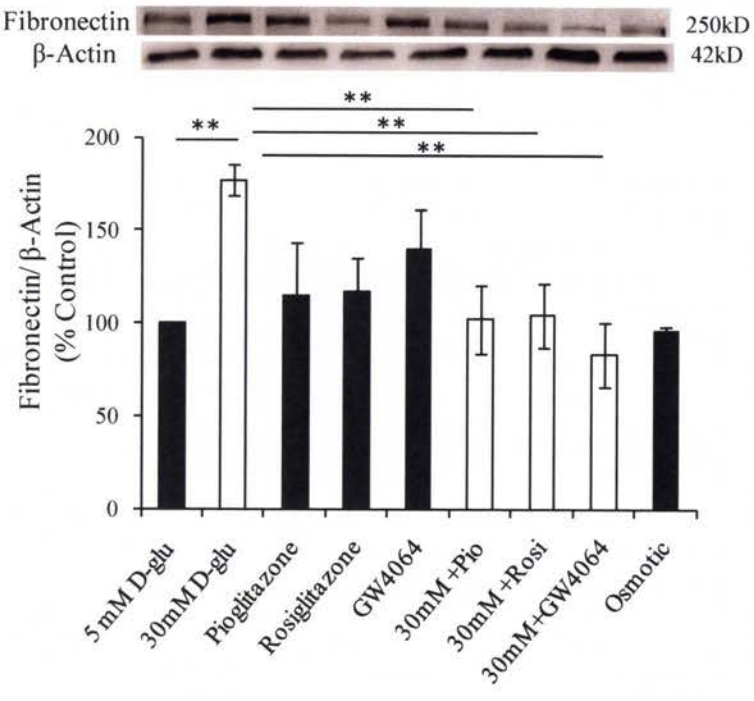

Figure 5.4.4.2 Effect of PPARγ and FXR agonists on fibronectin protein expression in high glucose conditions.

*High glucose induced fibronectin production in HK-2 cells. Both PPARγ and FXR agonists were able to suppress high glucose-induced fibronectin protein expression. Results are expressed as means ± SEM, * $p<0.05$ vs. Control; ** $p < 0.01$ vs. Control, n=4.*

5.4.5 FXR agonists but not PPARγ agonists suppressed high glucose induced type IV collagen expression

At 48 hours, exposure to high glucose induces another ECM protein, type IV collagen production in HK-2 cells, to 131.3 ± 7.7 %, $p < 0.05$, when compared to control. Both PPARγ agonists failed to significantly suppress high glucose-induced type IV collagen production. Only the FXR agonists suppressed its expression to 63.3 ± 7.9%, $p \leq$

0.01 (Figure 5.4.5.1). L-glucose did not alter type IV collagen expression in similar experimental conditions.

5.4.6 High glucose induced TGF-β1 mRNA expression was suppressed by both PPARγ and FXR agonists

24 hrs exposure to high glucose induced TGF-β1 mRNA expression to 1.46 ± 0.26 fold-change, $p<0.05$ when compared to control (Figure 5.4.6.1). Both pioglitazone and rosiglitazone, and GW 4064 inhibited high glucose-induced TGF-β1 mRNA expression to 0.87 ± 0.07 fold-change, 0.84 ± 0.1 fold-change and 0.82 ± 0.12 fold-change, $p<0.01$, respectively.

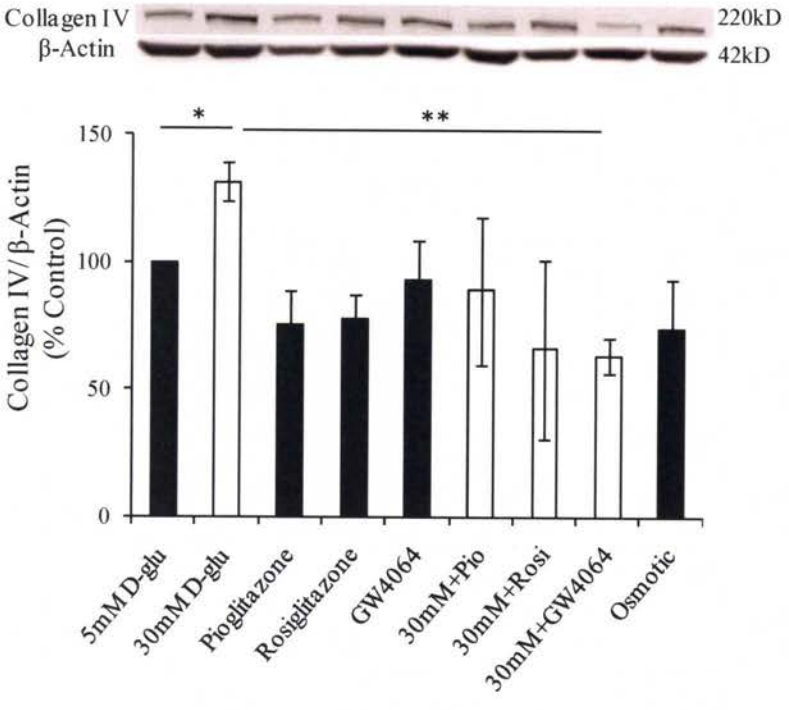

Figure 5.4.5.1 Effect of PPARγ and FXR agonists on type IV collagen protein expression in high glucose conditions

*Type IV collagen, which is the most abundant collagen expressed in the kidney, was induced by high glucose exposure for 48 hours. Only the FXR agonist significantly suppressed high glucose induced type IV collagen production in these cells. Results are expressed as means ± SEM, * $p<0.05$ vs. Control; ** $p < 0.01$ vs. Control (n=4).*

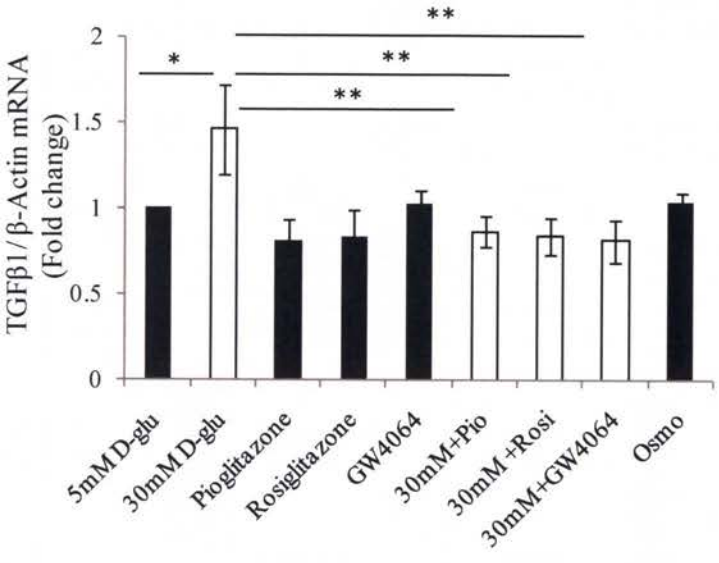

Figure 5.4.6.1 Effect of PPARγ and FXR agonists on high glucose-induced TGF-β1 mRNA.

*High glucose induced TGF-β1 mRNA expression in HK-2 cells. Both PPARγ and FXR agonists can inhibit high glucose-induced TGF-β1 mRNA. Results are expressed as means ± SEM, * $p<0.05$ vs. Control; ** $p < 0.01$ vs. Control (n=4).*

5.4.7 PPARγ agonist but not FXR agonists suppresses high glucose-induced MCP-1 production

An increase in MCP-1 production in the supernatant of cells exposed to high glucose for 48 hours was observed compared with cells exposed to control conditions, (119.3 ± 4.1% control, $p<0.05$, Figure 5.4.7.1). Both pioglitazone and rosiglitazone suppressed high glucose-induced MCP-1 production to 78.6 ± 4.4% and 80.7 ± 8.1%,

$p<0.05$, compared with cells exposed to high glucose. Even though GW 4064 suppressed MCP-1 production in high glucose conditions, it failed to reach statistical significance.

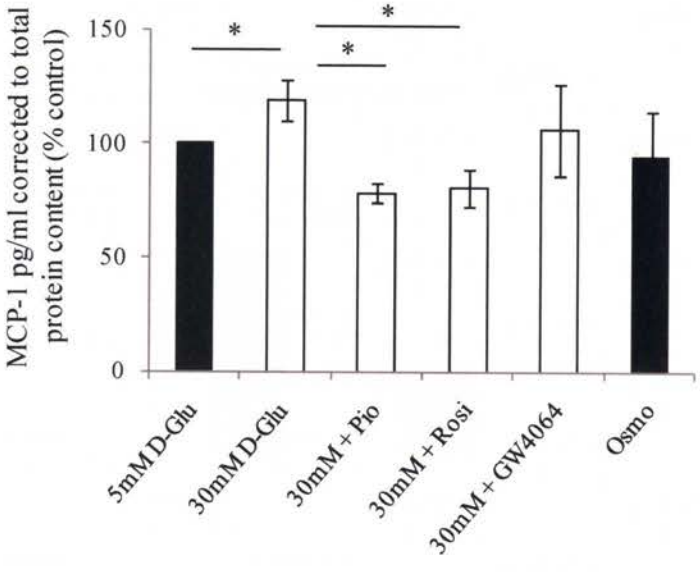

Figure 5.4.7.1 PPARγ agonists inhibit high glucose-induced MCP-1 production in HK-2 cells.

*Forty eight hours exposure high glucose induced MCP-1 production measured in the conditioned media. Both rosiglitazone and pioglitazone suppress high glucose-induced MCP-1 production. However, GW4064 failed to inhibit MCP-1 production in HK-2 cells. Results are expressed as means ± SEM, * $p<0.05$ vs. Control ($n=4$).*

5.4.8 FXR silenced cells have increased fibronectin and type IV collagen expression

FXR silencing was confirmed by both mRNA and protein expression of FXR by RT-PCR and western blotting. A near 40% reduction of FXR protein expression was achieved in all experiments as compared to the control (Figure 5.4.8.1).

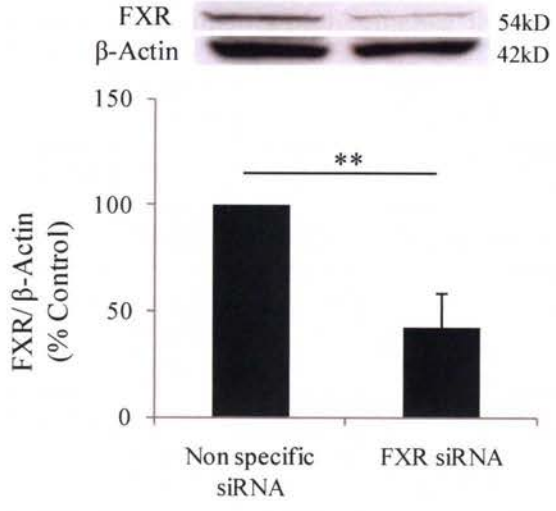

Figure 5.4.8.1 FXR silencing in HK-2 cells.

Subconfluent HK-2 cells were transfected with commercially purchased siRNA specific for FXR. Forty eight hours later, cells were harvested and protein lysates were used for western blotting. Near forty percent reduction of endogenous FXR was observed in cells transfected with FXR siRNA, 42.8±15.9% as compared to cells transfected with a non specific siRNA. Results are expressed as means ± SEM, **p<0.01 vs. control (n=4).

FXR silenced HK-2 cells exhibit increased ECM production compared to cells transfected with random non-specific siRNA. Both fibronectin and type IV collagen

expression were increased in FXR silenced cells to 111.6±1.9%, $p<0.01$ and 140.5±20.6%, $p<0.05$, when compared to the control (Figure 5.4.8.2a & b). Exposure to 30 mM D-glucose for 72 hours increased fibronectin expression in the HK-2 cells transfected with non specific siRNA to 110±2.5%, $p<0.05$, which is further increased to 116.2±1.7 in the presence of FXR siRNA (Figure 5.4.8.2a). Similarly, type IV collagen expression was increased, upon exposure to high glucose in HK-2 cells transfected with non specific siRNA to 130.8±19.9% which is comparable to type IV collagen expression in FXR silenced cells grown in medium containing 5 mM D-glucose. Type IV collagen is further increased to 226.4±34.7%, $p<0.05$, in FXR silenced cells when exposed to high glucose for 72 hours (Figure 5.4.8.2b).

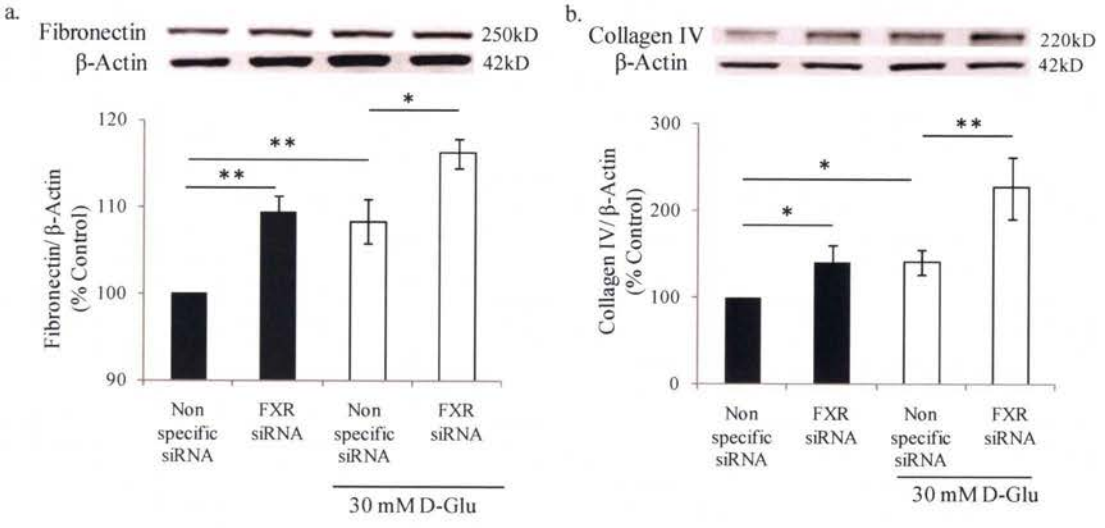

Figure 5.4.8.2 ECM expression in FXR silenced HK-2 cells.

FXR knock down HK-2 cells were then exposed to 5 mM D-glucose (black solid bars) and 30 mM D-glucose (white empty bars) for 72 hours. FXR silenced HK-2 cells exhibit increased fibronectin (a) and type IV collagen (b) expression. On exposure to high glucose,

*these ECM proteins are further up-regulated. Results are expressed as means ± SEM,*p<0.05 vs. control, **p<0.01 vs. control, (n=4).*

5.4.9 FXR silenced cells have increased SREBP-1 expression which is further up-regulated on exposure to high glucose

Increased SREBP-1 expression was found in FXR silenced cells, 132.4±6.1%, $p<0.05$, when compared to cells treated with NS siRNA. Exposure to 30 mM D-glucose further increased SREBP-1 expression to 175.2±16.3% confirming that FXR has an inhibitory regulatory role on SREBP-1 expression (Figure 5.4.9.1).

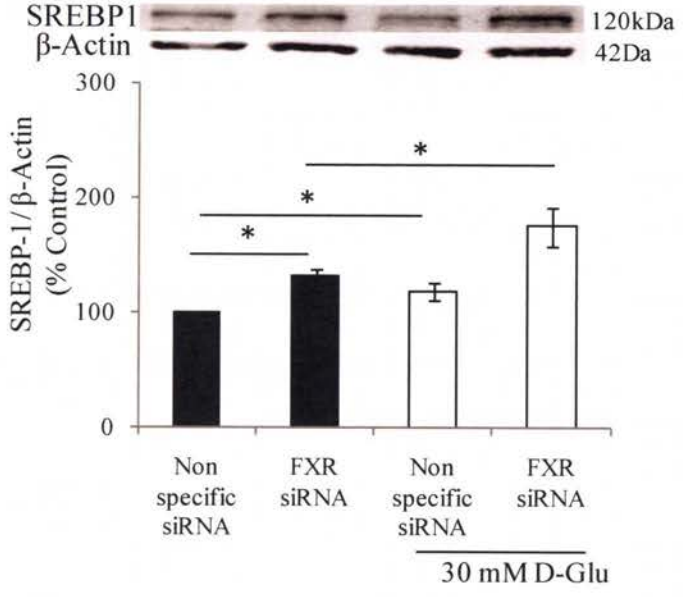

Figure 5.4.9.1 Effect of FXR silencing on SREBP-1 expression.

SREBP-1 is increased in FXR silenced cells under basal conditions which is further up-regulated in high glucose condition (c). Results are expressed as means ± SEM ,$p<0.05$ vs. control, (n=4).*

5.5 Discussion

Although patients with diabetic nephropathy typically have concomitant hyperglycemia and dyslipidemia, the contribution of lipid-induced renal injury to diabetic nephropathy is not well characterized. Recently, there is growing evidence to suggest that dysregulated lipid metabolism may play a role in the pathogenesis of diabetic nephropathy[447]. Hyperglycemia induces circulating or locally produced inflammatory and profibrotic factors, such as MCP-1, TGF-β1, endothelin 1 and angiotensin II in the kidney[159]. Insulin resistance alters adipocyte metabolism, which leads to the release of free

fatty acids in plasma. It is believed hyperglycemia and free fatty acid induces kidney mesangial cell production of reactive oxygen species (ROS) through a SREBP-1 dependent pathway[14]. Nephrectomy in rats resulted in the accumulation of lipids in the remnant kidney which was considered to be due to the effect of increased tubular reabsorption of filtered protein-bound lipids, the influx of oxidized lipoproteins, the synthesis of fatty acids, and the inhibition of pathways involved in fatty-acid catabolism. In response to hyperglycemia, albuminuria and lipid byproducts, PTCs increase synthesis of pro-fibrotic and pro-inflammatory cytokines[141].

FXR is a potential pharmacological target for the treatment of obesity and the metabolic syndrome[381] because of its modulatory effects on bile acid, lipids and glucose metabolism. Several studies have shown that FXR activation can ameliorate diabetic nephropathy by modulating lipid metabolism, fibrosis, inflammation, and oxidative stress[33, 384, 448]. The molecular mechanism of lipid-lowering effects of FXR agonist in kidney disease has remained elusive. It has been shown that this is mediated predominantly by altering the kidney SREBP-1 activity and its lipogenic target genes[376]. Despite the mRNA expression of FRX in mice PTCs being five times more than that of the glomeruli, there is lack of direct evidence linking FXR with SREBP-1c in kidney PTCs[33]. Jun *et al.* have demonstrated that *in vitro* exposure to high glucose can induce fatty acid accumulation and a fibrotic response in HKC cells (human proximal tubular cell line), which is inhibited by silencing SREBP-1[449]. However, the authors did not study its association with FXR in PTCs.

In this study, we have demonstrated that FXR is expressed in the nuclei of normal adult kidney tubules and this is markedly down regulated in individuals with diabetes

mellitus. This reduction is observed in structurally well preserved tubules with no significant tubulointerstitial damage, suggesting it is an early tubular response to hyperglycemia. This is further confirmed by *in vitro* studies using HK-2 cells, where 24 hours exposure to high glucose is sufficient to down regulate FXR mRNA expression, which is further down regulated at 72 hours. This confirms that exposure to high glucose can directly suppress FXR mRNA expression in PTCs. This observation is of interest because loss of FXR is known to disrupt normal glucose homeostasis and leads to the development of insulin resistance which is associated with elevated serum triglycerides and lipid accumulation[450]. We have shown that, SHP mRNA, a target gene of FXR was significantly down regulated at 72 hours, and consistent with that, SREBP-1c mRNA expression was up-regulated. We have shown here in kidney PTCs, reduction of FXR in high glucose leads to a reduction in SHP, which in turn leads to increased SREBP-1c expression. This is analogous to the proposed mechanism of FXR regulation in the liver by bile acids, which has invoked SHP as a mediator[373].

The presence of lipids deposits in the kidney of diabetic patients and in experimental models of DM has been well described. Seventy two hours of exposure to high glucose can stimulate triglyceride rich lipid droplets accumulation and up-regulation of SREBP-1 in human PTCs. Using FXR-/- and SHP-/- animal models, it has been shown that FXR mediates its effect on SREBP-1c expression through SHP-dependent and SHP-independent pathways[451]. Additionally, FXR can impact on triglyceride metabolism by modulating kidney PPARα, PPARγ and PGC-1α expression. The reciprocal effects of SREBP-1c and SHP at 72 hours of high glucose exposure, is potentially a consequence of lipid accumulation rather than high glucose itself.

Consistent with the previous observation, exposure to high glucose induced ECM production. The FXR agonist, GW4064 suppressed high glucose-induced fibronectin and collagen IV production. Conversely, FXR silenced cells exhibit increased basal ECM production which is further up-regulated when PTCs were exposed to high glucose conditions for 72 hours, suggesting a potentiating effect of high glucose and FXR suppression on ECM production. At the same time point, SREBP-1 protein expression in FXR silenced cells is increased which is further up-regulated after exposure to high glucose. Collectively, these results suggest that high glucose suppresses FXR expression, but conversely, a basal level of FXR expression is important to maintain ECM homeostasis. In addition, SREBP-1c and hyperglycemia act synergistically to induce ECM and an FXR agonist can abrogate high glucose induced ECM production.

Our laboratory has previously reported that exposure of HK-2 to high glucose and PPARγ agonists induce PPARγ expression at 48 hours[397]. In this study, we confirmed this observation. In addition we also confirmed that neither PPARγ nor FXR agonists affect FXR expression (data not shown). Both PPARγ and FXR agonists are equally potent in suppressing high glucose-induced fibronectin mRNA and protein expression. However, only FXR agonist is effective in suppressing collagen IV expression in HK-2 cells. This is consistent with previous observations that PPARγ agonists are less effective in suppressing collagen IV production. FXR agonists are equally effective in suppressing high glucose-induced TGF-β1 mRNA upregulation. However, only PPARγ agonists but not FXR agonists, are able to suppress high glucose–induced MCP-1 production. These data suggest that PPARγ agonists are more likely to have anti-inflammatory effects compared to a FXR agonist, which is more potent in modulating ECM production in human proximal tubular

cells. GW4064 has confirmed efficacy at 48 hours, as demonstrated by its antifibrotic effects in the absence of cytotoxicity and cell cycle arrest across the range of doses used in the experiments presented in this thesis. Even though the mechanistic interaction of these nuclear receptors is not addressed in this study, the results proposed the potential mechanisms in these different contexts of the metabolic syndrome-induced nephropathy include the effects of profibrotic and proinflammatory cytokines such as TGF-β1 and MCP-1, oxidative stress and microenvironment homeostasis.

CHAPTER 6: Circulating bone morphogenetic protein-7 and transforming growth factor-β1 as predictive biomarkers for renal outcome in patients with type 2 diabetes mellitus

6.1 Specific background and review

As will be clear from the information presented in the prior chapters of this thesis, an increase in renal parenchymal ECM accumulation has been shown to be the end result of a complex interplay of factors inherent in DM, and also to play a role in the development of diabetic nephropathy[452]. Clinical and experimental studies have demonstrated that tubulointerstitial fibrosis correlates more closely with progressive deterioration of renal function than does glomerular damage[65, 453, 454]. Currently an objective scoring system for measuring interstitial fibrosis on renal biopsy specimens is the gold standard for assessing tubulointerstitial injury. Hence there is a strong need for less invasive biomarkers to predict those at risk of progressive diabetic nephropathy.

TGF-β1 and BMP-7 are secretory cytokines belonging to the transforming growth factor superfamily. TGF-β1 is well recognized for its pro-fibrotic role and is known to increase in diabetes as a consequence of hyperglycemia, advanced glycation end product accumulation and intrarenal accumulation of angiotensin II. As discussed in Chapters 1 and 4, TGF-β1 is secreted in a latent biologically inactive form which is activated by proteloytic cleavage by serine proteinases *in vivo*[167]. Among its many actions, activated TGF-β1 influences cell growth and matrix production and promotes extracellular matrix accumulation by both glomerular and tubular epithelial cells.

Increased expression of TGF-β1 has been demonstrated in renal biopsies from patients with established diabetic nephropathy. The EURODIAB follow up study has demonstrated that circulating and urinary TGF-β1 correlates with proliferative retinopathy and nephropathy in patients with type 1 DM[222]. In patients with type 2 DM, circulating total TGF-β1 has been shown to be elevated when compared to the non diabetic population[223]. In a small cohort of patients with type 2 diabetes, Hellmich *et al* [224] have shown a higher level of circulating active TGF-β1 in those with nephropathy compared to those without nephropathy. However, the sample size of this study was too small to ascertain whether circulating TGF-β1 could be used as a biomarker to predict patients at risk for developing diabetic nephropathy.

African Americans with hypertension and ESKD exhibit higher circulating levels of TGF-β1 as compared to the Caucasian population[214, 215]. The proposed explanation, in addition to the conventional genetic and lifestyle risk factors, includes differences in the bidirectional activities of TGF-β1 and the renin angiotensin aldosterone system (RAAS) in the induction of TGF-β1 activation[216-219]. Recently, a cross sectional study reported a positive association between the circulating TGF-β1 and a variety of established risk factors for CKD progression[220]. In the same study, these investigators reported that TGF-β1 protein levels were predictive of microalbuminuria in African Americans when compared to the Caucasian population. However, a recent multicenter cohort study demonstrated that most African Americans with CKD due to hypertension continue to progress despite being treated with RAAS inhibitors[221]. Hence, further investigation into whether there is consistent association between circulating TGF-β1 and progression of CKD is required.

BMP-7, also known as osteogenic protein-1 (OP-1) is one of the many currently known bone morphogenetic proteins. As detailed in Chapter 3, it is of particular interest to the nephrology community not only because of its role in kidney development, but also because BMP-7 is highly expressed in adult kidney, and is recognized as a natural antagonist to the pro-fibrotic actions of TGF-β1 [80, 341, 455]. Local BMP-7 concentration and its receptors play a major regulatory role in BMP-7 biological activity. The data presented in Chapter 3 of this thesis demonstrates that BMP-7 is not useful as a treatment for chronic kidney disease when TGFβ-1 levels are elevated, but whether a reduction in BMP-7 may predispose to progressive nephropathy is not clear.

As described in Chapter 3, distal tubules are the main site of BMP-7 production. However, proximal tubules, glomeruli and other renal epithelial cells all have BMP receptors which are required for BMP-7 binding, suggestive that BMP-7 is secreted into the blood stream and then acts at different sites [345]. Loss of tubular BMP-7 is seen in progressive diabetic nephropathy [456] and exogenous administration of recombinant human BMP-7 in diabetic animals has been shown to retard the progression of renal disease [342, 343]. It has also been shown in animal models that circulating BMP-7 correlates with the functional renal mass and has therefore been proposed as a biomarker to monitor the progression of chronic renal disease [333]. This implies quantification of circulating BMP-7 and its protein expression may serve as a biomarker for progression of CKD.

The Action in Diabetes and Vascular Disease: Preterax and Diamicron Modified Release Controlled Evaluation (ADVANCE) Collaborative Group study, is a factorial randomised, double blinded controlled trial conducted at 215 collaborating centres in 20 countries from Asia, Australasian, Europe, and North America, involving 11,140 patients

with type 2 DM. Participants were separately randomised to (i) perindopril and indapamide or matching placebo, as well as (ii) standard HbA1c <7.0) or intensive glucose control (HbA1c<6.5%). Primary end points were composites of major macrovascular events (death from cardiovascular causes, nonfatal myocardial infarction, or nonfatal stroke) and major microvascular events (new or worsening nephropathy or retinopathy), with a median follow up period of 5 years. The glycaemic arm of the study was reported in 2008, and concluded that intensive glucose control, yielded a 10% relative reduction in the combined outcome of major macrovascular and microvascular events, primarily as a consequence of a 21% relative reduction in nephropathy.

We utilised serum samples collected at the study entry point to assess firstly, the baseline circulating levels of TGFβ-1 and BMP-7 in people with type 2 DM; secondly, whether baseline circulating levels of TGF-β1, BMP-7 and their ratio are related to the risk of progression of diabetic nephropathy; thirdly, whether any relationships identified are independent of other baseline clinical parameters, and finally the impact of these parameters on clinical risk prediction models.

6.2 Materials and methods

6.2.1 Study participants and selection

Baseline serum samples collected from a subset of participants in the ADVANCE study were used in this study. At enrolment, participants provided informed consent for the future use of their serum samples for analyses relevant to the primary and secondary outcomes of the study. Ethical approval detailing the specific analyses of the serum

specimens for the purpose of this study was obtained from the research office of the Royal North Shore Hospital. Eligibility criteria in the ADVANCE Study were a diagnosis of type 2 DM at 30 years of age or older, an age of at least 55 years at the time of study entry, and a history of major macrovascular or microvascular disease or at least one other risk factor for vascular disease. For the purpose of this study 'cases' were individuals who developed a renal endpoint during the 5 year follow up period, defined as doubling of serum creatinine to at least 200umol/l, need for renal replacement therapy, or death due to renal disease. Of the 120 participants in ADVANCE who reached the renal endpoints, serum from 64 patients was assayed for total and active TGF-β1 and circulating BMP-7. For each of these cases, two controls matched for a range of parameters which include age, sex, race, baseline eGFR (<60 vs. >60), albuminuria status (no albuminuria, microalbuminuria or macroalbuminuria), baseline blood pressure, baseline HbA1c, known macrovascular disease (cerebrovascular accident, myocardial infarct, peripheral vascular disease), history of retinopathy and treatment allocation (blood pressure lowering intensive glucose lowering, both or neither). A propensity score matching method[457] was used to select a total of 128 controls, and serum was available for analysis from 72 of these. Serum was not available for the controls matched to 12 cases, so these cases were excluded from the primary analysis. For the remaining 52 cases, 32 had one matching control and 20 had two matching controls. The final data set for the primary analysis therefore consisted of 52 cases and 72 controls.

6.2.2 Laboratory measurements

All measurements were performed in local laboratories. Blood glucose and urinary albumin measurements were performed on samples collected at study using local laboratories at each site. Each glycated haemoglobin measurement was standardized. The modification of diet in renal disease (MDRD) study formula was used to calculate the estimated glomerular filtration rate (eGFR).

6.2.3 Circulating transforming growth factor-β1 (TGF-β1) measurement

Peripheral venous blood was obtained from the study participants at study entry in heparin coated tubes and stored at -80°C until assayed for TGF-β1 protein. Serum TGF-β1 protein concentration was measured using an isoform-specific TGF-β1 ELISA according to the manufacturer's protocol (TGFβ1 $E_{max}^{®}$ ImmunoAssay System, Madison, WI, USA) Both active and total (latent+active) TGFβ1 were measured. Total TGF-β1 was obtained by acidification with 1N HCl for 15 minutes at room temperature followed by neutralization with 1N NaOH. A TGF-β1 standard curve was constructed by using 1000, 500, 250, 125, 62.5, and 31.25 pg/ml recombinant TGF-β1 protein, and used to quantify TGF-β1 protein concentration. The minimum detectable level was 32 pg/ml and the intra-assay and inter-assay median coefficients of variation are 3.1% and 12.7%, respectively. This assay typically has less than 3% cross-reactivity with TGF-β2 and TGF-β3 at10 ng/ml.

6.2.4 Human BMP-7 ELISA measurement

Circulating BMP-7 levels were determined using an immunoassay kit assay (R & D, MN, USA) with slight modification as follows. 150 μL of heparinised serum without assay diluent was used. The absorbance at 450nm, corrected by readings at 540 nm were obtained, and plotted against the standard to determine the circulating level of BMP-7. The minimum detectable level is 0.79 pg/ml, and the intra-assay and inter-assay median coefficients of variation are reported to be 4.6% and 7.8%, respectively.

6.2.5 Statistical analysis

Descriptive results for the subjects' baseline characteristics and biomarkers are expressed as either mean ± S.D or median, (interquartile range, IQR), or n (%). Statistical comparisons between groups were made by *t*-test for normally distributed data. The Wilcoxon test was used for non-normally distributed data and the *Chi-square* test used for categorical data. Spearman correlation tests were performed to investigate the relationship between the biomarkers. Conditional logistic regression models were conducted to identify the predictive risk for the biomarkers using unadjusted and adjusted models. Sensitivity analyses were performed by using all available cases and controls and by using 1 vs. 1 matched case-control data. Receiver operating characteristic (ROC) curves were produced to assess the discriminatory ability for the development of renal failure for each biomarker, all biomarkers combined, with or without other covariates. ROC curve is a graphical of sensitivity, or true positive rate. Analyses were performed using the software package SAS 9.2. P values <0.05 were considered significant.

6.3 Results

6.3.1 Baseline characteristics of cases and controls

Serum from a total of 124 participants are analysed (52 cases and 72 controls). The demographic and clinical baseline characteristics of study participants are shown in Table 6.3.1.1. The mean (SD) age of the cases and controls was 69.58±6.68 and 69.92±7.4, respectively. The two groups had similar other baseline characteristics except the HbA1c, serum creatinine, urinary albumin: creatinine ratio (ACR) and history of microvascular disease. The baseline serum creatinine of the cases was 133.8±102.8 μmol/L and that of the control was 92.3±20.6 μmol/L, $p<0.0001$. However, the eGFR difference between groups was not statistically significant. The cases also have a higher number of participants with history of microvascular disease, 16±30% ($p<0.05$) and a higher HbA1c 7.46±1.14% ($p=0.0001$), when compared to the control groups, 11±15.3% and 7.7 ±1.93%.

6.3.2 Individuals who developed renal endpoints have higher baseline total circulating TGF-β1, lower circulating BMP-7 and a lower BMP-7/ total TGF-β1 ratio

Individuals who developed renal endpoints had a significantly higher circulating total TGF-β1, 12684.7 pg/ml, (IQR 7610.4 pg/ml, 17383.3 pg/ml), when compared to those who did not reach the defined renal endpoints, 7501.6 pg/ml (IQR 5323.0 pg/ml, 11485.0 pg/ml), $p<0.01$. Conversely, circulating BMP-7 levels were significantly lower in those who reached renal endpoints at 6.89 pg/ml (IQR 0.29 pg/ml, 9.75 pg/ml) vs. 19.33 pg/ml (IQR 10.02 pg/ml, 84.26 pg/ml), $p<0.0001$. Hence the ratio of BMP-7/ total TGF-β1 was

lower in individuals with type 2 diabetes mellitus who progress to a renal endpoint, 0.0005 (IQR 0.00, 0.001) vs. 0.0027 (IQR 0.0014, 0.0103), p<0.0001. (Table 6.3.1.1)

Table 6.3.1.1 **Characteristics of cases and controls at baseline**

Variable	**Cases (n=52)**		**Controls (n=72)**		**p-value***
	Mean (SD)				
Age (years)	69.58	6.68	69.92	7.40	0.4479
Diabetes duration (years)	10.71	7.19	7.53	6.00	0.1595
Systolic blood pressure (mmHg)	157.9	22.34	157.1	24.09	0.5730
Haemoglobin A1c (%)	7.46	1.14	7.70	1.93	0.0001
creatinine clearance (MDRD) (ml/min/1.72m^2)	54.34	21.46	69.43	16.89	0.0633
Body Mass Index	30.15	5.53	30.44	4.64	0.1680
Creatinine (μmol/L)	133.8	102.8	92.33	20.66	<0.0001
	n (%)				
SEX (female)	16	30.8	17	23.6	0.3735
History of macrovascular disease (yes)	22	42.3	23	31.9	0.2363
History of microvascular disease (yes)	16	30.8	11	15.3	0.0392
	Median (IQR, 25th and 75th percentile)				
UAC ratio (μg/mg)	44.29	14.14, 378.35	12.33	5.30, 34.39	<0.0001
total TGF-β1 (pg/ml)	12684.7	7610.4, 17383.3	7501.6	5323.0, 11485.0	0.0029
BMP-7 (pg/ml)	6.89	0.29, 9.75	19.33	10.02, 84.26	<0.0001
Ratio BMP-7/TGF-β1	0.0005	0.0000, 0.0010	0.0027	0.0014, 0.0103	<0.0001

*p-values are tested by Chi-square test, t-test and Wilcoxon test.

6.3.3 Absence of correlation between baseline circulating total TGF-β1 and BMP-7

Figure 6.3.3.1 is the scatter plot matrix representing the levels of these biomarkers in both cases and controls. Using Spearman correlation tests, there is no correlation

between baseline circulating total TGF-β1 and BMP-7, with or without adjustment for baseline eGFR and urinary ACR (Tablet 6.3.3.1).

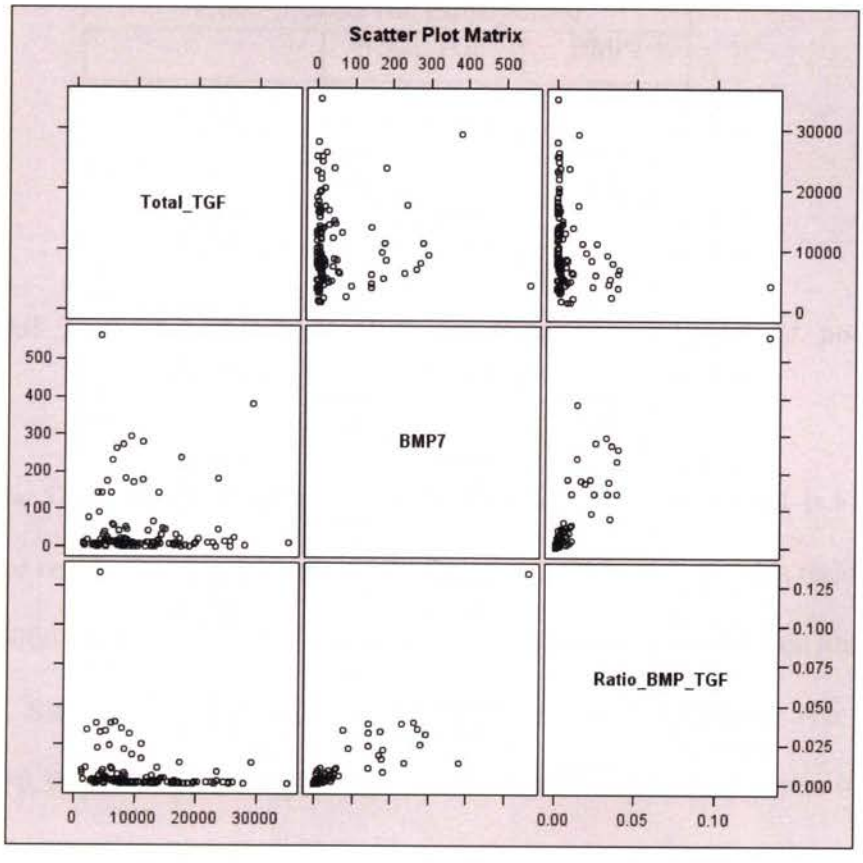

Figure 6.3.3.1 Scatter plot matrix of circulating total TGF-β1, BMP-7 and BMP-7: total TGF-β1 ratio.

Table 6.3.3.1 **Correlation study of BMP-7 and total TGF-β1 adjusted for eGFR and UACR**

Spearman Partial Correlation Coefficients, N = 114		
Prob > |r| under H0: Partial Rho=0		
	Total_TGF	BMP7
Total TGF-β1	1	-0.00672
		0.944
BMP-7	-0.00672	1
	0.944	

6.3.4 High total TGF-β1 and low BMP-7 are sensitive predictors of poor renal outcomes

Using the 52 cases and 72 controls, elevated circulating total TGF-β1 is a sensitive predictor of poor renal outcomes in individual with type 2 DM, with an odds ratio (OR) of 1.90 for each 6000 pg/ml higher TGF- β1 level at baseline (95% confidence limits 1.24-2.90, p=0.003). Similarly, high circulating BMP-7 levels predict a lower risk of renal endpoints (OR=0.39 per 10 pg/ml higher baseline level, 95% confidence limits 0.21-0.74, p=0.004) and for BMP-7: total TGF-β1 ratio, OR=0.46 per 0.001 higher level (95% CI 0.22-0.74, p= 0.004). Adjustment for sex, eGFR, HbA1c, urinary ACR, BMI, diabetes duration, history of macrovascular and microvascular disease did not materially change the results with ORs of 1.92 for total TGF-β1 (95% CI 1.08-3.39, p= 0.025) and 0.21 for BMP-7 (95% CI 0.05 – 0.84, p=0.028).

Further sensitivity analyses also revealed similar results; including all available cases (64) and controls (128) yielded similar results for TGF-β1 (OR=1.73, 95% CI 1.30-2.30, p= 0.0002) and for BMP-7 (OR=0.4, 95% CI 0.25-0.62 p<0.0001). Restricting the analyses to 52 cases and 1 control for each case (n= 104 in total) also found similar results:

TGF-β1 (OR=2, 95% CI 1.22-3.28, p= 0.006) and for BMP-7 (OR=0.43, 95% CI 0.28-0.81, p= 0.009).

Table 6.3.4.1 Odds ratio of each biomarker

Odds Ratio Estimates from unadjusted model					Odds Ratio Estimates from adjusted model*			
Effect	Point Estimate	95% Wald Confidence Limits		p-value	Point Estimate	95% Wald Confidence Limits		p-value
Total TGF-β1 (per 6000 pg/ml increase)	1.733	1.303	2.303	0.0002	1.877	1.331	2.648	0.0003
BMP-7 (per 10 pg/ml crease)	0.395	0.249	0.624	<.0001	0.328	0.179	0.603	0.0003
Ratio BMP-7/TGF-β1 (per 0.001 units increase)	0.440	0.303	0.639	<.0001	0.289	0.162	0.517	<.0001

*adjusted sex, creatinine clearance, HbA1c, albumin/ creatinine ratio (UACR), BMI, diabetes duration, history of macrovascular disease and history of microvascular disease, n=192.

6.3.5 Circulating BMP-7 is a better predictor of poor renal outcome

ROC curves were plotted for each of these biomarkers in an unadjusted or adjusted model (adjusted by UACR and eGFR). The area under the curve for total TGF-β1 and BMP-7 was 0.66 and 0.82, respectively (Figure 6.3.5.1A & B). When these ROC curves for each biomarker were compared, BMP-7 is significantly better than total TGF-β1 (p=0.001), but similar to the BMP-7: total TGF-β1 ratio (p=NS), in predicting poor renal outcomes in individuals with type 2 diabetes mellitus. To ascertain whether the relationship between TGF-β1 and BMP-7 are independent of kidney function and albuminuria, the ROC curves were each adjusted for eGFR and UACR. The areas under a curve (AUC) were similar or better after adjustment, TGF-β1 is 0.77 and BMP-7 is 0.83. Circulating

BMP-7 levels are found to be a good predictor for renal endpoints in individuals with type 2 diabetes independent of the baseline eGFR and UACR.

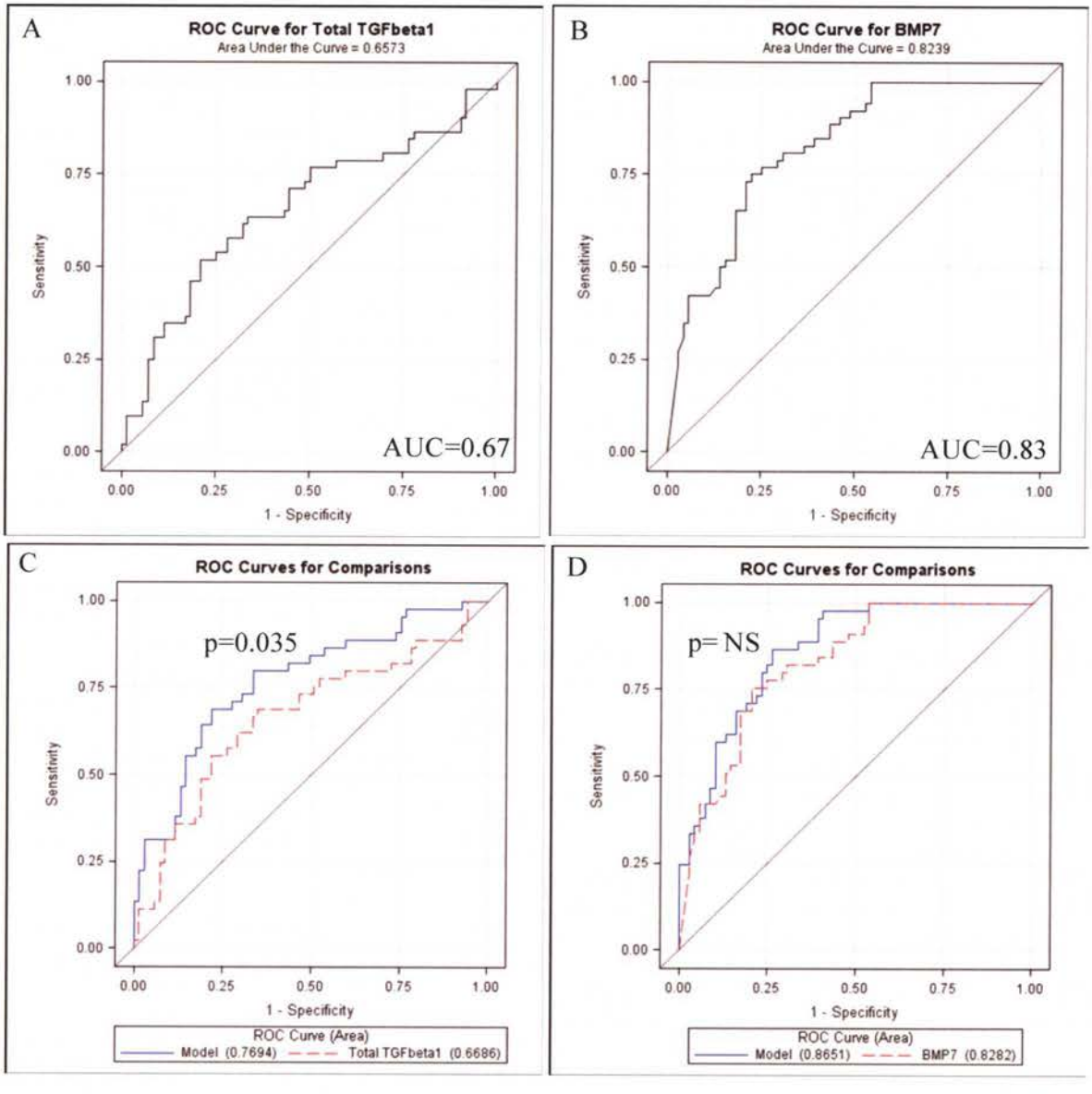

Figure 6.3.5.1 Comparison of ROC curves for individual biomarker raw values, and in models adjusted for eGFR and UACR.

ROC curves for total TGF-β1 raw values (A) and for BMP-7 raw values (B). Comparison of area under the curve for total TGF-β1 alone vs. adjusted for eGFR and UACR, p=0.035,

(C). AUC of the unadjusted and adjusted ROC curves for BMP-7 (0.83 vs. 0.86, p= NS) were similar (D). NS=statistical not significant.

6.3.6 Circulating total TGF-β1 adds little predictive value for poor renal outcomes.

The AUC of the ROC curves for BMP-7 improves significantly from 0.83 to 0.90, p=0.02, when adjusted for all other variables (Figure 6.3.6.1A). This suggests that circulating BMP-7 level provides addition predictive value on top of the conventional risk factors for renal progression such as sex, eGFR, HbA1c, UACR, BMI, duration of diabetes, history of macro- and microvascular disease. The AUC of the fully adjusted ROC including both BMP-7 and TGF-β1 is 0.93, is not different to that of the fully adjusted ROC for BMP-7 alone (Figure 6.3.6.1B). This suggests that total circulating TGF-β1 adds little value in predicting renal endpoints as compared to BMP-7, when all other known risk factors for diabetic kidney disease are taken into consideration.

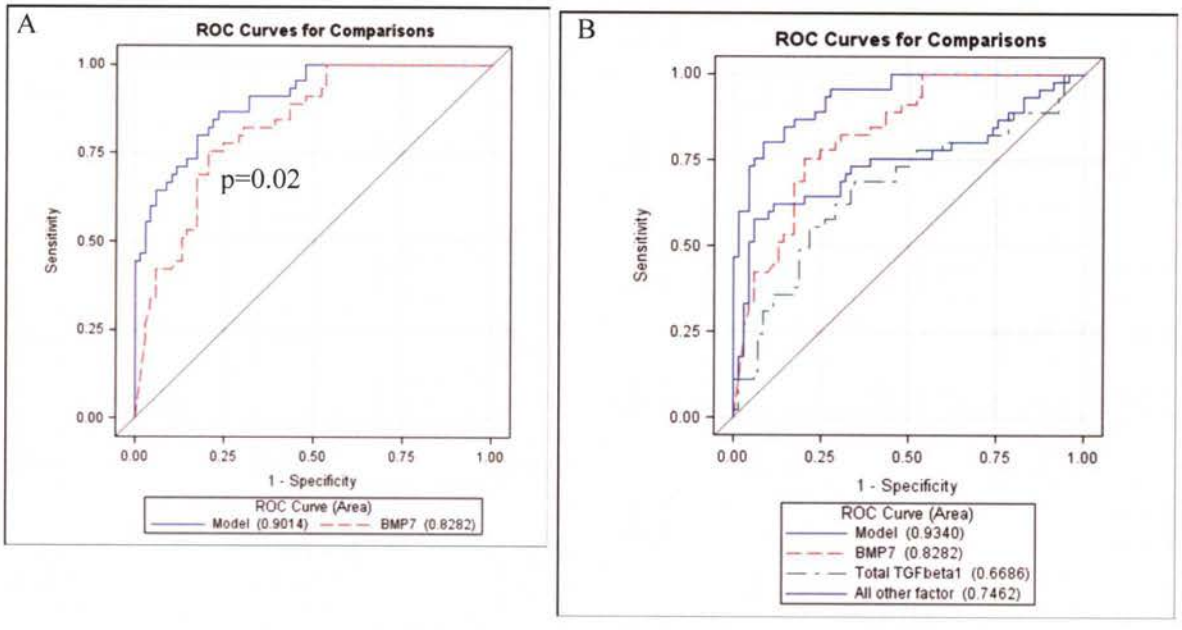

Figure 6.3.6.1 Comparison of ROC curves of individual biomarkers adjusted for all studied risk factors

Comparison of ROC *curves for circulating BMP-7 of unadjusted and adjusted for all studied variables. These variables sex, eGFR, HbA1c, UACR, BMI, diabetes duration, history of macro- and microvascular disease, which all are known risk factors for renal progression (A). ROC curves of individual biomarkers, both BMP-7 and TGF-β1 combined with other risk factors or other risk factors alone (B).*

6.4 Discussion

At present, proteinuria and eGFR are the best known predictors for the future functional decline of renal function in patients with diabetic nephropathy. However recent reports have described a number of people with diabetes who progress to Stage 5 CKD with normal or low levels of proteinuria. Furthermore, the presence of macroalbuminuria

and impaired renal function usually reflects irreversible advanced nephropathy. Therefore, there is a need for biomarkers that can predict poor renal outcome in the early stages of diabetes mellitus so as to better deploy community and hospital based preventative resources.

In this study we found that elevated circulating total TGF-β1, reduced BMP-7 and low BMP-7: TGF-β1 ratio, are associated with increased risk of progressive renal failure resulting in defined renal endpoints in a high risk cohort with type 2 DM. This association remained stable in multivariate analyses taking into account sex, eGFR, HbA1c, UACR, BMI, duration of diabetes mellitus, history of macrovascular and microvascular disease, and appears to be independent of these known risk factors for diabetic kidney disease. The results were also similar in sensitivity analyses using more and less restricted numbers of cases and controls which further supports the robustness of the findings.

The adjusted OR estimates for circulating BMP-7 was 0.39, suggesting that individuals with type 2 DM have a 61% lower risk of developing renal endpoints if BMP-7 level is 10 pg/ml higher at baseline. Conversely, the adjusted OR estimates for total TGF-β is 1.89, suggesting that the risk of developing renal endpoints is 89% higher if the circulating total TGF-β1 is 6000 pg/ml higher in individuals with type 2 DM.

Interaction and correlation studies confirmed that both circulating BMP-7 and TGF-β1 are independent of baseline eGFR and/or UACR, suggesting that these biomarkers are independent predictors irrespective of the baseline renal function and albuminuria status. This is of importance because some biomarkers may increase because of decreased excretion secondary to reduced eGFR. Similarly, some biomarkers may be influenced by

low albumin due to urinary albumin loss. These results suggest that levels of these biomarkers should provide additional prognostic information to that obtained using kidney function and albuminuria

We have demonstrated in Chapter 3, loss of tubular BMP-7 occurs early in kidney biopsy specimens of individuals with diabetic nephropathy, well before established fibrotic histological changes. We have also shown significantly lower circulating BMP-7 levels in patients with ESKD secondary to diabetic nephropathy receiving hemodialysis, when compared to healthy controls. This could either be due to circulating BMP-7 correlating with viable renal mass as previously reported [325], or diabetes mellitus *per se* suppressing BMP-7 production. The circulating BMP-7 level in normal healthy subjects is reported to be 207.2±45pg/ml (Chapter 3). The level observed in our studies is hence low in "control" individuals with type 2 DM and is even lower in those who progressed to a renal endpoint. This is consistent with observations in animal models of diabetic nephropathy[419, 458]. We have demonstrated in this study, circulating BMP-7 is a sensitive biomarker in predicting renal endpoints in individuals with type 2 DM (AUC=0.83), which remains strong after adjusting for UACR and eGFR (AUC=0.86). Even though the HbA1c at baseline is different between the cases and controls, the adjusted multivariate analysis did not affect the predictive value of BMP-7. Circulating BMP-7 appears to be a better predictor than circulating total TGF-β1 of progressive renal disease, and improves the predictive value of renal endpoints significantly, when other conventional risk factors for renal progression in type 2 DM are considered.

Conversely, although circulating total TGF-β1 is a strong predictor for renal progression, it is correlates with UACR and eGFR, and unlike BMP-7, it added little

advantage in predicting renal endpoints when these predictors of risk were taken into account. We measured both total (latent+ active) and active form of TGF-β1 in this study. However, almost 60% of the clinical specimens have no measurable levels of active TGF-β1. Although it is well documented that kidney biopsy specimens of individuals with diabetic nephropathy exhibit increased TGF-β1 expression[6], and therapeutic benefits of RAAS blockade in preventing diabetic nephropathy progression is mechanistically linked to lowering of TGF-β1 in addition to reduction proteinuria[459], the significance of elevated circulating total TGF-β1 in individuals with worsened renal outcome remains unclear. Huang *et al.* have reported renal protection by latent TGF-β in experimental mouse models of ureteral obstruction[166] and crescentic glomerulonephritis[165], which raised an intriguing hypothesis that the active TGF-β1 is pathogenic whereas an excess of the latent form could be protective. This remains difficult to study in the human scenario given the complex mechanisms for activation of TGF-β1.

The major limitation of this study is the relatively small samples size, although the strong and highly statistical significant results support the robustness of the findings. Confirmation of these findings, ideally by testing the derived model in a prospective cohort study, is warranted based on the results and offers the potential to substantially improve our ability to predict the risk of clinically important renal events in the large population at high risk due to the presence of diabetes. This will allow better targeting and evaluation of strategies that could prevent progressive renal disease.

In summary, circulating BMP-7 level is an independent predictor of future renal endpoints in individuals with type 2 diabetes mellitus. It adds predictive value to the currently used models to predict poor renal prognosis, namely a reduction in renal function

at diagnosis and an increase in urinary albumin excretion. These findings will enable nephrologists to risk stratify individuals with type 2 DM who may progress to ESKD in order to institute appropriate early risk factor modification strategies and therapeutic interventions.

CHAPTER 7: Conclusion and future direction

Chronic kidney disease (CKD) remains a growing epidemic worldwide, driven largely by the rise in obesity, hypertension and diabetes mellitus in the Western world. End stage kidney disease represents a small proportion of patients with CKD but is associated with devastating social and financial consequences to both the individual and the community. The Australian Diabetes, Obesity and Lifestyle (AusDiab) study is the largest Australian longitudinal population-based study examining the natural history of diabetes, pre-diabetes, heart disease and kidney disease; reported in 2005, 1 in 7 Australians over age 25 years have at least one clinical sign of CKD, such as reduced estimated glomerular filtration rate, or the presence of proteinuria or haematuria. This represents 1.7 million people in the Australian population. Importantly, more than 4.5 million Australia people have one or more risk factors for CKD, namely obesity, hypertension and diabetes mellitus as stated above. The renoprotective effects of glycaemic and blood pressure control, and specific interruption of the renin-angiotensin-aldosterone system are modest at best. There is increasing evidence that dyslipidemia induces or accelerates renal cell dysfunction, and reduction of serum lipids confers a renoprotective effect in animal models. However, a significant treatment gap exists. Hence alternative novel therapies to reduce the development and progression of CKD are required. This thesis focuses on three different novel agents, namely bone morphogenetic protein-7 (BMP-7), the cation independent mannose 6-phosphate receptor (CI-M6PR) inhibitor (PXS-25), and a farnesoid X receptor (FXR) agonist, GW4064, and to assess their role in prevention of CKD.

The HK-2 cells were used as the primary model for studies undertaken in this thesis and the animal model of streptozotocin (STZ)-induced diabetes was used where appropriate. HK-2 cells were exposed to media containing high glucose and/or transforming growth factor-β1 (TGF-β1), or were subjected to a hypoxic environment to mimic the microenvironment of CKD.

Using recombinant human BMP-7 and BMP-7 overexpression studies, I have demonstrated that BMP-7 can prevent TGF-β1 induced EMT only if TGF-β1 is removed as a trigger which is unlikely in the clinical course of treatment intervention in CKD. This thesis has demonstrated that TGF-β1 suppresses tubular cell BMPR-IA expression, which is the crucial type I BMP receptor for BMP-7 ligand receptor binding and its downstream signalling. The suppressive effect on BMPR-IA is also observed in KLF-6 overexpressing cells, supporting the observation reported previously by our laboratory that there is an interdependent relationship of KLF-6 and TGF-β1 in EMT. *In vivo* studies confirmed a reduction in BMP-7 and BMPR-IA but an increase in KLF-6 expression in established diabetic nephropathy. Hence, TGF-β1 and KLF-6 synergistically induce suppression of BMPR-IA and downstream reduction of BMP-7 signalling. These findings suggest that the presence of TGF-β1 in multiple forms of nephropathy mitigate against the use of recombinant human BMP7 as an antifibrotic therapeutic agent. These findings are contrary to other reports in murine models of CKD, in which administration of rhBMP-7 is able to reverse interstitial fibrosis and prevent the decline of renal function. However, BMP-7 administration in most, if not all of these models are delivered prior to the insult that induces CKD. This suggests that in established renal disease, where the local microenvironment of TGF-β1 is high, systemic administration of BMP-7 is unlikely to be

useful. This again highlights the complexity of interaction between a pro-fibrotic and antifibrotic agent in the setting of EMT.

Despite BMP-7 having been used in clinical trials to treat long bone fractures with malunion, convincing evidence of BMP-7 in delaying progression of kidney disease in humans is not supported, at least at the cellular level based on my experiments.

I also confirmed that PXS-25, a CI-M6PR inhibitor which selectively inhibits CI-M6PR dependent activation of latent to active TGF-β1, may have a role in preventing high glucose induced ECM accumulation in HK-2 cells. As a consequence of this study, I conclude that both hyperglycemia and hypoxia can independently induce endogenous active TGF-β1 production in human proximal tubular cells. However; there is no additive effect in both high glucose and hypoxic conditions. High glucose induces ECM accumulation namely, fibronectin and collagen IV, as does hypoxia, but only hyperglycemia induces increased matrix proteins that were suppressed by concurrent PXS-25 exposure. There is lack of *in vivo* data in these study, which is a project planned to be undertaken in the future. The major limitation of an animal study is selection of appropriate animal model that can dissect the contributory role of hyperglycemia and hypoxia in an *in vivo* setting. It is also of interest to compare the differential contribution of other pathways that are involved in TGF-β1 activation in high glucose condition e.g. thrombospondin-1 (TSP-1).

FXRs are well known for their role in bile acid, lipid and carbohydrate metabolism. Their role in fibrosis and inflammation in an *in vitro* model is studied in this thesis using GW4064, a FXR agonist. High glucose suppressed FXR mRNA and protein expression,

suppressed short heterodimer partner (SHP) and induced sterol regulatory element-binding protein-1 (SREBP-1) mRNA. FXR silenced cells have increased fibronectin, collagen IV and SREBP-1 expression, which is further increased on exposure to high glucose, suggesting a potentiating role of SREBP-1 and high glucose conditions. Despite similar suppression of high glucose-induced TGF-β1 mRNA, FXR agonists more effectively suppress ECM production compared to peroxisome proliferator activated receptors gamma (PPARγ) agonists. Conversely, PPARγ agonists have a greater anti-inflammatory effect. These results further support the synergistic effect of glucose and lipid in the contribution of renal interstitial fibrosis seen in metabolic syndrome. Although cytotoxicity of GW4064 was not observed using the concentration in this study, increasing reports suggest unwanted side effects in animal models. Hence, more physiological agonists such as 6-ethylchenodeoxycholic acids (6-ECDCAs) should be considered as future therapies to limit CKD initiation and progression. Future experiments should be designed to dissect the pathways whereby FXR regulates ECM deposition, taking note that complete blockade of such a multifunctional nuclear receptor is more likely to be accompanied by unwanted side effects. Pharmacological therapies specifically targeting FXR-mediated antifibrotic signalling pathways are likely to be of more value.

Although I have shown that BMP-7 may not be a suitable antifibrotic therapeutic option, myself and colleagues have shown that circulating BMP-7 may be a useful biomarker in predicting poor renal outcome in individuals with type 2 DM. Using baseline serum samples of 64 participants who developed primary renal endpoints, from the ADVANCE collaborative trial (majority participants are individuals with type 2 DM with significant micro- and macrovascular risk factors), we discovered high total circulating

TGF-β1, low circulating BMP-7 and low BMP-7: total TGF-β1 ratio are independent risk factors for poor renal outcome in individuals with type 2 DM. In addition, circulating BMP-7 is a more sensitive biomarker to discriminate poor renal outcomes in individuals with type 2 diabetes mellitus than total circulating TGF-β1 We aim to increase the number of cases and controls to increase statistical power, then undertaking subgroup analysis of these biomarkers in participants who received intensive or standard glycaemic control, and with or without ACE inhibitor/ diuretics therapy. These interesting data will require validation with an increased number of participants in a prospective trial, which should include other forms of progressive kidney disease. A cost-effective analysis would be useful to compare the predictive value of these biomarkers with that of conventional markers such as ACR and eGFR.

In summary, this thesis highlights the complexity of the mechanisms contributing to renal fibrosis and EMT, and hence the challenges needed for effective novel therapeutic agents. We have demonstrated the mechanistic interaction of BMP-7, a natural antagonist of TGF-β1 through a receptor-ligand and intracellular signalling pathway; inhibition of conversion of latent to active TGF-β1 using a CI-M6PR inhibitor, PXS-25; and FXR agonist, and a nuclear receptor agonist through its interaction with its target genes, in contributing to renal fibrosis. All are involved in the progression of renal disease and the challenge remains as to where therapies are best targeted to achieve improved outcomes.

BIBLIOGRAPHY

1. Remuzzi, G, Benigni, A, Remuzzi, A: Mechanisms of progression and regression of renal lesions of chronic nephropathies and diabetes. *J Clin Invest,* 116: 288-296, 2006.
2. De Vecchi, AF, Dratwa, M, Wiedemann, ME: Healthcare systems and end-stage renal disease (ESRD) therapies--an international review: costs and reimbursement/funding of ESRD therapies. *Nephrol Dial Transplant,* 14 Suppl 6: 31-41, 1999.
3. Wild, S, Roglic, G, Green, A, *et al.*: Global prevalence of diabetes: estimates for the year 2000 and projections for 2030. *Diabetes care,* 27: 1047-1053, 2004.
4. AusDiab 2005: the Australian diabetes, obesity and lifestyle study, Melbourne: International Diabetes Institute, 2006: p1-88.
5. Australian Institute of Health and Welfare. Diabetes prevalence in Australia: an assessment of national data sources. Diabetes Series no. 12. Canberra: Australian Institute of Health and Welfare, 2009.
6. Ritz, E, Orth, SR: Nephropathy in patients with type 2 diabetes mellitus. *N Engl J Med,* 341: 1127-1133, 1999.
7. McDonald S, Excell L, N, D: New patients commencing treatment in 2008. *In*: ANZDATA Registry Report 2009. Adelaide: Australia and New Zealand Dialysis and Transplant Registry. Chapter 2: 1-12, 2009.
8. Weiner, DE, Tighiouart, H, Amin, MG, *et al.*: Chronic kidney disease as a risk factor for cardiovascular disease and all-cause mortality: a pooled analysis of community-based studies. *J Am Soc Nephrol,* 15: 1307-1315, 2004.
9. Go, AS, Chertow, GM, Fan, D, *et al.*: Chronic kidney disease and the risks of death, cardiovascular events, and hospitalization. *N Engl J Med,* 351: 1296-1305, 2004.
10. Foley, RN, Murray, AM, Li, S, *et al.*: Chronic kidney disease and the risk for cardiovascular disease, renal replacement, and death in the United States Medicare population, 1998 to 1999. *J Am Soc Nephrol,* 16: 489-495, 2005.
11. Verhave, JC, Gansevoort, RT, Hillege, HL, *et al.*: An elevated urinary albumin excretion predicts de novo development of renal function impairment in the general population. *Kidney Int Suppl*: S18-21, 2004.
12. van der Velde, M, Halbesma, N, de Charro, FT, *et al.*: Screening for albuminuria identifies individuals at increased renal risk. *J Am Soc Nephrol,* 20: 852-862, 2009.
13. Hillege, HL, Fidler, V, Diercks, GF, *et al.*: Urinary albumin excretion predicts cardiovascular and noncardiovascular mortality in general population. *Circulation,* 106: 1777-1782, 2002.
14. de Zeeuw, D, Remuzzi, G, Parving, HH, *et al.*: Proteinuria, a target for renoprotection in patients with type 2 diabetic nephropathy: lessons from RENAAL. *Kidney Int,* 65: 2309-2320, 2004.
15. Joles, JA, Koomans, HA: Causes and consequences of increased sympathetic activity in renal disease. *Hypertension,* 43: 699-706, 2004.
16. Reaven, GM: Banting lecture 1988. Role of insulin resistance in human disease. *Diabetes,* 37: 1595-1607, 1988.
17. Gurnell, M, Savage, DB, Chatterjee, VK, *et al.*: The metabolic syndrome: peroxisome proliferator-activated receptor gamma and its therapeutic modulation. *J Clin Endocrinol Metab,* 88: 2412-2421, 2003.
18. Scott, CL: Diagnosis, prevention, and intervention for the metabolic syndrome. *Am J Cardiol,* 92: 35i-42i, 2003.
19. Grundy, SM, Cleeman, JI, Daniels, SR, *et al.*: Diagnosis and management of the metabolic syndrome. An American Heart Association/National Heart, Lung, and Blood Institute Scientific Statement. Executive summary. *Cardiol Rev,* 13: 322-327, 2005.

20. Kurella, M, Lo, JC, Chertow, GM: Metabolic syndrome and the risk for chronic kidney disease among nondiabetic adults. *J Am Soc Nephrol,* 16: 2134-2140, 2005.
21. Peralta, CA, Kurella, M, Lo, JC, *et al.*: The metabolic syndrome and chronic kidney disease. *Curr Opin Nephrol Hypertens,* 15: 361-365, 2006.
22. Rashidi, A, Ghanbarian, A, Azizi, F: Are patients who have metabolic syndrome without diabetes at risk for developing chronic kidney disease? Evidence based on data from a large cohort screening population. *Clin J Am Soc Nephrol,* 2: 976-983, 2007.
23. Chen, J, Muntner, P, Hamm, LL, *et al.*: The metabolic syndrome and chronic kidney disease in U.S. adults. *Ann Intern Med,* 140: 167-174, 2004.
24. Sarafidis, PA, Ruilope, LM: Insulin resistance, hyperinsulinemia, and renal injury: mechanisms and implications. *Am J Nephrol,* 26: 232-244, 2006.
25. Weinberg, JM: Lipotoxicity. *Kidney Int,* 70: 1560-1566, 2006.
26. Arita, Y, Kihara, S, Ouchi, N, *et al.*: Paradoxical decrease of an adipose-specific protein, adiponectin, in obesity. *Biochem Biophys Res Commun,* 257: 79-83, 1999.
27. Martin, A, David, V, Vico, L, *et al.*: Impaired energetic metabolism after central leptin signaling leads to massive appendicular bone loss in hindlimb-suspended rats. *J Bone Miner Res,* 23: 2040-2047, 2008.
28. Nishida, Y, Oda, H, Yorioka, N: Effect of lipoproteins on mesangial cell proliferation. *Kidney Int Suppl,* 71: S51-53, 1999.
29. Walker, WG: Relation of lipid abnormalities to progression of renal damage in essential hypertension, insulin-dependent and non insulin-dependent diabetes mellitus. *Miner Electrolyte Metab,* 19: 137-143, 1993.
30. Alexander, MP, Patel, TV, Farag, YM, *et al.*: Kidney pathological changes in metabolic syndrome: a cross-sectional study. *Am J Kidney Dis,* 53: 751-759, 2009.
31. Kambham, N, Markowitz, GS, Valeri, AM, *et al.*: Obesity-related glomerulopathy: an emerging epidemic. *Kidney Int,* 59: 1498-1509, 2001.
32. Guan, Y, Breyer, MD: Peroxisome proliferator-activated receptors (PPARs): novel therapeutic targets in renal disease. *Kidney Int,* 60: 14-30, 2001.
33. Jiang, T, Wang, XX, Scherzer, P, *et al.*: Farnesoid X receptor modulates renal lipid metabolism, fibrosis, and diabetic nephropathy. *Diabetes,* 56: 2485-2493, 2007.
34. Chawla, A, Repa, JJ, Evans, RM, *et al.*: Nuclear receptors and lipid physiology: opening the X-files. *Science,* 294: 1866-1870, 2001.
35. Brenner, BM, Cooper, ME, de Zeeuw, D, *et al.*: Effects of losartan on renal and cardiovascular outcomes in patients with type 2 diabetes and nephropathy. *N Engl J Med,* 345: 861-869, 2001.
36. Lewis, EJ, Hunsicker, LG, Bain, RP, *et al.*: The effect of angiotensin-converting-enzyme inhibition on diabetic nephropathy. The Collaborative Study Group. *N Engl J Med,* 329: 1456-1462, 1993.
37. The GISEN Group (Gruppo Italiano di Studi Epidemiologici in Nefrologia). Randomised placebo-controlled trial of effect of ramipril on decline in glomerular filtration rate and risk of terminal renal failure in proteinuric, non-diabetic nephropathy *Lancet,* 349: 1857-1863, 1997.
38. Catapano, F, Chiodini, P, De Nicola, L, *et al.*: Antiproteinuric response to dual blockade of the renin-angiotensin system in primary glomerulonephritis: meta-analysis and metaregression. *Am J Kidney Dis,* 52: 475-485, 2008.
39. Soma, J, Sato, K, Saito, H, *et al.*: Effect of tranilast in early-stage diabetic nephropathy. *Nephrol Dial Transplant,* 21: 2795-2799, 2006.
40. Soma, J, Sugawara, T, Huang, YD, *et al.*: Tranilast slows the progression of advanced diabetic nephropathy. *Nephron,* 92: 693-698, 2002.
41. Gambaro, G, Kinalska, I, Oksa, A, *et al.*: Oral sulodexide reduces albuminuria in microalbuminuric and macroalbuminuric type 1 and type 2 diabetic patients: the Di.N.A.S. randomized trial. *J Am Soc Nephrol,* 13: 1615-1625, 2002.
42. Heerspink, HL, Greene, T, Lewis, JB, *et al.*: Effects of sulodexide in patients with type 2 diabetes and persistent albuminuria. *Nephrol Dial Transplant,* 23: 1946-1954, 2008.

43. Bolton, WK, Cattran, DC, Williams, ME, *et al.*: Randomized trial of an inhibitor of formation of advanced glycation end products in diabetic nephropathy. *Am J Nephrol,* 24: 32-40, 2004.
44. Tuttle, KR, Bakris, GL, Toto, RD, *et al.*: The effect of ruboxistaurin on nephropathy in type 2 diabetes. *Diabetes Care,* 28: 2686-2690, 2005.
45. Chen, YM, Lin, SL, Chiang, WC, *et al.*: Pentoxifylline ameliorates proteinuria through suppression of renal monocyte chemoattractant protein-1 in patients with proteinuric primary glomerular diseases. *Kidney Int,* 69: 1410-1415, 2006.
46. Wenzel, RR, Littke, T, Kuranoff, S, *et al.*: Avosentan reduces albumin excretion in diabetics with macroalbuminuria. *J Am Soc Nephrol,* 20: 655-664, 2009.
47. Black, HR, Bakris, GL, Weber, MA, *et al.*: Efficacy and safety of darusentan in patients with resistant hypertension: results from a randomized, double-blind, placebo-controlled dose-ranging study. *J Clin Hypertens* 9: 760-769, 2007.
48. Athyros, VG, Mikhailidis, DP, Papageorgiou, AA, *et al.*: The effect of statins versus untreated dyslipidaemia on renal function in patients with coronary heart disease. A subgroup analysis of the Greek atorvastatin and coronary heart disease evaluation (GREACE) study. *J Clin Pathol,* 57: 728-734, 2004.
49. Sandhu, S, Wiebe, N, Fried, LF, *et al.*: Statins for improving renal outcomes: a meta-analysis. *J Am Soc Nephrol,* 17: 2006-2016, 2006.
50. Gouva, C, Nikolopoulos, P, Ioannidis, JP, *et al.*: Treating anemia early in renal failure patients slows the decline of renal function: a randomized controlled trial. *Kidney Int,* 66: 753-760, 2004.
51. Carlini, RG, Alonzo, EJ, Dominguez, J, *et al.*: Effect of recombinant human erythropoietin on endothelial cell apoptosis. *Kidney Int,* 55: 546-553, 1999.
52. Agarwal, R, Acharya, M, Tian, J, *et al.*: Antiproteinuric effect of oral paricalcitol in chronic kidney disease. *Kidney Int,* 68: 2823-2828, 2005.
53. Alborzi, P, Patel, NA, Peterson, C, *et al.*: Paricalcitol reduces albuminuria and inflammation in chronic kidney disease: a randomized double-blind pilot trial. *Hypertension,* 52: 249-255, 2008.
54. Freedman, BI, Wuerth, JP, Cartwright, K, *et al.*: Design and baseline characteristics for the aminoguanidine Clinical Trial in Overt Type 2 Diabetic Nephropathy (ACTION II). *Control Clin Trials,* 20: 493-510, 1999.
55. Tuttle, KR, McGill, JB, Haney, DJ, *et al.*: Kidney outcomes in long-term studies of ruboxistaurin for diabetic eye disease. *Clin J Am Soc Nephrol,* 2: 631-636, 2007.
56. Holmes, DR, Jr., Savage, M, LaBlanche, JM, *et al.*: Results of Prevention of REStenosis with Tranilast and its Outcomes (PRESTO) trial. *Circulation,* 106: 1243-1250, 2002.
57. Williams, ME, Bolton, WK, Khalifah, RG, *et al.*: Effects of pyridoxamine in combined phase 2 studies of patients with type 1 and type 2 diabetes and overt nephropathy. *Am J Nephrol,* 27: 605-614, 2007.
58. McCormick, BB, Sydor, A, Akbari, A, *et al.*: The effect of pentoxifylline on proteinuria in diabetic kidney disease: a meta-analysis. *Am J Kidney Dis,* 52: 454-463, 2008.
59. Douglas, K, O'Malley, PG, Jackson, JL: Meta-analysis: the effect of statins on albuminuria. *Ann Intern Med,* 145: 117-124, 2006.
60. Strippoli, GF, Navaneethan, SD, Johnson, DW, *et al.*: Effects of statins in patients with chronic kidney disease: meta-analysis and meta-regression of randomised controlled trials. *BMJ,* 336: 645-651, 2008.
61. Singh, AK, Szczech, L, Tang, KL, *et al.*: Correction of anemia with epoetin alfa in chronic kidney disease. *N Engl J Med,* 355: 2085-2098, 2006.
62. Drueke, TB, Locatelli, F, Clyne, N, *et al.*: Normalization of hemoglobin level in patients with chronic kidney disease and anemia. *N Engl J Med,* 355: 2071-2084, 2006.
63. Gilbert, RE, Cooper, ME: The tubulointerstitium in progressive diabetic kidney disease: more than an aftermath of glomerular injury? *Kidney Int,* 56: 1627-1637, 1999.

64. Bohle, A, Mackensen-Haen, S, von Gise, H: Significance of tubulointerstitial changes in the renal cortex for the excretory function and concentration ability of the kidney: a morphometric contribution. *Am J Nephrol,* 7: 421-433, 1987.
65. Nath, KA: Tubulointerstitial changes as a major determinant in the progression of renal damage. *Am J Kidney Dis,* 20: 1-17, 1992.
66. Kaissling, B, Le Hir, M: The renal cortical interstitium: morphological and functional aspects. *Histochem Cell Biol,* 130: 247-262, 2008.
67. Hinz, B: The myofibroblast: paradigm for a mechanically active cell. *J Biomech,* 43: 146-155, 2010.
68. Eyden, B: The myofibroblast: an assessment of controversial issues and a definition useful in diagnosis and research. *Ultrastruct Pathol,* 25: 39-50, 2001.
69. Hewitson, TD, Wu, HL, Becker, GJ: Interstitial myofibroblasts in experimental renal infection and scarring. *Am J Nephrol,* 15: 411-417, 1995.
70. Wiggins, R, Goyal, M, Merritt, S, *et al.*: Vascular adventitial cell expression of collagen I messenger ribonucleic acid in anti-glomerular basement membrane antibody-induced crescentic nephritis in the rabbit. A cellular source for interstitial collagen synthesis in inflammatory renal disease. *Lab Invest,* 68: 557-565, 1993.
71. Liu, Y: Epithelial to mesenchymal transition in renal fibrogenesis: pathologic significance, molecular mechanism, and therapeutic intervention. *J Am Soc Nephrol,* 15: 1-12, 2004.
72. Zeisberg, EM, Potenta, SE, Sugimoto, H, *et al.*: Fibroblasts in kidney fibrosis emerge via endothelial-to-mesenchymal transition. *J Am Soc Nephrol,* 19: 2282-2287, 2008.
73. Grimm, PC, Nickerson, P, Jeffery, J, *et al.*: Neointimal and tubulointerstitial infiltration by recipient mesenchymal cells in chronic renal-allograft rejection. *N Engl J Med,* 345: 93-97, 2001.
74. Lin, SL, Kisseleva, T, Brenner, DA, *et al.*: Pericytes and perivascular fibroblasts are the primary source of collagen-producing cells in obstructive fibrosis of the kidney. *Am J Pathol,* 173: 1617-1627, 2008.
75. Darby, IA, Hewitson, TD: Fibroblast differentiation in wound healing and fibrosis. *Int Rev Cytol,* 257: 143-179, 2007.
76. Geiger, B, Bershadsky, A, Pankov, R, *et al.*: Transmembrane crosstalk between the extracellular matrix--cytoskeleton crosstalk. *Nat Rev Mol Cell Biol,* 2: 793-805, 2001.
77. Marastoni, S, Ligresti, G, Lorenzon, E, *et al.*: Extracellular matrix: a matter of life and death. *Connect Tissue Res,* 49: 203-206, 2008.
78. Miyazono, K, Heldin, CH: Latent forms of TGF-beta: molecular structure and mechanisms of activation. *Ciba Found Symp,* 157: 81-89; discussion 89-92, 1991.
79. Cohen, EP: Fibrosis causes progressive kidney failure. *Med Hypotheses,* 45: 459-462, 1995.
80. Zeisberg, M, Hanai, J, Sugimoto, H, *et al.*: BMP-7 counteracts TGF-beta1-induced epithelial-to-mesenchymal transition and reverses chronic renal injury. *Nat Med,* 9: 964-968, 2003.
81. Mizuno, S, Matsumoto, K, Nakamura, T: Hepatocyte growth factor suppresses interstitial fibrosis in a mouse model of obstructive nephropathy. *Kidney Int,* 59: 1304-1314, 2001.
82. el-Khatib, MT, Becker, GJ, Kincaid-Smith, PS: Morphometric aspects of reflux nephropathy. *Kidney Int,* 32: 261-266, 1987.
83. Sumual, S, Saad, S, Tang, O, *et al.*: Differential regulation of Snail by hypoxia and hyperglycemia in human proximal tubule cells. *Int J Biochem Cell Biol,* 42: 1689-1697, 2010.
84. Wong, MG, Suzuki, Y, Tanifuji, C, *et al.*: Peritubular ischemia contributes more to tubular damage than proteinuria in immune-mediated glomerulonephritis. *J Am Soc Nephrol,* 19: 290-297, 2008.
85. Higgins, DF, Kimura, K, Bernhardt, WM, *et al.*: Hypoxia promotes fibrogenesis in vivo via HIF-1 stimulation of epithelial-to-mesenchymal transition. *J Clin Invest,* 117: 3810-3820, 2007.
86. Haase, VH: Pathophysiological Consequences of HIF Activation: HIF as a modulator of fibrosis. *Ann N Y Acad Sci,* 1177: 57-65, 2009.
87. Olson, MW, Toth, M, Gervasi, DC, *et al.*: High affinity binding of latent matrix metalloproteinase-9 to the alpha2(IV) chain of collagen IV. *J Biol Chem,* 273: 10672-10681, 1998.

88. Gomez, DE, Alonso, DF, Yoshiji, H, *et al.*: Tissue inhibitors of metalloproteinases: structure, regulation and biological functions. *Eur J Cell Biol,* 74: 111-122, 1997.
89. McLennan, SV, Fisher, E, Martell, SY, *et al.*: Effects of glucose on matrix metalloproteinase and plasmin activities in mesangial cells: possible role in diabetic nephropathy. *Kidney Int Suppl,* 77: S81-87, 2000.
90. McLennan, SV, Martell, SY, Yue, DK: High glucose concentration inhibits the expression of membrane type metalloproteinase by mesangial cells: possible role in mesangium accumulation. *Diabetologia,* 43: 642-648, 2000.
91. Tomooka, S, Border, WA, Marshall, BC, *et al.*: Glomerular matrix accumulation is linked to inhibition of the plasmin protease system. *Kidney int,* 42: 1462-1469, 1992.
92. Wagner, SN, Atkinson, MJ, Wagner, C, *et al.*: Sites of urokinase-type plasminogen activator expression and distribution of its receptor in the normal human kidney. *Histochem Cell Biol,* 105: 53-60, 1996.
93. Eddy, AA: Plasminogen activator inhibitor-1 and the kidney. *Am J Physiol Renal Physiol,* 283: F209-220, 2002.
94. Ronco, P, Lelongt, B, Piedagnel, R, *et al.*: Matrix metalloproteinases in kidney disease progression and repair: a case of flipping the coin. *Semin Nephrol,* 27: 352-362, 2007.
95. Cheng, S, Pollock, AS, Mahimkar, R, *et al.*: Matrix metalloproteinase 2 and basement membrane integrity: a unifying mechanism for progressive renal injury. *FASEB J,* 20: 1898-1900, 2006.
96. Lovett, DH, Johnson, RJ, Marti, HP, *et al.*: Structural characterization of the mesangial cell type IV collagenase and enhanced expression in a model of immune complex-mediated glomerulonephritis. *Am J Pathol,* 141: 85-98, 1992.
97. Shiau, MY, Tsai, ST, Tsai, KJ, *et al.*: Increased circulatory MMP-2 and MMP-9 levels and activities in patients with type 1 diabetes mellitus. *Mt Sinai J Med,* 73: 1024-1028, 2006.
98. Strutz, F, Okada, H, Lo, CW, *et al.*: Identification and characterization of a fibroblast marker: FSP1. *J Cell Biol,* 130: 393-405, 1995.
99. Liu, Y: New insights into epithelial-mesenchymal transition in kidney fibrosis. *J Am Soc Nephrol,* 21: 212-222, 2010.
100. Kalluri, R, Neilson, EG: Epithelial-mesenchymal transition and its implications for fibrosis. *J Clin Invest,* 112: 1776-1784, 2003.
101. Zavadil, J, Bottinger, EP: TGF-beta and epithelial-to-mesenchymal transitions. *Oncogene,* 24: 5764-5774, 2005.
102. Kalluri, R, Weinberg, RA: The basics of epithelial-mesenchymal transition. *J Clin Invest,* 119: 1420-1428, 2009.
103. Burns, WC, Kantharidis, P, Thomas, MC: The role of tubular epithelial-mesenchymal transition in progressive kidney disease. *Cells Tissues Organs,* 185: 222-231, 2007.
104. Neilson, EG: Mechanisms of disease: Fibroblasts--a new look at an old problem. *Nat Clin Pract Nephrol,* 2: 101-108, 2006.
105. Fan, JM, Huang, XR, Ng, YY, *et al.*: Interleukin-1 induces tubular epithelial-myofibroblast transdifferentiation through a transforming growth factor-beta1-dependent mechanism in vitro. *Am J Kidney Dis,* 37: 820-831, 2001.
106. Zeisberg, M, Neilson, EG: Biomarkers for epithelial-mesenchymal transitions. *J Clin Invest,* 119: 1429-1437, 2009.
107. Iwano, M, Plieth, D, Danoff, TM, *et al.*: Evidence that fibroblasts derive from epithelium during tissue fibrosis. *J Clin Invest,* 110: 341-350, 2002.
108. Yang, J, Shultz, RW, Mars, WM, *et al.*: Disruption of tissue-type plasminogen activator gene in mice reduces renal interstitial fibrosis in obstructive nephropathy. *J Clin Invest,* 110: 1525-1538, 2002.
109. Liu, Y, Rajur, K, Tolbert, E, *et al.*: Endogenous hepatocyte growth factor ameliorates chronic renal injury by activating matrix degradation pathways. *Kidney Int,* 58: 2028-2043, 2000.

110. Lan, HY: Tubular epithelial-myofibroblast transdifferentiation mechanisms in proximal tubule cells. *Curr Opin Nephrol Hypertens,* 12: 25-29, 2003.
111. Rossini, M, Cheunsuchon, B, Donnert, E, *et al.*: Immunolocalization of fibroblast growth factor-1 (FGF-1), its receptor (FGFR-1), and fibroblast-specific protein-1 (FSP-1) in inflammatory renal disease. *Kidney Int,* 68: 2621-2628, 2005.
112. Nishitani, Y, Iwano, M, Yamaguchi, Y, *et al.*: Fibroblast-specific protein 1 is a specific prognostic marker for renal survival in patients with IgAN. *Kidney Int,* 68: 1078-1085, 2005.
113. Rastaldi, MP, Ferrario, F, Giardino, L, *et al.*: Epithelial-mesenchymal transition of tubular epithelial cells in human renal biopsies. *Kidney Int,* 62: 137-146, 2002.
114. Simonson, MS: Phenotypic transitions and fibrosis in diabetic nephropathy. *Kidney Int,* 71: 846-854, 2007.
115. Hertig, A, Verine, J, Mougenot, B, *et al.*: Risk factors for early epithelial to mesenchymal transition in renal grafts. *Am J Transplant,* 6: 2937-2946, 2006.
116. Hertig, A, Anglicheau, D, Verine, J, *et al.*: Early epithelial phenotypic changes predict graft fibrosis. *J Am Soc Nephrol,* 19: 1584-1591, 2008.
117. Vongwiwatana, A, Tasanarong, A, Rayner, DC, *et al.*: Epithelial to mesenchymal transition during late deterioration of human kidney transplants: the role of tubular cells in fibrogenesis. *Am J Transplant,* 5: 1367-1374, 2005.
118. Yang, J, Liu, Y: Dissection of key events in tubular epithelial to myofibroblast transition and its implications in renal interstitial fibrosis. *Am J Pathol,* 159: 1465-1475, 2001.
119. Bottinger, EP, Bitzer, M: TGF-beta signaling in renal disease. *J Am Soc Nephrol,* 13: 2600-2610, 2002.
120. Yang, J, Liu, Y: Blockage of tubular epithelial to myofibroblast transition by hepatocyte growth factor prevents renal interstitial fibrosis. *J Am Soc Nephrol,* 13: 96-107, 2002.
121. Masszi, A, Fan, L, Rosivall, L, *et al.*: Integrity of cell-cell contacts is a critical regulator of TGF-beta 1-induced epithelial-to-myofibroblast transition: role for beta-catenin. *Am J Pathol,* 165: 1955-1967, 2004.
122. Strutz, F, Zeisberg, M, Ziyadeh, FN, *et al.*: Role of basic fibroblast growth factor-2 in epithelial-mesenchymal transformation. *Kidney Int,* 61: 1714-1728, 2002.
123. Burns, WC, Twigg, SM, Forbes, JM, *et al.*: Connective tissue growth factor plays an important role in advanced glycation end product-induced tubular epithelial-to-mesenchymal transition: implications for diabetic renal disease. *J Am Soc Nephrol,* 17: 2484-2494, 2006.
124. Tan, X, Li, Y, Liu, Y: Paricalcitol attenuates renal interstitial fibrosis in obstructive nephropathy. *J Am Soc Nephrol,* 17: 3382-3393, 2006.
125. Fan, JM, Huang, XR, Ng, YY, *et al.*: Interleukin-1 induces tubular epithelial-myofibroblast transdifferentiation through a transforming growth factor-beta1-dependent mechanism in vitro. *American journal of kidney diseases : the official journal of the National Kidney Foundation,* 37: 820-831, 2001.
126. Pollack, V, Sarkozi, R, Banki, Z, *et al.*: Oncostatin M-induced effects on EMT in human proximal tubular cells: differential role of ERK signaling. *Am J Physiol Renal Physiol,* 293: F1714-1726, 2007.
127. Nightingale, J, Patel, S, Suzuki, N, *et al.*: Oncostatin M, a cytokine released by activated mononuclear cells, induces epithelial cell-myofibroblast transdifferentiation via Jak/Stat pathway activation. *J Am Soc Nephrol,* 15: 21-32, 2004.
128. Yang, J, Dai, C, Liu, Y: Hepatocyte growth factor gene therapy and angiotensin II blockade synergistically attenuate renal interstitial fibrosis in mice. *J Am Soc Nephrol,* 13: 2464-2477, 2002.
129. Carvajal, G, Rodriguez-Vita, J, Rodrigues-Diez, R, *et al.*: Angiotensin II activates the Smad pathway during epithelial mesenchymal transdifferentiation. *Kidney Int,* 74: 585-595, 2008.
130. Patel, S, Mason, RM, Suzuki, J, *et al.*: Inhibitory effect of statins on renal epithelial-to-mesenchymal transition. *Am J Nephrol,* 26: 381-387, 2006.

131. Wu, MJ, Wen, MC, Chiu, YT, *et al.*: Rapamycin attenuates unilateral ureteral obstruction-induced renal fibrosis. *Kidney Int,* 69: 2029-2036, 2006.
132. Copeland, JW, Beaumont, BW, Merrilees, MJ, *et al.*: Epithelial-to-mesenchymal transition of human proximal tubular epithelial cells: effects of rapamycin, mycophenolate, cyclosporin, azathioprine, and methylprednisolone. *Transplantation,* 83: 809-814, 2007.
133. Cheng, S, Lovett, DH: Gelatinase A (MMP-2) is necessary and sufficient for renal tubular cell epithelial-mesenchymal transformation. *Am J Pathol,* 162: 1937-1949, 2003.
134. Zhang, G, Kernan, KA, Collins, SJ, *et al.*: Plasmin(ogen) promotes renal interstitial fibrosis by promoting epithelial-to-mesenchymal transition: role of plasmin-activated signals. *J Am Soc Nephrol,* 18: 846-859, 2007.
135. Manotham, K, Tanaka, T, Matsumoto, M, *et al.*: Transdifferentiation of cultured tubular cells induced by hypoxia. *Kidney Int,* 65: 871-880, 2004.
136. Djamali, A, Reese, S, Yracheta, J, *et al.*: Epithelial-to-mesenchymal transition and oxidative stress in chronic allograft nephropathy. *Am J Transplant,* 5: 500-509, 2005.
137. Li, JH, Wang, W, Huang, XR, *et al.*: Advanced glycation end products induce tubular epithelial-myofibroblast transition through the RAGE-ERK1/2 MAP kinase signaling pathway. *Am J Pathol,* 164: 1389-1397, 2004.
138. Li, J, Qu, X, Bertram, JF: Endothelial-myofibroblast transition contributes to the early development of diabetic renal interstitial fibrosis in streptozotocin-induced diabetic mice. *Am J Pathol,* 175: 1380-1388, 2009.
139. Humphreys, BD, Lin, SL, Kobayashi, A, *et al.*: Fate tracing reveals the pericyte and not epithelial origin of myofibroblasts in kidney fibrosis. *Am J Pathol,* 176: 85-97, 2010.
140. Ferguson, MW, O'Kane, S: Scar-free healing: from embryonic mechanisms to adult therapeutic intervention. *Philos Trans R Soc Lond B Biol Sci,* 359: 839-850, 2004.
141. Segerer, S, Kretzler, M, Strutz, F, *et al.*: Mechanisms of tissue injury and repair in renal diseases. In: *Diseases of the Kidney and Urinary Tract.* edited by R, S., Philadelphia, Lippincott, 2007.
142. Segerer, S, Schlondorff, D: Role of chemokines for the localization of leukocyte subsets in the kidney. *Semin Nephrol,* 27: 260-274, 2007.
143. Anders, HJ, Schlondorff, D: Toll-like receptors: emerging concepts in kidney disease. *Curr Opin Nephrol Hypertens,* 16: 177-183, 2007.
144. Anders, HJ, Banas, B, Schlondorff, D: Signaling danger: toll-like receptors and their potential roles in kidney disease. *J Am Soc Nephrol,* 15: 854-867, 2004.
145. Thomas, MC, Forbes, JM, Cooper, ME: Advanced glycation end products and diabetic nephropathy. *Am J Ther,* 12: 562-572, 2005.
146. Singh, DK, Winocour, P, Farrington, K: Mechanisms of disease: the hypoxic tubular hypothesis of diabetic nephropathy. *Nat Clin Pract Nephrol,* 4: 216-226, 2008.
147. Anders, HJ, Vielhauer, V, Schlondorff, D: Chemokines and chemokine receptors are involved in the resolution or progression of renal disease. *Kidney Int,* 63: 401-415, 2003.
148. Wada, T, Sakai, N, Matsushima, K, *et al.*: Fibrocytes: a new insight into kidney fibrosis. *Kidney int,* 72: 269-273, 2007.
149. Schlondorff, DO: Overview of factors contributing to the pathophysiology of progressive renal disease. *Kidney Int,* 74: 860-866, 2008.
150. Eckardt, KU, Rosenberger, C, Jurgensen, JS, *et al.*: Role of hypoxia in the pathogenesis of renal disease. *Blood Purif,* 21: 253-257, 2003.
151. Nangaku, M: Hypoxia and tubulointerstitial injury: a final common pathway to end-stage renal failure. *Nephron Exp Nephrol,* 98: e8-12, 2004.
152. Nangaku, M: Chronic hypoxia and tubulointerstitial injury: a final common pathway to end-stage renal failure. *J Am Soc Nephrol,* 17: 17-25, 2006.
153. Nath, KA, Croatt, AJ, Hostetter, TH: Oxygen consumption and oxidant stress in surviving nephrons. *Am J Physiol,* 258: F1354-1362, 1990.

154. Miyata, T, de Strihou, CY: Diabetic nephropathy: a disorder of oxygen metabolism? *Nat Rev Nephrol,* 6: 83-95, 2010.
155. Marx, J: Cell biology. How cells endure low oxygen. *Science,* 303: 1454-1456, 2004.
156. Lawrence, DA: Transforming growth factor-beta: a general review. *Eur Cytokine Netw,* 7: 363-374, 1996.
157. Wrana, JL: TGF-beta receptors and signalling mechanisms. *Miner Electrolyte Metab,* 24: 120-130, 1998.
158. Miettinen, PJ, Ebner, R, Lopez, AR, *et al.*: TGF-beta induced transdifferentiation of mammary epithelial cells to mesenchymal cells: involvement of type I receptors. *J Cell Biol,* 127: 2021-2036, 1994.
159. Ziyadeh, FN, Wolf, G: Pathogenesis of the podocytopathy and proteinuria in diabetic glomerulopathy. *Curr Diabetes Rev,* 4: 39-45, 2008.
160. Sharma, K, Jin, Y, Guo, J, *et al.*: Neutralization of TGF-beta by anti-TGF-beta antibody attenuates kidney hypertrophy and the enhanced extracellular matrix gene expression in STZ-induced diabetic mice. *Diabetes,* 45: 522-530, 1996.
161. Ziyadeh, FN, Sharma, K, Ericksen, M, *et al.*: Stimulation of collagen gene expression and protein synthesis in murine mesangial cells by high glucose is mediated by autocrine activation of transforming growth factor-beta. *J Clin Invest,* 93: 536-542, 1994.
162. Miyazono, K, Olofsson, A, Colosetti, P, *et al.*: A role of the latent TGF-beta 1-binding protein in the assembly and secretion of TGF-beta 1. *EMBO J,* 10: 1091-1101, 1991.
163. Kulkarni, AB, Huh, CG, Becker, D, *et al.*: Transforming growth factor beta 1 null mutation in mice causes excessive inflammatory response and early death. *Proc Natl Acad Sci U S A,* 90: 770-774, 1993.
164. Shull, MM, Ormsby, I, Kier, AB, *et al.*: Targeted disruption of the mouse transforming growth factor-beta 1 gene results in multifocal inflammatory disease. *Nature,* 359: 693-699, 1992.
165. Huang, XR, Chung, AC, Zhou, L, *et al.*: Latent TGF-beta1 protects against crescentic glomerulonephritis. *J Am Soc Nephrol,* 19: 233-242, 2008.
166. Huang, XR, Chung, AC, Wang, XJ, *et al.*: Mice overexpressing latent TGF-beta1 are protected against renal fibrosis in obstructive kidney disease. *Am J Physiol Renal Physiol,* 295: F118-127, 2008.
167. Khalil, N: TGF-beta: from latent to active. *Microbes Infect,* 1: 1255-1263, 1999.
168. Khalil, N, Corne, S, Whitman, C, *et al.*: Plasmin regulates the activation of cell-associated latent TGF-beta 1 secreted by rat alveolar macrophages after in vivo bleomycin injury. *Am J Respir Cell Mol Biol,* 15: 252-259, 1996.
169. Miyazono, K, Heldin, CH: Role for carbohydrate structures in TGF-beta 1 latency. *Nature,* 338: 158-160, 1989.
170. Schultz-Cherry, S, Hinshaw, VS: Influenza virus neuraminidase activates latent transforming growth factor beta. *J Virol,* 70: 8624-8629, 1996.
171. Schultz-Cherry, S, Chen, H, Mosher, DF, *et al.*: Regulation of transforming growth factor-beta activation by discrete sequences of thrombospondin 1. *J Biol Chem,* 270: 7304-7310, 1995.
172. Oursler, MJ, Riggs, BL, Spelsberg, TC: Glucocorticoid-induced activation of latent transforming growth factor-beta by normal human osteoblast-like cells. *Endocrinology,* 133: 2187-2196, 1993.
173. Abe, M, Oda, N, Sato, Y: Cell-associated activation of latent transforming growth factor-beta by calpain. *J Cell Physiol,* 174: 186-193, 1998.
174. Antonelli-Orlidge, A, Saunders, KB, Smith, SR, *et al.*: An activated form of transforming growth factor beta is produced by cocultures of endothelial cells and pericytes. *Proc Natl Acad Sci U S A,* 86: 4544-4548, 1989.
175. Sato, Y, Rifkin, DB: Inhibition of endothelial cell movement by pericytes and smooth muscle cells: activation of a latent transforming growth factor-beta 1-like molecule by plasmin during co-culture. *J Cell Biol,* 109: 309-315, 1989.

176. Loskutoff, DJ, Quigley, JP: PAI-1, fibrosis, and the elusive provisional fibrin matrix. *J Clin Invest,* 106: 1441-1443, 2000.
177. Lijnen, HR: Plasmin and matrix metalloproteinases in vascular remodeling. *Thromb Haemost,* 86: 324-333, 2001.
178. Lyons, RM, Gentry, LE, Purchio, AF, *et al.*: Mechanism of activation of latent recombinant transforming growth factor beta 1 by plasmin. *J Cell Biol,* 110: 1361-1367, 1990.
179. Kagami, S, Border, WA, Miller, DE, *et al.*: Angiotensin II stimulates extracellular matrix protein synthesis through induction of transforming growth factor-beta expression in rat glomerular mesangial cells. *J Clin Invest,* 93: 2431-2437, 1994.
180. Wolf, G, Mueller, E, Stahl, RA, *et al.*: Angiotensin II-induced hypertrophy of cultured murine proximal tubular cells is mediated by endogenous transforming growth factor-beta. *J Clin Invest,* 92: 1366-1372, 1993.
181. Gibbons, GH, Pratt, RE, Dzau, VJ: Vascular smooth muscle cell hypertrophy vs. hyperplasia. Autocrine transforming growth factor-beta 1 expression determines growth response to angiotensin II. *J Clin Invest,* 90: 456-461, 1992.
182. Negrete, H, Studer, RK, Craven, PA, *et al.*: Role for transforming growth factor beta in thromboxane-induced increases in mesangial cell fibronectin synthesis. *Diabetes,* 44: 335-339, 1995.
183. Riser, BL, Cortes, P, Heilig, C, *et al.*: Cyclic stretching force selectively up-regulates transforming growth factor-beta isoforms in cultured rat mesangial cells. *Am J Pathol,* 148: 1915-1923, 1996.
184. Studer, RK, Negrete, H, Craven, PA, *et al.*: Protein kinase C signals thromboxane induced increases in fibronectin synthesis and TGF-beta bioactivity in mesangial cells. *Kidney Int,* 48: 422-430, 1995.
185. Ghosh, P, Dahms, NM, Kornfeld, S: Mannose 6-phosphate receptors: new twists in the tale. *Nat Rev Mol Cell Biol,* 4: 202-212, 2003.
186. Godar, S, Horejsi, V, Weidle, UH, *et al.*: M6P/IGFII-receptor complexes urokinase receptor and plasminogen for activation of transforming growth factor-beta1. *Eur J Immunol,* 29: 1004-1013, 1999.
187. Gary-Bobo, M, Nirde, P, Jeanjean, A, *et al.*: Mannose 6-phosphate receptor targeting and its applications in human diseases. *Curr Med Chem,* 14: 2945-2953, 2007.
188. Dennis, PA, Rifkin, DB: Cellular activation of latent transforming growth factor beta requires binding to the cation-independent mannose 6-phosphate/insulin-like growth factor type II receptor. *Proc Natl Acad Sci U S A,* 88: 580-584, 1991.
189. Blasi, F, Carmeliet, P: uPAR: a versatile signalling orchestrator. *Nat Rev Mol Cell Biol,* 3: 932-943, 2002.
190. Leksa, V, Godar, S, Cebecauer, M, *et al.*: The N terminus of mannose 6-phosphate/insulin-like growth factor 2 receptor in regulation of fibrinolysis and cell migration. *J Biol Chem,* 277: 40575-40582, 2002.
191. Greupink, R, Reker-Smit, C, Proost, JH, *et al.*: Pharmacokinetics of a hepatic stellate cell-targeted doxorubicin construct in bile duct-ligated rats. *Biochem Pharmacol,* 73: 1455-1462, 2007.
192. Greupink, R, Bakker, HI, van Goor, H, *et al.*: Mannose-6-phosphate/insulin-Like growth factor-II receptors may represent a target for the selective delivery of mycophenolic acid to fibrogenic cells. *Pharm Res,* 23: 1827-1834, 2006.
193. O'Kane, S, Ferguson, MW: Transforming growth factor beta s and wound healing. *Int J Biochem Cell Biol,* 29: 63-78, 1997.
194. Bates, SJ, Morrow, E, Zhang, AY, *et al.*: Mannose-6-phosphate, an inhibitor of transforming growth factor-beta, improves range of motion after flexor tendon repair. *J Bone Joint Surg Am,* 88: 2465-2472, 2006.
195. Zhu, Y, Li, X, Kyazike, J, *et al.*: Conjugation of mannose 6-phosphate-containing oligosaccharides to acid alpha-glucosidase improves the clearance of glycogen in pompe mice. *J Biol Chem,* 279: 50336-50341, 2004.

196. Zhu, Y, Li, X, Schuchman, EH, *et al.*: Dexamethasone-mediated up-regulation of the mannose receptor improves the delivery of recombinant glucocerebrosidase to Gaucher macrophages. *J Pharmacol Exp Ther,* 308: 705-711, 2004.
197. Lee, ES, Na, K, Bae, YH: Doxorubicin loaded pH-sensitive polymeric micelles for reversal of resistant MCF-7 tumor. *J Control Release,* 103: 405-418, 2005.
198. Storm, G, Roerdink, FH, Steerenberg, PA, *et al.*: Influence of lipid composition on the antitumor activity exerted by doxorubicin-containing liposomes in a rat solid tumor model. *Cancer Res,* 47: 3366-3372, 1987.
199. Adams, JC: Thrombospondin-1. *Int J Biochem Cell Biol,* 29: 861-865, 1997.
200. Yevdokimova, N, Wahab, NA, Mason, RM: Thrombospondin-1 is the key activator of TGF-beta1 in human mesangial cells exposed to high glucose. *J Am Soc Nephrol,* 12: 703-712, 2001.
201. Yung, S, Lee, CY, Zhang, Q, *et al.*: Elevated glucose induction of thrombospondin-1 up-regulates fibronectin synthesis in proximal renal tubular epithelial cells through TGF-beta1 dependent and TGF-beta1 independent pathways. *Nephrol Dial Transplant,* 21: 1504-1513, 2006.
202. Yehualaeshet, T, O'Connor, R, Green-Johnson, J, *et al.*: Activation of rat alveolar macrophage-derived latent transforming growth factor beta-1 by plasmin requires interaction with thrombospondin-1 and its cell surface receptor, CD36. *Am J Pathol,* 155: 841-851, 1999.
203. Barcellos-Hoff, MH, Dix, TA: Redox-mediated activation of latent transforming growth factor-beta 1. *Mol Endocrinol,* 10: 1077-1083, 1996.
204. Nath, KA, Grande, J, Croatt, A, *et al.*: Redox regulation of renal DNA synthesis, transforming growth factor-beta1 and collagen gene expression. *Kidney Int,* 53: 367-381, 1998.
205. Munger, JS, Huang, X, Kawakatsu, H, *et al.*: The integrin alpha v beta 6 binds and activates latent TGF beta 1: a mechanism for regulating pulmonary inflammation and fibrosis. *Cell,* 96: 319-328, 1999.
206. Ludbrook, SB, Barry, ST, Delves, CJ, *et al.*: The integrin alphavbeta3 is a receptor for the latency-associated peptides of transforming growth factors beta1 and beta3. *Biochem J,* 369: 311-318, 2003.
207. Moyano, JV, Greciano, PG, Buschmann, MM, *et al.*: Autocrine TGF-{beta}1 Activation Mediated by Integrin {alpha}V{beta}3 Regulates Transcriptional Expression of LM-332 in Madin-Darby Canine Kidney (MDCK) Epithelial Cells. *Mol Biol Cell,* 2010.
208. Gils, A, Declerck, PJ: Plasminogen activator inhibitor-1. *Curr Med Chem,* 11: 2323-2334, 2004.
209. Sato, Y, Tsuboi, R, Lyons, R, *et al.*: Characterization of the activation of latent TGF-beta by co-cultures of endothelial cells and pericytes or smooth muscle cells: a self-regulating system. *J Cell Biol,* 111: 757-763, 1990.
210. Schaefer, L, Macakova, K, Raslik, I, *et al.*: Absence of decorin adversely influences tubulointerstitial fibrosis of the obstructed kidney by enhanced apoptosis and increased inflammatory reaction. *Am J Pathol,* 160: 1181-1191, 2002.
211. Juarez, P, Vilchis-Landeros, MM, Ponce-Coria, J, *et al.*: Soluble betaglycan reduces renal damage progression in db/db mice. *Am J Physiol Renal Physiol,* 292: F321-329, 2007.
212. Miyazono, K, Ichijo, H, Heldin, CH: Transforming growth factor-beta: latent forms, binding proteins and receptors. *Growth Factors,* 8: 11-22, 1993.
213. Li, J, Campanale, NV, Liang, RJ, *et al.*: Inhibition of p38 mitogen-activated protein kinase and transforming growth factor-beta1/Smad signaling pathways modulates the development of fibrosis in adriamycin-induced nephropathy. *Am J Pathol,* 169: 1527-1540, 2006.
214. Suthanthiran, M, Khanna, A, Cukran, D, *et al.*: Transforming growth factor-beta 1 hyperexpression in African American end-stage renal disease patients. *Kidney int,* 53: 639-644, 1998.
215. Suthanthiran, M, Li, B, Song, JO, *et al.*: Transforming growth factor-beta 1 hyperexpression in African-American hypertensives: A novel mediator of hypertension and/or target organ damage. *Proc Natl Acad Sci U S A,* 97: 3479-3484, 2000.
216. Huang, Y, Noble, NA, Zhang, J, *et al.*: Renin-stimulated TGF-beta1 expression is regulated by a mitogen-activated protein kinase in mesangial cells. *Kidney int,* 72: 45-52, 2007.

217. Gaedeke, J, Peters, H, Noble, NA, *et al.*: Angiotensin II, TGF-beta and renal fibrosis. *Contrib Nephrol*: 153-160, 2001.
218. Border, WA, Noble, NA: Interactions of transforming growth factor-beta and angiotensin II in renal fibrosis. *Hypertension,* 31: 181-188, 1998.
219. Yu, L, Border, WA, Anderson, I, *et al.*: Combining TGF-beta inhibition and angiotensin II blockade results in enhanced antifibrotic effect. *Kidney int,* 66: 1774-1784, 2004.
220. Suthanthiran, M, Gerber, LM, Schwartz, JE, *et al.*: Circulating transforming growth factor-beta1 levels and the risk for kidney disease in African Americans. *Kidney int,* 76: 72-80, 2009.
221. Appel, LJ, Wright, JT, Jr., Greene, T, *et al.*: Long-term effects of renin-angiotensin system-blocking therapy and a low blood pressure goal on progression of hypertensive chronic kidney disease in African Americans. *Arch Intern Med,* 168: 832-839, 2008.
222. Chaturvedi, N, Schalkwijk, CG, Abrahamian, H, *et al.*: Circulating and urinary transforming growth factor beta1, Amadori albumin, and complications of type 1 diabetes: the EURODIAB prospective complications study. *Diabetes Care,* 25: 2320-2327, 2002.
223. Sharma, K, Ziyadeh, FN, Alzahabi, B, *et al.*: Increased renal production of transforming growth factor-beta1 in patients with type II diabetes. *Diabetes,* 46: 854-859, 1997.
224. Hellmich, B, Schellner, M, Schatz, H, *et al.*: Activation of transforming growth factor-beta1 in diabetic kidney disease. *Metabolism,* 49: 353-359, 2000.
225. Massague, J, Gomis, RR: The logic of TGFbeta signaling. *FEBS Lett,* 580: 2811-2820, 2006.
226. Feng, XH, Derynck, R: Specificity and versatility in tgf-beta signaling through Smads. *Annu Rev Cell Dev Biol,* 21: 659-693, 2005.
227. Li, Y, Yang, J, Dai, C, *et al.*: Role for integrin-linked kinase in mediating tubular epithelial to mesenchymal transition and renal interstitial fibrogenesis. *J Clin Invest,* 112: 503-516, 2003.
228. Li, Y, Dai, C, Wu, C, *et al.*: PINCH-1 promotes tubular epithelial-to-mesenchymal transition by interacting with integrin-linked kinase. *J Am Soc Nephro,* 18: 2534-2543, 2007.
229. Li, Y, Yang, J, Luo, JH, *et al.*: Tubular epithelial cell dedifferentiation is driven by the helix-loop-helix transcriptional inhibitor Id1. *J Am Soc Nephro,* 18: 449-460, 2007.
230. Phanish, MK, Wahab, NA, Colville-Nash, P, *et al.*: The differential role of Smad2 and Smad3 in the regulation of pro-fibrotic TGFbeta1 responses in human proximal-tubule epithelial cells. *Biochem J,* 393: 601-607, 2006.
231. Sato, M, Muragaki, Y, Saika, S, *et al.*: Targeted disruption of TGF-beta1/Smad3 signaling protects against renal tubulointerstitial fibrosis induced by unilateral ureteral obstruction. *J Clin Invest,* 112: 1486-1494, 2003.
232. Zavadil, J, Cermak, L, Soto-Nieves, N, *et al.*: Integration of TGF-beta/Smad and Jagged1/Notch signalling in epithelial-to-mesenchymal transition. *EMBO J,* 23: 1155-1165, 2004.
233. Lan, HY: Smad7 as a therapeutic agent for chronic kidney diseases. *Front Biosci,* 13: 4984-4992, 2008.
234. Li, JH, Zhu, HJ, Huang, XR, *et al.*: Smad7 inhibits fibrotic effect of TGF-Beta on renal tubular epithelial cells by blocking Smad2 activation. *J Am Soc Nephro,* 13: 1464-1472, 2002.
235. Yang, J, Dai, C, Liu, Y: A novel mechanism by which hepatocyte growth factor blocks tubular epithelial to mesenchymal transition. *J Am Soc Nephrol,* 16: 68-78, 2005.
236. Fan, L, Sebe, A, Peterfi, Z, *et al.*: Cell contact-dependent regulation of epithelial-myofibroblast transition via the rho-rho kinase-phospho-myosin pathway. *Mol Biol Cell,* 18: 1083-1097, 2007.
237. Masszi, A, Di Ciano, C, Sirokmany, G, *et al.*: Central role for Rho in TGF-beta1-induced alpha-smooth muscle actin expression during epithelial-mesenchymal transition. *Am J Physiol Renal Physiol,* 284: F911-924, 2003.
238. Bhowmick, NA, Zent, R, Ghiassi, M, *et al.*: Integrin beta 1 signaling is necessary for transforming growth factor-beta activation of p38MAPK and epithelial plasticity. *J Biol Chem,* 276: 46707-46713, 2001.
239. Thornton, TM, Pedraza-Alva, G, Deng, B, *et al.*: Phosphorylation by p38 MAPK as an alternative pathway for GSK3beta inactivation. *Science,* 320: 667-670, 2008.

240. Zeng, R, Yao, Y, Han, M, *et al.*: Biliverdin reductase mediates hypoxia-induced EMT via PI3-kinase and Akt. *J Am Soc of Nephrol,* 19: 380-387, 2008.
241. Teixeira Vde, P, Blattner, SM, Li, M, *et al.*: Functional consequences of integrin-linked kinase activation in podocyte damage. *Kidney int,* 67: 514-523, 2005.
242. Guo, L, Sanders, PW, Woods, A, *et al.*: The distribution and regulation of integrin-linked kinase in normal and diabetic kidneys. *Am J Pathol,* 159: 1735-1742, 2001.
243. Kretzler, M, Teixeira, VP, Unschuld, PG, *et al.*: Integrin-linked kinase as a candidate downstream effector in proteinuria. *FASEB J,* 15: 1843-1845, 2001.
244. Legate, KR, Montanez, E, Kudlacek, O, *et al.*: ILK, PINCH and parvin: the tIPP of integrin signalling. *Nat Rev Mol Cell Biol,* 7: 20-31, 2006.
245. Li, Y, Tan, X, Dai, C, *et al.*: Inhibition of integrin-linked kinase attenuates renal interstitial fibrosis. *J Am Soc Nephrol,* 20: 1907-1918, 2009.
246. Moon, RT, Kohn, AD, De Ferrari, GV, *et al.*: WNT and beta-catenin signalling: diseases and therapies. *Nat Rev Genet,* 5: 691-701, 2004.
247. Clevers, H: Wnt/beta-catenin signaling in development and disease. *Cell,* 127: 469-480, 2006.
248. Surendran, K, McCaul, SP, Simon, TC: A role for Wnt-4 in renal fibrosis. *Am J Physiol Renal Physiol,* 282: F431-441, 2002.
249. Surendran, K, Schiavi, S, Hruska, KA: Wnt-dependent beta-catenin signaling is activated after unilateral ureteral obstruction, and recombinant secreted frizzled-related protein 4 alters the progression of renal fibrosis. *J Am SocNephrol,* 16: 2373-2384, 2005.
250. He, W, Dai, C, Li, Y, *et al.*: Wnt/beta-catenin signaling promotes renal interstitial fibrosis. *J Am Soc Nephrol,* 20: 765-776, 2009.
251. Dang, DT, Pevsner, J, Yang, VW: The biology of the mammalian Kruppel-like family of transcription factors. *Int J Biochem Cell Biol,* 32: 1103-1121, 2000.
252. Koritschoner, NP, Bocco, JL, Panzetta-Dutari, GM, *et al.*: A novel human zinc finger protein that interacts with the core promoter element of a TATA box-less gene. *J Biol Chem,* 272: 9573-9580, 1997.
253. Onyango, P, Koritschoner, NP, Patrito, LC, *et al.*: Assignment of the gene encoding the core promoter element binding protein (COPEB) to human chromosome 10p15 by somatic hybrid analysis and fluorescence in situ hybridization. *Genomics,* 48: 143-144, 1998.
254. Fischer, EA, Verpont, MC, Garrett-Sinha, LA, *et al.*: Klf6 is a zinc finger protein expressed in a cell-specific manner during kidney development. *J Am Soc Nephrol,* 12: 726-735, 2001.
255. Jeng, YM, Hsu, HC: KLF6, a putative tumor suppressor gene, is mutated in astrocytic gliomas. *Int J Cancer,* 105: 625-629, 2003.
256. Kremer-Tal, S, Reeves, HL, Narla, G, *et al.*: Frequent inactivation of the tumor suppressor Kruppel-like factor 6 (KLF6) in hepatocellular carcinoma. *Hepatology,* 40: 1047-1052, 2004.
257. Narla, G, Heath, KE, Reeves, HL, *et al.*: KLF6, a candidate tumor suppressor gene mutated in prostate cancer. *Science,* 294: 2563-2566, 2001.
258. Reeves, HL, Narla, G, Ogunbiyi, O, *et al.*: Kruppel-like factor 6 (KLF6) is a tumor-suppressor gene frequently inactivated in colorectal cancer. *Gastroenterology,* 126: 1090-1103, 2004.
259. Kim, Y, Ratziu, V, Choi, SG, *et al.*: Transcriptional activation of transforming growth factor beta1 and its receptors by the Kruppel-like factor Zf9/core promoter-binding protein and Sp1. Potential mechanisms for autocrine fibrogenesis in response to injury. *J Biol Chem,* 273: 33750-33758, 1998.
260. Ratziu, V, Lalazar, A, Wong, L, *et al.*: Zf9, a Kruppel-like transcription factor up-regulated in vivo during early hepatic fibrosis. *Proc Natl Acad Sci U S A,* 95: 9500-9505, 1998.
261. Zhao, JL, Austen, KF, Lam, BK: Cell-specific transcription of leukotriene C(4) synthase involves a Kruppel-like transcription factor and Sp1. *J Biol Chem,* 275: 8903-8910, 2000.
262. Kojima, S, Hayashi, S, Shimokado, K, *et al.*: Transcriptional activation of urokinase by the Kruppel-like factor Zf9/COPEB activates latent TGF-beta1 in vascular endothelial cells. *Blood,* 95: 1309-1316, 2000.

263. DiFeo, A, Narla, G, Camacho-Vanegas, O, *et al.*: E-cadherin is a novel transcriptional target of the KLF6 tumor suppressor. *Oncogene,* 25: 6026-6031, 2006.
264. Tarabishi, R, Zahedi, K, Mishra, J, *et al.*: Induction of Zf9 in the kidney following early ischemia/reperfusion. *Kidney Int,* 68: 1511-1519, 2005.
265. Holian, J, Qi, W, Kelly, DJ, *et al.*: Role of Kruppel-like factor 6 in transforming growth factor-beta1-induced epithelial-mesenchymal transition of proximal tubule cells. *Am J Physiol Renal Physiol,* 295: F1388-1396, 2008.
266. Qi, W, Chen, X, Holian, J, *et al.*: Transcription Factors Kruppel-Like Factor 6 and Peroxisome Proliferator-Activated Receptor-{gamma} Mediate High Glucose-Induced Thioredoxin-Interacting Protein. *Am J Pathol,* 2009.
267. Urist, MR, Iwata, H, Ceccotti, PL, *et al.*: Bone morphogenesis in implants of insoluble bone gelatin. *Proc Natl Acad Sci U S A,* 70: 3511-3515, 1973.
268. Ducy, P, Karsenty, G: The family of bone morphogenetic proteins. *Kidney Int,* 57: 2207-2214, 2000.
269. Reddi, AH: BMPs: from bone morphogenetic proteins to body morphogenetic proteins. *Cytokine Growth Factor Rev,* 16: 249-250, 2005.
270. Griffith, DL, Keck, PC, Sampath, TK, *et al.*: Three-dimensional structure of recombinant human osteogenic protein 1: structural paradigm for the transforming growth factor beta superfamily. *Proc Natl Acad Sci U S A,* 93: 878-883, 1996.
271. Constam, DB, Robertson, EJ: Regulation of bone morphogenetic protein activity by pro domains and proprotein convertases. *J Cell Biol,* 144: 139-149, 1999.
272. Brown, MA, Zhao, Q, Baker, KA, *et al.*: Crystal structure of BMP-9 and functional interactions with pro-region and receptors. *J Biol Chem,* 280: 25111-25118, 2005.
273. Schreuder, H, Liesum, A, Pohl, J, *et al.*: Crystal structure of recombinant human growth and differentiation factor 5: evidence for interaction of the type I and type II receptor-binding sites. *Biochem Biophys Res Commun,* 329: 1076-1086, 2005.
274. Allendorph, GP, Vale, WW, Choe, S: Structure of the ternary signaling complex of a TGF-beta superfamily member. *Proc Natl Acad Sci U S A,* 103: 7643-7648, 2006.
275. Kessler, E, Takahara, K, Biniaminov, L, *et al.*: Bone morphogenetic protein-1: the type I procollagen C-proteinase. *Science,* 271: 360-362, 1996.
276. Kang, Q, Sun, MH, Cheng, H, *et al.*: Characterization of the distinct orthotopic bone-forming activity of 14 BMPs using recombinant adenovirus-mediated gene delivery. *Gene Ther,* 11: 1312-1320, 2004.
277. Callis, TE, Cao, D, Wang, DZ: Bone morphogenetic protein signaling modulates myocardin transactivation of cardiac genes. *Circ Res,* 97: 992-1000, 2005.
278. Vukicevic, S, Helder, MN, Luyten, FP: Developing human lung and kidney are major sites for synthesis of bone morphogenetic protein-3 (osteogenin). *J Histochem Cytochem,* 42: 869-875, 1994.
279. Hino, J, Kangawa, K, Matsuo, H, *et al.*: Bone morphogenetic protein-3 family members and their biological functions. *Front Biosci,* 9: 1520-1529, 2004.
280. Luyten, FP, Chen, P, Paralkar, V, *et al.*: Recombinant bone morphogenetic protein-4, transforming growth factor-beta 1, and activin A enhance the cartilage phenotype of articular chondrocytes in vitro. *Exp Cell Res,* 210: 224-229, 1994.
281. Oxburgh, L, Dudley, AT, Godin, RE, *et al.*: BMP4 substitutes for loss of BMP7 during kidney development. *Dev Biol,* 286: 637-646, 2005.
282. Miljkovic, ND, Cooper, GM, Marra, KG: Chondrogenesis, bone morphogenetic protein-4 and mesenchymal stem cells. *Osteoarthritis Cartilage,* 16: 1121-1130, 2008.
283. Cho, TJ, Gerstenfeld, LC, Einhorn, TA: Differential temporal expression of members of the transforming growth factor beta superfamily during murine fracture healing. *J Bone Miner Res,* 17: 513-520, 2002.

284. Zuzarte-Luis, V, Montero, JA, Rodriguez-Leon, J, *et al.*: A new role for BMP5 during limb development acting through the synergic activation of Smad and MAPK pathways. *Dev Biol,* 272: 39-52, 2004.
285. Gitelman, SE, Kobrin, MS, Ye, JQ, *et al.*: Recombinant Vgr-1/BMP-6-expressing tumors induce fibrosis and endochondral bone formation in vivo. *J Cell Biol,* 126: 1595-1609, 1994.
286. Rickard, DJ, Hofbauer, LC, Bonde, SK, *et al.*: Bone morphogenetic protein-6 production in human osteoblastic cell lines. Selective regulation by estrogen. *J Clin Invest,* 101: 413-422, 1998.
287. Lefer, AM, Tsao, PS, Ma, XL, *et al.*: Anti-ischaemic and endothelial protective actions of recombinant human osteogenic protein (hOP-1). *J Mol Cell Cardiol,* 24: 585-593, 1992.
288. Reddi, AH: Cartilage-derived morphogenetic proteins and cartilage morphogenesis. *Microsc Res Tech,* 43: 131-136, 1998.
289. Simic, P, Vukicevic, S: Bone morphogenetic proteins in development and homeostasis of kidney. *Cytokine Growth Factor Rev,* 16: 299-308, 2005.
290. Ozkaynak, E, Schnegelsberg, PN, Oppermann, H: Murine osteogenic protein (OP-1): high levels of mRNA in kidney. *Biochem Biophys Res Commun,* 179: 116-123, 1991.
291. Chen, C, Grzegorzewski, KJ, Barash, S, *et al.*: An integrated functional genomics screening program reveals a role for BMP-9 in glucose homeostasis. *Nat Biotechnol,* 21: 294-301, 2003.
292. Esquela, AF, Lee, SJ: Regulation of metanephric kidney development by growth/differentiation factor 11. *Dev Biol,* 257: 356-370, 2003.
293. Harmon, EB, Apelqvist, AA, Smart, NG, *et al.*: GDF11 modulates NGN3+ islet progenitor cell number and promotes beta-cell differentiation in pancreas development. *Development,* 131: 6163-6174, 2004.
294. Andersson, O, Reissmann, E, Ibanez, CF: Growth differentiation factor 11 signals through the transforming growth factor-beta receptor ALK5 to regionalize the anterior-posterior axis. *EMBO Rep,* 7: 831-837, 2006.
295. Reddi, AH: Cartilage morphogenetic proteins: role in joint development, homoeostasis, and regeneration. *Ann Rheum Dis,* 62 Suppl 2: ii73-78, 2003.
296. Lo, L, Dormand, EL, Anderson, DJ: Late-emigrating neural crest cells in the roof plate are restricted to a sensory fate by GDF7. *Proc Natl Acad Sci U S A,* 102: 7192-7197, 2005.
297. Yamashita, H, Shimizu, A, Kato, M, *et al.*: Growth/differentiation factor-5 induces angiogenesis in vivo. *Exp Cell Res,* 235: 218-226, 1997.
298. Zeng, Q, Li, X, Beck, G, *et al.*: Growth and differentiation factor-5 (GDF-5) stimulates osteogenic differentiation and increases vascular endothelial growth factor (VEGF) levels in fat-derived stromal cells in vitro. *Bone,* 40: 374-381, 2007.
299. Zhao, GQ, Deng, K, Labosky, PA, *et al.*: The gene encoding bone morphogenetic protein 8B is required for the initiation and maintenance of spermatogenesis in the mouse. *Genes Dev,* 10: 1657-1669, 1996.
300. Chen, H, Shi, S, Acosta, L, *et al.*: BMP10 is essential for maintaining cardiac growth during murine cardiogenesis. *Development,* 131: 2219-2231, 2004.
301. Knight, PG, Glister, C: TGF-beta superfamily members and ovarian follicle development. *Reproduction,* 132: 191-206, 2006.
302. Hogan, B: Bone morphogenetic proteins in development. *Curr Opin Genet Dev,* 6: 432-438., 1996.
303. Sampath, TK, Coughlin, JE, Whetstone, RM, *et al.*: Bovine osteogenic protein is composed of dimers of OP-1 and BMP-2A, two members of the transforming growth factor-beta superfamily. *J Biol Chem,* 265: 13198-13205, 1990.
304. Vukicevic, S, Basic, V, Rogic, D, *et al.*: Osteogenic protein-1 (bone morphogenetic protein-7) reduces severity of injury after ischemic acute renal failure in rat. *J Clin Invest,* 102: 202-214, 1998.
305. Massague, J: Receptors for the TGF-beta family. *Cell,* 69: 1067-1070, 1992.
306. Martinez, G, Loveland, KL, Clark, AT, *et al.*: Expression of bone morphogenetic protein receptors in the developing mouse metanephros. *Exp Nephrol,* 9: 372-379, 2001.

307. Kitten, AM, Kreisberg, JI, Olson, MS: Expression of osteogenic protein-1 mRNA in cultured kidney cells. *J Cell Physiol,* 181: 410-415, 1999.
308. Gould, SE, Day, M, Jones, SS, *et al.*: BMP-7 regulates chemokine, cytokine, and hemodynamic gene expression in proximal tubule cells. *Kidney Int,* 61: 51-60, 2002.
309. ten Dijke, P, Yamashita, H, Sampath, TK, *et al.*: Identification of type I receptors for osteogenic protein-1 and bone morphogenetic protein-4. *J Biol Chem,* 269: 16985-16988, 1994.
310. Wieser, R, Wrana, JL, Massague, J: GS domain mutations that constitutively activate T beta R-I, the downstream signaling component in the TGF-beta receptor complex. *EMBO J,* 14: 2199-2208, 1995.
311. Miyazono, K, Maeda, S, Imamura, T: BMP receptor signaling: transcriptional targets, regulation of signals, and signaling cross-talk. *Cytokine Growth Factor Rev,* 16: 251-263, 2005.
312. Miyazono, K, ten Dijke, P, Heldin, CH: TGF-beta signaling by Smad proteins. *Adv Immunol,* 75: 115-157, 2000.
313. Kusanagi, K, Inoue, H, Ishidou, Y, *et al.*: Characterization of a bone morphogenetic protein-responsive Smad-binding element. *Mol Biol Cell,* 11: 555-565, 2000.
314. Ishida, W, Hamamoto, T, Kusanagi, K, *et al.*: Smad6 is a Smad1/5-induced smad inhibitor. Characterization of bone morphogenetic protein-responsive element in the mouse Smad6 promoter. *J Biol Chem,* 275: 6075-6079, 2000.
315. Murakami, G, Watabe, T, Takaoka, K, *et al.*: Cooperative inhibition of bone morphogenetic protein signaling by Smurf1 and inhibitory Smads. *Mol Biol Cell,* 14: 2809-2817, 2003.
316. Zhang, Y, Chang, C, Gehling, DJ, *et al.*: Regulation of Smad degradation and activity by Smurf2, an E3 ubiquitin ligase. *Proc Natl Acad Sci U S A,* 98: 974-979, 2001.
317. Fuentealba, LC, Eivers, E, Ikeda, A, *et al.*: Integrating patterning signals: Wnt/GSK3 regulates the duration of the BMP/Smad1 signal. *Cell,* 131: 980-993, 2007.
318. Motazed, R, Colville-Nash, P, Kwan, JT, *et al.*: BMP-7 and Proximal Tubule Epithelial Cells: Activation of Multiple Signaling Pathways Reveals a Novel Anti-fibrotic Mechanism. *Pharm Res,* 25: 2440-2446, 2008.
319. Bosukonda, D, Shih, MS, Sampath, KT, *et al.*: Characterization of receptors for osteogenic protein-1/bone morphogenetic protein-7 (OP-1/BMP-7) in rat kidneys. *Kidney Int,* 58: 1902-1911, 2000.
320. Gregory, KE, Ono, RN, Charbonneau, NL, *et al.*: The prodomain of BMP-7 targets the BMP-7 complex to the extracellular matrix. *J Biol Chem,* 280: 27970-27980, 2005.
321. Vukicevic, S, Latin, V, Chen, P, *et al.*: Localization of osteogenic protein-1 (bone morphogenetic protein-7) during human embryonic development: high affinity binding to basement membranes. *Biochem Biophys Res Commun,* 198: 693-700, 1994.
322. Yanagita, M: Balance between bone morphogenetic proteins and their antagonists in kidney injury. *Ther Apher Dial,* 11 Suppl 1: S38-43, 2007.
323. Yanagita, M, Oka, M, Watabe, T, *et al.*: USAG-1: a bone morphogenetic protein antagonist abundantly expressed in the kidney. *Biochem Biophys Res Commun,* 316: 490-500, 2004.
324. Lin, J, Patel, SR, Cheng, X, *et al.*: Kielin/chordin-like protein, a novel enhancer of BMP signaling, attenuates renal fibrotic disease. *Curr Opin Investig Drugs,* 6: 255-261., 2005.
325. Lund, RJ, Davies, MR, Brown, AJ, *et al.*: Successful treatment of an adynamic bone disorder with bone morphogenetic protein-7 in a renal ablation model. *J Am Soc Nephrol,* 15: 359-369, 2004.
326. Luo, G, Hofmann, C, Bronckers, AL, *et al.*: BMP-7 is an inducer of nephrogenesis, and is also required for eye development and skeletal patterning. *Genes Dev,* 9: 2808-2820, 1995.
327. Godin, RE, Robertson, EJ, Dudley, AT: Role of BMP family members during kidney development. *Int J Dev Biol,* 43: 405-411, 1999.
328. Archdeacon, P, Detwiler, RK: Bone morphogenetic protein 7 (BMP7): a critical role in kidney development and a putative modulator of kidney injury. *Adv Chronic Kidney Dis,* 15: 314-320, 2008.
329. Piscione, TD, Yager, TD, Gupta, IR, *et al.*: BMP-2 and OP-1 exert direct and opposite effects on renal branching morphogenesis. *Am J Physiol,* 273: F961-975, 1997.

330. Raatikainen-Ahokas, A, Hytonen, M, Tenhunen, A, *et al.*: BMP-4 affects the differentiation of metanephric mesenchyme and reveals an early anterior-posterior axis of the embryonic kidney. *Dev Dyn,* 217: 146-158, 2000.
331. King, JA, Marker, PC, Seung, KJ, *et al.*: BMP5 and the molecular, skeletal, and soft-tissue alterations in short ear mice. *Dev Biol,* 166: 112-122, 1994.
332. Godin, RE, Takaesu, NT, Robertson, EJ, *et al.*: Regulation of BMP7 expression during kidney development. *Development,* 125: 3473-3482, 1998.
333. Zeisberg, M: Bone morphogenic protein-7 and the kidney: current concepts and open questions. *Nephrol Dial Transplant,* 21: 568-573, 2006.
334. De Petris, L, Hruska, K, Chiechio, S: Bone morphogenetic protein-7 delays podocyte injury due to high glucose. *Nephrol Dial Transplant,* 22: 3442-3450, 2007.
335. Chan, WL, Leung, JC, Chan, LY, *et al.*: BMP-7 protects mesangial cells from injury by polymeric IgA. *Kidney Int*: 1026-1039, 2008.
336. Zeisberg, M, Shah, AA, Kalluri, R: Bone morphogenic protein-7 induces mesenchymal to epithelial transition in adult renal fibroblasts and facilitates regeneration of injured kidney. *Jour biol chemistry,* 280: 8094-8100, 2005.
337. Zeisberg, EM, Tarnavski, O, Zeisberg, M, *et al.*: Endothelial-to-mesenchymal transition contributes to cardiac fibrosis. *Nat Med,* 13: 952-961, 2007.
338. Zhang, XL, Selbi, W, de la Motte, C, *et al.*: Bone morphogenic protein-7 inhibits monocyte-stimulated TGF-beta1 generation in renal proximal tubular epithelial cells. *J Am Soc Nephrol,* 16: 79-89, 2005.
339. Marumo, T, Hishikawa, K, Yoshikawa, M, *et al.*: Epigenetic regulation of BMP7 in the regenerative response to ischemia. *J Am Soc Nephrol,* 19: 1311-1320, 2008.
340. Hruska, KA, Guo, G, Wozniak, M, *et al.*: Osteogenic protein-1 prevents renal fibrogenesis associated with ureteral obstruction. *Am J Physiol Renal Physiol,* 79: F1060-1067, 2000.
341. Zeisberg, M, Bottiglio, C, Kumar, N, *et al.*: Bone morphogenic protein-7 inhibits progression of chronic renal fibrosis associated with two genetic mouse models. *Am J Physiol Renal Physiol,* 285: F1060-1067, 2003.
342. Wang, S, Chen, Q, Simon, TC, *et al.*: Bone morphogenic protein-7 (BMP-7), a novel therapy for diabetic nephropathy. *Kidney Int,* 63: 2037-2049, 2003.
343. Wang, S, de Caestecker, M, Kopp, J, *et al.*: Renal bone morphogenetic protein-7 protects against diabetic nephropathy. *J Am Soc Nephrol,* 17: 2504-2512, 2006.
344. Nguyen, TQ, Goldschmeding, R: Bone morphogenetic protein-7 and connective tissue growth factor: novel targets for treatment of renal fibrosis? *Pharm Res,* 25: 2416-2426, 2008.
345. Wetzel, P, Haag, J, Campean, V, *et al.*: Bone morphogenetic protein-7 expression and activity in the human adult normal kidney is predominantly localized to the distal nephron. *Kidney Int,* 70: 717-723, 2006.
346. Ichijo, T, Voutetakis, A, Cotrim, AP, *et al.*: The Smad6-histone deacetylase 3 complex silences the transcriptional activity of the glucocorticoid receptor: potential clinical implications. *J Biol Chem,* 280: 42067-42077, 2005.
347. Ikeda, Y, Jung, YO, Kim, H, *et al.*: Exogenous bone morphogenetic protein-7 fails to attenuate renal fibrosis in rats with overload proteinuria. *Nephron Exp Nephrol,* 97: e123-135, 2004.
348. Dudas, PL, Argentieri, RL, Farrell, FX: BMP-7 fails to attenuate TGF-beta1-induced epithelial-to-mesenchymal transition in human proximal tubule epithelial cells. *Nephrol Dial Transplant,* 24: 1406-1416, 2009.
349. Evans, RM: The steroid and thyroid hormone receptor superfamily. *Science,* 240: 889-895, 1988.
350. Wang, XX, Jiang, T, Levi, M: Nuclear hormone receptors in diabetic nephropathy. *Nat Rev Nephrol,* 6: 342-351, 2010.
351. Kumar, R, Thompson, EB: The structure of the nuclear hormone receptors. *Steroids,* 64: 310-319, 1999.

352. Thompson, EB, Kumar, R: DNA binding of nuclear hormone receptors influences their structure and function. *Biochem Biophys Res Commun,* 306: 1-4, 2003.
353. Mangelsdorf, DJ, Ong, ES, Dyck, JA, *et al.*: Nuclear receptor that identifies a novel retinoic acid response pathway. *Nature,* 345: 224-229, 1990.
354. Bookout, AL, Mangelsdorf, DJ: Quantitative real-time PCR protocol for analysis of nuclear receptor signaling pathways. *Nucl Recept Signal,* 1: e012, 2003.
355. Wang, YD, Chen, WD, Moore, DD, *et al.*: FXR: a metabolic regulator and cell protector. *Cell Res,* 18: 1087-1095, 2008.
356. Forman, BM, Goode, E, Chen, J, *et al.*: Identification of a nuclear receptor that is activated by farnesol metabolites. *Cell,* 81: 687-693, 1995.
357. Seol, W, Choi, HS, Moore, DD: Isolation of proteins that interact specifically with the retinoid X receptor: two novel orphan receptors. *Mol Endocrinol,* 9: 72-85, 1995.
358. Makishima, M, Okamoto, AY, Repa, JJ, *et al.*: Identification of a nuclear receptor for bile acids. *Science,* 284: 1362-1365, 1999.
359. Wang, H, Chen, J, Hollister, K, *et al.*: Endogenous bile acids are ligands for the nuclear receptor FXR/BAR. *Mol Cell,* 3: 543-553, 1999.
360. Parks, DJ, Blanchard, SG, Bledsoe, RK, *et al.*: Bile acids: natural ligands for an orphan nuclear receptor. *Science,* 284: 1365-1368, 1999.
361. Huang, W, Ma, K, Zhang, J, *et al.*: Nuclear receptor-dependent bile acid signaling is required for normal liver regeneration. *Science,* 312: 233-236, 2006.
362. Yang, F, Huang, X, Yi, T, *et al.*: Spontaneous development of liver tumors in the absence of the bile acid receptor farnesoid X receptor. *Cancer Res,* 67: 863-867, 2007.
363. Modica, S, Murzilli, S, Salvatore, L, *et al.*: Nuclear bile acid receptor FXR protects against intestinal tumorigenesis. *Cancer Res,* 68: 9589-9594, 2008.
364. Lee, FY, Lee, H, Hubbert, ML, *et al.*: FXR, a multipurpose nuclear receptor. *Trends Biochem Sci,* 31: 572-580, 2006.
365. Bookout, AL, Jeong, Y, Downes, M, *et al.*: Anatomical profiling of nuclear receptor expression reveals a hierarchical transcriptional network. *Cell,* 126: 789-799, 2006.
366. Otte, K, Kranz, H, Kober, I, *et al.*: Identification of farnesoid X receptor beta as a novel mammalian nuclear receptor sensing lanosterol. *Mol Cell Biol,* 23: 864-872, 2003.
367. Zhang, Y, Kast-Woelbern, HR, Edwards, PA: Natural structural variants of the nuclear receptor farnesoid X receptor affect transcriptional activation. *J Biol Chem,* 278: 104-110, 2003.
368. Lefebvre, P, Cariou, B, Lien, F, *et al.*: Role of bile acids and bile acid receptors in metabolic regulation. *Physiol Rev,* 89: 147-191, 2009.
369. Thomas, C, Pellicciari, R, Pruzanski, M, *et al.*: Targeting bile-acid signalling for metabolic diseases. *Nat Rev Drug Discov,* 7: 678-693, 2008.
370. Grober, J, Zaghini, I, Fujii, H, *et al.*: Identification of a bile acid-responsive element in the human ileal bile acid-binding protein gene. Involvement of the farnesoid X receptor/9-cis-retinoic acid receptor heterodimer. *J Biol Chem,* 274: 29749-29754, 1999.
371. Li, H, Chen, F, Shang, Q, *et al.*: FXR-activating ligands inhibit rabbit ASBT expression via FXR-SHP-FTF cascade. *Am J Physiol Gastrointest Liver Physiol,* 288: G60-66, 2005.
372. Shibata, M, Morizane, T, Uchida, T, *et al.*: Irregular regeneration of hepatocytes and risk of hepatocellular carcinoma in chronic hepatitis and cirrhosis with hepatitis-C-virus infection. *Lancet,* 351: 1773-1777, 1998.
373. Goodwin, B, Jones, SA, Price, RR, *et al.*: A regulatory cascade of the nuclear receptors FXR, SHP-1, and LRH-1 represses bile acid biosynthesis. *Mol Cell,* 6: 517-526, 2000.
374. Edwards, PA, Kast, HR, Anisfeld, AM: BAREing it all: the adoption of LXR and FXR and their roles in lipid homeostasis. *J Lipid Res,* 43: 2-12, 2002.
375. Sirvent, A, Claudel, T, Martin, G, *et al.*: The farnesoid X receptor induces very low density lipoprotein receptor gene expression. *FEBS Lett,* 566: 173-177, 2004.

376. Watanabe, M, Houten, SM, Wang, L, *et al.*: Bile acids lower triglyceride levels via a pathway involving FXR, SHP, and SREBP-1c. *J Clin Invest,* 113: 1408-1418, 2004.
377. Stayrook, KR, Bramlett, KS, Savkur, RS, *et al.*: Regulation of carbohydrate metabolism by the farnesoid X receptor. *Endocrinology,* 146: 984-991, 2005.
378. Fiorucci, S, Antonelli, E, Rizzo, G, *et al.*: The nuclear receptor SHP mediates inhibition of hepatic stellate cells by FXR and protects against liver fibrosis. *Gastroenterology,* 127: 1497-1512, 2004.
379. Li, YT, Swales, KE, Thomas, GJ, *et al.*: Farnesoid x receptor ligands inhibit vascular smooth muscle cell inflammation and migration. *Arterioscler Thromb Vasc Biol,* 27: 2606-2611, 2007.
380. Hartman, HB, Gardell, SJ, Petucci, CJ, *et al.*: Activation of farnesoid X receptor prevents atherosclerotic lesion formation in LDLR-/- and apoE-/- mice. *J Lipid Res,* 50: 1090-1100, 2009.
381. Wang, XX, Jiang, T, Shen, Y, *et al.*: The farnesoid X receptor modulates renal lipid metabolism and diet-induced renal inflammation, fibrosis, and proteinuria. *Am J Physiol Renal Physiol,* 297: F1587-1596, 2009.
382. Brown, MS, Goldstein, JL: The SREBP pathway: regulation of cholesterol metabolism by proteolysis of a membrane-bound transcription factor. *Cell,* 89: 331-340, 1997.
383. Shimano, H, Shimomura, I, Hammer, RE, *et al.*: Elevated levels of SREBP-2 and cholesterol synthesis in livers of mice homozygous for a targeted disruption of the SREBP-1 gene. *J Clin Invest,* 100: 2115-2124, 1997.
384. Proctor, G, Jiang, T, Iwahashi, M, *et al.*: Regulation of renal fatty acid and cholesterol metabolism, inflammation, and fibrosis in Akita and OVE26 mice with type 1 diabetes. *Diabetes,* 55: 2502-2509, 2006.
385. Wang, Z, Jiang, T, Li, J, *et al.*: Regulation of renal lipid metabolism, lipid accumulation, and glomerulosclerosis in FVBdb/db mice with type 2 diabetes. *Diabetes,* 54: 2328-2335, 2005.
386. Sun, L, Halaihel, N, Zhang, W, *et al.*: Role of sterol regulatory element-binding protein 1 in regulation of renal lipid metabolism and glomerulosclerosis in diabetes mellitus. *J Biol Chem,* 277: 18919-18927, 2002.
387. Jiang, T, Wang, Z, Proctor, G, *et al.*: Diet-induced obesity in C57BL/6J mice causes increased renal lipid accumulation and glomerulosclerosis via a sterol regulatory element-binding protein-1c-dependent pathway. *J Biol Chem,* 280: 32317-32325, 2005.
388. Ishigaki, N, Yamamoto, T, Shimizu, Y, *et al.*: Involvement of glomerular SREBP-1c in diabetic nephropathy. *Biochem Biophys Res Commun,* 364: 502-508, 2007.
389. Fiorucci, S, Rizzo, G, Antonelli, E, *et al.*: Cross-talk between farnesoid-X-receptor (FXR) and peroxisome proliferator-activated receptor gamma contributes to the antifibrotic activity of FXR ligands in rodent models of liver cirrhosis. *J Pharmacol Exp Ther,* 315: 58-68, 2005.
390. Mencarelli, A, Renga, B, Distrutti, E, *et al.*: Antiatherosclerotic effect of farnesoid X receptor. *Am J Physiol Heart Circ Physiol,* 296: H272-281, 2009.
391. Zhang, Y, Castellani, LW, Sinal, CJ, *et al.*: Peroxisome proliferator-activated receptor-gamma coactivator 1alpha (PGC-1alpha) regulates triglyceride metabolism by activation of the nuclear receptor FXR. *Genes Dev,* 18: 157-169, 2004.
392. Kaimal, R, Song, X, Yan, B, *et al.*: Differential Modulation of Farnesoid X Receptor Signaling Pathway by Thiazolidinediones. *J Pharmacol Exp Ther*, 2009.
393. Pirisi, L, Creek, KE, Doniger, J, *et al.*: Continuous cell lines with altered growth and differentiation properties originate after transfection of human keratinocytes with human papillomavirus type 16 DNA. *Carcinogenesis,* 9: 1573-1579, 1988.
394. Hawley-Nelson, P, Vousden, KH, Hubbert, NL, *et al.*: HPV16 E6 and E7 proteins cooperate to immortalize human foreskin keratinocytes. *EMBO J,* 8: 3905-3910, 1989.
395. Ryan, MJ, Johnson, G, Kirk, J, *et al.*: HK-2: an immortalized proximal tubule epithelial cell line from normal adult human kidney. *Kidney Int,* 45: 48-57, 1994.
396. Qi, W, Chen, X, Gilbert, RE, *et al.*: High glucose-induced thioredoxin-interacting protein in renal proximal tubule cells is independent of transforming growth factor-beta1. *Am J Pathol,* 171: 744-754, 2007.

397. Panchapakesan, U, Sumual, S, Pollock, CA, *et al.*: PPARgamma agonists exert antifibrotic effects in renal tubular cells exposed to high glucose. *Am J Physiol Renal Physiol,* 289: F1153-1158, 2005.
398. Qi, W, Johnson, DW, Vesey, DA, *et al.*: Isolation, propagation and characterization of primary tubule cell culture from human kidney. *Nephrology,* 12: 155-159, 2007.
399. Vesey, DA, Qi, W, Chen, X, *et al.*: Isolation and primary culture of human proximal tubule cells. *Methods Mol Biol,* 466: 19-24, 2009.
400. Johnson, DW, Saunders, HJ, Baxter, RC, *et al.*: Paracrine stimulation of human renal fibroblasts by proximal tubule cells. *Kidney Int,* 54: 747-757, 1998.
401. Johnson, DW, Saunders, HJ, Brew, BK, *et al.*: Human renal fibroblasts modulate proximal tubule cell growth and transport via the IGF-I axis. *Kidney Int,* 52: 1486-1496, 1997.
402. Kelly, DJ, Wilkinson-Berka, JL, Allen, TJ, *et al.*: A new model of diabetic nephropathy with progressive renal impairment in the transgenic (mRen-2)27 rat (TGR). *Kidney Int,* 54: 343-352, 1998.
403. Kelly, DJ, Skinner, SL, Gilbert, RE, *et al.*: Effects of endothelin or angiotensin II receptor blockade on diabetes in the transgenic (mRen-2)27 rat. *Kidney Int,* 57: 1882-1894, 2000.
404. Gilbert, RE, Cox, A, Wu, LL, *et al.*: Expression of transforming growth factor-beta1 and type IV collagen in the renal tubulointerstitium in experimental diabetes: effects of ACE inhibition. *Diabetes,* 47: 414-422, 1998.
405. Pfaffl, MW: A new mathematical model for relative quantification in real-time RT-PCR. *Nucleic Acids Res,* 29: e45, 2001.
406. Nath, KA: The tubulointerstitium in progressive renal disease. *Kidney Int,* 54: 992-994, 1998.
407. Chan, WL, Leung, JC, Chan, LY, *et al.*: BMP-7 protects mesangial cells from injury by polymeric IgA. *Kidney Int*: 1026-1039, 2008.
408. Zeisberg, M, Shah, AA, Kalluri, R: Bone morphogenic protein-7 induces mesenchymal to epithelial transition in adult renal fibroblasts and facilitates regeneration of injured kidney. *J Biol Chem,* 280: 8094-8100, 2005.
409. Qi, W, Chen, X, Twigg, S, *et al.*: Tranilast attenuates connective tissue growth factor-induced extracellular matrix accumulation in renal cells. *Kidney Int,* 69: 989-995, 2006.
410. Yoshikawa, M, Hishikawa, K, Marumo, T, *et al.*: Inhibition of histone deacetylase activity suppresses epithelial-to-mesenchymal transition induced by TGF-beta1 in human renal epithelial cells. *J Am Soc Nephrol,* 18: 58-65, 2007.
411. Kowanetz, M, Valcourt, U, Bergstrom, R, *et al.*: Id2 and Id3 define the potency of cell proliferation and differentiation responses to transforming growth factor beta and bone morphogenetic protein. *Mol Cell Biol,* 24: 4241-4254, 2004.
412. Roberts, AB, McCune, BK, Sporn, MB: TGF-beta: regulation of extracellular matrix. *Kidney Int,* 41: 557-559, 1992.
413. Helder, MN, Ozkaynak, E, Sampath, KT, *et al.*: Expression pattern of osteogenic protein-1 (bone morphogenetic protein-7) in human and mouse development. *Histochem Cytochem,* 43: 1035-1044, 1995.
414. Brewer, KC, Mwizerva, O, Goldstein, AM: BMPRIA is a promising marker for evaluating ganglion cells in the enteric nervous system--a pilot study. *Hum Pathol,* 36: 1120-1126, 2005.
415. Schnaper, HW, Jandeska, S, Runyan, CE, *et al.*: TGF-beta signal transduction in chronic kidney disease. *Front Biosci,* 14: 2448-2465, 2009.
416. Li, T, Surendran, K, Zawaideh, MA, *et al.*: Bone morphogenetic protein 7: a novel treatment for chronic renal and bone disease. *Curr Opin Nephrol Hypertens,* 13: 417-422., 2004.
417. Zeisberg, M, Kalluri, R: Reversal of experimental renal fibrosis by BMP7 provides insights into novel therapeutic strategies for chronic kidney disease. *Pediatr Nephrol,* 23: 1395-1398, 2008.
418. Veerasamy, M, Nguyen, TQ, Motazed, R, *et al.*: Differential regulation of E-cadherin and alpha-smooth muscle actin by BMP 7 in human renal proximal tubule epithelial cells and its implication in renal fibrosis. *Am J Physiol Renal Physiol,* 297: F1238-1248, 2009.

419. Wang, SN, Lapage, J, Hirschberg, R: Loss of tubular bone morphogenetic protein-7 in diabetic nephropathy. *J Am Soc Nephrol,* 12: 2392-2399, 2001.
420. Roxburgh, SA, Kattla, JJ, Curran, SP, *et al.*: Allelic depletion of grem1 attenuates diabetic kidney disease. *Diabetes,* 58: 1641-1650, 2009.
421. Ruggenenti, P, Remuzzi, G: Nephropathy of type 1 and type 2 diabetes: diverse pathophysiology, same treatment? *Nephrol Dial Transplant,* 15: 1900-1902, 2000.
422. Nath, KA: Tubulointerstitial changes as a major determinant in the progression of renal damage. *Am J Kidney Dis,* 20: 1-17., 1992.
423. Fine, LG, Bandyopadhay, D, Norman, JT: Is there a common mechanism for the progression of different types of renal diseases other than proteinuria? Towards the unifying theme of chronic hypoxia. *Kidney Int Suppl,* 75: S22-26, 2000.
424. Choi, YJ, Chakraborty, S, Nguyen, V, *et al.*: Peritubular capillary loss is associated with chronic tubulointerstitial injury in human kidney: altered expression of vascular endothelial growth factor. *Hum Pathol,* 31: 1491-1497, 2000.
425. Zhang, H, Akman, HO, Smith, EL, *et al.*: Cellular response to hypoxia involves signaling via Smad proteins. *Blood,* 101: 2253-2260, 2003.
426. Sanchez-Elsner, T, Botella, LM, Velasco, B, *et al.*: Synergistic cooperation between hypoxia and transforming growth factor-beta pathways on human vascular endothelial growth factor gene expression. *J Biol Chem,* 276: 38527-38535, 2001.
427. Gustafsson, MV, Zheng, X, Pereira, T, *et al.*: Hypoxia requires notch signaling to maintain the undifferentiated cell state. *Dev Cell,* 9: 617-628, 2005.
428. Higgins, DF, Biju, MP, Akai, Y, *et al.*: Hypoxic induction of Ctgf is directly mediated by Hif-1. *Am J Physiol Renal Physiol,* 287: F1223-1232, 2004.
429. Orphanides, C, Fine, LG, Norman, JT: Hypoxia stimulates proximal tubular cell matrix production via a TGF-beta1-independent mechanism. *Kidney Int,* 52: 637-647, 1997.
430. Kietzmann, T, Roth, U, Jungermann, K: Induction of the plasminogen activator inhibitor-1 gene expression by mild hypoxia via a hypoxia response element binding the hypoxia-inducible factor-1 in rat hepatocytes. *Blood,* 94: 4177-4185, 1999.
431. Wahl, SM: Transforming growth factor-beta: innately bipolar. *Curr Opin Immunol,* 19: 55-62, 2007.
432. Ma, LJ, Jha, S, Ling, H, *et al.*: Divergent effects of low versus high dose anti-TGF-beta antibody in puromycin aminonucleoside nephropathy in rats. *Kidney Int,* 65: 106-115, 2004.
433. Crawford, SE, Stellmach, V, Murphy-Ullrich, JE, *et al.*: Thrombospondin-1 is a major activator of TGF-beta1 in vivo. *Cell,* 93: 1159-1170, 1998.
434. Wang, W, Koka, V, Lan, HY: Transforming growth factor-beta and Smad signalling in kidney diseases. *Nephrology,* 10: 48-56, 2005.
435. Fraser, D, Brunskill, N, Ito, T, *et al.*: Long-term exposure of proximal tubular epithelial cells to glucose induces transforming growth factor-beta 1 synthesis via an autocrine PDGF loop. *Am J Pathol,* 163: 2565-2574, 2003.
436. Brownlee, M: Biochemistry and molecular cell biology of diabetic complications. *Nature,* 414: 813-820, 2001.
437. Falanga, V, Zhou, L, Yufit, T: Low oxygen tension stimulates collagen synthesis and COL1A1 transcription through the action of TGF-beta1. *J Cell Physiol,* 191: 42-50, 2002.
438. Okada, Y, Gonoji, Y, Naka, K, *et al.*: Matrix metalloproteinase 9 (92-kDa gelatinase/type IV collagenase) from HT 1080 human fibrosarcoma cells. Purification and activation of the precursor and enzymic properties. *J Biol Chem,* 267: 21712-21719, 1992.
439. Liu, Y: Renal fibrosis: new insights into the pathogenesis and therapeutics. *Kidney Int,* 69: 213-217., 2006.
440. Virchow, R: Cellular Pathology, as Based Upon Physiological and Pathological Histoloy. *2nd Edition.* Chance R, Trans. New York, 1860 pp 383-408.

441. Ruan, X, Zheng, F, Guan, Y: PPARs and the kidney in metabolic syndrome. *Am J Physiol Renal Physiol,* 294: F1032-1047, 2008.
442. Cases, A, Coll, E: Dyslipidemia and the progression of renal disease in chronic renal failure patients. *Kidney Int Suppl*: S87-93, 2005.
443. Tuttle, KR: Linking metabolism and immunology: diabetic nephropathy is an inflammatory disease. *J Am Soc Nephrol,* 16: 1537-1538, 2005.
444. Mora, C, Navarro, JF: Inflammation and diabetic nephropathy. *Curr Diab Rep,* 6: 463-468, 2006.
445. Qi, W, Chen, X, Holian, J, *et al.*: Transforming growth factor-beta1 differentially mediates fibronectin and inflammatory cytokine expression in kidney tubular cells. *Am J Physiol Renal Physiol,* 291: F1070-1077, 2006.
446. Panchapakesan, U, Pollock, CA, Chen, XM: The effect of high glucose and PPAR-gamma agonists on PPAR-gamma expression and function in HK-2 cells. *Am J Physiol Renal Physiol,* 287: F528-534, 2004.
447. Rutledge, JC, Ng, KF, Aung, HH, *et al.*: Role of triglyceride-rich lipoproteins in diabetic nephropathy. *Nat Rev Nephrol,* 6: 361-370, 2010.
448. Zhang, Y, Lee, FY, Barrera, G, *et al.*: Activation of the nuclear receptor FXR improves hyperglycemia and hyperlipidemia in diabetic mice. *Proc Natl Acad Sci U S A,* 103: 1006-1011, 2006.
449. Jun, H, Song, Z, Chen, W, *et al.*: In vivo and in vitro effects of SREBP-1 on diabetic renal tubular lipid accumulation and RNAi-mediated gene silencing study. *Histochem Cell Biol,* 131: 327-345, 2009.
450. Ma, K, Saha, PK, Chan, L, *et al.*: Farnesoid X receptor is essential for normal glucose homeostasis. *J Clin Invest,* 116: 1102-1109, 2006.
451. Fiorucci, S, Rizzo, G, Donini, A, *et al.*: Targeting farnesoid X receptor for liver and metabolic disorders. *Trends Mol Med,* 13: 298-309, 2007.
452. Fioretto, P, Mauer, M: Histopathology of diabetic nephropathy. *Semin Nephrol,* 27: 195-207, 2007.
453. Risdon, RA, Sloper, JC, De Wardener, HE: Relationship between renal function and histological changes found in renal-biopsy specimens from patients with persistent glomerular nephritis. *Lancet,* 2: 363-366, 1968.
454. Striker, GE, Schainuck, LI, Cutler, RE, *et al.*: Structural-functional correlations in renal disease. I. A method for assaying and classifying histopathologic changes in renal disease. *Hum Pathol,* 1: 615-630, 1970.
455. Wang, S, Hirschberg, R: BMP7 antagonizes TGF-beta -dependent fibrogenesis in mesangial cells. *Am J Physiol Renal Physiol,* 284: F1006-1013, 2003.
456. Loss of tubular bone morphogenetic protein-7 in diabetic nephropathy. *J Dent Res,* 80: 1895-1902., 2001.
457. Woodward, M: *Epidemiology: study design and data analysis,* Boca Raton, Florida, Chapmam and Hall/CRC, 2005.
458. Mitu, GM, Wang, S, Hirschberg, R: BMP7 is a podocyte survival factor and rescues podocytes from diabetic injury. *Am J Physiol Renal Physiol,* 293: F1641-1648, 2007.
459. Sharma, K, Eltayeb, BO, McGowan, TA, *et al.*: Captopril-induced reduction of serum levels of transforming growth factor-beta1 correlates with long-term renoprotection in insulin-dependent diabetic patients. *Am J Kidney Dis,* 34: 818-823, 1999.